

**AN INVESTIGATION INTO MECHANISMS
UNDERLYING ABERRANT PAIN RESPONSES,
AND POTENTIAL THERAPEUTIC INTERVENTIONS,
IN THE HFD/STZ MODEL OF DIABETIC
NEUROPATHY**

Frederika Maria Byrne, BSc. (Hons)

Thesis submitted to the University of Nottingham
for the degree of Doctor of Philosophy

July 2014

Abstract

It is estimated that 366 million people were living with diabetes in 2011, and this is predicted to rise to 522 million by 2030. One of the most common complications of diabetes is diabetic neuropathy, where patients experience various symptoms of neuropathic pain including mechanical allodynia. Using a high fat diet (HFD) in combination with streptozotocin (STZ) produces a model of diabetes which mimics aspects of type 2 diabetes. The aim of this thesis was to characterise pain responses in the HFD/STZ model and to explore some of the peripheral and spinal mechanisms associated with the changes in somatosensory processing. The effectiveness of a variety of drugs in alleviating/preventing neuropathic pain was also investigated in this model.

The effects of the HFD/STZ model on mechanical sensitivity, and changes in metabolic parameters were investigated, and it was found to cause a robust development of mechanical hypersensitivity and a large increase in plasma glucose and a contrasting decrease in plasma insulin. The impacts of the HFD/STZ model on peripheral nerve function and pathology, and spinal mechanisms of central sensitisation, were explored to help identify the mechanisms underpinning the behavioural pain phenotype in these rats. No neuronal degeneration was detected in DRGs or the spinal cord at the timepoints investigated, and a decrease in microglial activation and GFAP immunoreactivity was observed at later timepoints (day 50). Changes in neuronal responses in the dorsal horn of the spinal cord were then investigated, and there was a trend towards a decrease in mechanically evoked responses of spinal neurones in the HFD/STZ group, but no changes in the threshold for electrical activation of C-fibres, nor any significant changes to electrically evoked responses, were observed. There was no change in spontaneous firing, possibly due to the search criteria used.

The effects of different types of interventions on aberrant pain responses were also investigated. As neuropathic pain often proves intractable, one of the key objectives is to develop new drugs, or to find alternative uses of current drugs, that are able to provide symptomatic relief of pain. The gold standard treatment for pain in diabetic neuropathy, pregabalin (10mgkg^{-1} , p.o.), was effective at alleviating established mechanical hypersensitivity at day 37 in the HFD/STZ model. A novel MAGL inhibitor, MJN110 (5mgkg^{-1} , i.p.), was found to be as effective as pregabalin in this model, highlighting a possible role for endocannabinoid modulators in providing pain relief in diabetes. The antidiabetic pioglitazone (10mgkg^{-1} , p.o.), however, was unable to alleviate mechanical hypersensitivity when administered at day 21 for 28 days. Two other antidiabetic drugs, linagliptin (3mgkg^{-1} , p.o.) and metformin (200mgkg^{-1} , p.o.), did show promise in preventing the development of mechanical hypersensitivity in this model when administered from day 4, independent of glycemic control. It is worth investigating these findings further since both of these drugs are already licensed and have undergone all necessary safety testing, and so could rapidly be put to use if effective.

In conclusion, this thesis has highlighted the role that the HFD/STZ model can play in investigating underlying mechanisms of diabetic peripheral neuropathic pain, and its use in exploring potential new therapeutic options for alleviating this pain.

Publications

Niphakis MJ, Cognetta AB, Chang JW, Buczynski MW, Parsons LH, **Byrne F**, Burston JJ, Chapman V, Cravatt BF (2013). Evaluation of NHS carbamates as a potent and selective class of endocannabinoid hydrolase inhibitors. *ACS Chem Neurosci*.

Abstracts

F.M. Byrne, R. Mason, S. Cheetham, S. Vickers, V. Chapman. Pain behaviour in an animal model of diabetic neuropathy. Poster session presented at: 7th Congress of the European Federation of IASP Chapters (EFIC); Hamburg, Germany; Sept 21-24 2011.

F.M. Byrne, S. Cheetham, V. Chapman. Characterisation of the high fat diet/streptozotocin model of diabetes and the effects of the PPAR γ ligand pioglitazone. Poster session presented at: 14th World Congress on Pain 7th (IASP); Milan, Italy; August 27-31, 2012.

Acknowledgements

Firstly I would like to thank my supervisor, Prof. Vicky Chapman, for all her help and support along the way, her excellent advice, and for reading drafts even on a sunny Saturday afternoon. I would also like to thank the BBSRC and RenaSci for their funding, and the help of various RenaSci staff in setting up the model.

In our lab group I need to thank: Devi, for everything, especially for making me feel at home when I first joined the lab; James, who couldn't be more helpful if he tried (and trust me, he has); Steve, for his never-ending patience when I requested yet more ephys assistance; and Charlie, least of all for her baking prowess.

Thank you to my amazing film buddies – Ian, Lizi, Adrian and Ricky - for accompanying me on numerous visits to the cinema, and so much more beside. And thank you to the other friends who reminded me that there is life outside the lab, even when it was difficult to remember: Chris, Steve, Glen and Alex; Justine for all our extended lunch hours; and to Pippa, who is the best friend I could ask for.

Finally, thank you to my family; to my Mum for always being at the end of the phone through four long and tumultuous years, and for Dad for bravely volunteering (!) to proof-read this thesis (although any mistakes are obviously my own). And lastly, to Mike, who needs the biggest thanks for putting up with me during the long and arduous ephys period, for all the 5-star cooking before I proceeded to thank him by falling asleep on the sofa, and for being a wonderfully calming presence in my life.

There's nothing we can't do if we work hard, never sleep,
and shirk all other responsibilities in our lives.

- **Leslie Knope**

Abbreviations

15d-PGJ2:	15-deoxy- Δ -12,14-prostaglandin J2
2-AG:	2-arachidonoyl glycerol
AEA:	arachidonoyl ethanolamine (anandamide)
AGE:	advanced glycation end-product
AMPA:	α -amino-3-hydroxy-5-methyl-4-isoxazolepropionic acid
AMPK:	AMP-activated protein kinase
ANCOVA:	analysis of covariance
ANOVA:	analysis of variance
ATP:	adenosine triphosphate
AUC:	area under the curve
BADGE:	bisphenolAdiglycidyl ether
BB:	biobreeding
BDNF:	brain-derived neurotrophic factor
CB1:	cannabinoid receptor 1
CB2:	cannabinoid receptor 2
CCI:	chronic constriction injury
CGRP:	calcitonin-gene related peptide
CNS:	central nervous system
DAG:	diacylglycerol
DCCT:	diabetes control and complications trial
DPN:	diabetic peripheral neuropathy
DPNP:	diabetic peripheral neuropathic pain
DPP-4:	dipeptidyl-peptidase-IV
DRG:	dorsal root ganglion
EAA:	excitatory amino acid
EAAT:	excitatory amino acid transporter
ERK:	extracellular signal-regulated kinase
FAAH:	fatty acid amide hydrolase
FAE:	fatty acid ethanolamide
GABA:	γ -aminobutyric acid
GDNF:	glial-derived neurotrophic factor
GFAP:	glial fibrillary acidic protein
GIP:	glucose-dependent insulinotropic polypeptide
GLP-1:	glucagon-like peptide-1
GLT:	glutamate transporter
GPCR:	G protein-coupled receptor
GSH:	reduced glutathione
HbA1c:	glycosylated haemoglobin
HFD:	high fat diet
HFD/STZ:	high fat diet (in combination with) streptozotocin
i.p.:	intraperitoneal
IASP:	international association for the study of pain
Iba1:	ionised calcium binding adapter molecule 1
IENF:	intra-epidermal nerve fibre
IGF:	insulin-like growth factor
IRS-1:	insulin receptor substrate 1
KCC2:	potassium chloride co-transporter 2
L:	lamina

LC-MS/MS: liquid chromatography/tandem mass spectrometry
MAGL: monoacylglycerol lipase
MAPK: mitogen activated protein kinase
MCP-1: monocyte chemoattractant protein-1
MMP: matrix metalloproteinase
mTOR: mammalian target of rapamycin
mTORC1: mammalian target of rapamycin complex 1
NAA: N-acetylaspartate
NAD: nicotinamide
NCV: nerve conduction velocity
NF κ B: nuclear factor κ B
NGF: nerve growth factor
NMDA: N-methyl-D-aspartate
NO: nitric oxide
NOD: non-obese diabetic
NRG1: neuregulin 1
NS: nociceptive specific
OEA: oleoylethanolamide
OGTT: oral glucose tolerance test
p.o.: oral
PAG: periaqueductal gray
PARP: poly(ADP-ribose) polymerase
PBS: phosphate buffered saline
PEA: palmitoylethanolamide
PFA: paraformaldehyde
PG: prostaglandin
PKC: protein kinase C
PNL: partial sciatic nerve ligation
PPAR: peroxisome proliferator-activated receptor
PSDC: postsynaptic dorsal column
RAGE: receptor for AGE
ROS: reactive oxygen species
RT: room temperature
RVM: rostral ventromedial medulla
SNI: spared nerve injury
SNL: spinal nerve ligation
SP: substance P
SPBT: spinoparabrachial tract
STT: spinothalamic tract
STZ: streptozotocin
THC: Δ 9-tetrahydrocannabinol
TLR: toll-like receptor
TNF- α : tumour necrosis factor- α
TRPV1: transient receptor potential vanilloid 1
TTBS: trizma triton X-100 buffered saline
TZD: thiazolidinedione
URB597: cyclohexylcarbamic acid 3'-carbamoyl-biphenyl-3-yl ester
VLPAG: ventrolateral PAG
WDR: wide dynamic range
ZDF: zucker diabetic fatty

Table of contents

Chapter 1.	1
General Introduction	1
1.1. Diabetes	2
1.1.1. Current treatments for diabetes	3
1.1.1.1. Pioglitazone	3
1.1.1.2. Metformin	5
1.1.1.3. Linagliptin	5
1.1.2. Animal models of diabetes	6
1.2. Diabetic neuropathy	11
1.2.1. Mechanisms associated with diabetic neuropathy	11
1.2.1.1. Microangiopathy	12
1.2.1.2. Oxidative stress	12
1.2.1.3. Polyol pathway	13
1.2.1.4. Advanced glycation end-products (AGEs)	14
1.2.1.5. PKC activation	14
1.2.1.6. Hexosamine pathway	15
1.2.1.7. Poly(ADP) ribose polymerase	15
1.2.1.8. Insulin and C-peptide	15
1.3. Pain	17
1.3.1. Primary afferent nociceptors	17
1.3.2. The organisation of the dorsal horn of the spinal cord	20
1.3.3. Ascending pain pathways	22
1.3.4. Descending control of pain	24
1.3.5. Neuropathic pain	26
1.3.6. Origins of pain in diabetes	27
1.3.6.1. Involvement of primary afferent fibres	28
1.3.6.2. Involvement of spinal sensitisation	30
1.3.6.3. Involvement of higher centres	32
1.4. Aims of the thesis	35

Chapter 2.	36
Assessment of the HFD/STZ diabetic model	36
2.1. Introduction	37
2.1.1. The STZ model of diabetes	37
2.1.2. Neuropathy in the STZ model	38
2.1.3. Criticisms of the STZ model	39
2.1.4. Alternatives to the STZ model	39
2.1.5. The HFD/STZ model	40
2.1.6. HFD/STZ: a model of diabetic neuropathy?	41
2.1.7. Aim of the study	42
2.2. Methods	43
2.2.1. Animals	43
2.2.2. The HFD/STZ model of diabetes	43
2.2.3. Development of the HFD/STZ model	43
2.2.4. Behavioural testing	45
2.2.5. Blood sampling	46
2.2.6. Oral glucose tolerance test (OGTT)	46
2.2.7. Total pancreatic insulin content	46
2.2.8. Statistics	47
2.3. Results	48
2.3.1. Effects of HFD/STZ on body weight, and food and water intake	48
2.3.2. Effects of HFD/STZ on metabolic parameters	48
2.3.3. Effects of HFD/STZ on mechanical withdrawal thresholds	54
2.4. Discussion	56
2.4.1. Metabolic effects in the HFD/STZ model	56
2.4.2. Mechanical withdrawal thresholds in the HFD/STZ model	56
Chapter 3.	60
Investigating the impact of the HFD/STZ model on peripheral nerve function, and spinal mechanisms of central sensitisation	60
3.1. Introduction	61
3.1.1. Fluoro-Jade B	61
3.1.2. CGRP	62

3.1.3. Microglia.....	65
3.1.4. Astrocytes	68
3.1.5. Aim of the Study.....	71
3.2. Methods -----	72
3.2.1. Animals	72
3.2.2. DRG and spinal cord immunohistochemistry	72
3.2.2.1. NeuN and Fluoro-Jade B-----	74
3.2.2.2. CGRP-----	74
3.2.2.3. Iba1 and GFAP -----	75
3.2.3. Quantification of antibody staining	75
3.2.3.1. NeuN and Fluoro-Jade B-----	76
3.2.3.2. CGRP-----	77
3.2.3.3. Iba1 and GFAP -----	77
3.2.4. Statistics.....	78
3.3. Results-----	79
3.3.1. Effects of HFD/STZ on body weight, and food and water intake	79
3.3.2. Effects of HFD/STZ on metabolic parameters and development of mechanical hypersensitivity	79
3.3.3. Effects of HFD/STZ on degenerating neurones	83
3.3.4. Effects of HFD/STZ on expression of CGRP.....	87
3.3.5. Effects of HFD/STZ on activation of glia	89
3.4. Discussion -----	95
3.4.1. Fluoro-Jade B staining	96
3.4.2. CGRP expression	98
3.4.3. Microglial activation.....	98
3.4.4. Astroglial activation	100
Chapter 4.-----	103
Electrophysiological characterisation of spinal neuronal responses in the HFD/STZ model of diabetes, and the effects of pioglitazone intervention-----	103
4.1. Introduction -----	104
4.1.1. Involvement of primary afferent fibres in the STZ model....	104

4.1.2.	Involvement of WDR neurones in the dorsal horn of the spinal cord in the STZ model.....	105
4.1.3.	Pioglitazone and other PPAR γ agonists.....	106
4.1.4.	PPAR γ agonists in inflammatory pain	106
4.1.5.	PPAR γ agonists in neuropathic pain	108
4.1.6.	PPAR γ agonists in diabetic neuropathy	108
4.1.7.	Aim of the study	111
4.2.	Methods	112
4.2.1.	Animals	112
4.2.2.	<i>In vivo</i> electrophysiology	112
4.2.2.1.	Induction of anaesthesia	112
4.2.2.2.	Tracheal cannulation	113
4.2.2.3.	Laminectomy	113
4.2.2.4.	Electrophysiological recordings	114
4.2.2.5.	Characterising neurones	115
4.2.2.6.	Production of glass coated tungsten microelectrodes-	116
4.2.2.7.	Choice of anaesthetic	117
4.2.3.	Administration of drugs	118
4.2.4.	Statistics.....	119
4.3.	Results	120
4.3.1.	Effects of HFD/STZ on hindpaw evoked responses of WDR neurones in the dorsal horn	120
4.3.2.	Effects of pioglitazone on mechanically evoked responses of dorsal horn neurones	123
4.3.3.	Effects of pioglitazone on metabolic parameters.....	125
4.3.4.	Effects of pioglitazone on mechanical withdrawal thresholds.....	126
4.4.	Discussion	128
4.4.1.	Effects of the HFD/STZ model on electrophysiological parameters.....	128
4.4.2.	Metabolic effects of pioglitazone in the HFD/STZ model....	131
4.4.3.	Effects of pioglitazone on pain behaviour and neuronal responses in the HFD/STZ model	132

Chapter 5.	135
Comparison of analgesic versus antidiabetic interventions on aberrant pain responses in the HFD/STZ model	135
5.1. Introduction	136
5.1.1. Existing and novel analgesics for diabetic neuropathy	136
5.1.1.1. Pregabalin	137
5.1.1.2. Cannabinoid ligands	138
5.1.1.2.1. MAGL inhibitors	141
5.1.1.2.2. FAAH inhibitors	142
5.1.2. Antidiabetic drugs	144
5.1.2.1. Metformin	144
5.1.2.2. Linagliptin	145
5.1.3. Aim of the Study	146
5.2. Methods	147
5.2.1. Animals	147
5.2.2. Administration of drugs	147
5.2.3. Quantification of endocannabinoids in spinal cord using liquid chromatography/tandem mass spectrometry (LC-MS/MS)	149
5.2.4. Drugs	150
5.2.5. Statistics	151
5.3. Results	152
5.3.1. Acute effects of MJN110, URB597 and Pregabalin on established mechanical hypersensitivity	152
5.3.2. Acute effects of MNJ110 and URB597 on endocannabinoid levels in spinal cord and brain	155
5.3.3. Effects of Metformin and Linagliptin on metabolic parameters	158
5.3.4. Effects of Metformin and Linagliptin on the development of mechanical hypersensitivity	161
5.4. Discussion	162
5.4.1. Cannabinoids in the HFD/STZ model	162
5.4.2. Antidiabetics in the HFD/STZ model	165

Chapter 6.	171
General Discussion	171
6.1. HFD/STZ: a model of type 2 diabetes?	173
6.2. Assessment of mechanical hypersensitivity in the HFD/STZ model	175
6.3. Mechanisms underlying the development of mechanical hypersensitivity.	177
6.4. Possible treatments for diabetic neuropathy	182
6.5. Conclusions.	185
References	186

Chapter 1.

General Introduction

1.1. Diabetes

Diabetes mellitus is a metabolic disorder characterised by elevated blood glucose. Globally, it is estimated that 366 million people were living with diabetes in 2011, and this is predicted to rise to 522 million by 2030 (IDF, 2012). Diabetes can be divided into two main categories: type 1 and type 2 diabetes, with type 2 accounting for approximately 90% of diabetic cases (Rydén *et al.*, 2007). Type 1 diabetes is an autoimmune disease in which the pancreatic β -cells in the islets of Langerhans are gradually destroyed by T cells, leading to the pancreas being unable to secrete enough insulin (Atkinson *et al.*, 2001; Bluestone *et al.*, 2010). In type 2 diabetes, the first stage is peripheral insulin resistance, where the sensitivity of tissues to insulin decreases (Rydén *et al.*, 2007). The β -cells initially secrete more insulin to compensate for the insulin resistance, but eventually become less effective (Campbell, 2009). The hallmark of diabetes is hyperglycaemia – where fasting blood glucose is $\geq 7\text{mM}$, or glycosylated haemoglobin (HbA1c) is $\geq 6.5\%$ (American Diabetes Association, 2013). Insulin levels generally have to fall below 0.5ngml^{-1} for hyperglycaemia to develop (Dobretsov *et al.*, 2007). In healthy individuals, insulin is secreted from β -cells in response to elevated levels of glucose. The roles of insulin include: stimulating amino acid synthesis; suppressing gluconeogenesis; decreasing lipogenesis in fat tissue; and promoting the uptake of glucose in skeletal muscle and the liver, where it is stored as glycogen (Dobretsov *et al.*, 2007). Glucagon, which is released by pancreatic α -cells, performs an opposing role; causing an increase in the release of glucose.

Diabetes leads to a wide variety of complications: microvascular diseases such as retinopathy, nephropathy and neuropathy (including diabetic autonomic neuropathy and focal neuropathy), as well as macrovascular diseases such as cardiovascular disease (Forbes *et al.*, 2013). The focus of this thesis, however, is diabetic peripheral neuropathy (DPN), also known as sensorimotor neuropathy or distal symmetric neuropathy.

1.1.1. Current treatments for diabetes

Exogenous insulin is necessary in the control of type 1 diabetes, but there are a number of drugs available for the treatment of type 2 diabetes (for review see Stumvoll *et al.*, 2005), and these include:

- Thiazolidinediones (TZDs), such as pioglitazone, which help to improve insulin resistance and increase glucose uptake into peripheral tissues.
- Metformin, a biguanide, which reduces hepatic glucose production.
- Glucagon-like peptide 1 (GLP-1) agonists (Gutniak *et al.*, 1992), and dipeptidyl peptidase-IV (DPP-4) inhibitors such as linagliptin, which cause insulin secretion, as well as inhibiting hepatic glucagon secretion and slowing gastric emptying.
- Sulfonylureas, such as glibenclamide, which stimulate insulin secretion from the pancreas.

Those relevant to this thesis are discussed in more detail below.

1.1.1.1. Pioglitazone

TZDs such as pioglitazone act through a peroxisome proliferator-activated receptor (PPAR): PPAR γ . PPARs are members of the nuclear hormone receptor superfamily (Dreyer *et al.*, 1992; Issemann *et al.*, 1990), and are activated by fatty acids, eicosanoids and synthetic compounds (Youssef *et al.*, 2004). Once activated, they form heterodimers with retinoid X receptors (Kota *et al.*, 2005). They are able to regulate the transcription of a wide variety of target genes through binding to a specific peroxisome proliferator response element in the promoter region of these genes (Berger *et al.*, 2002), and they then stimulate transcription through recruitment of coactivators (Tan *et al.*, 2005).

There are three different PPAR isoforms – α , β/δ , and γ (Berger *et al.*, 2005). PPAR γ is primarily expressed in the adipose tissue, but is also

found at lower levels in kidney, liver, and Schwann cells (Desvergne *et al.*, 1999), as well as microglia and astrocytes in the brain (Bernardo *et al.*, 2008; Moreno *et al.*, 2004). It can also be found in pain pathways where it has been measured in adipocytes in the epineurium of the sciatic nerve, in L5 dorsal root ganglia (DRG), and in neurones in the dorsal horn of the spinal cord (Churi *et al.*, 2008; Maeda *et al.*, 2008).

TZDs have been shown to alter the mRNA levels of a myriad of genes, but primarily those involved in glucose and lipid metabolism (Sears *et al.*, 2007). They normalise expression of the glucose transporter, GLUT4, in adipose tissue and increase expression of GLUT1 in adipose tissue and skeletal muscle (Kramer *et al.*, 2001). They are able to enhance adipocyte insulin signalling, and lipid uptake and metabolism, as well as attenuating lipolysis and free fatty acid release. TZDs are also able to stimulate the redistribution of lipids from insulin-resistant visceral fat depots into subcutaneous fat (Miyazaki *et al.*, 2002) through promoting apoptosis in mature adipocytes in visceral fat, and stimulating adipogenesis in subcutaneous fat, resulting in an increase in smaller, more insulin-responsive adipocytes (Okuno *et al.*, 1998). As more lipolysis takes place in visceral fat (Arner, 1995), the change to more insulin responsive adipocytes in subcutaneous fat leads to a decrease in levels of free fatty acids, therefore enhancing insulin sensitivity (Willson *et al.*, 2000).

TZDs are also able to reduce levels of pro-inflammatory cytokines, such as tumour necrosis factor- α (TNF α) (Dandona *et al.*, 2004), which is increased in obese rodents (Hotamisligil *et al.*, 1993; Xu *et al.*, 2003) and also in patients with type 2 diabetes (Katsuki *et al.*, 1998; Zinman *et al.*, 1999). TNF α has been linked to insulin resistance due to interference with the insulin signalling cascade (Hotamisligil *et al.*, 1996; Hotamisligil *et al.*, 1993).

All of these mechanisms mean TZDs are able to act as potent insulin sensitisers in peripheral tissue, as well as lowering blood glucose,

HbA1c, insulin and triglyceride levels and increasing HDL cholesterol levels (Aronoff *et al.*, 2000; Diamant *et al.*, 2003; Rosenblatt *et al.*, 2001). TZDs may even preserve β -cell function - increasing islet mass, preserving insulin content and improving insulin secretion (Campbell *et al.*, 2007; Kawasaki *et al.*, 2005; Kawashima *et al.*, 2011). This may be through a decrease in lipotoxicity in the β cells, resulting in an inhibition of excessive apoptosis (Berger *et al.*, 2005).

1.1.1.2. Metformin

Metformin improves glycemic control and decreases blood sugar levels through multiple mechanisms: a reduction in hepatic glucose output; the inhibition of gluconeogenesis; and by improving the sensitivity of muscle to insulin, leading to increased glucose uptake (Stumvoll *et al.*, 1995).

Metformin causes increased phosphorylation and activation of AMP-activated protein kinase (AMPK), which is termed 'the energy sensor of the cell' (Tillu *et al.*, 2012). AMPK responds to the cellular AMP:ATP ratio, and is an important regulator of lipid and glucose metabolism. When it is activated, it downregulates the expression of several genes through phosphorylation of multiple targets, including those involved in gluconeogenesis and lipogenesis in the liver. This leads to a reduction of lipid stores in muscle and liver (Kahn *et al.*, 2005) and inhibition of hepatic glucose production (Zhou *et al.*, 2001a). AMPK also switches on pathways that lead to the uptake and metabolism of glucose in muscle by increasing the translocation of the glucose transporter GLUT4 to the plasma membrane (Hardie, 2007).

1.1.1.3. Linagliptin

Linagliptin competitively and reversibly inhibits DPP-4 (Eckhardt *et al.*, 2007), an enzyme that cleaves GLP-1 and glucose-dependent insulinotropic polypeptide (GIP), two incretin hormones which are rapidly secreted from gut endocrine cells after eating (Drucker *et al.*,

2006). These hormones activate GPCRs and cause glucose-dependent insulin secretion. GLP-1 also inhibits hepatic glucagon secretion, and slows gastric emptying (Drucker, 2006). In humans it has been shown that an oral dose of glucose causes an increased release of insulin compared to an intravenous dose, termed the 'incretin effect', but this effect is often much lower in type 2 diabetics (Nauck *et al.*, 1993). At higher concentrations, GLP-1 is still able to exert its insulinotropic activity (Nauck *et al.*, 1993), and therefore augmentation of this incretin through inhibition of DPP-4 can help to control hyperglycaemia.

Linagliptin causes approximately 80% inhibition of DPP-4 (Rauch *et al.*, 2012) and has been shown to increase the levels of circulating GLP-1 by around 2-fold (Rauch *et al.*, 2012; Sarashina *et al.*, 2010), and cause a reduction of approximately 15% in peak glucagon (Rauch *et al.*, 2012). Linagliptin improves HbA1c, has a good safety profile, and is not associated with hypoglycaemia or weight gain (McGill, 2012). It is licensed to treat type 2 diabetes as a monotherapy, but can also be combined with other treatments such as metformin, utilising two complementary modes of action (Gallwitz, 2013).

1.1.2. Animal models of diabetes

Animal models of type 1 diabetes include those induced by chemical ablation of pancreatic β -cells, and rodents who spontaneously develop autoimmune diabetes (Table 1.1). Models of type 2 diabetes include both obese and non-obese rodents, with varying severity of symptoms. Table 1.2 briefly describes the main models of type 2 diabetes, some of which are described in more detail in Chapter 2. Full descriptions and advantages/disadvantages are discussed elsewhere (for review see Chatzigeorgiou *et al.*, 2009; King, 2012; Reed *et al.*, 1999; Rees *et al.*, 2005; Srinivasan *et al.*, 2007), but for brevity only those models mentioned in this thesis are described below.

The most frequently used model is the streptozotocin (STZ) model, as it is cheap and quick to set up, whereas the spontaneous autoimmune models are more expensive, disease onset is less predictable and they are also more time consuming. Non-obese diabetic (NOD) mice and biobreeding (BB) rats, however, can more accurately represent the disease in humans, as they share some of the genes that are linked with susceptibility to type 1 diabetes (for review see Driver *et al.*, 2011; Yang *et al.*, 2006). There are, however, concerns that observations from these highly inbred genetic strains are not representative of the heterogeneity of the human population (Srinivasan *et al.*, 2005). The rodent models summarised in Table 1.1 and 1.2 produce many of the symptoms associated with diabetes, as well as signs of peripheral nerve dysfunction such as nerve conduction velocity (NCV) slowing, and development of mechanical sensitivity, and have been used to investigate pathogenic pathways in early diabetic neuropathy (Forbes *et al.*, 2013). However the majority of these models tend to lack the advanced clinical characteristics of microvascular complications such as segmental demyelination, neurodegeneration, and subsequent axon or fibre loss (Sharma *et al.*, 1974), possibly due to their relatively short lifespan. They are therefore not as useful for studying the long term complications, such as loss of sensory function, unless a long-term study is run. However nerve pathology, such as atrophy of sural axons and loss of large-calibre dermal and small-calibre epidermal axons, can be seen after 4 months of diabetes in ZDF rats (Brussee *et al.*, 2008). This aspect is discussed further in Chapter 3.

It has been postulated that STZ may have a direct neurotoxic effect that is partly responsible for the development of some of the signs of diabetic neuropathy (Bishnoi *et al.*, 2011; Pabbidi *et al.*, 2008b). It has been shown that the timecourse and the degree of thermal and mechanical hypersensitivity were similar in STZ rats that went on to develop hyperglycaemia and those rats that didn't (Bishnoi *et al.*, 2011), and a similar effect was also seen with thermal hyperalgesia in STZ-treated mice (Pabbidi *et al.*, 2008b). They hypothesised that this may be

due to a direct neuronal effect of STZ, which leads to enhanced expression and function of the TRPV1 receptor in DRGs, as well as microglial activation, and increased levels of pro-inflammatory cytokines.

However, other studies have ruled out a direct effect of STZ (Davidson *et al.*, 2009; Romanovsky *et al.*, 2010). Evidence for this comes from studies that show that when STZ rats are treated with insulin they exhibit a decrease in hyperglycaemia and attenuated pain sensation (Courteix *et al.*, 1996; Romanovsky *et al.*, 2006), as well as a reversal of the upregulation of T-current density in small-sized DRG cells (Messinger *et al.*, 2009). This suggests that these aberrant pain sensations must be due to a combination of hyperglycaemia and hypoinsulinaemia, and not just a direct effect of STZ (Romanovsky *et al.*, 2004). Mechanical hyperalgesia has also been shown to correlate with plasma insulin levels in normoglycaemic STZ rats, further substantiating a role of decreased insulin in the development of hypersensitivity (Romanovsky *et al.*, 2006). Finally, pressure pain thresholds were restored to original levels in normoglycaemic STZ rats after four weeks, in parallel with the spontaneous recovery of insulin production in these animals (Romanovsky *et al.*, 2010). Therefore, in this thesis, it was presumed that any development of mechanical hypersensitivity was not a direct neurotoxic effect of STZ.

In this array of animal models of diabetes, the development of diabetic peripheral neuropathic pain (DPNP) can be investigated through a variety of methods. Most commonly, the development of mechanical hypersensitivity is examined using von Frey hairs, and the paw pressure test can be used to assess hyperalgesia. To look at thermal thresholds, both the Hargreaves and the hot plate test can be used. Finally, the formalin test can also be used in the diabetic model itself. Although this is not clinically relevant, it enables the investigation of the effect of hyperglycaemia on prolonged activation of nociceptive pathways in the peripheral and central nervous system (Calcutt, 2002).

Table 1.1 Summary of rodent models of type 1 diabetes

Method of induction	Model	Features
Chemical	High dose STZ (45-90mgkg ⁻¹ in rats)	STZ is used to destroy a high percentage of the pancreatic β -cells resulting in little endogenous insulin production, which leads to hyperglycaemia and weight loss.
	Multiple low doses of STZ (20-30mgkg ⁻¹ in rats)	This induces insulinitis, which causes a decrease in islet number and therefore a decrease in insulin secretion capacity.
Spontaneous autoimmune	NOD mice	NOD mice develop insulinitis at around 3–4 weeks of age, which causes β -cell destruction. Overt diabetes becomes apparent at around 12-30 weeks, and mice rapidly lose weight and require insulin treatment.
	BB rats	BB rats develop diabetes between 8-16 weeks of age. The level of diabetes is quite severe, and the rats rely on insulin therapy to survive.

Table 1.2 Summary of rodent models of type 2 diabetes

Method of induction	Model	Features
Obese models	Lep ob/ob mice	Mutation in the leptin gene. Obesity and mild hyperglycaemia develop by 4 weeks, and increase over time. Hyperinsulinaemia is also present.
	Lepr db/db mice	Autosomal recessive mutation in the leptin receptor. Mice become obese, hyperglycaemic, hyperinsulinaemic and insulin resistant within 4 weeks and develop hypoinsulinaemia later, with a peak in hyperglycaemia between 3-4 months of age.
	Zucker diabetic fatty (ZDF) rats	Mutated leptin receptor. Rats are initially hyperinsulinaemic with severe insulin resistance. When levels of insulin decrease, they become hyperglycaemic at 8-10 weeks of age.
Induced obesity	High fat diet (HFD) fed C57BL/6J mice	A high fat diet (typically where around 60% of energy is derived from fat) can lead to obesity and the development of hyperinsulinaemia, insulin resistance and glucose intolerance.
Chemically induced	Nicotinamide (NAD) + STZ	Rats administered NAD 15 minutes before STZ develop moderate, stable hyperglycaemia without any changes in plasma insulin levels as NAD has a protective effect on the cytotoxic action of STZ, resulting in only minor damage to pancreatic β -cell mass.
	Neonatal STZ	STZ administration to neonatal rats can lead to hyperglycaemia at 6 weeks, due to a decrease in normal β -cell mass and β -cell dysfunction.
	HFD/STZ	The HFD causes insulin resistance, followed by a low dose of STZ, which causes hyperglycaemia to develop as a proportion of the β -cells are destroyed.

1.2. Diabetic neuropathy

The prevalence of diabetic neuropathy varies from 10% within one year of diagnosis, to up to 50% 25 years after diagnosis (Pirart, 1978), with an average prevalence of approximately 30% (Said, 2007; Sugimoto *et al.*, 2000), and the likelihood increasing with poor control of plasma glucose levels (Tesfaye *et al.*, 1996). It has been estimated that approximately 16-21% of diabetic patients experience chronic painful DPN (Abbott *et al.*, 2011; Daousi *et al.*, 2004), and 40-50% of those with diabetic neuropathies experience pain (Veves *et al.*, 2008).

The positive symptoms of DPN can include tingling, burning, spontaneous pain, allodynia and hyperalgesia, whereas the negative symptoms include numbness and loss of sensation (Dobretsov *et al.*, 2007). The longest nerves are affected first, starting at the distal end, and so symptoms tend to follow a 'stocking and glove' distribution; starting in the toes, and spreading up the foot and eventually the leg, and can also be seen in the fingers and the hands (Zochodne, 2007). Early on there is a loss of intra-epidermal nerve fibres (IENFs). The loss of protective sensation in the foot can lead to ulceration, which can ultimately result in amputation (Vinik *et al.*, 2000).

1.2.1. Mechanisms associated with diabetic neuropathy

The first changes observed in diabetic neuropathy are a decrease in the NCV in motor and sensory neurones, shunting of excess glucose into the polyol pathway, microangiopathy and impairments of Na^+/K^+ -ATPase activity (Sima, 2003). Other important factors include inappropriate activation of protein kinase C (PKC) and poly(ADP-ribose) polymerase (PARP), and lack of neurotrophic support due to C-peptide and insulin deficiency (Obrosova, 2009b).

1.2.1.1. Microangiopathy

Microangiopathy leads to abnormalities in blood flow as observed in the sciatic nerve and DRG in the STZ model (Sasaki *et al.*, 1997). This is due to impaired vasodilation with nitric oxide (NO), and increased activity of vasoconstrictors (Zochodne, 2007). There is also an increase in vascular permeability due to a rise in permeability factors such as vascular endothelial growth factor (Brownlee, 2001). As the disease develops there can be loss of microvascular cells, and thickening of the capillary basement membrane of the vasa nervorum, due to overproduction of the extracellular matrix, which is induced by growth factors. All of these changes lead to ischaemic damage to neurones and axons, resulting in axonal degeneration in peripheral nerves, due to severe demyelination.

1.2.1.2. Oxidative stress

In diabetes, metabolic abnormalities lead to increased production of mitochondrial superoxide by the electron transport chain (Brownlee, 2001; Giacco *et al.*, 2010). This in turn results in activation of the intertwined mechanisms described below, resulting in a common fate: further oxidative stress. Excessive reactive oxygen series (ROS), such as superoxide and hydrogen peroxide, and reactive nitrogen series, such as peroxy nitrite, are produced, which can lead to damage to lipids, proteins and DNA (Edwards *et al.*, 2008). Peroxidation of lipids leads to formation of products which are toxic to the cell, and if DNA is damaged this can lead to apoptosis. Accumulation of all these products can also cause a loss of neuronal function, and neuronal degeneration (Vincent *et al.*, 2004a). Oxidative stress can also cause mitochondrial dysfunction, and when the mitochondrial permeability transition pore opens, there is a release of cytochrome c and initiation of the apoptotic cascade (Russell *et al.*, 2002). Treatment with antioxidants has been shown to prevent the NCV slowing that occurs as a result of peripheral nerve dysfunction in STZ rats (Cameron *et al.*, 1993; Vincent *et al.*, 2004b), but antioxidants such as α -lipoic acid have demonstrated

limited effects on neuropathic symptoms in randomised double-blind placebo trials (Vincent *et al.*, 2004b).

1.2.1.3. Polyol pathway

Hyperglycaemia results in more glucose being shunted through the polyol pathway. Figure 1.1 summarises this pathway; glucose is converted to sorbitol by aldose reductase with the oxidation of NADPH to NADP⁺, and then to fructose by sorbitol hydrogenase with NAD⁺ being reduced to NADH (Duby *et al.*, 2004).

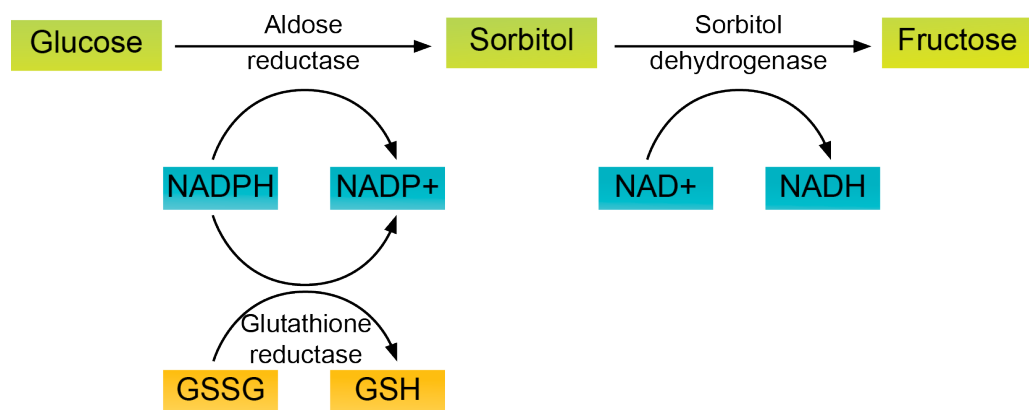


Figure 1.1 The key features of the polyol pathway, adapted from (Brownlee, 2001).

The polyol pathway uses up NADPH, which is important in the production of reduced glutathione (GSH), another antioxidant, and this depletion of GSH further promotes oxidative stress (Brownlee, 2005). The decrease in NADPH also leads to depletion of osmolytes such as taurine and nerve *myo*-inositol. Taurine is an antioxidant and vasodilator and its decrease leads to promotion of oxidative stress (Sima, 2003). A 1% taurine diet has been shown to improve the deficits in nerve conduction and blood flow that are seen in STZ mice (Pop-Busui *et al.*, 2001). The loss of *myo*-inositol causes a decrease in PKC, which leads to impaired Na⁺/K⁺-ATPase activity, resulting in increased levels of sodium which are associated with slowing of NCV (Cherian *et*

al., 1996). The increased accumulation of fructose also leads to the formation of advanced glycation end-products.

Diabetic transgenic mice overexpressing human aldose reductase had an increased accumulation of sorbitol and fructose, decreased PKC activity, more severe slowing of NCV and more severe neuronal atrophy. These symptoms were ameliorated by the aldose reductase inhibitor, WAY121-409 (Yagihashi *et al.*, 2001). On the other hand, diabetic mice with a knockout for the aldose reductase gene showed no reduction in NCV, and no change in GSH level (Chung *et al.*, 2003). Aldose reductase inhibitors, however, have failed to show promise in diabetic patients.

1.2.1.4. Advanced glycation end-products (AGEs)

AGEs are formed when glucose, fructose or galactose covalently bond with proteins via the Maillard reaction (Ahmed, 2005). These first form a Schiff base, and then an Amadori product, followed by the irreversible formation of AGEs (Ulrich *et al.*, 2001). AGEs can cause intermolecular cross-linking of proteins such as myelin, which can lead to demyelination (Brownlee, 2001). They can also bind to receptors, such as the Receptor for AGE (RAGE), which is found in DRGs, peripheral nerves, Schwann cells and epidermal fibres (Bierhaus *et al.*, 2004; Toth *et al.*, 2008). RAGE activates nuclear factor kappa B (NF κ B), leading to an increased expression of cytokines. RAGE also activates NADPH oxidases, leading to the generation of ROS (Wautier *et al.*, 2001; Yan *et al.*, 1994) and so further increasing oxidative stress in the cell (Vincent *et al.*, 2004a).

1.2.1.5. PKC activation

Hyperglycaemia also leads to increased production of diacylglycerol (DAG), which activates various PKC isoforms including PKC- β and - δ , leading to changes in gene expression (summarised in Brownlee,

2005): eNOS is downregulated, and endothelin-1 and TGF- β are upregulated, which can lead to negative changes in blood flow. NF κ B is also upregulated, which causes increased expression of pro-inflammatory genes. PKC- β inhibitors have been shown to improve some of the vascular deficits, such as decreased NCV and reduced blood flow, that are observed in STZ animals (Ahlgren *et al.*, 1994; Ishii *et al.*, 1996; Nakamura *et al.*, 1999). PKC also plays a role in pain pathways and hyperalgesic priming.

1.2.1.6. Hexosamine pathway

Hyperglycaemia leads to excess fructose-6-phosphate being diverted from glycolysis to enter the hexosamine pathway, where it is converted to uridine diphosphate-N-acetyl glucosamine. This attaches to the serine and threonine residues of transcription factors, and can lead to altered gene expression, including upregulation of pro-inflammatory genes (Brownlee, 2001).

1.2.1.7. Poly(ADP) ribose polymerase

The PARP pathway is stimulated by free radicals and cleaves NAD⁺ (Edwards *et al.*, 2008). This reduction in NAD⁺ can lead to a slowing of NCV, small fibre neuropathy, and development of painful symptoms such as thermal and mechanical hyperalgesia and tactile hypersensitivity (Edwards *et al.*, 2008). It also affects glycolysis and mitochondrial respiration, which causes a decrease in energy production and can lead to cell death (Negi *et al.*, 2010).

1.2.1.8. Insulin and C-peptide

As well as the importance of hyperglycaemia in diabetic neuropathy, the deficiency of insulin and C-peptide is also important, especially in type 1 diabetes. This is supported by the Diabetes Control and Complications Trial (DCCT), which shows that tight glycaemic control is effective at

reducing the development of diabetic neuropathy by 60%, but not in preventing it entirely, suggesting that other factors must also be important (Sugimoto *et al.*, 2000). C-peptide links the A and B chains of proinsulin together, and is cleaved by proteases. C-peptide has been shown to: improve Na⁺/K⁺-ATPase activity and ameliorate the decrease in NCV, as well as helping to prevent paranodal swelling and axonal degeneration (Zhang *et al.*, 2001b); improve indices of sensory nerve function (by decreasing thermal thresholds) (Johansson *et al.*, 2000); and prevent thermal hyperalgesia in BB/Wor rats (Kamiya *et al.*, 2004). Both insulin and insulin-like growth factors (IGFs) are important neurotrophic factors involved in supporting peripheral neurones, and continuous subcutaneous infusion of IGF-2 was able to attenuate hyperalgesia in ZDF rats (Zhuang *et al.*, 1997). In STZ mice, insulin can decrease mortality and sensory loss, as well as improving neuropathic pain (Francis *et al.*, 2009), and in STZ rats insulin can improve NCV, as well as increasing the number of myelinated fibres in the sural nerve (Singhal *et al.*, 1997). The importance of changes in insulin to the development of DPNP is discussed further in Chapter 2.

1.3. Pain

According to the International Association for the Study of Pain (IASP), pain can be defined as “an unpleasant sensory and emotional experience associated with actual or potential tissue damage, or described in terms of such damage”. Nociception, however, is the neural process involving detection of tissue injury, and refers to the physical response to pain, but is not tied to the emotional experience.

1.3.1. Primary afferent nociceptors

Nociception occurs through nociceptors, whose existence was first proposed by Sherrington (1906) over a century ago, and these are defined by IASP as “a high-threshold sensory receptor of the peripheral somatosensory nervous system that is capable of transducing and encoding noxious stimuli”. Nociceptors can detect noxious heat or cold, and intense mechanical stimulation and noxious chemicals, but do not respond to innocuous stimuli (Burgess *et al.*, 1967) such as touch or warming/cooling. Fibres that innervate the body arise from cell bodies in the DRG (Julius *et al.*, 2001). Nociceptors can be divided into three different sub-types depending on their conduction velocity: small diameter unmyelinated C-fibres, slightly larger A δ -fibres which are thinly myelinated, and myelinated, large diameter (>10 μ m) A β -neurones (for review see Willis *et al.*, 2004).

A β -fibres are rapidly conducting and act as low threshold mechanoreceptors - responsible for proprioception and the detection of innocuous stimuli, but some A β -fibres do function as nociceptors (Djoughri *et al.*, 2004). This is important as it is A β -fibres that are responsible for the development of allodynia (pain elicited by an innocuous stimuli), and after even a small drop in their threshold these nociceptive A β -fibres become responsive to innocuous stimuli (Djoughri *et al.*, 2004). It is A δ - and C-fibres that are mainly responsible for the detection of noxious stimuli. A δ -fibres are thought to be responsible for

the rapid acute pain sensations of pricking and aching, whereas slowly conducting C-fibres produce a delayed, more diffuse, dull burning pain sensation (Willis *et al.*, 2004).

Two populations of A δ -fibres exist: Type I and Type II (Treede *et al.*, 1995). Type I respond to high heat ($\sim 53^{\circ}\text{C}$), mechanical and chemical stimuli. They have a delayed onset to heat stimuli, but they then become sensitised and their discharge rate increases during a prolonged heat stimulus (Treede *et al.*, 1995). They sensitise to burn and chemical injury, and are responsible for development of primary hyperalgesia (Meyer *et al.*, 2005). Type II, on the other hand, are mostly mechanically insensitive, and have a lower thermal threshold ($\sim 43^{\circ}\text{C}$) and a rapid and fast adapting response to heat and are thought to signal the first pain sensation from heat (Campbell *et al.*, 1983; Treede *et al.*, 1998; Treede *et al.*, 1995).

C-fibre nociceptors can be polymodal, as some respond to noxious mechanical stimuli, intense heat and cold, as well as noxious chemical stimuli such as acid or capsaicin (Meyer *et al.*, 2005). However some C-fibre nociceptors are mechanically sensitive but do not respond to heat, whereas others can be mechanically insensitive but respond to noxious heat (Schmidt *et al.*, 1995). Furthermore, some C-nociceptors may initially be insensitive to both mechanical and thermal stimuli, known as 'silent' or 'sleeping' nociceptors, but are activated by irritant substances such as mustard oil in experimental conditions (Schmidt *et al.*, 1995), or inflammatory mediators released during inflammation, and can then become sensitised to further mechanical and thermal stimuli.

C-fibres can be divided into two classes based on their neurochemical content: peptidergic and non-peptidergic. Peptidergic neurones release substance P (SP) and calcitonin gene related peptide (CGRP) and express TrkA (a high affinity receptor for nerve growth factor (NGF)), and are reliant on NGF for normal function (Averill *et al.*, 1995; Molliver *et al.*, 1997). Approximately 80% of DRG neurones require NGF for

survival during embryonic development, but in the first three weeks of development approximately half of these neurones stop expressing TrkA, and these are then classified as non-peptidergic neurones (Bennett *et al.*, 1996; Molliver *et al.*, 1997). These neurones express the growth factor receptor, GFR α , as well as the receptor tyrosine kinase, RET, and are reliant on glial-derived neurotrophic factor (GDNF) for survival (Bennett *et al.*, 1998). They also express the P2X3 receptor (an ionotropic ATP receptor), and can be labelled with the plant lectin IB₄ (Molliver *et al.*, 1997).

Neurones can be desensitised by repeated stimulation. Repeated activation of the receptors present on the neurones can lead to a downregulation of these receptors, or an exhaustion of mediators. Nociceptors can be desensitised by application of capsaicin, a Transient Receptor Potential Vanilloid 1 (TRPV1) ligand. TRPV1 is expressed exclusively by small-diameter neurones within sensory ganglia (Caterina *et al.*, 2001; Caterina *et al.*, 1997). Capsaicin causes firing of nociceptors and an initial period of enhanced sensitivity, which is followed by a refractory period in which responses to noxious stimuli, including capsaicin, are reduced (Jancso, 1992).

The predominant excitatory neurotransmitter in primary afferent fibres is glutamate, but a wide variety of substances are involved in the central transmission and modulation of nociceptive information. These can include other excitatory amino acids (EAAs), neuropeptides such as SP and CGRP, adenosine triphosphate (ATP) and NO, as well as prostaglandins (PGs) and neurotrophins such as NGF.

Glutamate provides rapid transmission of excitatory pronociceptive inputs in the spinal cord, and can act on a variety of specific receptors. These include the metabotropic glutamate receptors: mGluR1-8, which are GPCRs and the ionotropic glutamate receptors: α -amino-3-hydroxy-5-methyl-isoxazole (AMPA), N-methyl-D-aspartate (NMDA) and kainite,

which are coupled to cation channels (Coggeshall *et al.*, 1997; Mayer *et al.*, 2004).

1.3.2. The organisation of the dorsal horn of the spinal cord

Primary afferent nociceptors synapse with neurones in the dorsal horn of the spinal cord, and projection neurones convey the information to higher centres in the brain, where the information is processed.

In 1952, the division of the dorsal horn of the spinal cord of a cat into six laminae was first described (Rexed, 1952). Figure 1.2 shows how the laminae are organised; with I-VI comprising the dorsal horn, VII-IX making up the ventral horn, with lamina X surrounding the central canal. Laminae I and II make up the superficial dorsal horn (with lamina II further subdivided into an outer (Ilo) and inner part (Ili)), and these together with V, VI and X are the main targets for primary nociceptive afferents. Lamina I receives nociceptive input from A δ - and C-fibres, whereas laminae III and IV contain neurones responsive to the innocuous stimulation delivered by A β -fibres, and lamina V receives both non-noxious and noxious input from monosynaptic A δ - and A β -inputs and polysynaptic C-fibre inputs (Basbaum *et al.*, 2009).

Three different populations of neurones exist within the dorsal horn of the spinal cord, and these are defined as: non-nociceptive, nociceptive specific (NS) and wide dynamic range (WDR) neurones (Willis *et al.*, 2004). Non-nociceptive neurones are located in Ili, III and IV, and are activated by innocuous stimuli. NS neurones are typically silent and are specifically activated by noxious stimuli mediated by peripheral nociceptors, and are found in both superficial (lamina I and Ilo) and deep (lamina V, VI and X) layers. WDR neurones are able to encode the intensity of noxious stimuli, and have a graded response to stimuli that range from low-threshold to those in the noxious range. They respond to thermal, mechanical and chemical stimuli mediated by A β -

A δ - and C-fibres. These are also found in lamina IV, V, VI and X, as well as laminae I and II. WDR neurones also display a 'wind-up' response (Price *et al.*, 1978), where the response of the neurone to repeated electrical stimulation at a set intensity, with a frequency of >0.5Hz, will increase dramatically, with each stimulus evoking a larger response than the last, and firing continuing even after cessation of stimulation (Mendell, 1966; Schouenborg *et al.*, 1985). NMDA antagonists are able to markedly reduce this wind-up and post stimulus discharge, suggesting that high frequency stimulation of NMDA receptors contributes to wind up through alleviation of the Mg²⁺ block (Dickenson *et al.*, 1987).

Dorsal horn neurones can also be classified by their output destination. Propriospinal neurones allow communication between the ipsilateral and contralateral sides, as well as between different segments (Willis *et al.*, 2004), and they are also able to initiate descending inhibition. Projection neurones are responsible for transmitting nociceptive information supraspinally, and are mostly found in laminae I, V and VI, whereas interneurones are responsible for inter- and intra-laminar transfer, integration and modulation of nociceptive information (Millan, 1999).

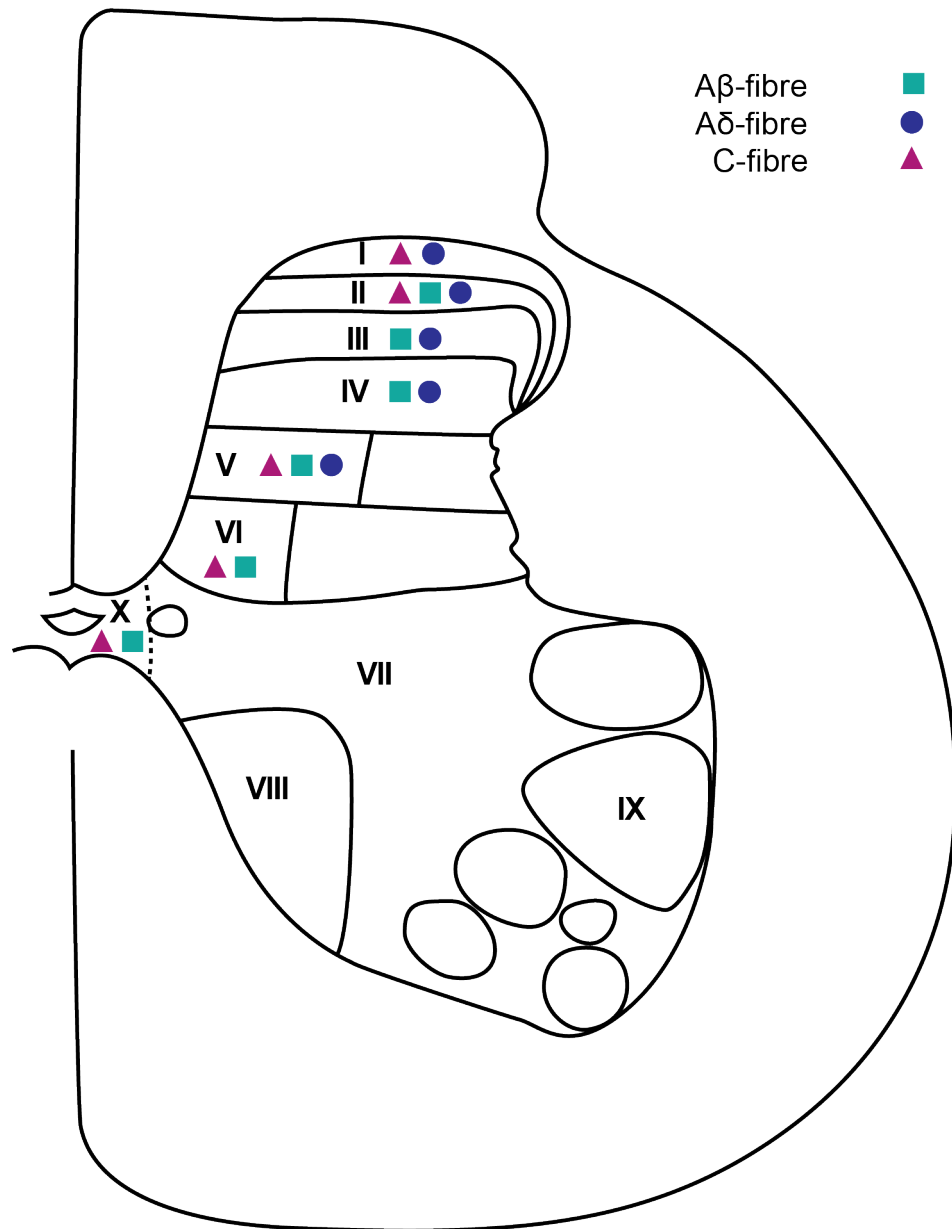


Figure 1.2. Organisation of the Rexed laminae in the grey matter of the spinal cord, adapted from (Rexed, 1952).

1.3.3. Ascending pain pathways

There are two types of ascending pathways: monosynaptic and polysynaptic. Monosynaptic pathways project directly from the dorsal horn to the higher brain centres and include the spinothalamic tract (STT), the spinomesencephalic tract, the spinoparabrachial tracts

(SPBT), and the spinothalamic tract. Polysynaptic pathways, on the other hand, include a relay station of second order neurones on their journey to higher brain centres, and these include the spinothalamic pathway, and the postsynaptic dorsal column (PSDC) pathway.

The STT transmits information to the thalamus, and it has projections originating from superficial lamina I and deeper laminae IV and V of the dorsal horn, and also laminae VII and VIII, with half of these originating in lamina I and the other 50% split evenly between the other laminae (Dostrovsky *et al.*, 2006). The STT neurones in each of the different regions of the spinal cord receive afferent input from different primary afferent fibres. Lamina I STT cells receive input from A δ - and C-fibres, and so respond to noxious stimulation including noxious heat and cold, as well as pinch and itch. STT cells in laminae IV-V receive input from A-fibres, and also respond to a variety of stimuli encoded by WDR cells. Finally, STT cells in laminae VII-VIII receive input from skin, and muscle and joint inputs (Dostrovsky *et al.*, 2005).

The SPBT projects to the medulla and brainstem, which is important for the integration of nociceptive information with homeostatic, arousal and autonomic processes, and this information is then conveyed to the forebrain (Tracey *et al.*, 2007).

The thalamus can be seen as the key relay site for nociceptive information as it receives nociceptive information from the STT, and is able to encode information about intensity and topographic localisation and then transfer it to cortical and subcortical structures (Millan, 2002). The thalamus has also been hypothesised to be important in chronic pain, and a decrease in thalamic blood flow contralateral to the site of pain has been observed in patients with cancer (Di Piero *et al.*, 1991), and a patient with a left medullary infarct (Garcia-Larrea *et al.*, 2006). In patients with diabetic neuropathy, a decrease in N-acetylaspartate (NAA), a marker of neuronal integrity, has been observed in the

thalamus, with a correlation between the reduction in NAA and the severity of the neuropathy (Selvarajah *et al.*, 2008). Another study found lower levels of NAA in the thalamus of diabetic patients, and that these were further decreased in those that experienced pain (Sorensen *et al.*, 2008).

1.3.4. Descending control of pain

The descending pain modulatory system, as seen in Figure 1.3, is an anatomical network that plays an important role in determining the experience of pain, as it can have facilitatory as well as inhibitory effects, and these can be altered depending on emotional or pathological state, and are affected by arousal and expectation (Fields *et al.*, 2005). It is thought that sustained facilitation of pain transmission may be an underlying mechanism of chronic pain (Porreca *et al.*, 2002).

The PAG-RVM (periaqueductal grey-rostral ventromedial medulla) system is important in the descending control of pain (Fields *et al.*, 1991). The PAG receives input from the dorsal horn and is connected to the hypothalamus and frontal cortex, as well as limbic forebrain structures such as the amygdala, and receives input from the spinomesencephalic tract (Millan, 2002). The PAG projects to the RVM, which is responsible for transmitting information to the dorsal horn of the spinal cord. The role of the PAG in descending control was first established in experiments where stimulation of, or microinjections into, the PAG resulted in behavioural analgesia to noxious stimuli (Mayer *et al.*, 1976; Mayer *et al.*, 1971), and similar effects have also been shown in humans (Mayer, 1984).

The RVM includes the nucleus raphe magnus and projects to both the superficial layer and the deep dorsal horn via the dorsolateral funiculus. It mediates bidirectional control as it can exert both facilitatory and inhibitory influences (Porreca *et al.*, 2002). Electrical stimulation of the RVM can be antinociceptive and cause decreased responses of dorsal

horn neurones (Fields *et al.*, 1991), but at a lower intensity it can also prove facilitatory (Zhuo *et al.*, 1990), and these effects can also be seen by microinjection with neurotransmitters (Zhuo *et al.*, 1992). If a lesion is created in the RVM or if it is inactivated with lidocaine, stimulation of the PAG no longer has an analgesic action, highlighting the importance of the RVM as a relay for the PAG to connect with the dorsal horn.

Within the RVM, there are three types of cells: ON, OFF and NEUTRAL (Fields *et al.*, 1991). OFF-cells are tonically active and pause their firing immediately before a withdrawal response as they are inhibited by noxious stimuli (Fields *et al.*, 1983; Porreca *et al.*, 2002). It is thought that it is the OFF-cells that cause descending inhibition of nociception, as decreases in OFF-cell firing have been shown to correlate with increased nociceptive transmission (Fields *et al.*, 1991), and activation of OFF-cells has been correlated with inhibition of nociceptive input (Fields *et al.*, 1999). ON-cells accelerate their firing before a withdrawal reflex occurs, and it has been postulated that ON-cells enable the RVM to have a facilitatory role in pain. Increased activity of ON-cells has been observed in models of hyperalgesia, and administering a drug in the RVM while monitoring neuronal activity, and also the threshold for a reflex to nociceptive stimulation, confirms that ON-cells are responsible for facilitation (for review see Heinricher *et al.*, 2009).

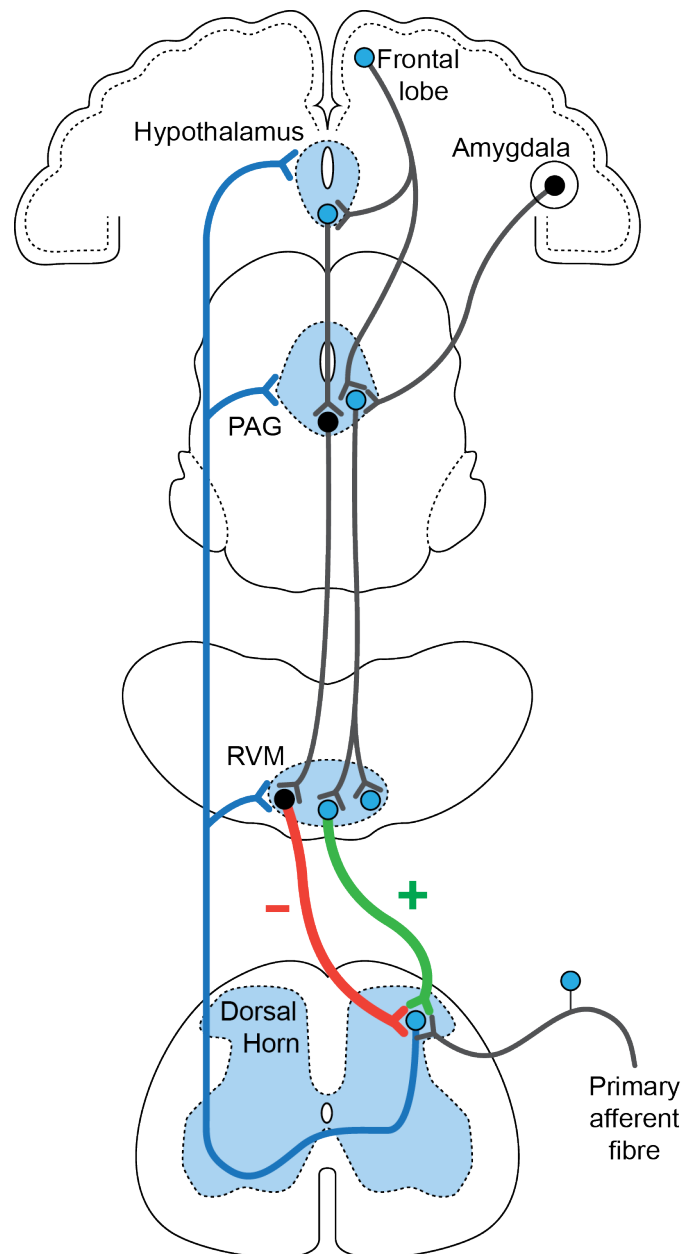


Figure 1.3. Descending control of pain. The modulatory pathway links higher brain centres to the PAG, which projects to the RVM, which exerts inhibitory (-) or facilitatory (+) effects on nociceptive processing. Adapted from (McMahon *et al.*, 2005).

1.3.5. Neuropathic pain

Neuropathic pain is defined by IASP as “pain caused by a lesion or disease of the somatosensory nervous system”, and is chronic and potentially irreversible. Acute pain, and the ability to detect noxious stimuli serves an important evolutionary role by acting as a warning

system to ensure an organism's survival and well being, through reflex withdrawal responses to a noxious stimuli and protective behaviour of a damaged tissue. Neuropathic pain, however, fulfils no physiological purpose and can be considered pathological (Millan, 1999).

It has been estimated that one in six of the general population are affected by neuropathic pain at some point, and symptoms include spontaneous pain, allodynia, hyperalgesia (heightened sensation of pain) and abnormal sensations such as dysesthesias and paresthesias (Campbell *et al.*, 2006). As well as being present in diabetic neuropathy, it can also be caused by nerve injury, autoimmune disease, infections such as shingles, and neurotoxicity (e.g. by chemotherapy agents) (Zimmermann, 2001).

1.3.6. Origins of pain in diabetes

Diabetic neuropathy is a progressive disease with pain experienced due to a wide variety of causes. Painful symptoms usually occur at the onset of diabetic neuropathy, although there tends to be no correlation between the intensity of pain symptoms and the extent of the sensory deficit, and can be influenced by the patient's psychological and emotional state (Guastella *et al.*, 2009).

Oxidative stress and the other processes described in section 1.2.1, lead to neuronal death. The loss of small A δ - and C-fibres leads to changes in pain sensation and temperature perception, whereas the loss of larger A β -fibres can cause a loss of vibration sensation, and tactile discrimination (Guastella *et al.*, 2009). Along with sensory loss, destruction of C-fibres also causes painful symptoms such as burning, as well as paresthesias and dysesthesias (Guastella *et al.*, 2009). As the disease progresses further and there is greater neuronal loss, chronic pain can still be experienced, even without peripheral stimulation, due to the development of central sensitisation, but eventually the sensory deficits overtake and there is sensory loss.

1.3.6.1. Involvement of primary afferent fibres

When nerves in diabetic patients become injured, this leads to the accumulation of sodium channels along portions of the injured axons. In the STZ model an increase in the expression of the TTX-S sodium channel, Na_v1.7, has been observed, along with a reduction in the expression of the TTX-R sodium channel, Na_v1.8, which is preferentially expressed in small DRG neurones (Hong *et al.*, 2004). An increase in Na_v1.3, and Na_v1.6 has also been observed, which would be expected to lead to a lowered firing threshold (Craner *et al.*, 2002). Despite a decrease in Na_v1.8, there is an increase in its phosphorylation, which results in a modification of the channel properties (Hong *et al.*, 2004), and post-translational modification of Na_v1.8 by methylglyoxal is associated with enhanced sensory neurone excitability (Bierhaus *et al.*, 2012). These changes in sodium channels result in an increase in TTX-S and TTX-R sodium currents in small DRG neurones, which correlates with the development of hyperalgesia and mechanical hypersensitivity, and persists in the long term (Hirade *et al.*, 1999; Hong *et al.*, 2004). In large A-fibre DRG neurones an increase in TTX-S Na_v1.2, Na_v1.3 and Na_v1.7, as well as TTX-R Na_v1.9 has been observed, resulting in an increase in sodium currents, and a shift of the voltage-dependent activation kinetics in the hyperpolarising direction (Craner *et al.*, 2002; Hong *et al.*, 2006). Normalisation of Na_v1.7 levels in STZ rats was able to reduce pain related behaviours (Chattopadhyay *et al.*, 2012). Increased nodal persistent sodium currents have been associated with neuropathic pain in humans with diabetic neuropathy (Misawa *et al.*, 2009).

The changes in these channels facilitate the generation of ectopic electrical impulses and hyperexcitability (Devor, 2005). In the STZ rat model, nociceptive fibres have been shown to fire in an exaggerated spontaneous manner (see Chapter 4 for more detail) (Ahlgren *et al.*, 1992; Chen *et al.*, 2001), and increased excitability of regenerating nerve fibres may also lead to aberrant discharge (Brown *et al.*, 1976).

Ectopic discharges are also seen in models of nerve damage such as the chronic constriction injury (CCI) model, and spinal nerve injury at both the level of peripheral neurones (Tal *et al.*, 1996; Wall *et al.*, 1983) as well as DRGs (Kajander *et al.*, 1992; Liu *et al.*, 2000; Study *et al.*, 1996; Xie *et al.*, 1995). Spontaneous firing has been shown to cause a reduction in thermal, mechanical and chemical thresholds (Howe *et al.*, 1977), and nerve injury can also lead to spontaneous discharges in neighbouring uninjured axons, as well as the injured neurones themselves (Ali *et al.*, 1999). Ectopic discharges can lead to spontaneous pain and paresthesias (Devor, 2006), as well as contributing to the development and maintenance of central sensitisation (discussed later). Transection of, or anaesthetising the dorsal roots in the spinal nerve ligation (SNL) model, and therefore blocking ectopic discharges, reduced behavioural signs of neuropathic pain (Yoon *et al.*, 1996).

As described previously, there is increased activation of PKC in diabetic neuropathy, and PKC also plays a role in nociceptive processing in primary afferents and hyperalgesic priming (for review see Velazquez *et al.*, 2007). PKC activation can cause depolarisation of unmyelinated C-fibres by increasing sodium conductance (Dray *et al.*, 1988; Rang *et al.*, 1988), and enhance currents caused by noxious thermal stimuli (Cesare *et al.*, 1996). PKC inhibitors have been shown to block this depolarisation (Burgess *et al.*, 1989; McGuirk *et al.*, 1992).

In rats, PKC activation is able to increase capsaicin induced TRPV1 currents by increasing depolarisation of TRPV1 (Zhou *et al.*, 2001b), which allows the receptor to conduct at lower, non-noxious temperatures, and also at physiologically relevant pHs (Crandall *et al.*, 2002), while PKC inhibitors decrease these currents (Zhou *et al.*, 2001b). Inflammatory mediators, such as bradykinin, galanin and TNF α enhance the activity of TRPV1 through PKC-dependent pathways, which may play a role in hyperalgesic priming (see references in Velazquez *et al.*, 2007). PKC inhibitors can decrease thermal

hyperalgesia and C-fibre hyperexcitability in STZ rats (Ahlgren *et al.*, 1994). As well as in the periphery, PKC can also modulate neurotransmission at the level of the spinal cord through increasing excitatory neurotransmission and decreasing inhibitory tone.

1.3.6.2. Involvement of spinal sensitisation

Sensitisation can occur at both the peripheral and central level, and is important in the development of pain in diabetic neuropathy. Peripheral sensitisation involves a reduced threshold for activation and an amplification in the responsiveness of primary afferent nociceptors, and occurs when these neurones are exposed to inflammatory mediators, which are released by damaged tissues (Dickenson *et al.*, 2002). Central sensitisation, which was first proposed thirty years ago (Woolf, 1983), develops following a primary afferent barrage, which leads to sustained activation of WDR neurones in the spinal cord. These neurones become sensitised, and at this point input from primary afferent neurones is no longer required to elicit responses from these neurones. To demonstrate this, pre-treatment with a local anaesthetic can prevent the cutaneous hyperalgesia that develops following intradermal capsaicin administration, but if the anaesthetic is only given after injection of capsaicin, there is no effect on hyperalgesia (LaMotte *et al.*, 1991), suggesting that peripheral inputs are required for the onset of hyperalgesia, but are not required to maintain it.

Central sensitisation is characterised by an increased responsiveness of nociceptive neurones in the central nervous system (CNS) to both normal and subthreshold afferent input. The recruitment of low-threshold A β -fibres means that their input is able to drive nociceptive pathways, resulting in a reduction in the threshold for activation. Central sensitisation also results in an increase in spontaneous activity, as well as an enlargement of peripheral receptive fields (Coderre *et al.*, 1997). These effects are due to increases in membrane excitability, synaptic facilitation, and decreases in inhibitory transmission (for references see

Latremoliere *et al.*, 2009). The result of central sensitisation is that pain is no longer coupled to the intensity or duration of a peripheral stimulus, and painful sensations can occur in the absence of noxious stimuli. There are a number of mechanisms underlying the development of central sensitisation, and a variety of receptor systems are involved.

GABAergic interneurons are important in both pre- and post-synaptic inhibition of responses of dorsal horn neurons. Blocking these interneurons with γ -Aminobutyric acid (GABA)_{A/B} antagonists causes mechanical hypersensitivity and thermal hyperalgesia in naive rats, whereas GABA_{A/B} agonists were able to abolish the mechanical hypersensitivity and thermal hyperalgesia seen in SNL rats (Malan *et al.*, 2002). Therefore the loss of inhibitory GABAergic interneurons causes disinhibition of neurons in the dorsal horn, leading to increased neurotransmission, which can contribute to central sensitisation.

When nerves are injured, this causes a phenotypic switch where damaged A-fibres begin to synthesise excitatory neurotransmitters that are normally associated with C-fibres, such as CGRP and SP (Miki *et al.*, 1998; Noguchi *et al.*, 1995). The release of substance P causes activation of post-synaptic NK1 receptors, which leads to downstream activation of intracellular signalling pathways such as mitogen-activated protein kinase (MAPK) and extracellular-signal related kinase (ERK). These pathways lead to activation of NMDA receptors, along with PKC, which potentiates these NMDA-currents through alleviation of the voltage dependent Mg²⁺ block (Chen *et al.*, 1992). Activation of NMDA receptors results in synaptic potentiation (Woolf *et al.*, 1991) where nociceptive stimuli produce larger postsynaptic potentials, resulting in hyperexcitability of dorsal horn neurons. NMDA receptor antagonists are able to reduce the facilitation of these responses (Woolf *et al.*, 1991), and NMDA receptor phosphorylation in the spinal cord coincides with the development of mechanical hypersensitivity in the SNL model (Gao *et al.*, 2005).

Upregulation of AMPA and NMDA receptors in the spinal cord has also been implicated in the development of central sensitisation, and the increase in AMPA receptor expression coincided with the development of mechanical and thermal hyperalgesia in the partial nerve ligation (PNL) model (Harris *et al.*, 1996). mRNA of AMPA and NMDA subunits is upregulated in the STZ model (Tomiyama *et al.*, 2005), and hyperalgesia and mechanical hypersensitivity can be prevented in this model by administration of AMPA- and NMDA-receptor antagonists (Begon *et al.*, 2000; Calcutt *et al.*, 1997; Malcangio *et al.*, 1998), demonstrating the important role these receptors play in central sensitisation.

Neurochemical changes in the spinal cord, such as the release of excitatory amino acids, cytokines and reactive oxygen species cause glial activation, which also plays an important role in the development of neuropathic pain and is discussed further in Chapter 3.

1.3.6.3. Involvement of higher centres

As well as the involvement of primary afferent fibres and spinal cord neurones, it has also been hypothesised that higher order pain signalling neurones are involved in the generation and/or amplification of pain signals. Fischer *et al.* (2009) made recordings from neurones in the thalamic ventral posterolateral nucleus, which relays sensory input from the periphery. Increases in spontaneous activity, evoked activity to both innocuous and noxious stimuli, as well as enlarged receptive fields were reported in the STZ rat model, and this spontaneous activity was generated even in the absence of signals from primary sensory neurones (Fischer *et al.*, 2009). STT neurones also display increased spontaneous activity, enlarged receptive fields and increased responses to mechanical stimuli (brush and pinch), which may be due to the aberrant activity that is observed in the afferent nerves in the STZ model (Chen *et al.*, 2002a).

There is also an increase in serotonergic neurones in the RVM and noradrenergic neurones in the A5 noradrenergic cell group in STZ rats, as well as increased levels of serotonin and noradrenaline at the spinal cord and increased c-Fos expression in the ventrolateral PAG (VLPAG) (Morgado *et al.*, 2011b). As the PAG is responsible for relaying messages from the higher brain centres, such as the amygdala and anterior cingulate cortex, via the RVM (Heinricher *et al.*, 2009), this suggests that in diabetes there may be impairments to descending pain modulation. The high levels of noradrenaline increase the release of GABA, which is increased in the STZ model (Malmberg *et al.*, 2006; Morgado *et al.*, 2008). This increase in GABA, unexpectedly, has an excitatory effect in diabetes, due to a decrease in the expression of the potassium chloride co-transporter 2 (KCC2) (Jolivald *et al.*, 2008; Morgado *et al.*, 2008). This leads to an increase in intracellular chloride concentrations, and when GABA binds to GABA_A receptors, there is an efflux of chloride creating a depolarising event (Coull *et al.*, 2003). This, in combination with increased serotonergic activity, results in enhanced activity of spinal neurones, and therefore increased facilitation.

A further study went on to demonstrate that Fos expression (a marker of neuronal activation) increases over time in diabetes, suggesting that spontaneous neuronal activity increases as the disease progresses (Morgado *et al.*, 2011a). The PAG, which has facilitatory as well as inhibitory effects on pain modulation (Heinricher *et al.*, 2009; Vanegas *et al.*, 2004), shows a universal increase in Fos expression at 4 weeks, but at 10 weeks this was limited to only the VLPAG. c-Fos expression is also increased in both superficial and deeper laminae of the dorsal horn in STZ rats (Morgado *et al.*, 2007).

A recent study has shown that in STZ rats there is a decrease in descending pain inhibition as evidenced by a decrease in the spontaneous activity of OFF-cells, as well as the absolute number, and this is coupled with an increase in spontaneous activity of ON-cells

indicating an increase in descending pain facilitation from the RVM (Silva *et al.*, 2013).

Increased C-fibre evoked wind-up is observed in the STZ mouse model (Kimura *et al.*, 2005), indicating the enhanced excitability of spinal cord neurones. While the conditioning stimulus generates both inhibitory and excitatory influences in normal animals, the decrease in μ -opioid receptors in the dorsal horn of the spinal cord in diabetes (Chen *et al.*, 2002b) means that there is less recruitment of the inhibitory system, leading to enhanced wind-up (Kimura *et al.*, 2005).

1.4. Aims of the thesis

The aim of this thesis was to characterise pain responses in the HFD/STZ model and to explore some of the peripheral and spinal mechanisms associated with the changes in somatosensory processing. The effectiveness of a variety of drugs in alleviating/preventing neuropathic pain was also investigated in this model.

The objectives were to:

- 1, study the development of mechanical hypersensitivity in the HFD/STZ model.
- 2, investigate underlying mechanisms by examining indices of neurodegeneration in the DRG and spinal cord, and the potential contribution of microglia and astrocytes in the spinal cord.
- 3, characterise the electrically and mechanically-evoked responses of wide dynamic range neurones in the dorsal horn of the spinal cord.
- 4, explore the possibility of using currently prescribed antidiabetics versus existing and novel analgesics to alleviate pain responses in this model.

Chapter 2.

Assessment of the HFD/STZ diabetic model

2.1. Introduction

2.1.1. The STZ model of diabetes

As discussed in Chapter 1, there is an array of animal models of diabetes. One of the most frequently used models is the STZ model, as it is quick, easy and cheap to set up.

Streptozotocin (2-deoxy-2-(3-(methyl-3-nitrosoureido)-D-glucopyranose) is a toxin which selectively destroys pancreatic β -cells, and is derived from *Streptomyces achromogenes*. It enters through the glucose transporter, GLUT2, and causes alkylation of DNA (Szkudelski, 2001). Other effects include formation of superoxide radicals, which cause the release of toxic amounts of nitric oxide, which also damages DNA (Szkudelski, 2001). Alkylation of DNA leads to overstimulation of PARP, which causes a decrease in NAD⁺, and subsequently ATP, leading to the necrosis of β -cells (Lenzen, 2008). It is this activation of PARP that is considered one of the main reasons for the diabetogenicity of STZ (Szkudelski, 2001). Depletion of NAD⁺ also results in the inhibition of insulin synthesis and secretion (Lenzen, 2008).

A wide range of doses of STZ are used in the induction of diabetes in rats, and these vary from multiple low doses (20mgkg⁻¹) (Skalska *et al.*, 2010; Taliyan *et al.*, 2012; Zhang *et al.*, 2008), to high doses of up to 75-90mgkg⁻¹ (Aubel *et al.*, 2004; Lindner *et al.*, 2006; Nadig *et al.*, 2012), with the majority ranging somewhere between 45-70mgkg⁻¹.

Administration of STZ leads to hyperglycaemia and hypoinsulinaemia, which is evident in the first few days after injection, and is maintained at a similar level as the model develops. Other symptoms that are typically associated with STZ administration are stunted growth, polydipsia, polyuria and polyphagia (Chatzigeorgiou *et al.*, 2009).

2.1.2. Neuropathy in the STZ model

The development of changes in mechanical and thermal thresholds in response to nociceptive and non-nociceptive stimuli has been extensively studied in the STZ model. A decrease in mechanical withdrawal thresholds is first seen 1-2 weeks after injection with STZ, and reduces further as the model progresses (Ahlgren *et al.*, 1993; Calcutt *et al.*, 1996; Courteix *et al.*, 1993; Dobretsov *et al.*, 2003; Fuchs *et al.*, 2010; Xu *et al.*, 2011). There are conflicting reports about whether thermal hyperalgesia (Courteix *et al.*, 1993; Fuchs *et al.*, 2010; Ulugol *et al.*, 2004) or hypoalgesia (Bianchi *et al.*, 2012; Fox *et al.*, 1999; Malcangio *et al.*, 1998; Piriz *et al.*, 2009) is seen in the STZ model. Recent reports have suggested that STZ causes thermal hyperalgesia in the early stages, which is followed by thermal hypoalgesia after approximately six weeks (Bishnoi *et al.*, 2011; Pabbidi *et al.*, 2008a; Pabbidi *et al.*, 2008b), similar to what is seen clinically (Obrosova, 2009a).

A variety of drugs are effective at reversing the manifestation of pain behaviours in the STZ model. Four weeks after STZ administration, high single doses of morphine (20mgkg⁻¹) and baclofen (16mgkg⁻¹) were able to reverse mechanical hyperalgesia in the paw pressure test, and chronic treatment (for 6 days) with MK-801 (0.1mgkg⁻¹) completely reversed mechanical hyperalgesia (Malcangio *et al.*, 1998). Another study looked at the acute effect of five drugs on mechanical withdrawal thresholds at 3 and 7 weeks after STZ injection (Yamamoto *et al.*, 2009). Pregabalin (30mgkg⁻¹) was the most effective and reversed the decrease in withdrawal thresholds at both timepoints. Mexiletine (100mgkg⁻¹) and morphine (10mgkg⁻¹), however, were only able to partially reverse the decrease in withdrawal thresholds at 3 weeks, and were ineffective by 7 weeks. Other studies have also shown hyporesponsiveness to morphine, with its antinociceptive abilities abolished 12 weeks after STZ administration (Nielsen *et al.*, 2007). Amitriptyline (3mgkg⁻¹) was only able to partially alleviate mechanical

hypersensitivity at 7 weeks, and diclofenac (10mgkg^{-1}) was ineffective at all timepoints.

2.1.3. Criticisms of the STZ model

The STZ model has been criticised as it can leave animals in poor condition. Fox *et al.* (1999) expressed doubts as to its validity as a model of diabetic neuropathy, as the animals suffered from diarrhoea, polyuria, enlarged and distended bladders, and reduced growth. These rats were assessed to be chronically ill, as they appeared very lethargic and displayed no exploratory behaviour, and 24% were removed before the end of the four week study. They hypothesised that the behavioural results obtained might not be valid as they could be caused by general ill-health rather than neuropathy itself. The body condition score of rats has also been correlated with withdrawal thresholds (Hoybergs *et al.*, 2008), emphasising the importance of monitoring rats for weight loss and general body condition, to ensure that any behavioural data obtained cannot be attributed solely to their poor condition.

2.1.4. Alternatives to the STZ model

While the STZ model has been widely used, it is a model of type 1 diabetes, but only a small proportion of cases of diabetes are accounted for by type 1 diabetes, with 90-95% of sufferers having type 2 diabetes (Cheng, 2005). There are several alternatives to the single high-dose of STZ that can produce a model which more closely resembles type 2 diabetes:

Nicotinamide, an antioxidant, can be administered 15 minutes before STZ, which leads to moderate hyperglycaemia, glucose intolerance and reduced insulin stores (Masiello *et al.*, 1998). NAD is able to scavenge free radicals, as well as causing inhibition of PARP, and increasing levels of NAD⁺, and this helps to reduce the amount of damage that is

caused to β -cells (Szkudelski, 2012). This model can therefore be considered more typical of type 2 diabetes, and doses of each compound can be adjusted to alter the severity of diabetes that is produced. This model is also quite stable and so can be used for longer-term studies looking at different diabetic complications (Szkudelski, 2012).

Another alternative is to give an intraperitoneal (i.p.) injection of STZ to neonatal rats, which leads to only partial destruction of the β -cell population. This leads to moderate hyperglycaemia which increases with age, abnormal glucose intolerance and an initial increase in insulin levels as the rat attempts to maintain glucose homeostasis (Takada *et al.*, 2007). However, by 12 weeks of age, the rats show a decrease in pancreatic insulin content, indicating that the β -cells have become exhausted, resulting in overt hyperglycaemia. These features are similar to the natural course of type 2 diabetes in humans. While those two models are both valid alternatives to the STZ model, they do not take into account the risk factors which often contribute to the development of type 2 diabetes such as a poor diet, and a sedentary lifestyle, which both contribute to obesity, and can lead to diabetes (Cheng, 2005).

2.1.5. The HFD/STZ model

In 1998, Luo *et al.* reported an alternative to the high dose STZ model. A low dose of STZ in combination with either a high fat or high sugar diet was shown to induce diabetes in mice, with a disease progression more similar to that of type 2 diabetes in humans. The diet caused the mice to become insulin resistant, resulting in a compensatory increase in the production of insulin. This is similar to that of the prediabetes state which involves impaired fasting glucose and impaired glucose tolerance, which is associated with insulin resistance (Bock *et al.*, 2006). It was only following injection of STZ, when a proportion of the β -cells were destroyed, leading to a decrease in the production of insulin,

that the mice developed hyperglycaemia. Importantly, the same dose of STZ did not cause any changes in the mice that were fed a normal diet (Luo *et al.*, 1998).

In 2005, this model was replicated in rats (Srinivasan *et al.* (2005), which were fed a high fat diet (58% calories as fat) for two weeks, which led to increased body weight, blood plasma glucose, insulin, triglycerides and total cholesterol, and a decrease in the glucose disappearance rate during an insulin-glucose tolerance test, indicating that the rats were becoming insulin resistant. STZ injection (35mgkg^{-1}) in the HFD rats resulted in frank hyperglycaemia, but only decreased insulin to what would be considered a normal level. They proposed that this model was more clinically relevant, and also had the benefit of being much cheaper than genetic models of type 2 diabetes. Further studies investigated the influence of the dose of STZ, in combination with a high fat diet, on this model of diabetes (Zhang *et al.*, 2008). STZ at 45mgkg^{-1} , given as a single dose, was shown to result in diabetes more than 50% of the time, compared to $25\text{-}35\text{mgkg}^{-1}$ STZ. They also found that only the higher dose was able to produce a blood glucose concentration of over 10mM (24.5mM). This finding, and data from my own pilot experiments, prompted me to select 45mgkg^{-1} STZ for the studies described in this thesis.

2.1.6. HFD/STZ: a model of diabetic neuropathy?

While the HFD/STZ model has been shown to produce all the metabolic changes we would expect – polyuria, polydipsia, stunted growth rate, and related changes in glucose and insulin, the development of mechanical hypersensitivity has not yet been widely investigated. Of the handful of groups who have assessed altered nociception in the HFD/STZ model, results have not always been in agreement, and the length of time the high fat diet is fed before injection, the percentage of fat in the diet, and the dose of STZ have varied between groups. Davidson *et al.* (2011b; 2012) fed a high fat diet for 8 weeks followed by

30mgkg⁻¹ of STZ and in the Hargreaves test they observed a hypoalgesic response, with an increase in withdrawal latency from the thermal stimulus, which was confirmed by Yang *et al.* (2011) who gave 4 weeks of a high fat and high sucrose diet, followed by 35mgkg⁻¹ of STZ. Conversely, Kumar *et al.* (2009) fed rats a HFD for 2 weeks and administered 35mgkg⁻¹ of STZ, but saw a hyperalgesic response in the tail-immersion and hot-plate test. Similar discrepancies in the findings of thermal nociception have also been reported in the STZ model, where there are reports of both thermal hypoalgesia and hyperalgesia.

2.1.7. Aim of the study

The aim of this study was to investigate the effects of a HFD in combination with STZ on metabolic parameters and mechanical and thermal sensitivity, to determine whether the metabolic changes produced in this model resulted in the development of hypersensitivity.

2.2. Methods

2.2.1. Animals

All experiments were carried out under Personal Home Office Licence 40/9559 and Project Home Office Licence 40/3124, in accordance with the UK Home Office Animals (Scientific Procedures) Act 1986 and IASP guidelines. 18 male Sprague-Dawley rats (200-250g), obtained from Charles River (Kent, U.K.), were individually housed on a normal light cycle (lights on: 07:00 - 19:00) with free access to the high fat diet (60% fat by caloric content; D12492 diet; Research Diets, New Jersey, USA) and tap water at all times. Food and water intake, and body weight were monitored at least twice weekly.

2.2.2. The HFD/STZ model of diabetes

After three weeks consumption of the high fat diet, the rats were divided into two stratified groups on the basis of body weight and mechanical withdrawal thresholds, and they received an i.p. injection of STZ (45mgkg^{-1} , at 3mlkg^{-1} ; $n=12$) or citric acid buffer ($n=6$). STZ (batch/lot number 019K1022) was purchased from Sigma Aldrich (Poole, UK), and dissolved in 0.05M citric acid, pH 4.5.

A blood sample was drawn from the tail vein, and a minimum plasma glucose concentration of 15mM was required to confirm diabetes. Any HFD/STZ rat with a plasma glucose concentration lower than this was excluded from any further analysis.

2.2.3. Development of the HFD/STZ model

In a pilot study, a dose of STZ (55mgkg^{-1}) caused two spontaneous deaths, and several rats that were in poor health throughout the study, leading to a lower dose of 45mgkg^{-1} being chosen for this study. This dose produced all of the same metabolic symptoms that were seen

previously, but left the rats in better health. An even lower dose has been shown to result in a much smaller percentage of rats going on to develop diabetes (Zhang *et al.*, 2008), whereas in this study all 12 of the rats injected with STZ had plasma glucose levels of >15mM.

As was established in the introduction, it is of utmost importance that rats are regularly monitored to ensure that any behavioural data obtained cannot be explained away as a side effect of their poor condition, and animals seen to be in very ill-health must not be allowed to continue in a study. Therefore in this, and future studies, a set of strict guidelines was followed to decide if/when to remove a rat from a study. It was decided that rats showing a combination of the following symptoms must be humanely killed:

- Lethargy.
- Lack of response to stimuli such as handling.
- Partially closed eyes.
- Significant lack of grooming.
- Huddling in corners, “fluffed up” appearance, sitting hunched over, cold.
- Weight loss of greater than 25% of their initial bodyweight.

Rats were therefore closely monitored at all times, and body weight was measured and general condition was observed at least once a day. Rats that exhibited weight loss of 18% or greater (irrespective of any other symptoms) in the first week after dosing with STZ, were drawn to the attention of the NACWO, and their continuance in the study was carefully considered. Any rats exhibiting weight loss of between 20% and 25% of their initial bodyweight with no other symptoms or loss of condition were allowed to remain on the study, but were checked twice daily.

2.2.4. Behavioural testing

von Frey testing was carried out to assess the sensitivity of the hindpaws to mechanical stimulation using calibrated von Frey hairs of bending forces 1, 1.4, 2, 4, 6, 8, 10 and 15g (Semmes-Weinstein monofilaments, Linton Instrumentation, Norfolk, UK). The day before behavioural testing commenced, the rats were acclimatised to the apparatus by placing them in the testing equipment (transparent Perspex boxes with a wire mesh floor; Medical Engineering Unit, University of Nottingham, UK) and leaving them to settle for half an hour, and then applying a 10g von Frey hair five times to each hindpaw. On the day of testing, the rats were allowed to habituate for 30 minutes before testing began. A modified form of the up-down method (Dixon, 1980) was utilised to determine the mechanical withdrawal threshold. von Frey filaments were applied to the plantar surface of each hindpaw in turn for five seconds, with an interval of >3 seconds between repetitions. Stimulations were performed three times, or until a withdrawal response was elicited. The 6g von Frey hair was applied first: if there was a response, the next lowest von Frey hair was applied; and if there was no response, the next highest von Frey hair was applied. This was repeated until there was either no response at the highest weight (15g) or the lowest force that elicited a withdrawal response was found (Guasti *et al.*, 2009). All behavioural testing was carried out between 08.00-12.00. As diabetic neuropathy produces a bilateral injury, the average withdrawal response of both hindpaws was calculated.

The Hargreaves test was performed to evaluate thermal sensitivity (Hargreaves *et al.*, 1988). Rats were placed in a clear Plexiglass chamber on an elevated platform and allowed to habituate for 30 minutes. A radiant heat source was positioned underneath the hindpaw, and the time from initiation of radiant heat until paw withdrawal was measured automatically. There was a cut off of 20 seconds to avoid tissue damage. Each paw was tested five times, with at least 5 minutes

between each trial to avoid sensitisation, and the mean withdrawal latency was calculated.

All behavioural testing was performed blind to the treatment groups.

2.2.5. Blood sampling

After a four hour fast, 100µl of blood was taken from the lateral tail vein by vein stab and collected into lithium heparinised tubes (Sarstedt Microvette CB300) and plasma was separated by centrifugation (2,400 g for 5 min at 4°C) to produce a single aliquot of plasma (approximately 50µl) which was frozen (-80°C) and subsequently assayed for glucose (Thermoelectron infinity glucose reagent; Microgenics, UK) and insulin (Mercodia rat insulin ELISA; Diagenics, Milton Keynes, UK).

2.2.6. Oral glucose tolerance test (OGTT)

An oral glucose tolerance test was performed at day 120. Rats were deprived of food overnight and the following day the lateral tail vein was cannulated, and a baseline blood sample (120µl) was taken immediately before the glucose load (2g/kg p.o.), along with an aliquot of whole blood (25µl) for HbA1c determination (direct enzymatic HbA1c assay; Diazyme, Germany) into an EDTA vial (Sarstedt Microvette CB300K2E). Further blood samples were taken 15, 30, 45, 60, 120 and 180 minutes post glucose administration and plasma was separated by centrifugation as described above.

2.2.7. Total pancreatic insulin content

The pancreas (n=1 for HFD/Veh, n=3 for HFD/STZ) was removed, weighed and homogenized in acid ethanol (0.18 mol/l in 70%[vol./vol.] ethanol) for subsequent determination of total pancreatic insulin content (Mercodia rat insulin ELISA).

2.2.8. Statistics

Statistical advice was sought from a statistician at RenaSci.

Analysis of body weight, food intake and water intake was by an analysis of covariance (ANCOVA) with Tukey's post-hoc test, with the average of day -7 to 0 as the covariate. Analysis of plasma glucose, plasma insulin, the OGTT, HbA1c and mechanical withdrawal thresholds was by a Mann Whitney test. Additional analysis of the OGTT was by a Friedman test with Dunn's multiple comparison post-hoc test. Analysis of the Hargreaves test was by an unpaired t-test.

In all analyses, a p value of less than 0.05 was considered statistically significant.

2.3. Results

2.3.1. Effects of HFD/STZ on body weight, and food and water intake

Prior to injection with STZ, both groups of HFD rats exhibited a steady weight gain of ~53g per week (Figure 2.1A). The day after injection with STZ there was a dip in the body weight of the HFD/STZ group, and after this they exhibited a significantly stunted growth rate in comparison to the HFD/Veh group ($p < 0.001$), with a difference of ~260g between the two groups at the end of the study ($521 \pm 30\text{g}$ vs. $782 \pm 52\text{g}$ at day 120). The HFD/STZ group exhibited a fourfold increase in daily water consumption ($22.0 \pm 0.8\text{g}$ vs. $88.3 \pm 6.2\text{g}$ at 120 days post STZ), compared to the HFD/Veh controls ($p < 0.001$) and this was evident from the first days after injection with STZ (Figure 2.1B). The HFD/STZ group also exhibited a small increase in food consumption, compared to the HFD/Veh group (Figure 2.1C), although this was only significant at certain points throughout the study ($p < 0.05$).

2.3.2. Effects of HFD/STZ on metabolic parameters

The present study also demonstrated that the HFD/STZ model caused changes in metabolic parameters that are indicative of diabetes. At day -5, prior to injection of STZ, the mean plasma glucose concentration was $8.5 \pm 0.4\text{mM}$ in the HFD/Veh group and $8.4 \pm 0.5\text{mM}$ in the HFD/STZ group. Following injection with STZ this remained stable in the HFD/Veh group at $8.9 \pm 0.4\text{mM}$, whereas it increased threefold to $24.0 \pm 0.9\text{mM}$ ($p < 0.001$) in the HFD/STZ group (Figure 2.2A). In the HFD/STZ group, plasma insulin concentration decreased ($1.05 \pm 0.17\text{ngml}^{-1}$) whereas there was a slight increase in the HFD/Veh group ($3.02 \pm 0.49\text{ngml}^{-1}$) compared to levels prior to STZ injection ($2.41 \pm 0.63\text{ngml}^{-1}$ in the HFD/Veh group and $2.01 \pm 0.33\text{ngml}^{-1}$ in the HFD/STZ group at day -5; Figure 2.2B; $p < 0.001$). These values were maintained throughout the rest of the study.

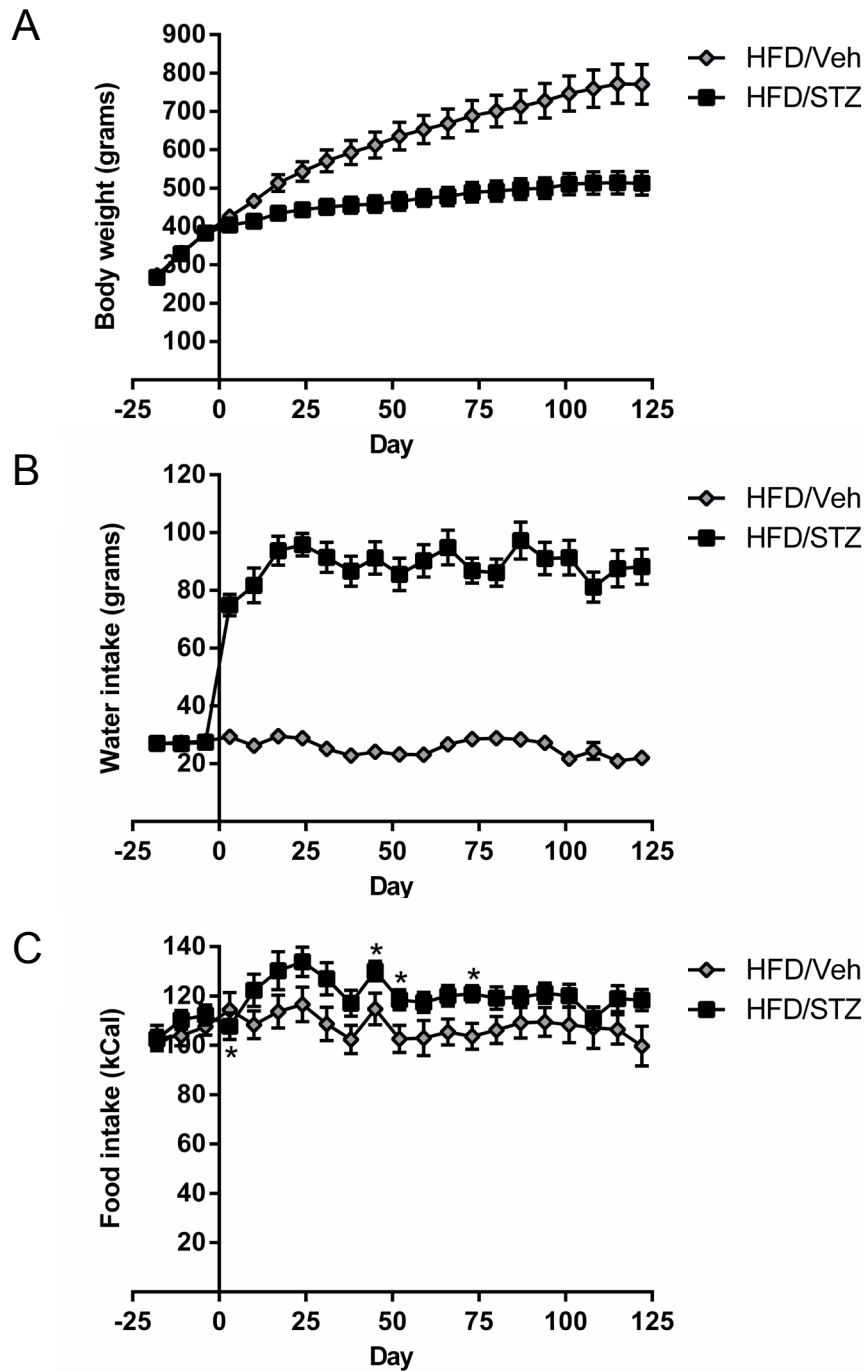


Figure 2.1 Effects of HFD/STZ (n=12) on **(A)** body weight, **(B)** water intake and **(C)** food intake, in comparison with HFD/Veh (n=6). All data represent mean \pm SEM, analysis was by an ANCOVA (with the average of day -7 to 0 as a covariate): * $p < 0.05$, ** $p < 0.01$.

In comparison to HFD/Veh controls, body weight and water intake, $p < 0.001$ from day 1

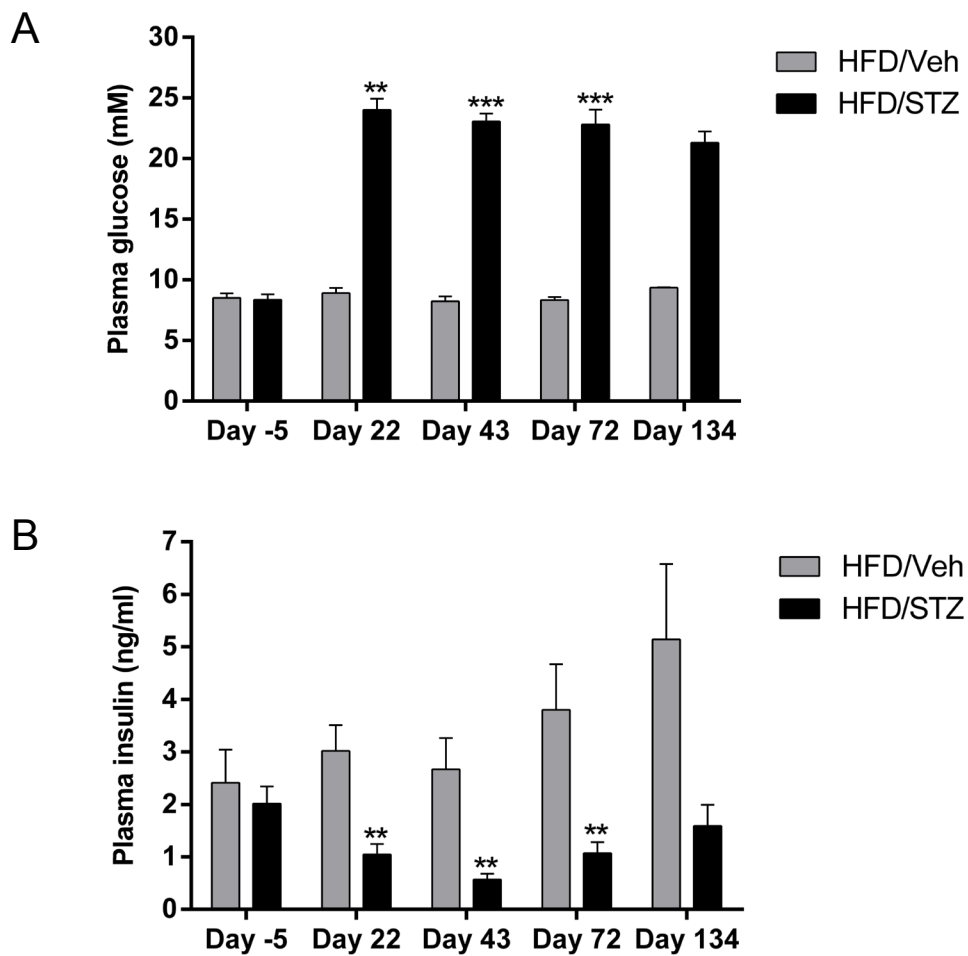


Figure 2.2 Effects of HFD/STZ (n=12) on **(A)** fasting plasma glucose and **(B)** fasting plasma insulin, in comparison with HFD/Veh (n=6). Blood was collected after a four hour fast. All data represent mean \pm SEM (day 134 n=2 for HFD/Veh, n=6 for HFD/STZ, no statistical analysis was performed at this time point). The error bar at day 134 for glucose is too small to be visible. Analysis was by a Mann-Whitney: ** p<0.01, *** p<0.001.

A measure of average plasma glucose concentration is HbA1c. HbA1c is formed when haemoglobin reacts with glucose molecules, and is found in red blood cells. These cells have a life cycle of about two months, thus the amount of glycosylated haemoglobin they contain is directly related to the average plasma glucose concentration during this time (Koenig *et al.*, 1976). As shown in Figure 2.3, HbA1c levels were significantly increased ($p < 0.01$) in the HFD/STZ group compared to the HFD/Veh controls.

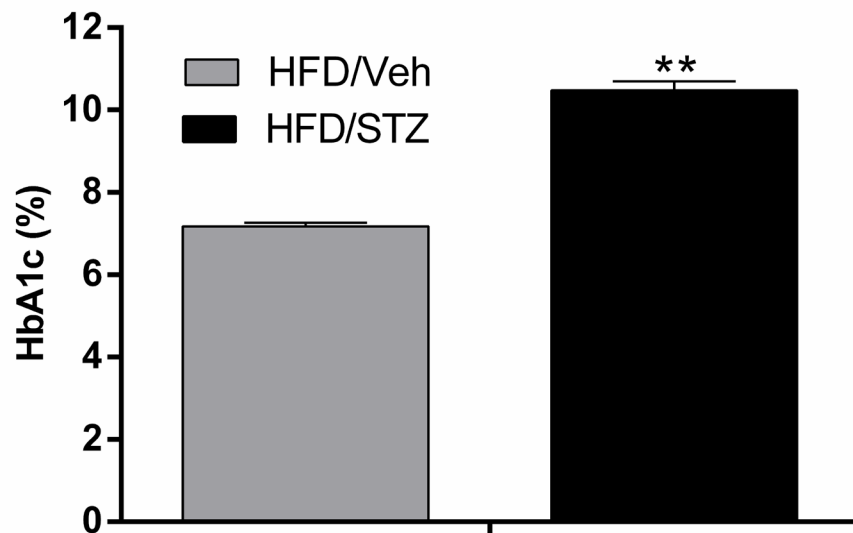


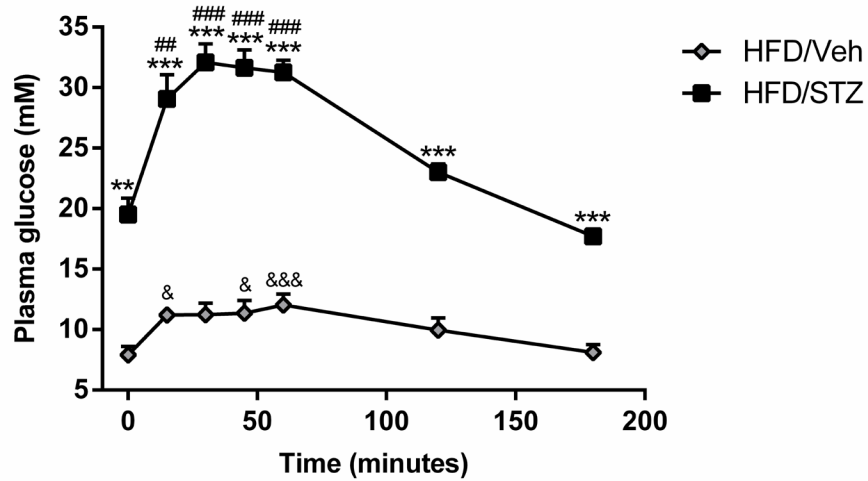
Figure 2.3 Effects of HFD/STZ (n=12) on HbA1c levels, in comparison with HFD/Veh (n=6). All data represent mean \pm SEM, analysis was by a Mann Whitney: ** $p < 0.01$

An OGTT was performed to determine how quickly glucose was cleared from the blood following the delivery of a glucose load. In the HFD/Veh group there was an increased production of insulin, which was significant from 30 minutes until 60 minutes ($p < 0.01$), and had returned to basal levels after 120 minutes (Figure 2.4B). This increase in insulin prevented a large fluctuation in the plasma glucose concentration, resulting in only a small, but significant ($p < 0.05$) increase from 15 to 60 minutes (Figure 2.4A). Significantly less insulin was produced in the HFD/STZ group ($p < 0.001$, compared to HFD/Veh); with only a significant increase from basal levels seen at 15 minutes ($p < 0.05$), and as a result there was a much larger increase in plasma glucose concentration ($p < 0.001$, compared to HFD/Veh, Figure 2.4A). However, as with the HFD/Veh group, plasma glucose concentration had returned close to basal levels at 120 minutes post glucose administration.

Finally, pancreatic insulin content in the HFD/STZ group was also quantified at the end of the study. Levels of pancreatic insulin in the HFD/STZ group were very low ($5700 \pm 1400 \mu\text{g}$ insulin/g pancreas). Due to time limitations and the resources required for this test, pancreatic insulin concentration was only assessed in one sample from the HFD/Veh group ($95200 \mu\text{g}$ insulin/g pancreas), and therefore statistical analysis could not be performed.

All of these results confirm that the HFD/STZ model of diabetes produces robust metabolic changes that can be correlated with the disease in humans.

A



B

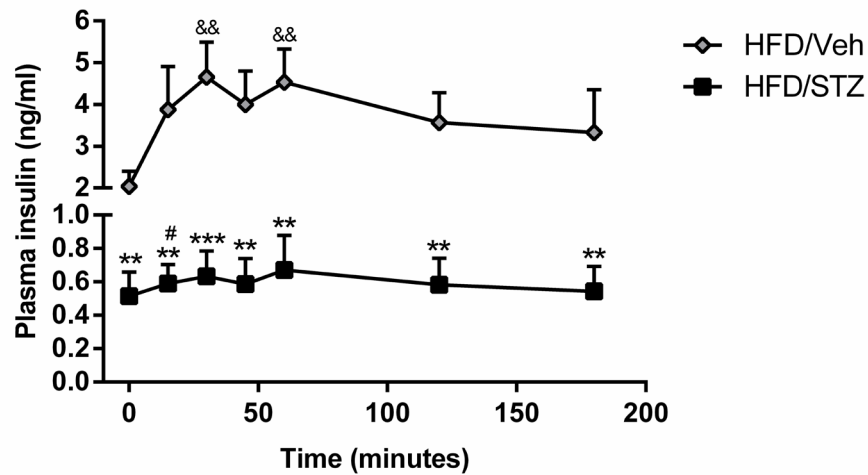


Figure 2.4 Effects of HFD/STZ (n=12) on **(A)** plasma glucose and **(B)** plasma insulin during an OGTT, in comparison with HFD/Veh (n=6). Rats were fasted overnight, and the next morning (day 120) a glucose load was given ($2\text{g}\cdot\text{kg}^{-1}$, p.o.) and blood samples were collected at 0, 15, 30, 45, 60, 120 and 180 minutes. All data represent mean \pm SEM, analysis was by a Mann Whitney:

** $p < 0.01$, *** $p < 0.001$ (HFD/STZ vs. HFD/Veh)

Additional analysis was by a Friedman test with Dunn's multiple comparison post-hoc test:

& $p < 0.05$, && $p < 0.01$, &&& $p < 0.001$ (HFD/Veh vs. HFD/Veh at T0)

$p < 0.05$, ### $p < 0.01$, #### $p < 0.001$ (HFD/STZ vs. HFD/STZ at T0)

2.3.3. Effects of HFD/STZ on mechanical withdrawal thresholds

The mean mechanical withdrawal threshold of the hindpaws of HFD/Veh controls throughout the study (14.1 ± 0.6 g) was consistent with responses in naive rats. Following injection of STZ, there was a progressive decrease in the mechanical withdrawal threshold of the hindpaws in the HFD/STZ rats, compared to the HFD/Veh controls. A significant difference in the hindpaw withdrawal thresholds of the two groups was first evident at day 46 (Figure 2.5). By day 120, the mean mechanical withdrawal threshold of the HFD/STZ group was 7.0 ± 0.7 g compared to 14.2 ± 0.5 g in the HFD/Veh group. This decrease in mechanical withdrawal threshold is indicative of the presence of mechanical hypersensitivity. It is noteworthy that the development of mechanical hypersensitivity is very slow in comparison to the metabolic changes.

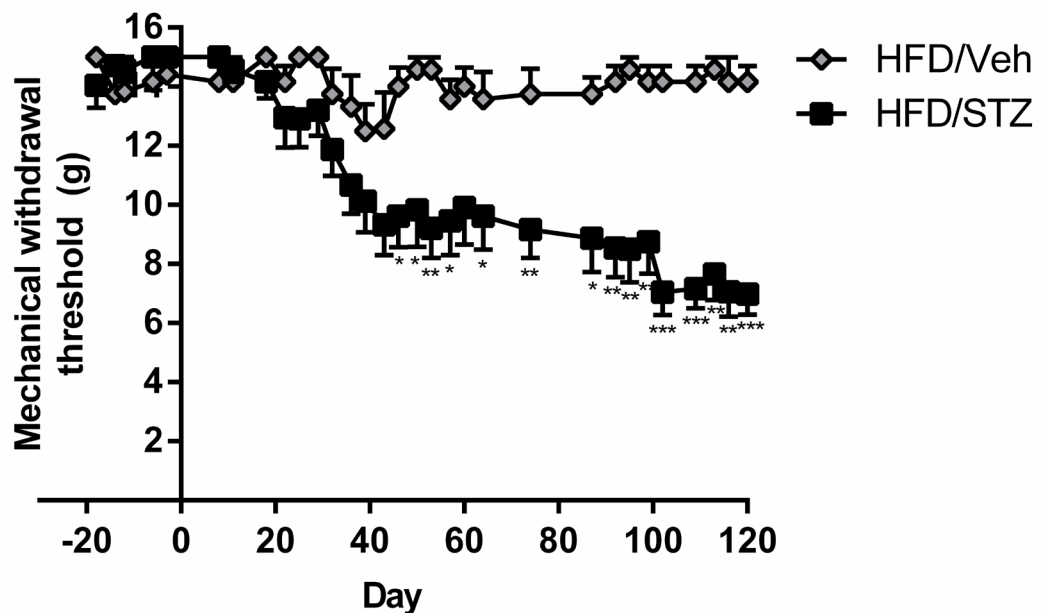


Figure 2.5 Effects of HFD/STZ (n=12) on mechanical withdrawal threshold of the hindpaws, in comparison with HFD/Veh (n=6). All data represent mean \pm SEM, analysis was by a Mann-Whitney:

* $p < 0.05$, ** $p < 0.01$, *** $p < 0.001$

Finally, the Hargreaves test was carried out on two consecutive days at the end of the study to determine whether the thermal withdrawal latency was altered in the HFD/STZ rats compared to the HFD/Veh controls. There were no significant differences in the thermal withdrawal latency between the two groups at these two timepoints (Figure 2.6).

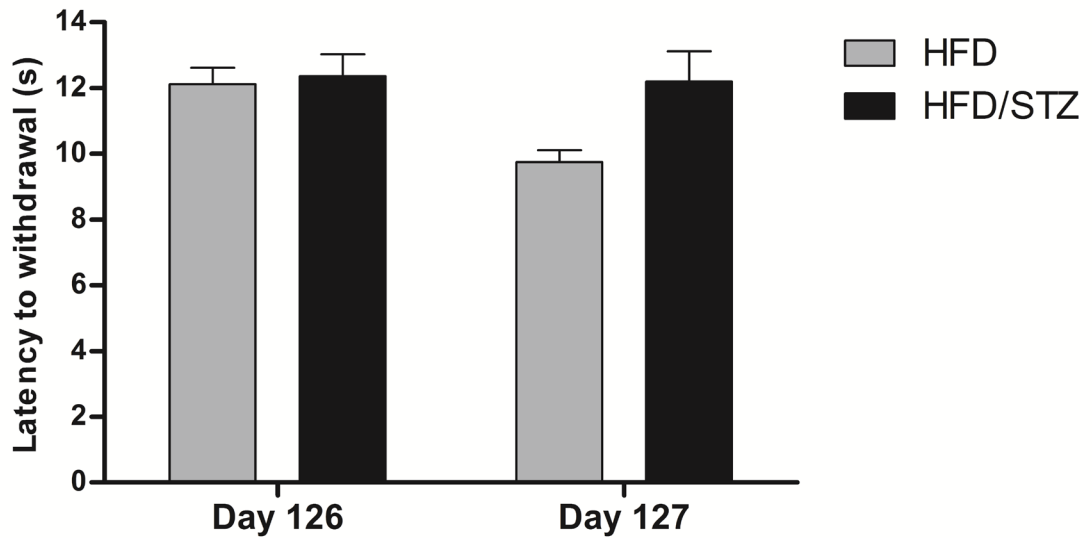


Figure 2.6 Effects of HFD/STZ (n=12) on thermal withdrawal latency in the Hargreaves test, in comparison with HFD/Veh (n=6). All data represent mean \pm SEM, analysis was by an unpaired t-test.

2.4. Discussion

2.4.1. Metabolic effects in the HFD/STZ model

In the present study, the combination of a HFD and a single dose of STZ were examined for their ability to produce a type 2-like model of diabetes. The HFD/STZ model resulted in all of the metabolic changes that were expected (Srinivasan *et al.*, 2005). There was a decreased growth rate, and a huge increase in water consumption, which resulted in a large increase in urine production. These changes were evident in the first few days after STZ injection, and were significant from the first week onwards. The rats also developed hyperglycaemia, and hypoinsulinaemia, with a large rise in plasma glucose levels, and a corresponding decrease in plasma insulin. Injection of STZ significantly reduced food intake during the first week, but after this the intake fluctuated in both groups but remained relatively stable, with the HFD/STZ group taking in more calories than the HFD/Veh controls in general, which was significant at several timepoints. In the OGTT, administration of glucose in the HFD/Veh rats caused a significant increase in the production of insulin, followed by a rapid decrease in plasma glucose levels. However, in the diabetic HFD/STZ rats, the insulin-secretory response was greatly decreased and the level of plasma insulin was only significantly changed from basal levels at 15 minutes. This increase did not bring it close to the basal level of the HFD/Veh rats, resulting in a much larger increase in plasma glucose levels.

2.4.2. Mechanical withdrawal thresholds in the HFD/STZ model

The mechanical withdrawal threshold of the hindpaws in the HFD/Veh group was stable throughout the duration of the study, but in the HFD/STZ group the mechanical withdrawal threshold was decreased significantly by day 46 and this decrease persisted for a further ten

weeks until the study was terminated. The timecourse of the changes in mechanical withdrawal threshold of the hindpaws in the HFD/STZ rats was slower than the rapid metabolic changes produced in this model. This indicates that the development of mechanical hypersensitivity is not just a direct consequence of hyperglycaemia, but must also be due to other underlying mechanisms, some of which will be investigated in Chapters 3 and 4.

The timecourse of the change in mechanical withdrawal thresholds in the HFD/STZ model reported in this first study is slower than the rapid development of mechanical hypersensitivity reported in the STZ-alone model, where changes are first seen after 1-2 weeks (Ahlgren *et al.*, 1993; Calcutt *et al.*, 1996; Courteix *et al.*, 1993; Dobretsov *et al.*, 2003; Fuchs *et al.*, 2010; Xu *et al.*, 2011). However in the studies in Chapters 3-5 there was a slightly faster progression, with a significant decrease in mechanical withdrawal thresholds first reported between 2-3 weeks after STZ injection.

There has only been one other report looking at the development of mechanical hypersensitivity in the HFD/STZ model so far, in which 2 weeks of high fat diet followed by 35mgkg⁻¹ of STZ was reported to not alter mechanical withdrawal thresholds of the hindpaw, mechanical hyperalgesia in the pinprick test or thermal/cold thresholds, compared to a higher dose of STZ alone (Ferhatovic *et al.*, 2013). However this study resulted in a much more moderate model of diabetes, with lower plasma glucose levels and a steady increase in body weight.

Previous studies suggest that it is not just prolonged hyperglycaemia that is responsible for the development of mechanical hypersensitivity, but also insulin deficiency. Insulin implantation has been shown to prevent the development of mechanical hypersensitivity, and established hypersensitivity was reversed by prolonged insulin treatment, but not by a single insulin injection (Calcutt *et al.*, 1996). Similarly, Hoybergs *et al.* (2007) showed that low-dose insulin

administration, which did not significantly change hyperglycaemia, reversed tactile hypersensitivity and mechanical hyperalgesia. Furthermore, in a long term (24 week) study, insulin implantations at day 7 after STZ restored blood glucose, and also prevented the development of mechanical hypersensitivity (Otto *et al.*, 2011). Thus it seems likely that the development of mechanical hypersensitivity is related, in part, to a prolonged insulin deficiency (Calcutt *et al.*, 1996).

The relationship between plasma insulin and glucose and the development of mechanical hypersensitivity was further investigated by Romanovsky *et al.* (2004). In this study, mechanical hypersensitivity was compared between STZ treated rats that became hyperglycaemic (20-25mM) and those that maintained normal blood sugar levels, but displayed a decrease in pancreatic β -cell area and plasma insulin levels, similar to early stage type 1 diabetes (Romanovsky *et al.*, 2010). Interestingly, both groups of rats showed a decrease in mechanical withdrawal thresholds as soon as 1 week after STZ injection, which was fully developed at 3 weeks (Romanovsky *et al.*, 2004). They concluded that it could not be solely hyperglycaemia that was responsible for the development of hyperalgesia. In a further study, Romanovsky *et al.* (2006) found that in STZ treated rats that did not go on to develop hyperglycaemia, plasma insulin levels were correlated with paw pressure withdrawal thresholds. Furthermore, low-dose injections of insulin, which increased plasma insulin without affecting plasma glucose levels, reversed changes in mechanical sensitivity (Romanovsky *et al.*, 2006). More recently, Otto *et al.* (2011) hypothesised that insulin deficiency and impaired insulin signalling results in a loss of neurotrophic support which contributes to changes in sensory afferent fibre function.

Finally, at the end of this study, the thermal nociceptive thresholds were examined in all of the HFD/STZ and HFD/Veh control rats over two days. No difference was seen on the first day, and the withdrawal latency was slightly longer in the HFD/STZ rats on the second day, but

no significance was seen. As no significant changes in thermal withdrawal thresholds were seen in this first study, and due to the inconsistencies in the literature so far, the remaining work in this thesis focuses on the changes in mechanical withdrawal thresholds in this model of diabetes.

Chapter 3.

Investigating the impact of the HFD/STZ model on peripheral nerve function, and spinal mechanisms of central sensitisation

3.1. Introduction

The work in this chapter will investigate the impact of the HFD/STZ model on peripheral nerve function and spinal mechanisms of central sensitisation, to help identify the mechanisms underpinning the behavioural pain phenotype in these rats.

Fluoro-Jade-B and CGRP are used as measures of peripheral nerve function and pathology, as well as for investigating changes in the spinal cord.

3.1.1. Fluoro-Jade B

Fluoro-Jade B is a fluorescent ligand which is used to detect and quantify degenerating neurones. It stains cell bodies, dendrites, axons and axon terminals, and although the exact mechanism is unknown, it has been speculated that it may bind to a polyamine (Schmued *et al.*, 2000).

Fluoro-Jade has been used to detect whether neuronal death is induced in the brain in diabetic models when exposed to hypoglycaemia. No neuronal death was detected in the hippocampus or the cortex at 1 or 4 weeks in STZ treated rats, or in the hypothalamus at 8 weeks following STZ treatment (Lechuga-Sancho *et al.*, 2006). However neuronal death has been induced in the cortex by hypoglycaemia at 1 week in STZ treated rats (Bree *et al.*, 2009). Fluoro-Jade has also been used to detect degenerating neurones in the spinal cord (Kudo *et al.*, 2006; Marmiroli *et al.*, 2009; Nguyen *et al.*, 2004; Orendacova *et al.*, 2005; Saganová *et al.*, 2006) and DRGs (Lazaridis *et al.*, 2011; Marmiroli *et al.*, 2009) in a variety of models that induce neuronal death, although there are some reports that it also stains astrocytes in the spinal cord (Anderson *et al.*, 2003).

As no neuronal death has been detected in the brain of STZ rats, I was interested in investigating whether any neuronal death occurs in the DRGs or spinal cord of HFD/STZ rats, and whether this might play a role in the progression of diabetic neuropathy.

3.1.2. CGRP

CGRP plays an important role in the transmission and modulation of peripheral and central nociceptive processing (Neugebauer, 2009). CGRP is synthesised and stored in primary afferent axons, especially small DRG cells and unmyelinated axons (van Rossum *et al.*, 1997; Willis *et al.*, 2004). CGRP receptors are mostly found in laminae I and II in the spinal cord, the major terminal site of nociceptive primary afferents, but they can also be found in deeper laminae (Ye *et al.*, 1999).

Levels of CGRP in the spinal cord can be increased by noxious stimuli (Morton *et al.*, 1989; Schaible *et al.*, 1994) and by inflammation (Schaible *et al.*, 1994; Willis *et al.*, 2004), as well as electrical stimulation of unmyelinated afferents (Morton *et al.*, 1989; Schaible *et al.*, 1994) and administration of carrageenan (Garry *et al.*, 1992). The CCI model of neuropathic pain is, however, associated with a decrease in CGRP immunoreactivity (Bennett *et al.*, 1989; Yu *et al.*, 1996). Spinal application of CGRP has pro-nociceptive effects (Li *et al.*, 2001; Oku *et al.*, 1987; Sun *et al.*, 2004a; Sun *et al.*, 2003; Sun *et al.*, 2004b), and a CGRP antagonist (CGRP₈₋₃₇), or anti-CGRP antiserum, prevents or reduces central sensitisation of dorsal horn neurones (Neugebauer *et al.*, 1996; Sun *et al.*, 2004a; Sun *et al.*, 2004b; Yu *et al.*, 2002), as well as attenuating hypersensitivity in animal models of inflammatory and neuropathic pain (Jang *et al.*, 2004; Kawamura *et al.*, 1989; Kuraishi *et al.*, 1988; Sun *et al.*, 2003; Yu *et al.*, 1996). CGRP knock-out mice showed no pain responses in the hot plate test, and no development of secondary hyperalgesia in a model of knee joint inflammation (Zhang *et al.*, 2001a)

The impacts of STZ induced diabetic neuropathy on levels of CGRP in different tissues in the rat have varied, as outlined below in Table 3.1. An increase in CGRP-positive fibres and basal CGRP release has been reported in the skin, whereas a decrease in CGRP content/mRNA levels/CGRP-positive neurones has been reported in nerves and DRGs. Finally, in the spinal cord, there was no change in basal CGRP release at 5 weeks in STZ treated rats, but an increase in capsaicin-stimulated release of CGRP was observed (Bishnoi *et al.*, 2011).

Table 3.1 Summary of the effects of STZ-induced diabetes on CGRP expression/release in different tissues.

Tissue	Change	Reference
Skin	Doubling of basal and capsaicin-evoked release of CGRP in 8 week STZ rats	(Ellington <i>et al.</i> , 2002)
	Increase in CGRP-positive fibres in 12 week STZ rats	(Karanth <i>et al.</i> , 1990)
Vagus nerve	Decrease in CGRP content in 8 week STZ rats	(Calcutt <i>et al.</i> , 1998)
	No change in the levels of CGRP-positive neurones in the nodose ganglion in 8, 16 or 24 week STZ rats	(Regalia <i>et al.</i> , 2002)
Sciatic nerve	Decrease in CGRP content in 4 week STZ rats	(Brewster <i>et al.</i> , 1994; Diemel <i>et al.</i> , 1994)
DRGs	Decrease in mRNA levels in 4 week STZ rats	(Brewster <i>et al.</i> , 1994; Diemel <i>et al.</i> , 1994)
	Decrease in CGRP positive neurones in 4 week and 12 month STZ rats	(Adeghate <i>et al.</i> , 2006; Zochodne <i>et al.</i> , 2001)
Spinal cord	No change in basal CGRP release in 5 week STZ rats, but an increase in capsaicin-stimulated release of CGRP	(Bishnoi <i>et al.</i> , 2011)

3.1.3. Microglia

Glial cells are 10 to 50 times as numerous as neurones in the CNS and belong to one of three groups: microglia, astrocytes or oligodendrocytes (Gao *et al.*, 2010). Glia play an important role in central sensitisation in neuropathic pain, and so it is important to elucidate their role in the spinal cord in the HFD/STZ model.

Microglia represent 5-10% of glia in the CNS (Tsuda *et al.*, 2005). It is currently believed that microglia derive from the yolk sac macrophages that seed the rudimentary brain during early foetal development (for review see Ginhoux *et al.*, 2013). When 'resting', microglia have a small soma with thin, branching processes which survey the microenvironment for stimuli such as CNS trauma, ischemia and infection (Tsuda *et al.*, 2005).

There are a wide variety of pathways that lead to activation of microglia (Smith, 2010), and these include:

- Matrix metalloproteinase 9 (MMP9), which is thought to contribute to the initiation of neuropathic pain through IL-1 β cleavage (Kawasaki *et al.*, 2008).
- Fractalkine, a chemokine which is cleaved by MMPs, and its receptor CX₃CR1, which is mainly expressed by microglia. CX₃CR1 expression is increased during neuropathic pain, and it is thought that fractalkine can attract CX₃CR1-expressing microglia to sites of ongoing pathology (Verge *et al.*, 2004).
- Monocyte chemoattractant protein-1 (MCP-1, OR CCL2), and its receptor CCR2, which is upregulated in microglia following nerve injury (Zhang *et al.*, 2006a)
- Toll-like receptors (TLRs), which cause activation of NF κ B, and the subsequent release of IL-1 β , IL-6 and TNF α , resulting in a positive feedback loop in the pain-pathway (Kim *et al.*, 2007a). TLR4 activation has been shown to correlate with the onset of

behavioural sensitivity in the spared nerve injury (SNI) model (Tanga *et al.*, 2004).

- Neuregulin-1 (NRG1), a growth factor, is released by primary afferents and binds to erbB2, 3 and 4, which are expressed by microglia. Blockade of erbB2 reduces accumulation of microglia and attenuates hypersensitivity in the SNL model (Calvo *et al.*, 2010).
- ATP and its receptors (especially P2X4 and P2X7) (Hide *et al.*, 2000; Inoue *et al.*, 2007; Tsuda *et al.*, 2013).

Microglia can also be activated by ROS, NO, substance P (Zhou *et al.*, 2010), brain-derived neurotrophic factor (BDNF), PGs, glutamate (Tikka *et al.*, 2001) and heat shock proteins which are upregulated by peripheral nerve injury (Costigan *et al.*, 1998).

Once microglia are activated, they show dramatic changes in morphology including: hypertrophy and thickened and retracted processes (Eriksson *et al.*, 1993); increases in the levels of microglial markers such as ionized calcium binding adapter molecule 1 (Iba1) and CD11b (Tsuda *et al.*, 2005); as well as proliferation (Gehrmann *et al.*, 1995; Romero-Sandoval *et al.*, 2008a). Activation of microglia and phosphorylation of p38 MAPK is involved in Ca²⁺ sensitive intracellular signalling cascades and leads to the production of pro-inflammatory cytokines (Hanisch, 2002; Kim *et al.*, 2007a; Kreutzberg, 1996; Ledebor *et al.*, 2005; Zhuo *et al.*, 2011). They also release cytotoxic molecules such as ROS (Kim *et al.*, 2010), NO (Tikka *et al.*, 2001), and PGs (Candelario-Jalil *et al.*, 2007), as well as BDNF (Coull *et al.*, 2005), substance P, excitatory amino acids, and ATP. These substances can, in turn, activate nearby astrocytes, microglia and neurones (Zhou *et al.*, 2010).

Microglial activation in the spinal cord has been seen in a variety of animal models of pain, including the formalin model (Fu *et al.*, 2000; Fu *et al.*, 1999; Sweitzer *et al.*, 1999), models of peripheral nerve injury

(Colburn *et al.*, 1999; Coyle, 1998), and spinal nerve transection (Sweitzer *et al.*, 1999). Minocycline, a second-generation tetracycline with anti-inflammatory properties (for review see Garrido-Mesa *et al.*, 2013), selectively prevents the activation of microglia and blocks the release of pro-inflammatory cytokines IL-1 β and TNF α (Ledeboer *et al.*, 2005; Padi *et al.*, 2008). Minocycline is able to attenuate the development of neuropathic pain in sciatic inflammatory neuropathy and acute spinal immune activation with intrathecal HIV-1 gp120 (Ledeboer *et al.*, 2005), CCI (Padi *et al.*, 2008), and L5 spinal nerve transection (Raghavendra *et al.*, 2003). Minocycline is not, however, effective against already established hypersensitivity (Ledeboer *et al.*, 2005; Padi *et al.*, 2008; Raghavendra *et al.*, 2003).

As well as a role in models of nerve injury, microglia have also been shown to play a part in the development of painful symptoms in animal models of diabetes. Microglia are upregulated in the spinal cord of rats as soon as 4 days after injection with STZ (Talbot *et al.*, 2010), as well as at later timepoints; 2-4 weeks (Tsuda *et al.*, 2008); 3 weeks (Kim *et al.*, 2012b); 4 weeks (Morgado *et al.*, 2011a); and 5 weeks (Wodarski *et al.*, 2009). In STZ treated mice, a slower change in the number of microglia was reported, with no change evident at 1 month, but an increase at 3 months, peaking at 5 months, and decreasing slightly by 8 months post model induction (Toth *et al.*, 2010). An increase in the density of Iba1-positive endoneurial macrophages was also seen in the sciatic and tibial nerves of STZ rats (Nukada *et al.*, 2011). However, in the db/db mouse model of type 2 diabetes, no change in spinal microglial activation was observed at postnatal week 6 or 16 (Liao *et al.*, 2011).

An increase in ERK (Tsuda *et al.*, 2008), JNK and p38 phosphorylation (Sweitzer *et al.*, 2004) in both neuronal and microglial cells in the spinal cord and DRG of STZ treated rats has been reported, indicating an increase in their activation, which correlates with the hyperalgesic state (Daulhac *et al.*, 2006). Inhibitors of all three of these signalling

molecules were able to attenuate these painful symptoms (Daulhac *et al.*, 2006; Sweitzer *et al.*, 2004).

Treatment with minocycline in STZ animals also causes a decrease in microglial activation, as well as attenuating the increased levels of IL-1 β , B₁R, TNF α and TRPV1, and reversing cold and tactile hypersensitivity (Morgado *et al.*, 2011a; Pabreja *et al.*, 2011; Talbot *et al.*, 2010). Infusion of lidocaine in the early phase, but not the late phase, was also able to attenuate tactile hypersensitivity in STZ mice through inhibition of microglial activation (Suzuki *et al.*, 2011).

3.1.4. Astrocytes

Astrocytes are the most abundant cells in the CNS, and they are able to form networks with themselves and are closely associated with neurones and blood vessels (Saravia *et al.*, 2002). This enables them to play a role in maintaining the balance of the neuronal environment through homeostatic regulation of water, ions and pH (Montgomery, 1994), as well as protecting against toxic insults such as reactive oxygen species (Lamigeon *et al.*, 2001). Astrocytes also play a role in synaptic transmission, where excess amino acids such as glutamate are removed from the synaptic cleft by excitatory amino acid transporters (EAATs; Nakagawa *et al.*, 2010), preventing over-excitation and neurotoxicity. They also play a role in mediating glucose metabolism, as uptake of excess glutamate leads to stimulation of glycolysis, where glucose is converted to lactate. This produces ATP, which is used for the synthesis of glutamine from glutamate (Magistretti *et al.*, 1999).

Nociceptive stimuli, as well as pro-inflammatory cytokines, can lead to activation of astrocytes, as they express receptors for nociceptive neurotransmitters such as glutamate, substance P and CGRP (Marchand *et al.*, 2005). They can also be activated by MMP2 (Kawasaki *et al.*, 2008). When astrocytes are activated, they exhibit a

hypertrophic morphology, with thickened process, and upregulation of glial fibrillary acidic protein (GFAP), an intermediate cytoskeletal filament protein specific for astrocytes. In turn, activation of astrocytes leads to further production and release of pro-inflammatory cytokines, chemokines, prostaglandins, NO, ATP, D-serine and glutamate, which can contribute to enhanced pain sensitivity. As with microglia, activation of astrocytes leads to activation of ERK and JNK signalling pathways, which release pro-inflammatory factors which can lead to further astrocyte activation (Milligan *et al.*, 2009).

An increase in GFAP staining due to hypertrophy of activated astrocytes, known as astrogliosis, has been observed in the spinal cord in a variety of neuropathic and inflammatory pain models, paralleling the development of hypersensitivity (Garrison *et al.*, 1991; Obata *et al.*, 2006; Raghavendra *et al.*, 2004; Sweitzer *et al.*, 1999; Wang *et al.*, 2009). Whereas microglia numbers undergo a more rapid increase, and then a later decrease, astrogliosis has a more delayed initiation, but is then sustained long-term (up to 150 days in one study) (Raghavendra *et al.*, 2004; Tanga *et al.*, 2004; Zhang *et al.*, 2006a). It is therefore hypothesised that upregulation of astrocytes contributes to the maintenance of chronic pain, whereas microglial activation is responsible for the development. However this pattern is not always observed in all animal models of pain (see Colburn *et al.*, 1999; Romero-Sandoval *et al.*, 2008a). Fluorocitrate, which functionally and morphologically suppresses glial cell activation, reduced hypersensitivity for 5 days in a postoperative pain model (Obata *et al.*, 2006), as well as attenuating thermal and mechanical hyperalgesia in the zymosan model (Meller *et al.*, 1994), and attenuating the induction, and reversing the early phase of developed mechanical hypersensitivity, in neonatal capsaicin-treated adult rats (Nakagawa *et al.*, 2007).

In contrast to this upregulation of astrocytes in animal models of chronic pain, there are conflicting reports about the changes in levels of GFAP

staining in various models of diabetes. Some groups have shown a significant decrease in GFAP staining in areas of the brain including the cerebral cortex, hippocampus, cerebellum and corpus callosum in STZ rats (Coleman *et al.*, 2004; de Senna *et al.*, 2011; Lechuga-Sancho *et al.*, 2006; Renno *et al.*, 2012; Zuo *et al.*, 2011). In the retina, the intensity of GFAP staining in astrocytes was decreased as soon as 1 month following STZ injection, and decreased further as the studies progressed (Barber *et al.*, 2000; Rungger-Brandle *et al.*, 2000). Conversely, other groups have shown an increase in GFAP staining in the hippocampus, cerebral cortex, and cerebellum at 6 week in STZ rats (Baydas *et al.*, 2003), and in the hippocampus in NOD and STZ mice (Saravia *et al.*, 2002).

In the spinal cord, a decrease in the number of GFAP-immunoreactive astrocytes was seen in the dorsal and ventral horns, as well as the central region, with the number decreasing further between 6 and 12 weeks after STZ injection (Afsari *et al.*, 2008), and this has also been reported at 5 weeks in the same model (Wodarski *et al.*, 2009). However, there have also been reports of no change in GFAP expression at 4 weeks post-STZ (Tsuda *et al.*, 2008), and in a recent report an increase in GFAP expression was seen at 3 weeks (Kim *et al.*, 2012b). In the db/db mouse model of type 2 diabetes, an increase in the amount of GFAP staining was seen in the dorsal horn of the spinal cord from 8 weeks of age, and was maintained thereafter (Dauch *et al.*, 2012; Liao *et al.*, 2011). L- α -amino adipate (a specific astrocyte inhibitor) was able to attenuate mechanical hypersensitivity and phenyl-alpha-tert-butyl nitron (an antioxidant) significantly decreased the levels of GFAP, suggesting that oxidative stress may be an underlying cause of the increase in spinal GFAP expression (Liao *et al.*, 2011).

The role(s) of astrocytes and microglia in any of the models of diabetic neuropathy have yet to be fully elucidated, as seen in some of the conflicting results described above. It is therefore of upmost interest to

quantify levels of activated microglia and astrocytes in the spinal cord in the HFD/STZ model.

3.1.5. Aim of the Study

The aim of this study was to investigate the effect of the HFD/STZ model on immunohistochemical staining in the DRGs and spinal cord. Fluoro-Jade B staining was used to investigate whether any neuronal death could be detected in the DRGs or spinal cord, and the expression of CGRP positive neurones was also investigated, as well as the activation of microglia and astrocytes in the spinal cord.

3.2. Methods

For detailed methods of induction of diabetes, blood sampling and von Frey testing see Chapter 2.

3.2.1. Animals

All experiments were carried out under Home Office Licence 40/3124, in accordance with the UK Home Office Animals (Scientific Procedures) Act 1986 and IASP guidelines. 47 male Sprague-Dawley rats (200-250g), obtained from Charles River (Kent, UK), were individually housed on a normal light cycle (lights on: 07:00 - 19:00) with free access to either normal chow or a high fat diet (60% fat by caloric content; D12492 diet; Research Diets, New Jersey, USA) and water at all times. The rats were divided into two stratified groups on the basis of body weight, and the lean/Veh group were fed chow, and the HFD group were fed the high fat diet. After three weeks consumption of diet, the HFD group was stratified into two further subgroups on the basis of body weight and mechanical withdrawal thresholds, and the lean/Veh and HFD/Veh groups received an i.p. injection of citric acid buffer, and the HFD/STZ group received an i.p. injection of STZ (45mgkg^{-1}). Blood samples were taken at days -5, 8, 23 and 44. von Frey testing was carried out twice weekly.

3.2.2. DRG and spinal cord immunohistochemistry

Tissue was removed and prepared for immunohistochemistry at the following stages of the model: day 10 (Lean/Veh: n=6; HFD/Veh: n=6; HFD/STZ: n=3); day 30 (Lean/Veh: n=5; HFD/Veh: n=5; HFD/STZ: n=4); and day 50 (Lean/Veh: n=6; HFD/Veh: n=6; HFD/STZ: n=4).

Rats were overdosed with sodium pentobarbital and transcardially perfused with 0.9% saline followed by 4% paraformaldehyde (PFA; Sigma, U.K.) in 0.1M phosphate buffered saline (PBS). The lumbar

spinal cord, as well as L4, L5 and L6 DRGs were excised and post-fixed in 4% PFA for 48 hours and then stored in 30% sucrose in 0.1M PBS/0.02% sodium azide solution at 4°C. Spinal cord tissues were frozen with dry ice and fixed to a microtome stage (Leica SM2010R) with mounting media and sliced into 40µm sections through L4/L5. DRGs were suspended in mounting media, and frozen in a chilled acetone solution, and then sliced on a cryostat (Leica CM3050) into 15µm sections, and mounted onto Superfrost Plus microscope slides (Thermo-Scientific, UK).

Table 3.2 Primary and secondary antibodies used in immunohistochemistry experiments

Primary antibody (source)	Dilution/ conditions	Secondary antibody (all Molecular Probes, Oregon)	Dilution/ conditions
Rabbit anti-Iba1 (Wako, Japan)	1:1000, 72hrs, 4°C	Alexaflour 488 donkey anti-rabbit	1:500, 2hrs, RT
Mouse anti-GFAP (Thermo-Fisher, UK)	1:100, 18hrs, RT	Alexaflour 568 donkey anti-mouse	1:500, 2hrs, RT
Rabbit anti-CGRP (Millipore, UK)	1:1000, 18hrs, RT	Alexaflour 488 goat anti-rabbit	1:500, 2hrs, RT
Mouse anti-NeuN (Fisher Scientific, UK)	1:100, 1hr, RT	Alexaflour 568 donkey anti-mouse	1:500, 2hrs, RT

3.2.2.1. NeuN and Fluoro-Jade B

A pilot study was run double-labelling spinal cord and DRG sections with Fluoro-Jade B and GFAP as it has previously been reported that Fluoro-Jade B can stain astrocytes in the spinal cord, instead of degenerating neurones (Anderson *et al.*, 2003; Damjanac *et al.*, 2007). In this pilot study, there was no colocalisation between Fluoro-Jade B and GFAP (data not shown), and so double-labelling with NeuN was run in this study instead.

Neuronal cells were stained using NeuN and dying or degenerating neurones were stained using Fluoro-Jade B (Millipore) (Schmued *et al.*, 2000). The same protocol used for Iba1/GFAP was followed for staining with NeuN, but whereas the spinal cord sections were mounted after the secondary antibody had been washed off, the whole process was carried out on DRG sections which were already annealed to microscope slides. The sections were allowed to air-dry on a slide warmer at 50°C for half an hour, and then the following solutions were applied:

- 1% sodium hydroxide in 60% alcohol, 5 minutes
- 70% alcohol, 2 minutes
- distilled water, 2 minutes
- 0.06% potassium permanganate, 3 minutes
- distilled water, 2 minutes
- 0.0004% Fluoro-Jade B solution (freshly made up from stock solution each day)
- distilled water, 3 minutes (x3)

The slides were then dried on a slide warmer at 50°C, immersed in xylene for 1 minute, and then coverslipped with DPX.

3.2.2.2. CGRP

The same protocol was followed as for Iba1/CGAP except only using the CGRP primary and secondary antibodies (Table 3.2).

3.2.2.3. Iba1 and GFAP

Microglial cells were stained using Iba1 and astrocytes were stained using GFAP. Sections were blocked for 1 hour in 0.1M PBS containing 3% goat serum/0.3% Triton X-100 at room temperature (RT). Sections were then incubated with an Iba1 primary antibody (Table 3.2) diluted with Trizma Triton X-100 buffered saline (TTBS). Five 10 minute washes in 0.1M PBS were carried out, and then sections were incubated with secondary antibody (Table 3.2), and another five 10 minute washes were carried out. This process was then repeated on the same sections, this time using GFAP primary and secondary antibodies (Table 3.2). Sections were then mounted on gelatinised microscope slides, air-dried overnight at RT in the dark and cover-slipped using Fluoromount (Sigma).

3.2.3. Quantification of antibody staining

7 individual spinal cord sections and 6 DRG sections were analysed per rat. For Iba1 and GFAP, and NeuN and Fluoro-Jade B, images were taken of the dorsal horn, ventral horn and central region, whereas only images of the dorsal horn were taken for CGRP. The mean of the left and right half of the dorsal and ventral horn was calculated for each section.

Iba1 and GFAP, and CGRP stained sections were visualised using a 20× 0.4NA objective lens on a Leica DMIRE2 fluorescence microscope, running Volocity 5.5 (PerkinElmer) equipped with a Hamamatsu Orca ER camera. NeuN and Fluoro-Jade B stained sections were visualised using a 20× 0.4NA objective lens on a Leica DMIRB fluorescence microscope, running Volocity 5.5 equipped with a Hamamatsu Orca ER camera.

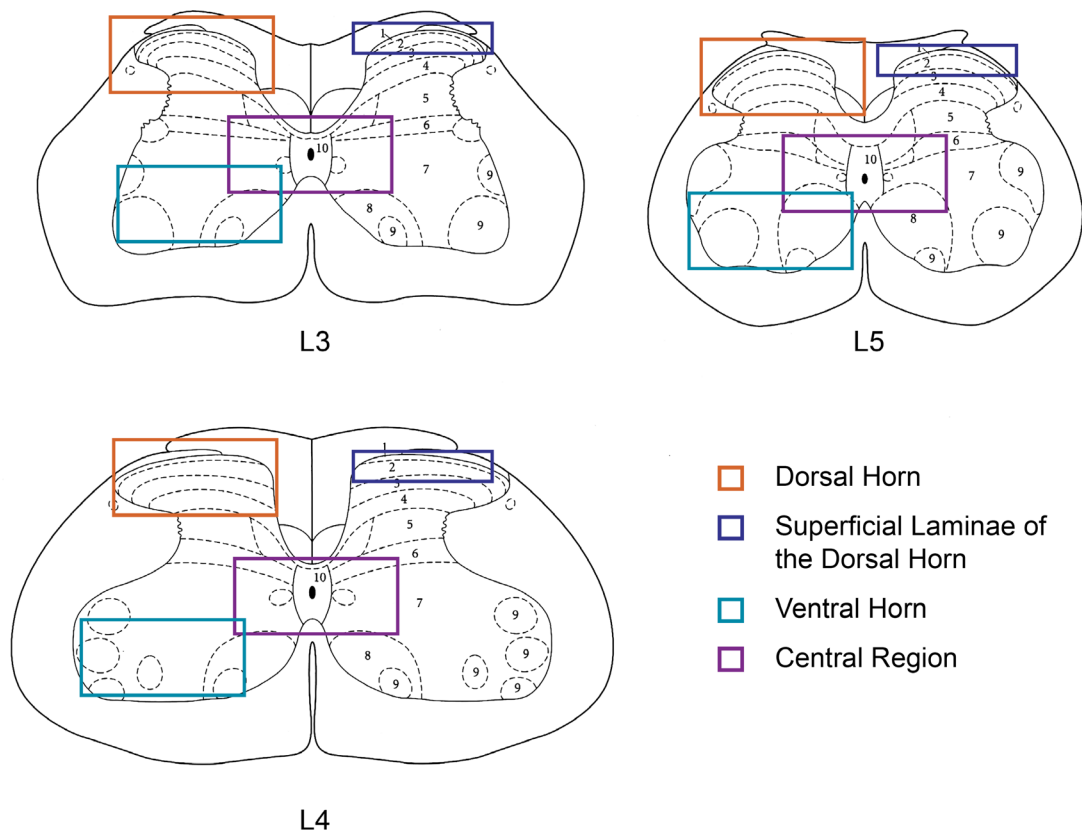


Figure 3.1 Schematic diagrams of L4, L5 and L6 of the spinal cord with: orange boxes marking the approximate dorsal horn region utilised for Iba1, GFAP and Fluoro-Jade B quantification; blue boxes marking the eyebrow region of the superficial dorsal horn used for CGRP quantification; and turquoise boxes and purple boxes marking the ventral horn and central region respectively that were utilised for GFAP quantification. Adapted from (Sagar *et al.*, 2011)

3.2.3.1. NeuN and Fluoro-Jade B

Images were acquired using an exposure time of 400ms for Fluoro-Jade B, and 600ms for NeuN. A heat map was applied on each image so that positively stained cells could be more easily identified from background staining. The total number of cells positively-stained with Fluoro-Jade B was counted manually for each DRG and spinal cord section.

3.2.3.2. CGRP

Images were acquired using an exposure time of 35ms. Immunofluorescence was quantified via region of interest analysis as “eyebrow” staining in the superficial dorsal horn, using threshold intensity values on Velocity 5.5 software.

3.2.3.3. Iba1 and GFAP

Images were acquired using an exposure time of 444ms for Iba1. Only activated, and not the total number of microglia, were counted manually in a quadrant of the dorsal horn in individual sections. Microglia were defined as activated if they displayed a clearly swollen cell body with reduced processes, which differ from normal or resting microglia where cell bodies are largely absent and large ramified processes are displayed (as illustrated in Figure 3.2). Assessment was performed by two independent blinded investigators, who quantified total number of activated microglia.

The mean fluorescence grey intensity was also measured. Background fluorescence was measured by taking an image of an area within the sample, using the parameters described above, which contained no labelled structures, that was then subtracted from all images using IMAGE J (NIH open software with Macbiophotonics plugins). Following background subtraction, mean fluorescence grey intensity was determined for each image using IMAGE J.

For quantification of GFAP, single-plane images of the superficial dorsal horn of the spinal cord were acquired using an exposure time of 393ms, and mean fluorescence grey intensity was measured as described above. All image analysis, cell counts and fluorescence measurements were performed “off-line” on captured images taken from stained sections.

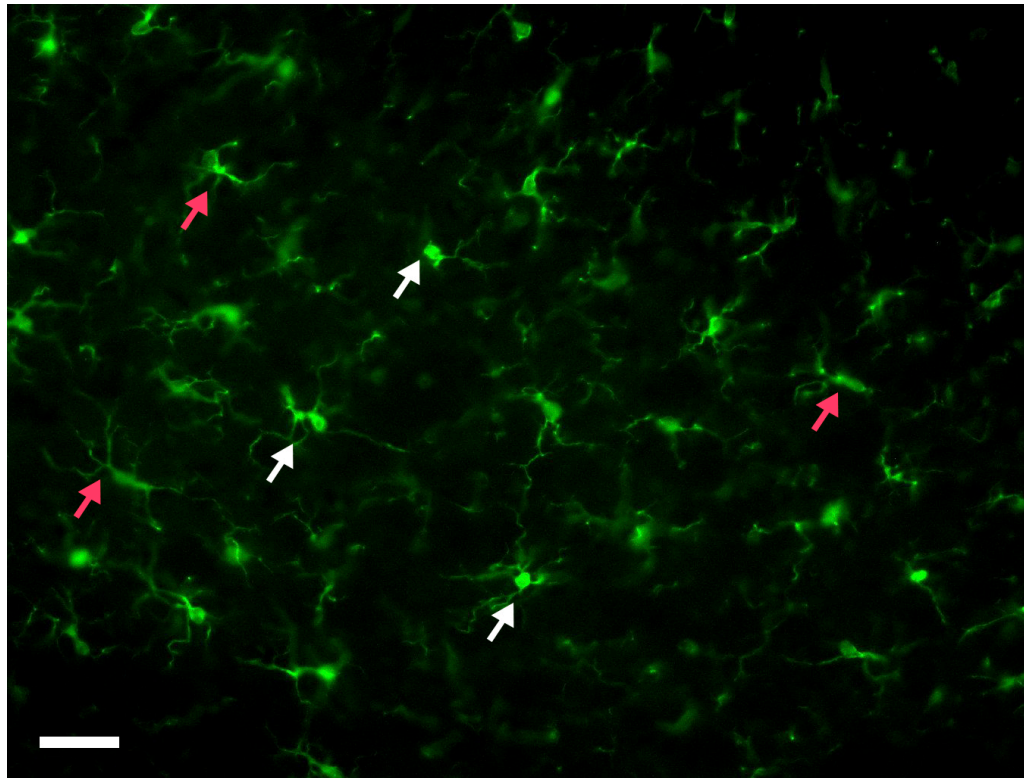


Figure 3.2 Scale bar is 100 μ m. An image at 40x magnification of Iba1 staining in the dorsal horn of the spinal cord. Pink arrows indicate examples of 'resting'/ramified microglia, and white arrows indicate examples of activated microglia.

3.2.4. Statistics

Analysis of body weight, food intake and water intake was by an ANCOVA with Tukey's post-hoc test, with the average of day -7 to 0 as the covariate. Analysis of plasma glucose, plasma insulin and mechanical withdrawal thresholds was by a Kruskal-Wallis test with Dunn's post-hoc test. Analysis of all immunohistochemistry was by a 2-way analysis of variance (ANOVA) with Bonferroni post-hoc test. In all analyses, a p value of less than 0.05 was considered statistically significant.

Rats were excluded from analysis of pain behaviour if in the two weeks before injection with STZ the average hindpaw mechanical withdrawal threshold was <10g. In this study, this represented 6 rats – 3 lean/Veh, 2 HFD/Veh and 1 HFD/STZ.

3.3. Results

3.3.1. Effects of HFD/STZ on body weight, and food and water intake

Consistent with the previous chapter, the HFD/STZ group exhibited a significantly stunted growth rate in comparison to both the lean/Veh and the HFD/Veh controls ($p < 0.001$), with the HFD/Veh group gaining significantly more weight than the lean/Veh controls ($p < 0.05$, Figure 3.3A). Water intake was significantly increased in the HFD/STZ group ($p < 0.001$), and there was no difference between the lean/Veh and the HFD/Veh controls (Figure 3.3B). The HFD/Veh group had a significantly higher caloric intake than the lean/Veh controls ($p < 0.05$, Figure 3.3C), whereas the HFD/STZ group had a significant decrease in caloric intake in the first week after injection with STZ ($p < 0.001$), and the caloric intake was then maintained at around the same level as the HFD/Veh controls, increasing significantly at various timepoints during the study.

3.3.2. Effects of HFD/STZ on metabolic parameters and development of mechanical hypersensitivity

Again, consistent with Chapter 2, there was a threefold increase in the plasma glucose levels in the HFD/STZ rats, and this remained stable for the duration of the study (Figure 3.4A). A small increase in plasma glucose concentration was also seen in the HFD/Veh group in comparison to the lean/Veh controls, although this was only significant at day -5 ($p < 0.05$). The plasma insulin concentration was significantly decreased in the HFD/STZ group at day 8 ($p < 0.001$), and this decreased further as the model developed (Figure 3.4B). There was an increase in the plasma insulin levels in the HFD/Veh group compared to the lean/Veh control group at day -5 ($p < 0.01$), indicating that the HFD leads to the development of hyperinsulinaemia.

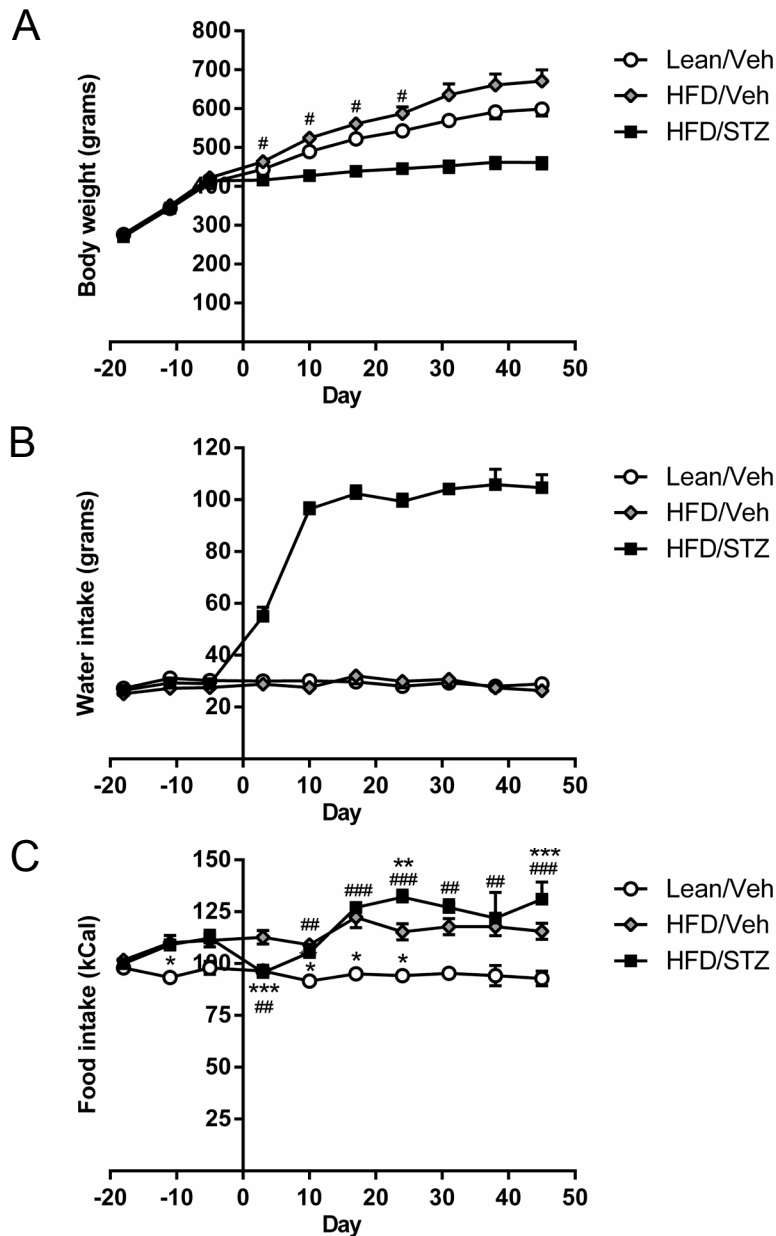


Figure 3.3 Effects of HFD/STZ on (A) body weight, (B) water intake and (C) food intake, in comparison with HFD/Veh and lean/Veh controls. Up to day 10: n=17 for lean/Veh and HFD/Veh, and n=11 for HFD/STZ. Up to day 30: n=11 for lean/Veh and HFD/Veh, and n=8 for HFD/STZ. Day 30 onwards: n=6 for lean/Veh and HFD/Veh, and n=4 for HFD/STZ. All data represent mean \pm SEM, analysis was by an ANCOVA (with day -7 to 0 as covariate) with Tukey's post-hoc test: (* vs. HFD/Veh, # vs. lean/Veh)
 * p<0.05, ** p<0.01, *** p<0.001; # p<0.05, ## p<0.01, ### p<0.001
 In comparison to HFD/Veh controls, body weight and water intake for HFD/STZ, p<0.001 from day 3.

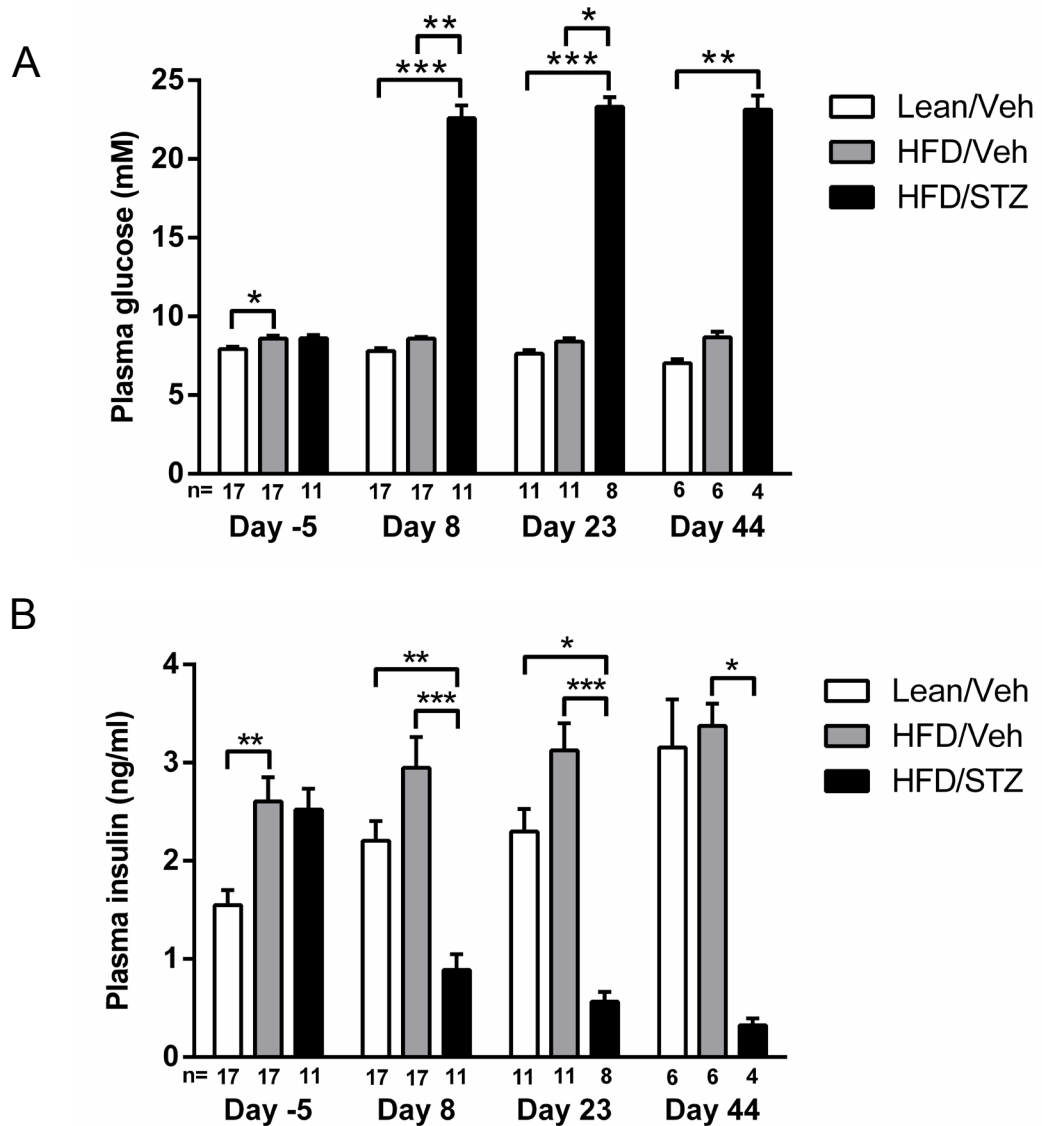


Figure 3.4 Effects of HFD/STZ on **(A)** fasting plasma glucose and **(B)** fasting plasma insulin, in comparison with HFD/Veh and lean/Veh controls. n numbers are displayed on the graphs. All data represent mean \pm SEM, analysis was by a Kruskal-Wallis test with Dunn's post-hoc test: * $p < 0.05$, ** $p < 0.01$, *** $p < 0.001$

Consistent with Chapter 2, the combination of HFD/STZ was associated with a progressive decrease in mechanical withdrawal thresholds of the hindpaws (Figure 3.5). There was no difference in mechanical withdrawal thresholds between the lean/Veh and the HFD/Veh controls, with the mechanical withdrawal thresholds of both groups stable at ~15g. At day 10, the first timepoint at which tissue was collected for immunohistochemistry, there was no significant difference in mechanical withdrawal thresholds. The decrease in mechanical withdrawal thresholds in the HFD/STZ group first became significant at day 15, and continued to decrease as the model progressed until day 50.

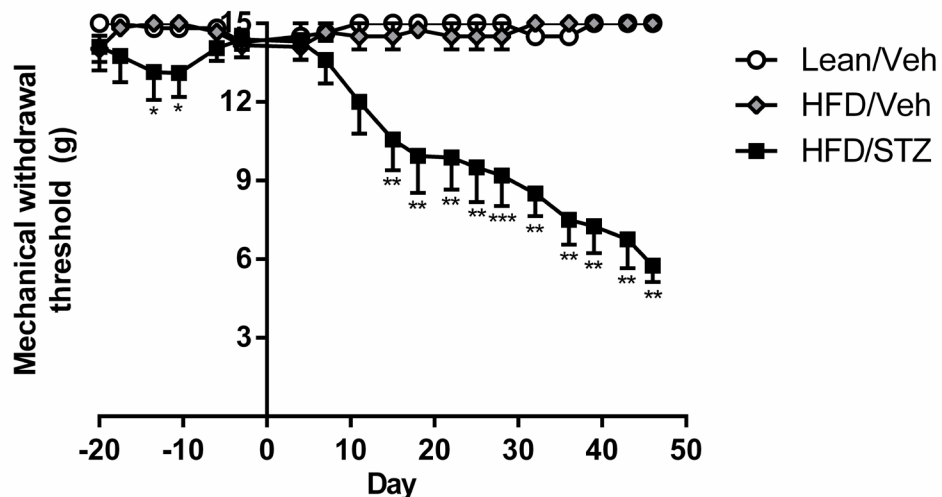


Figure 3.5 Effects of HFD/STZ on mechanical withdrawal thresholds of hindpaws, in comparison with HFD/Veh and lean/Veh controls. Up to day 10: n=14 for lean/Veh, n=15 for HFD/Veh, and n=10 for HFD/STZ. Up to day 30: n=9 for lean/Veh, n=10 for HFD/Veh, and n=8 for HFD/STZ. Day 30 onwards: n=5 for lean/Veh and HFD/Veh, and n=4 for HFD/STZ. All data represent mean \pm SEM, analysis was by a Kruskal-Wallis test with Dunn's post-hoc test:

(* vs. HFD/Veh) * $p < 0.05$, ** $p < 0.01$, *** $p < 0.001$

3.3.3. Effects of HFD/STZ on degenerating neurones

The effect of HFD/STZ treatment on the total number of Fluoro-Jade B positive cells per rat in DRGs (Figure 3.6A) and the dorsal horn of the spinal cord (Figure 3.6B) was quantified. Overall, there were very few Fluoro-Jade B positive cells present in either tissue. No significant changes in the number of Fluoro-Jade B positive cells in either the DRGs, or the spinal cord, were observed at any of the timepoints in the HFD/STZ model.

Tissues were also stained with NeuN to assess the colocalisation between NeuN and Fluoro-Jade B, ensuring that any Fluoro-Jade B positive cells were indeed neurones, and not astrocytes as has been previously reported (Damjanac *et al.*, 2007). All of the Fluoro-Jade B positive cells were found to colocalise with NeuN.

Figure 3.7A-C shows representative stitched merged images of DRGs, showing colocalisation between Fluoro-Jade B positive cells (green) and NeuN staining (red) and Figure 3.8A-C shows representative images of Fluoro-Jade B staining in dorsal horn spinal cord sections in a lean/Veh, HFD/Veh and HFD/STZ rat respectively. The intensity of staining of any Fluoro-Jade B positive cells observed in this model was very low when compared to models which produce severe neurodegeneration, as can be seen in Figure 3.8D.

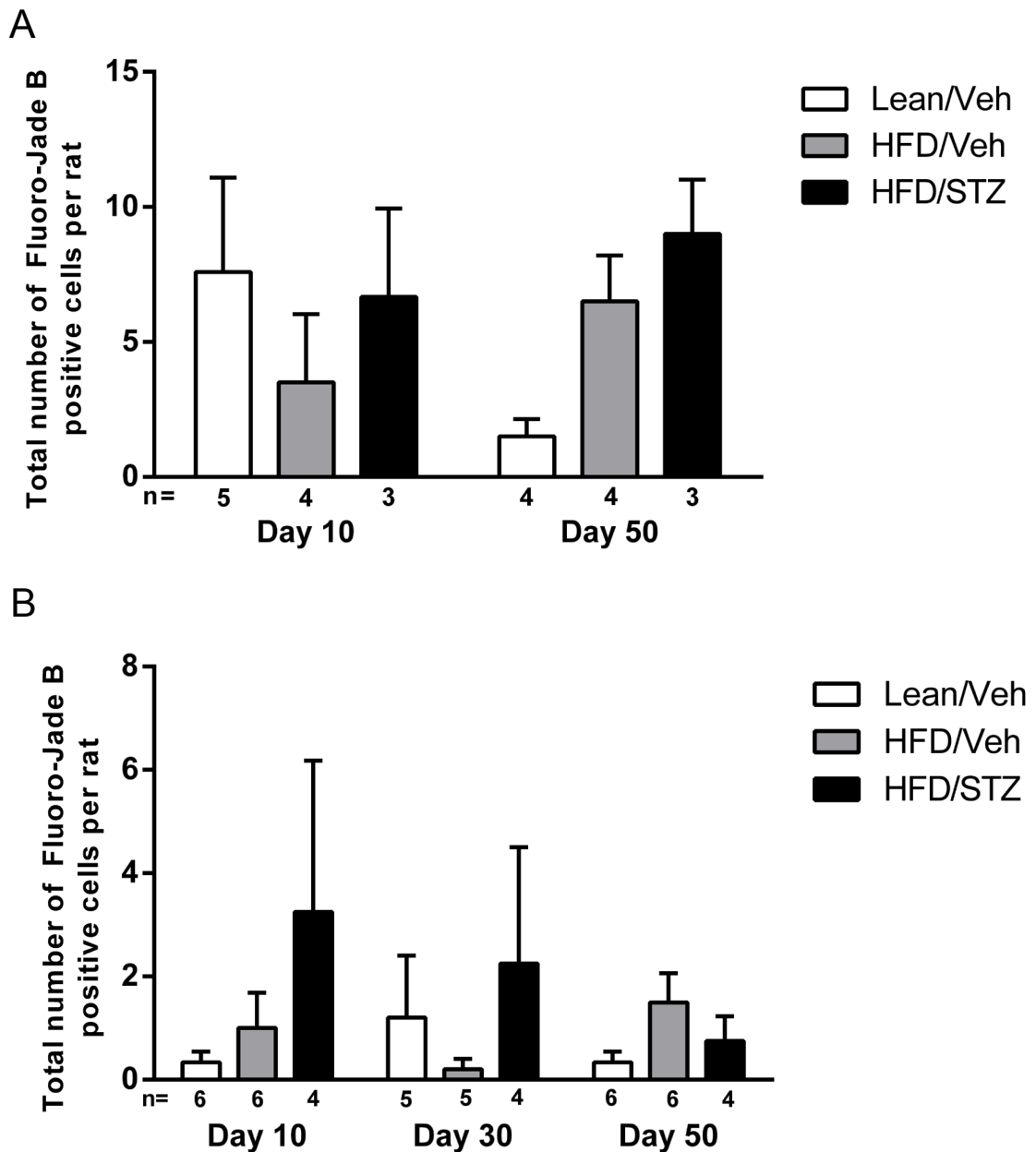


Figure 3.6 Effects of HFD/STZ on total number of Fluoro-Jade B positive cells per rat in **(A)** DRGs and **(B)** the dorsal horn of the spinal cord at different timepoints, in comparison with HFD/Veh and lean/Veh controls. n numbers, representing total number of rats, are displayed on the graphs (total number of Fluoro-Jade B positive cells in 7 spinal cord sections and 6 DRGs were quantified for each rat). All data represent mean \pm SEM, analysis was by a 2-way ANOVA.

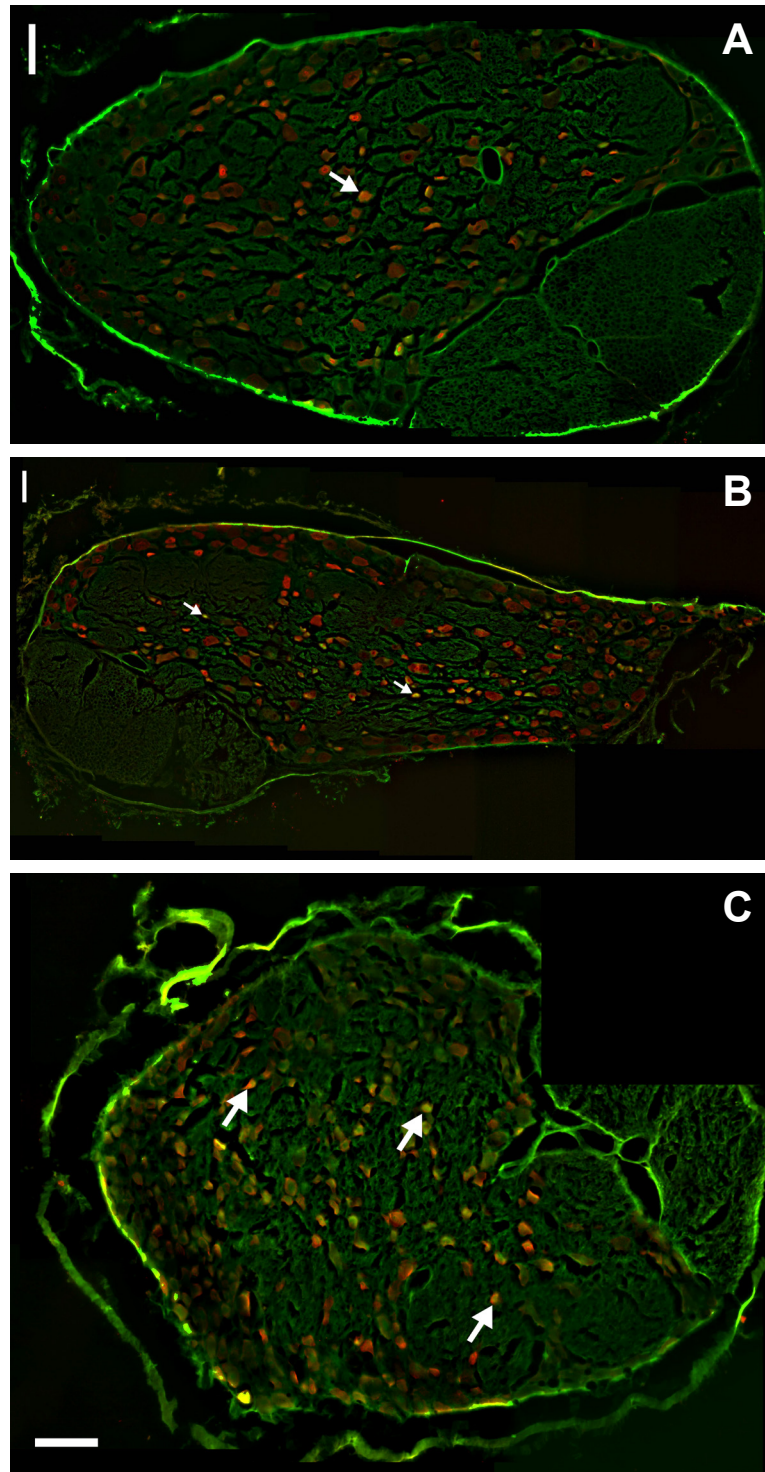


Figure 3.7 (A-C) Representative stitched merged images composed of 20x magnification tiles, showing colocalisation of Fluoro-Jade B staining (green) and NeuN staining (red) in DRGs in a Lean/Veh, HFD/Veh and HFD/STZ rat respectively. Scale bar is 100 μ m. Arrows indicate Fluoro-Jade B positive staining. Images have been altered in Image-J (minimum brightness set to 20, and maximum brightness set to 150 for Fluoro-Jade B, and 15 and 75 respectively for NeuN)

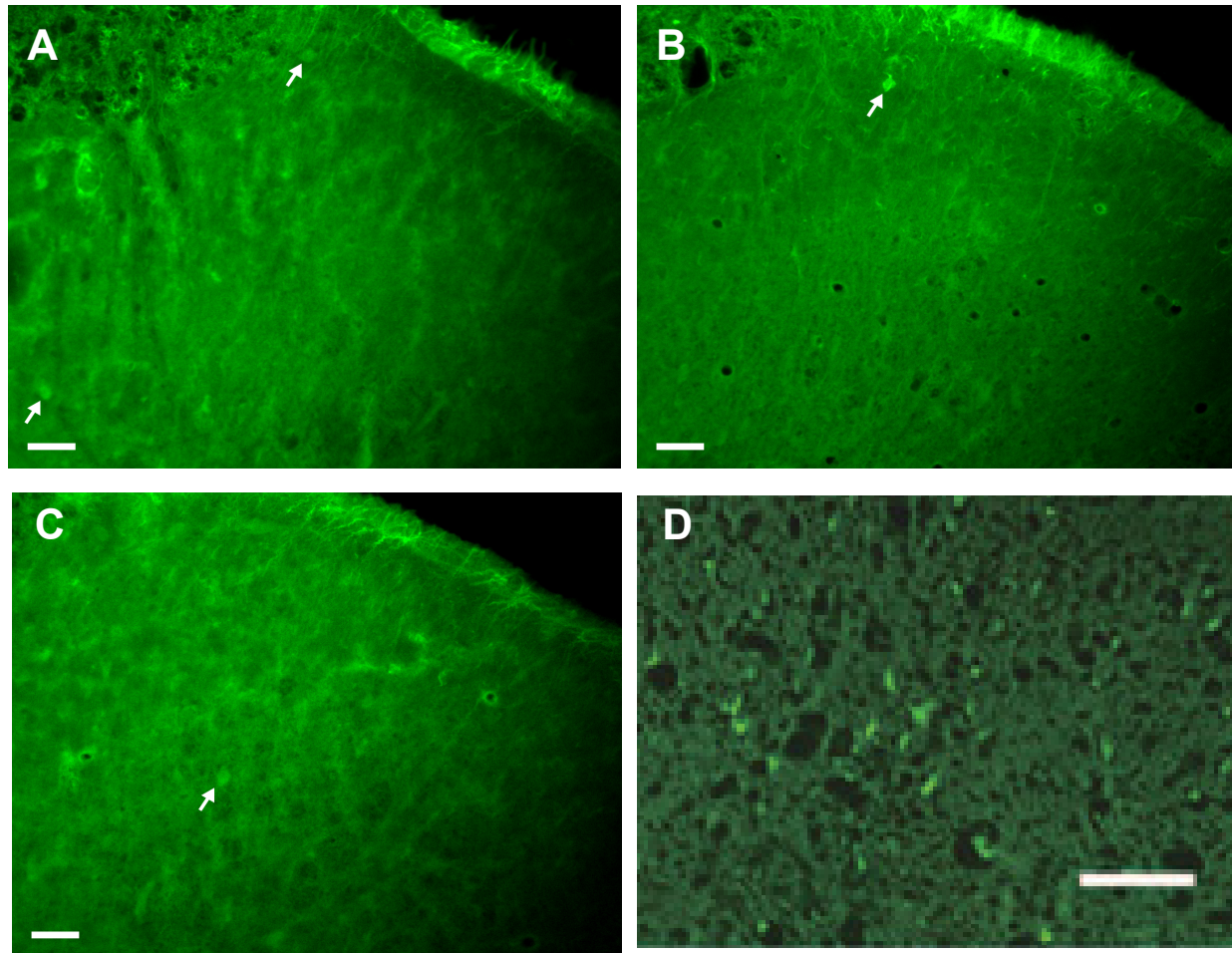


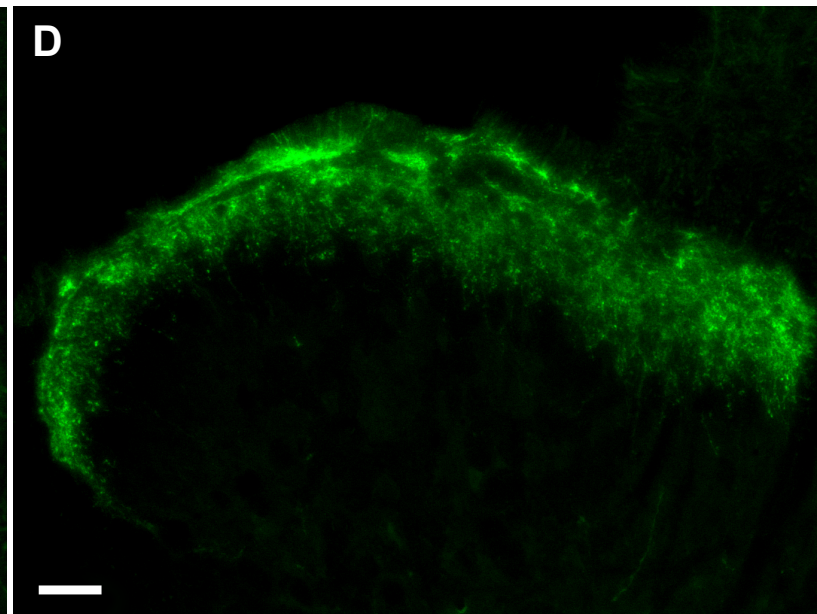
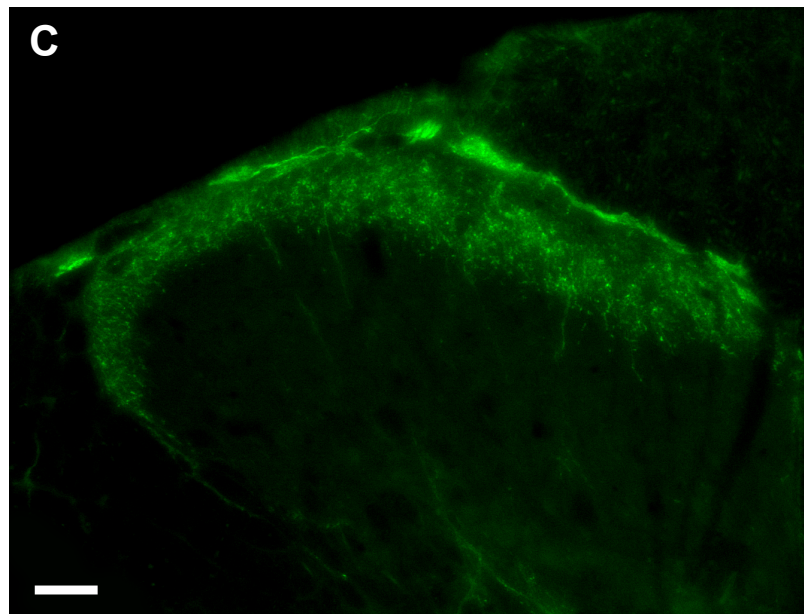
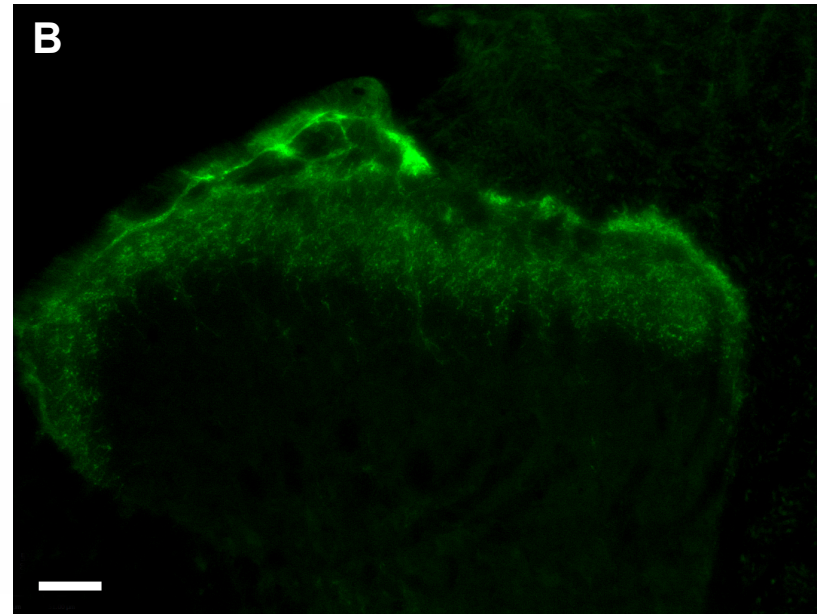
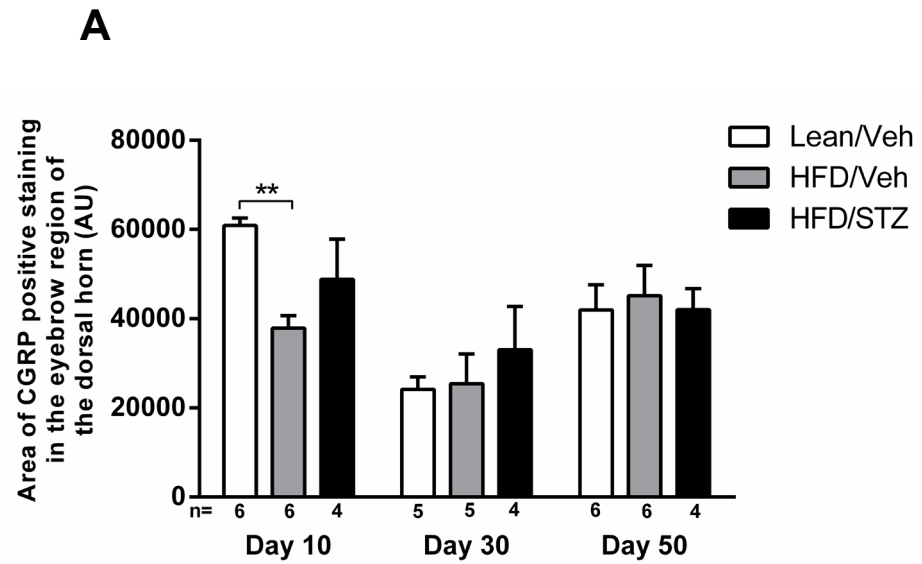
Figure 3.8 Scale bar is 50µm **(A-C)** Representative images at 20x magnification of Fluoro-Jade B staining in dorsal horn spinal cord sections in a Lean/Veh, HFD/Veh and HFD/STZ rat respectively. Arrows indicate positive staining. Images have been altered in Image-J (minimum brightness set to 20, and maximum brightness set to 150). **(D)** Image taken from Kudo *et al.* (2006) showing Fluoro-Jade B staining in the spinal cord after hemorrhagic shock and cardiac arrest, to compare intensity of staining.

3.3.4. Effects of HFD/STZ on expression of CGRP

The impact of the HFD/STZ model on peptidergic afferent fibre innervations into the dorsal horn was assessed by the quantification of CGRP immunofluorescence in the superficial laminae of the dorsal horn of the spinal cord. Overall, there were no differences in CGRP immunofluorescence in the superficial dorsal horn between any of the groups at any of the timepoints (Figure 3.9A), except for a significant decrease in the expression of CGRP in the HFD/Veh controls at day 10, in comparison to the lean/Veh group ($p < 0.01$). Figure 3.9B-D shows representative images of CGRP staining in dorsal horn spinal cord sections in a lean/Veh, HFD/Veh and HFD/STZ rat, respectively.

As seen on page 88:

Figure 3.9 (A) Effects of HFD/STZ on expression of CGRP in the superficial laminae of the dorsal horn, in comparison with HFD/Veh and lean/Veh controls. n numbers, representing total number of rats, are displayed on the graph (mean of 7 spinal cord sections per rat). All data represent mean \pm SEM, analysis was by a 2-way ANOVA with Bonferroni post-hoc test: ** $p < 0.01$. **(B-D)** Representative images at 20x magnification of CGRP staining in the superficial laminae of the dorsal horn of the spinal cord in a Lean/Veh, HFD/Veh and HFD/STZ rat respectively. Scale bar is 50 μ m. Images have been altered in Image-J (minimum brightness set to 20, and maximum brightness set to 100).



3.3.5. Effects of HFD/STZ on activation of glia

The number of activated microglia in the dorsal horn of the spinal cord was compared at different timepoints and between the different treatment groups. Although there were some small differences between the absolute numbers of activated microglia at the different timepoints in the lean/Veh and HFD/Veh groups, overall there was no significant change. In the HFD/STZ group there was a tendency for the number of activated microglia in the dorsal horn to be lower at all timepoints, but this was most evident at the later timepoints (Figure 3.10A). However statistical analysis with a 2-way ANOVA did not reveal any significant differences. It was evident, however, that there was a large amount of variability in the data, in particular at the early timepoints and in the lean/Veh and HFD/Veh groups. To overcome this issue the number of activated microglia in the HFD/Veh and HFD/STZ group were expressed as a percentage of the lean/Veh controls and a non parametric Mann-Whitney analysis was performed. This revealed a significant decrease ($p < 0.05$) in the number of activated microglia in the HFD/STZ group, in comparison with the HFD/Veh group at both day 30 and day 50 (Figure 3.10B). Analysis of the mean grey intensity of Iba1 staining revealed no differences between any of the groups at any of the different timepoints (Figure 3.10C). Figure 3.11A-C shows representative images of Iba1 staining in dorsal horn spinal cord sections in a lean/Veh, HFD/Veh and HFD/STZ rat respectively, with examples of activated microglia indicated with arrows.

The expression of GFAP in the dorsal horn of the spinal cord was also compared at different timepoints and between the different treatment groups. Again, there was no significant change in the expression of GFAP at the different timepoints in the lean/Veh and HFD/Veh treatment groups. In the HFD/STZ model there was a tendency for the expression of GFAP in the dorsal horn to be lower, and this was most evident at day 50 (Figure 3.12A). As with the microglia, statistical analysis with a 2-way ANOVA did not reveal any significant differences

as there was a large amount of variability in the data. When the expression of GFAP in the HFD/Veh and HFD/STZ group was expressed as a percentage of the lean/Veh control and a Mann-Whitney analysis was performed, this revealed a significant decrease ($p < 0.05$) in the expression of GFAP in the HFD/STZ group at day 50, in comparison with the HFD/Veh group. The expression of GFAP was also examined in the ventral horn and the central region, and this revealed a similar pattern, with a decrease in GFAP expression in the HFD/STZ group. In the ventral horn, a significant decrease ($p < 0.05$) can be seen in the HFD/STZ group, in comparison to both control groups at day 50, with no change evident until this later timepoint (Figure 3.12B). In the central region, a significant decrease in the HFD/STZ group, in comparison with both control groups is also seen at day 50, but in this region a decrease is also observed as soon as day 10, and this decrease is significant compared to the lean/Veh controls at this timepoint (Figure 3.12C). Figure 3.13A-C shows representative images of GFAP staining in dorsal horn spinal cord sections in a lean/Veh, HFD/Veh and HFD/STZ rat respectively.

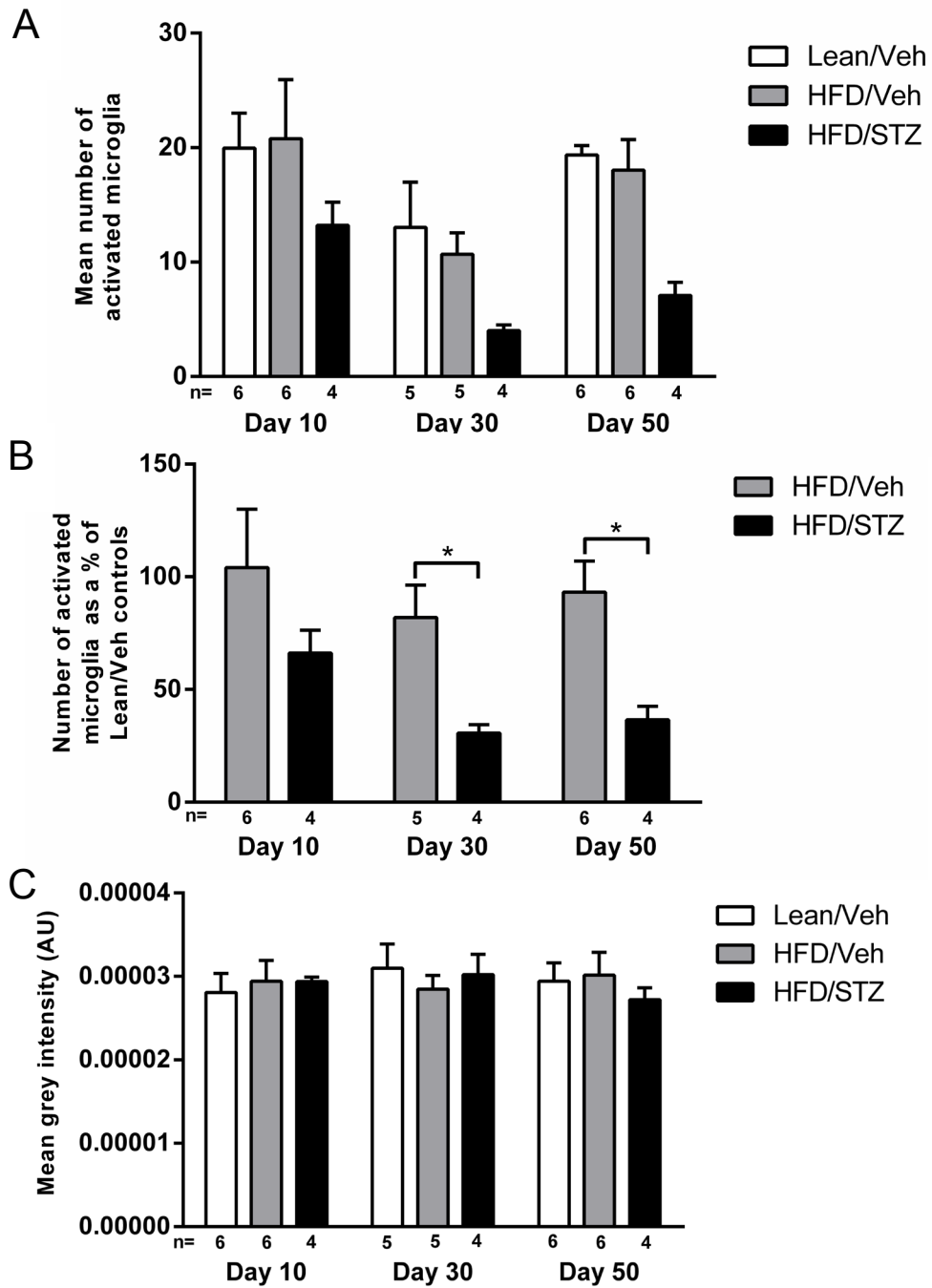


Figure 3.10 Effects of HFD/STZ on **(A)** number of activated microglia per quadrant in the dorsal horn **(B)** number of activated microglia (expressed as a percentage of lean/Veh controls) and **(C)** mean grey intensity of Iba1 staining in the dorsal horn at different timepoints, in comparison to HFD/Veh and lean/Veh controls. n numbers, representing total number of rats, are displayed on the graphs (mean of 7 spinal cord sections per rat). All data represent mean \pm SEM, analysis was by a 2-way ANOVA for A and C, and a Mann-Whitney test for B:

* $p < 0.05$

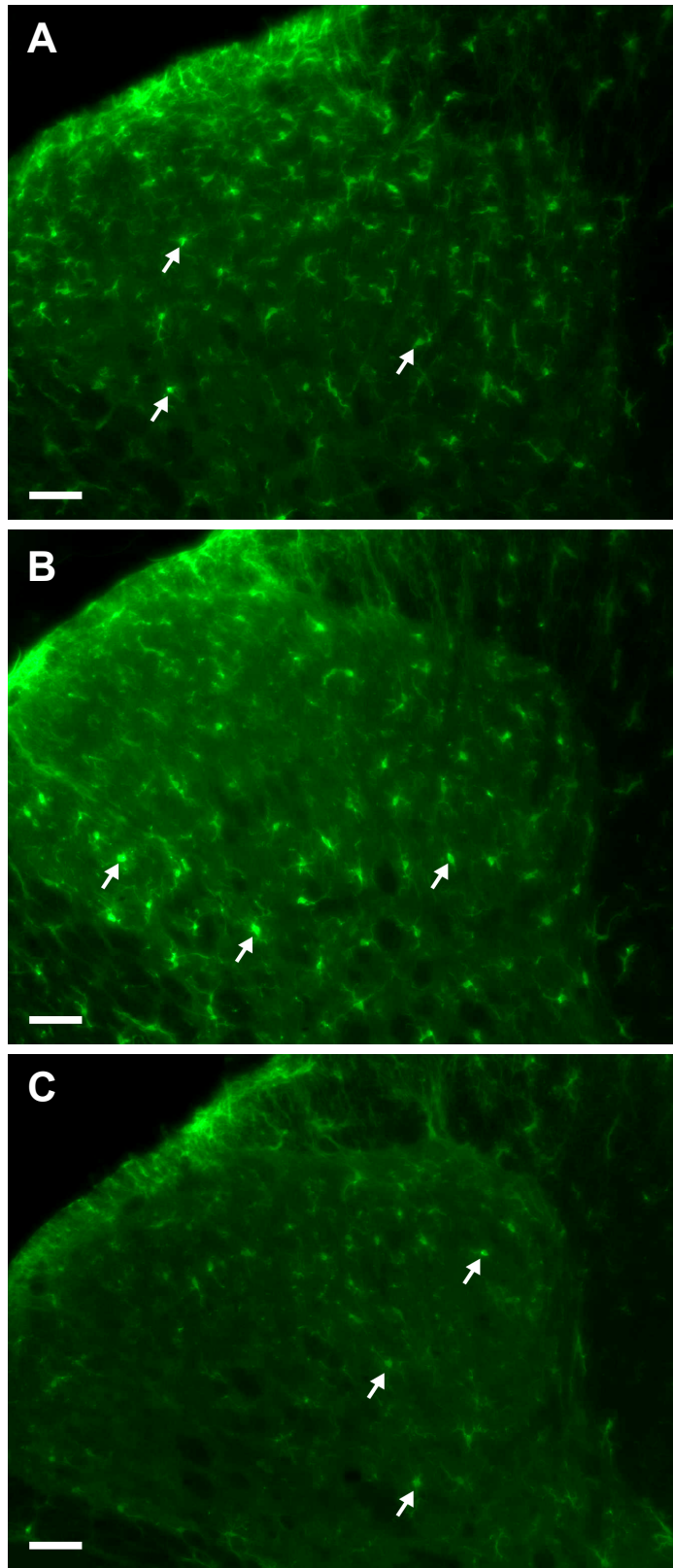


Figure 3.11 (A-C) Representative images at 20x magnification of Iba1 staining in the dorsal horn of the spinal cord in a Lean/Veh, HFD/Veh and HFD/STZ rat respectively. Scale bar is 50µm. Arrows indicate examples of activated microglia. Images have been altered in Image-J (minimum brightness set to 20, and maximum brightness set to 120).

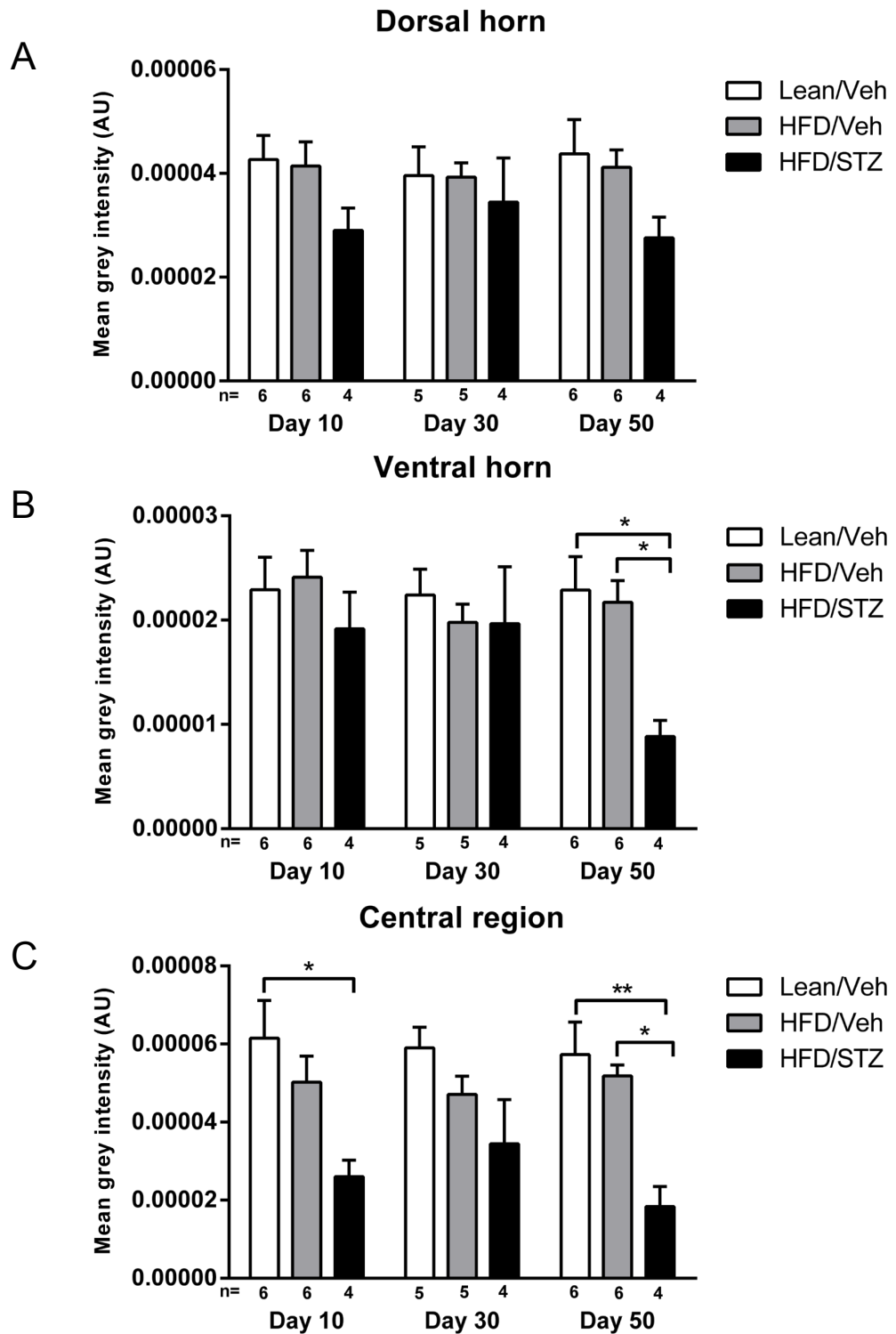


Figure 3.12 Effects of HFD/STZ on mean grey intensity of spinal GFAP immunofluorescence in the **(A)** dorsal horn, **(B)** ventral horn and **(C)** central region at different timepoints, in comparison with HFD/Veh and lean/Veh controls. n numbers, representing total number of rats, are displayed on the graphs (mean of 7 spinal cord sections per rat). All data represent mean \pm SEM, analysis was by a 2-way ANOVA with Bonferroni post-hoc test: * $p < 0.05$, ** $p < 0.01$

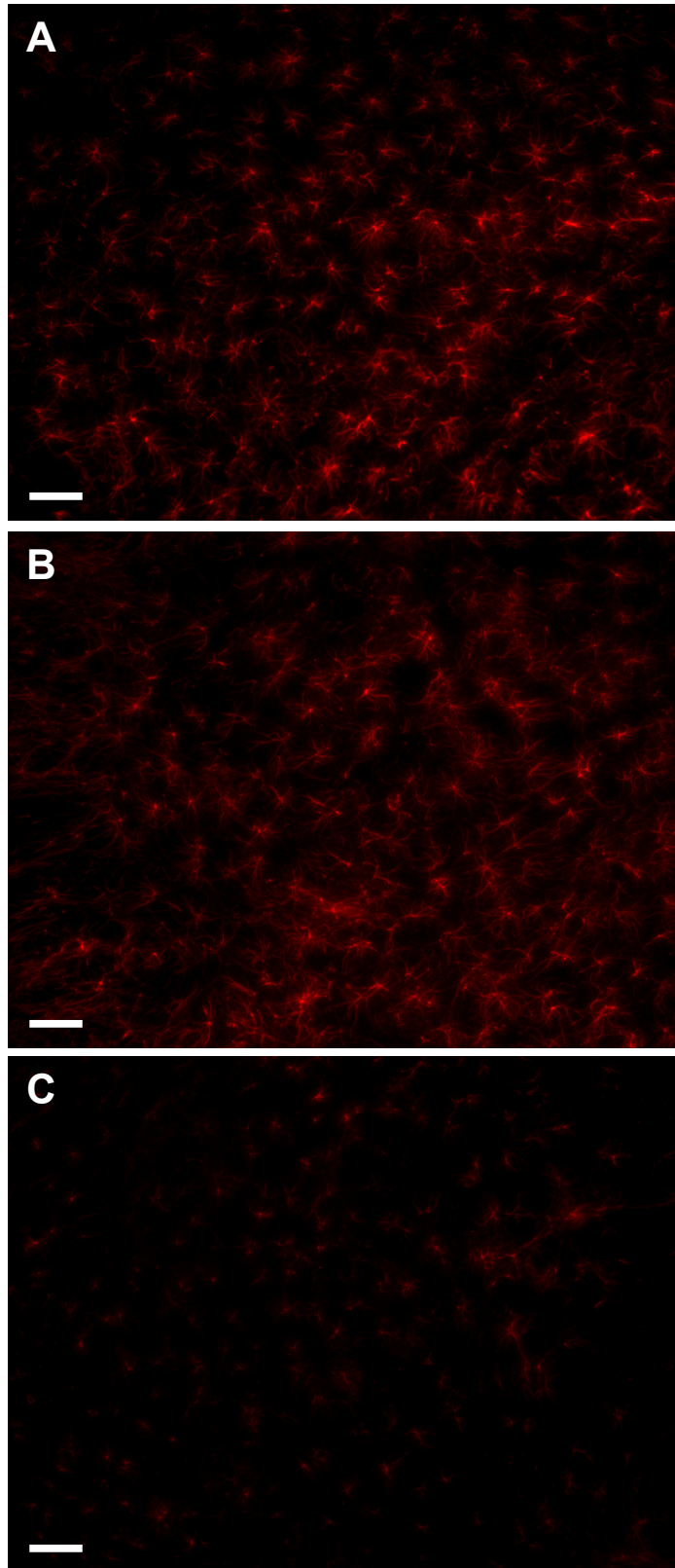


Figure 3.13 (A-C) Representative images at 20x magnification of GFAP staining in the ventral horn of the spinal cord in a Lean/Veh, HFD/Veh and HFD/STZ rat respectively. Scale bar is 50 μ m. Images have been altered in Image-J (minimum brightness set to 20, and maximum brightness set to 100).

3.4. Discussion

The inclusion of a lean/Veh group provided an important additional control to this study which was absent in Chapter 2. Specifically, this allowed me to demonstrate that the HFD produced an increase in glucose and insulin by the time the STZ injection was given, indicating that the rats may already be insulin resistant at this stage, as discussed in the previous chapter (Srinivasan *et al.*, 2005). The development of mechanical hypersensitivity in this study was consistent with the data presented in Chapter 2, although the decrease in mechanical withdrawal thresholds was evident at an earlier timepoint. The points at which tissue was collected represent timepoints: when there is no mechanical hypersensitivity (day 10); when there is an evident, but not maximal, decrease in withdrawal thresholds (day 30); and when mechanical hypersensitivity is well established (day 50). The aim was that using these timepoints would reveal any effects of time on the parameters being investigated.

The present study investigated the impact of the HFD/STZ model on peripheral nerve function. The number of Fluoro-Jade B positive cells in DRGs and spinal cord was assessed to determine the presence of neuronal degeneration. No changes in the total number of Fluoro-Jade B positive cells in the DRG or spinal cord are reported, with numbers of Fluoro-Jade B cells being very low in all groups. Immunohistochemistry was also used to investigate potential changes in the expression of CGRP, and activation of microglia and astrocytes in the spinal cord in the HFD/STZ model. Reports from previous studies of animal models of diabetes have been mixed, and some of the results herein are consistent with the current literature whereas others are at odds with what has been seen previously. The HFD/STZ model elicited no significant changes in CGRP expression in the spinal cord. A decrease in activated microglia in the dorsal horn was observed, and there was a significant decrease in GFAP expression in the dorsal and ventral horn,

as well as the central region, which became more obvious at the latest time point - 50 days after STZ injection.

3.4.1. Fluoro-Jade B staining

The number of Fluoro-Jade B positive cells present in the DRGs and dorsal horn of the spinal cord was very low in all three groups, and HFD/STZ had no significant effect on the number of positive cells. As Fluoro-Jade B stains for dying or degenerating neurones, this would suggest that there is very little neurodegeneration taking place in the HFD/STZ model at the timepoints studied. The intensity of the Fluoro-Jade B staining was also very low when compared to previous studies by other groups who used Fluoro-Jade in the spinal cord, where a very obvious staining of neurones was reported. However, these studies used models of ischemia, acute inflammation or neurodegeneration, where any neuronal death is very apparent (Kudo *et al.*, 2006; Nguyen *et al.*, 2004; Orendacova *et al.*, 2005; Saganová *et al.*, 2006). In future, it would be advantageous to also run a control group of rats which underwent an ischemic insult, so that the Fluoro-Jade B positive staining in the HFD/STZ model could easily be compared to the changes seen in a robust model of neuronal degeneration.

All of the Fluoro-Jade B positive cells were colocalised with NeuN, confirming that they were neurones. In a previous study, no colocalisation between Fluoro-Jade positive cells and NeuN was observed in a model using a moderate hypoglycaemic insult (Tkacs *et al.*, 2005). They hypothesised that when neurones undergo cell death, NeuN is broken down, and so this, along with the very low intensity staining of Fluoro-Jade B would suggest that any neurodegeneration taking place is not in the advanced stages.

Consistent with my data, no neuronal death has been detected with Fluoro-Jade in the brain of STZ rats at 2 or 8 weeks (Bree *et al.*, 2009; Lechuga-Sancho *et al.*, 2006; Won *et al.*, 2012), and so it is possible that no neuronal death occurs in diabetic rats until later timepoints.

These results in the spinal cord are in agreement with what has been seen in the literature so far. As reviewed in Mizisin *et al.* (2007), no changes in the grey matter of the spinal cord have been reported in animal models of diabetic neuropathy, with reductions in perikaryal volume of motor and sensory neurones, but no signs of neuronal degeneration (Sidenius *et al.*, 1980). However there have been conflicting reports about whether there is structural injury and neuronal loss in sensory ganglia. Two studies have revealed a significant increase in apoptosis in the DRG at 1 month (Russell *et al.*, 1999), and also 3 and 12 months following STZ treatment in rats (Schmeichel *et al.*, 2003). Zochodne *et al.* (2001) examined neuronal numbers in dorsal root ganglion at 2 and 12 months after STZ injection, and reported a significant reduction in neurone diameter and area, and a trend towards a decrease in neuronal number at the later timepoint. These results were confirmed in a similar study, with no neuronal loss observed, but instead an increase in the ratio of small type-B neurones to large type-A neurones (Kishi *et al.*, 2002), with a similar pattern observed at 1 month (Sidenius *et al.*, 1980). No neuronal loss has been reported in the DRG at 3 months in STZ treated rats (Severinsen *et al.*, 2007). In the diabetic BB rat, there is no change in neurone number at 4 months (Kamiya *et al.*, 2005b), but there is severe neuronal loss of SP and CGRP neurones in the DRG at 10 months of age (Kamiya *et al.*, 2006). In the present study, the latest timepoint was 7 weeks, and so in agreement with the aforementioned studies, no neuronal degeneration/loss was observed at this early stage of diabetic neuropathy. It would therefore be interesting to carry out a longer term study, to see if these effects could be observed after a longer duration of diabetes in this model. These data add to the hypothesis that the STZ model should be considered a model of the early stages of diabetic neuropathy, as it does not exhibit the sort of structural changes in nerves that we would expect to see in human diabetic neuropathy (Wattiez *et al.*, 2012).

3.4.2. CGRP expression

Changes in the levels of CGRP in diabetic animal models have not yet been fully elucidated. So far there have been reports of an increase in: the basal release of CGRP in the skin (Ellington *et al.*, 2002), the capsaicin-stimulated release of CGRP in the skin and spinal cord (Bishnoi *et al.*, 2011; Ellington *et al.*, 2002), and the number of CGRP-positive fibres in skin (Karanth *et al.*, 1990), whereas no change has been seen in: the levels of CGRP immunoreactive neurones in the nodose ganglion of the vagus nerve (Regalia *et al.*, 2002) or the spinal cord and DRG (Jiang *et al.*, 2004; Terenghi *et al.*, 1994). Conversely, a decrease has been seen in: CGRP content in the vagus nerve (Calcutt *et al.*, 1998), and the sciatic nerve (Brewster *et al.*, 1994; Diemel *et al.*, 1994), the number of CGRP-positive neurones in the DRG (Adeghate *et al.*, 2006), and finally the expression of CGRP mRNA in the DRG (Zochodne *et al.*, 2001) and sciatic nerve (Diemel *et al.*, 1992). Therefore the results reported here of no significant changes in CGRP expression in the spinal cord add another piece of the puzzle, but the full picture of the role of CGRP in diabetic neuropathy is yet to be elucidated.

3.4.3. Microglial activation

The changes in the number of Iba1 positive cells morphologically identified as activated microglia in the spinal cord in this study are not in agreement with the existing literature. In general, an upregulation of activated microglia in the spinal cord has been reported in STZ treated rats over a similar timescale to that investigated in this study. Changes in the number of activated microglia are seen as soon as 4 days after STZ injection (Talbot *et al.*, 2010), and then at various timepoints over the following five weeks. However the method by which activation of microglia is calculated varies between the different studies. Some use Iba1 as a marker of microglia (Talbot *et al.*, 2010; Tsuda *et al.*, 2008; Wodarski *et al.*, 2009), whereas others used CD11b/OX-42 (Kim *et al.*,

2012b; Morgado *et al.*, 2011a; Tsuda *et al.*, 2008). Whereas Iba1 stains all microglia, and their activation state can then be assessed by morphological changes, CD11b only stains classically activated microglia, and will not stain for alternatively activated or 'resting' microglia. In these studies, activation of microglia is then assessed by calculating mean pixel energy (Talbot *et al.*, 2010), or by densitometric analysis (Morgado *et al.*, 2011a), whereas others count cell bodies stained with Iba1 (Tsuda *et al.*, 2008; Wodarski *et al.*, 2009), and some go further and assess whether the microglia being counted appear activated. In future studies looking at microglia in the diabetic model, it would be sensible to use both antibodies, and a consistent method of detecting activation so that results could be more easily compared between groups. In this study, Iba1 was used, and only activated microglia were counted, assessed as those displaying large cell bodies and thickened retracted processes (Eriksson *et al.*, 1993). As the expected increase in microglial activation was not observed using this method, the mean grey intensity of these sections was also calculated to see whether this method would confirm these findings. Using this method, no change in Iba1 expression was seen between any of the three groups at the three different timepoints. As the greater numbers of activated microglia in the lean/Veh and HFD/Veh controls would be expected to show an increased expression of Iba1 (Tsuda *et al.*, 2005), it is possible that although there were fewer activated microglia in the HFD/STZ group, there was actually an overall increase in the number of microglia, even if they did not show the classic changes in morphology that are indicators of activation.

Tsuda *et al.* (2008) also investigated whether microglial activation was altered in different segments of the spinal cord, and found that they were most strongly activated in the L4 segment, with weaker Iba1 immunofluorescence in segments L5 and L6. In this study lumbar regions 4-6 of the spinal cord were all cut together, and so the different segments were unable to be identified with certainty, and so any positive results that may have been seen in L4 may have been masked

by the inclusion of L5 and 6. Therefore in a future study, these lumbar regions should be cut separately to see whether there are more regional specific changes

Another factor that would be interesting to investigate in future immunohistochemistry studies in the HFD/STZ model, would be to double-label cells with markers for phospho-ERK (Morgado *et al.*, 2011a; Sweitzer *et al.*, 2004; Tsuda *et al.*, 2008) and phospho-p38 (Morgado *et al.*, 2011a; Sweitzer *et al.*, 2004), as these MAPK pathways are often activated in microglia. As no increase in the number of activated microglia was observed in this study, double-labelling with these markers would either confirm that there is less activation of microglia, or may be able to show that although no increase in number is seen, there is in fact an increase in the activation of these MAPK pathways in the microglia, despite no change in the phenotypic state. It would also be of interest to see whether treatment with minocycline, which inhibits activation of microglia, would be effective at preventing the development of mechanical hypersensitivity in the HFD/STZ model. All of these further ideas would help to explain, or build upon, the results observed in this study.

3.4.4. Astroglial activation

To date previous studies of GFAP expression in the spinal cord in the STZ model have been mixed. A decrease in GFAP immunoreactivity has been reported by some groups (Afsari *et al.*, 2008; Wodarski *et al.*, 2009), no change by others (Tsuda *et al.*, 2008), and finally an increase in GFAP immunoreactivity in one recent report (Kim *et al.*, 2012b). My data report a significant decrease in GFAP-immunoreactive astrocytes in three different regions of the spinal cord in the HFD/STZ model, which is particularly evident at the latest timepoint. This finding is in agreement not only with studies in the spinal cord, but also in other regions of the CNS such as the brain and the retina, where decreases in GFAP expression have also been reported (Barber *et al.*, 2000;

Coleman *et al.*, 2004; de Senna *et al.*, 2011; Lechuga-Sancho *et al.*, 2006; Renno *et al.*, 2012; Rungger-Brandle *et al.*, 2000; Zuo *et al.*, 2011).

It is important to note that although a decrease in GFAP immunoreactivity in the brain of STZ treated rats has previously been reported, this did not correlate with a decrease in astrocyte number *per se* (Coleman *et al.*, 2004). The basis for these decreases in GFAP immunoreactivity may be related to the large decrease in insulin exhibited in these models (Afsari *et al.*, 2008). Co-application of insulin and thyroid hormone has been shown to alter the morphology of astrocytes, with cell processes becoming thicker and more distinct, as well as increasing the activity of glutamine synthase (Aizenman *et al.*, 1987), and enhancing the expression of GFAP in astrocytes (Toran-Allerand *et al.*, 1991). These effects of insulin on astrocytes were reversible (Aizenman *et al.*, 1987), suggesting that insulin may play an important role in regulating normal astrocytic function. The decrease in GFAP-immunoreactive astrocytes demonstrated in HFD/STZ rats may be indicative of an altered metabolic and functional role, meaning that the astrocytes are unable to maintain their neuronal support role in the CNS (Afsari *et al.*, 2008). This idea is further consolidated by the demonstration that insulin treatment restores GFAP levels in the diabetic STZ-treated rat (Coleman *et al.*, 2010).

The changes in GFAP immunoreactivity suggest that the contribution of astrocytes to spinal cord homeostasis in this model may be altered. Glutamate-transporter 1 (GLT-1 or EAAT2), and glutamate/aspartate transporter (GLAST) are predominantly expressed in astrocytes, with GLT-1 found predominantly in the superficial dorsal horn (Regan *et al.*, 2007; Rothstein *et al.*, 1994; Xin *et al.*, 2009). In nerve injury models of pain, astrocyte activation has been associated with decreased GLT-1 and GLAST (Sung *et al.*, 2003; Xin *et al.*, 2009), as well as a decrease in other glutamate transporters, such as excitatory amino-acid carrier 1 (Sung *et al.*, 2003; Wang *et al.*, 2006), resulting in a decrease in

glutamate uptake (Binns *et al.*, 2005). Whether the decrease in GFAP staining reported herein in the HFD/STZ model is associated with a decrease in these transporters remains to be determined. It has been hypothesised that decreased GLT-1 expression can lead to pain hypersensitivity, due to enhanced glutamatergic synaptic neurotransmission (Nakagawa *et al.*, 2010), and inhibition of glutamate transporters has been shown to produce spontaneous nociceptive behaviours and thermal and mechanical hypersensitivity (Liaw *et al.*, 2005; Weng *et al.*, 2006).

No changes in GLT-1 or GLAST expression, but an increased uptake of glutamate was observed in the brain of 4 and 8 week STZ treated rats (Coleman *et al.*, 2004; Coleman *et al.*, 2010). An increase in the level of glutamate in the peripheral nerve in 4 week STZ treated rats has also been reported (Li *et al.*, 2004), but the presence of mechanical hypersensitivity was not investigated in any of these studies. GCP11, which reduces glutamate release, attenuated hyperalgesia in the BB rat (Zhang *et al.*, 2006b). It would therefore be interesting to see whether the expression of GLTs, and the levels of glutamate, are altered in the spinal cord of HFD/STZ rats.

In conclusion, I have demonstrated a decrease in GFAP expression in the spinal cord, no change in CGRP expression, and no neuronal degeneration induced in the HFD/STZ model by 7 weeks. However, a decrease in activated microglia was observed in this study, and this warrants further investigation to see whether this result can be repeated in this model. As pain behaviour is evident in the HFD/STZ model, and some of the changes described in this chapter only go part way to explaining its development, the next stage was to investigate whether there is a change in neuronal responses, which was investigated in Chapter 4.

Chapter 4.

Electrophysiological characterisation of spinal neuronal responses in the HFD/STZ model of diabetes, and the effects of pioglitazone intervention

4.1. Introduction

4.1.1. Involvement of primary afferent fibres in the STZ model

A β -, A δ - and C-fibres have all been postulated to be important in the development of painful symptoms in diabetic neuropathy. Sustained mechanical stimulation (Chen *et al.*, 2001) and noxious chemical stimuli (Chen *et al.*, 2003) have been shown to elicit a greater number of action potentials in C-fibres in the STZ model than in controls, with only a subset of C-fibres (1 in 3) being markedly hyper-responsive (Ahlgren *et al.*, 1992; Chen *et al.*, 2003; Chen *et al.*, 2001). In agreement with this, a facilitation of responses to suprathreshold mechanical stimulation in C-fibres (Ahlgren *et al.*, 1994; Ahlgren *et al.*, 1992; Suzuki *et al.*, 2002), as well as an increase in spontaneous firing, and a decrease in response thresholds in response to ramp-pressure stimulation have all been observed in STZ rats (Suzuki *et al.*, 2002). This increase in afferent firing may lead to sensitisation of spinal nociceptive circuits (Kamiya *et al.*, 2005a).

Other groups have hypothesised that A β - and A δ -fibres also play a role in the development of painful symptoms. When resiniferatoxin was used to desensitise unmyelinated C-fibres, the development of mechanical hypersensitivity was unaffected in the STZ model (Khan *et al.*, 2002). Indeed, A β - and A δ -fibres developed abnormal spontaneous discharges, a decrease in their activation threshold, and an increase in evoked responses to von Frey filaments. A decrease in mechanical thresholds in A δ -fibres has also been seen in STZ treated rats between 3-7 weeks (Ahlgren *et al.*, 1992).

4.1.2. Involvement of WDR neurones in the dorsal horn of the spinal cord in the STZ model

As discussed in Chapter 1, the spinal cord plays a pivotal role in the integration and modulation of noxious inputs, and is a critical site involved in sensitisation mechanisms associated with chronic pain. Previous studies in models of diabetes have shown that dendritic spine remodelling in the spinal cord is seen at 4 weeks after STZ injection when mechanical hypersensitivity and hyperalgesia are apparent, but not before the painful symptoms develop at 1 week, suggesting that this too may play a role in neuropathic pain (Tan *et al.*, 2012). They also examined the activity of WDR neurones at L4-L5 in the spinal cord in the STZ model at 4 weeks, and an increase in spontaneous activity, enlarged receptive fields and increased peripherally evoked responses to brush, press, pinch and von Frey stimuli was observed (Tan *et al.*, 2012). An increase in the response of somatic WDR neurones to a brush stimulus in 4-11 week STZ treated rats was also seen when the thoracic region, T3, of the spinal cord was examined (Ghorbani *et al.*, 2011).

In a previous study of spinal dorsal horn WDR neurone activity (T12-L2) in 6 week STZ treated rats, an increase in spontaneous activity was reported (Pertovaara *et al.*, 2001), but there was no change in noxious heat-evoked responses, after discharges, or receptive field size, and there was a decrease in the responses evoked by mechanical stimulation (2, 4, 12 and 75g von Frey hairs).

Previous studies in STZ rats have therefore consistently demonstrated an increase in the spontaneous activity of WDR neurones, but the impact of these models of diabetic neuropathy on evoked responses of spinal neurones is less consistent. This may reflect the different models and timescales involved, as well as the experimental methods such as the depth of anaesthesia. It will be interesting to explore this aspect in

the HFD/STZ model to see how evoked neuronal responses to mechanical and electrical stimulation are altered.

4.1.3. Pioglitazone and other PPAR γ agonists

Pioglitazone is one of a class of drugs called the thiazolidinediones that are used to treat type 2 diabetes. The TZDs act on the nuclear receptor PPAR γ and their mechanisms of action are discussed in Chapter 1. Recently it has been demonstrated that they may also play a positive role in diseases such as atherosclerosis, cancer and neurodegenerative disorders such as Alzheimer's disease (Churi *et al.*, 2008). They have also shown promise in alleviating inflammatory and neuropathic pain through a variety of different mechanisms, as discussed below. I was therefore interested in investigating a potential role of pioglitazone in alleviating the mechanical hypersensitivity that is observed in the HFD/STZ model.

4.1.4. PPAR γ agonists in inflammatory pain

Table 4.1 summarises the effects of the PPAR γ agonists: 15-Deoxy- Δ -12,14-prostaglandin J₂ (15d-PGJ₂, a natural agonist of PPAR γ (Desvergne *et al.*, 1999)), rosiglitazone, and pioglitazone, in the carrageenan and post-incisional models of inflammatory pain. It can be seen that they are able to reduce inflammation, and that these effects were blocked by bisphenolAdiglycidyl ether (BADGE) or GW9662, two PPAR γ antagonists, indicating that their effects are mediated through this receptor (Cuzzocrea *et al.*, 2004; Morgenweck *et al.*, 2010).

It is hypothesised that these PPAR γ agonists might work by regulating macrophage polarity to induce an analgesic effect, which is elaborated on in the discussion, and transplanting rosiglitazone-treated peritoneal macrophages to the injured site in the post-incisional model had an analgesic effect (Hasegawa-Moriyama *et al.*, 2012; Takahashi *et al.*, 2011).

Table 4.1 Summary of the effects of acute doses of PPAR γ agonists in various models of inflammatory pain.

Drug	Model	Behavioural Outcomes	Biochemical outcomes	Reference
Rosiglitazone 100mgkg ⁻¹ , i.p.	Carrageenan in rats	-	Inhibited paw oedema (only when given before carrageenan)	(Taylor <i>et al.</i> , 2002)
Rosiglitazone 10mgkg ⁻¹ , i.p.	Carrageenan in rats	-	Inhibited paw oedema, and attenuated the increase in PARP, iNOS and COX-2 in the lungs. Effects blocked by BADGE	(Cuzzocrea <i>et al.</i> , 2004)
Pioglitazone 25-50mgkg ⁻¹ , i.p.	Carrageenan in rats	No effect on mechanical hypersensitivity	Inhibited paw oedema	(Oliveira <i>et al.</i> , 2007)
15d-PGJ2 200 μ g, i.t. Rosiglitazone 50 μ g, i.t.	Carrageenan in rats	Reduced thermal hyperalgesia	- Inhibited paw oedema - Attenuated increase in Fos-staining in the dorsal horn	(Morgenweck <i>et al.</i> , 2010)
Rosiglitazone 10 μ g into the paw	Post-incisional pain in mice (induces paw swelling and infiltration of immune cells)	Attenuated thermal hyperalgesia and mechanical hypersensitivity	- Inhibited paw oedema - Attenuated the infiltration of immune cells - Increased the ratio of M1 (pro-inflammatory): M2 (anti-inflammatory) macrophages	(Hasegawa-Moriyama <i>et al.</i> , 2012)

4.1.5. PPAR γ agonists in neuropathic pain

Table 4.2 summarises the effects of PPAR γ agonists in different models of neuropathic pain. The effects of these drugs are thought to be mediated, at least in part, by actions at the level of the spinal cord; perhaps through decreasing the activation of microglia, leading to a decrease in pro-inflammatory cytokines, and modifying central sensitisation. This could explain their long lasting effects after administration has ceased.

4.1.6. PPAR γ agonists in diabetic neuropathy

A limited number of studies have also evaluated the effects of PPAR γ agonists in models of diabetic neuropathy. Troglitazone treatment was shown to protect against the slowing of NCV and fibre atrophy in STZ rats, as well as acting as a free radical scavenger and reducing TNF α production (Qiang *et al.*, 1998). Rosiglitazone treatment was able to improve thermal hypoalgesia, as well as reducing oxidative stress in the sciatic nerve in STZ-treated mice, without having any effect on hyperglycaemia (Wiggin *et al.*, 2008). Evidence that rosiglitazone activated genes responsible for glucose metabolism, as well as oxidoreductase activity has been generated using microarray analysis (Wiggin *et al.*, 2008). Pioglitazone has also been shown to be effective at reducing oxidative stress (Majithiya *et al.*, 2005), as well as having a neuroprotective effect on NCV, restoring PKC activity, decreasing levels of ERK activity, and reducing macrophage infiltration in the STZ model (Yamagishi *et al.*, 2008).

Table 4.2 Summary of the effects of PPAR γ agonists in various models of neuropathic pain.

i.p: intraperitoneal; p.o: oral; i.t: intrathecal; i.c.v: intracerebroventricular; SNI: spared nerve injury; PNL: partial sciatic nerve ligation; CA: cold allodynia; MH: mechanical hypersensitivity; BADGE and GW9662 are PPAR γ antagonists

Drug	Model	Behavioural Outcomes	Biochemical outcomes	Reference
15d-PGJ2 100-200 μ g, i.t. Rosiglitazone 200 μ g, i.t. Acute dose	SNI in rats	<ul style="list-style-type: none"> - Decreased MH and CA - Effects blocked by BADGE - i.p./i.c.v administration were ineffective 	-	(Churi <i>et al.</i> , 2008)
Pioglitazone 0.3-30mgkg ⁻¹ , p.o. 1 - 10 mgkg ⁻¹ , i.p. Various	SNI in rats	<ul style="list-style-type: none"> - 7 days pre-SNI and 7 weeks post-SNI prevented mechanical and cold hypersensitivity - A single injection 15 minutes before SNI reduced hyperalgesia for the next 2 weeks. - 2 x daily injections for 7 days, 24 hours after SNI, decreased established hypersensitivity - Pioglitazone was still effective for a week after its termination - GW9662 blocked the ameliorative effects of pioglitazone 	<ul style="list-style-type: none"> - Attenuated the increase in GFAP-positive staining in the spinal cord - Attenuated the increase in p-ERK in the dorsal horn 	(Morgenweck <i>et al.</i> , 2013)
Pioglitazone 1-25mgkg ⁻¹ , p.o. 4 days	PNL in mice	Prevented the development of MH	Attenuated the increase in activated microglia	(Iwai <i>et al.</i> , 2008)

<p>Pioglitazone 25 mgkg⁻¹, p.o. Various</p>	<p>PNL in mice</p>	<ul style="list-style-type: none"> - Prevented the development of MH when administered for one week after PNL, and for a week after administration had ceased. - Reduced the magnitude of established MH when given on days 7 to 13, but a single acute dose had no effect 	<p>Attenuated the increase in TNF-α and IL-6 when administered for 7 days</p>	<p>(Maeda <i>et al.</i>, 2008).</p>
<p>Rosiglitazone 10 mgkg⁻¹, i.p. Day 1-3, 5-7 or 26-28</p>	<p>PNL in mice</p>	<ul style="list-style-type: none"> - Early administration attenuated the development of MH - No effect at the later timepoint 	<ul style="list-style-type: none"> - Early administration attenuated the increase in activated microglia and MMP-9, iNOS, and COX-2 	<p>(Takahashi <i>et al.</i>, 2011)</p>
<p>Rosiglitazone 5-10mgkg⁻¹, p.o 28 days</p>	<p>Tibial and sural nerve transection in rats</p>	<p>Attenuated mechanical and cold hyperalgesia, but not thermal hyperalgesia</p>	<p>Attenuated the increase in GSH, and the decrease in myeloperoxidase activity (a specific marker of inflammation)</p>	<p>(Jain <i>et al.</i>, 2009)</p>
<p>Pioglitazone 10mgkg⁻¹, p.o. 14 days</p>	<p>Spinal nerve transection in rats</p>	<p>Prevented the development of MH and mechanical hyperalgesia</p>	<ul style="list-style-type: none"> - Attenuated the increase in TNF-α, IL-6 and IL-1β and inhibited the activation of NFκB. - Attenuated the increase in GFAP-positive staining in the spinal cord 	<p>(Jia <i>et al.</i>, 2013; Jia <i>et al.</i>, 2010)</p>

4.1.7. Aim of the study

The primary aim of the work in this chapter was to characterise the impact of the HFD/STZ model of diabetes on the electrically and mechanically evoked responses of WDR neurones in the dorsal horn of the spinal cord at 7 and 11 weeks after model induction.

The second aim of this study was to investigate the ability of the PPAR γ ligand pioglitazone to alter already established mechanical hypersensitivity in the HFD/STZ model, and to determine whether this was associated with changes in the response profiles of WDR neurones in the spinal cord in HFD/STZ rats.

4.2. Methods

For detailed methods of induction of diabetes, blood sampling and von Frey testing see Chapter 2.

4.2.1. Animals

All experiments were carried out under Home Office Licence 40/3124, in accordance with the UK Home Office Animals (Scientific Procedures) Act 1986 and IASP guidelines. 47 male Sprague-Dawley rats (200-250g), obtained from Charles River (Kent, UK), were individually housed on a normal light cycle (lights on: 07:00 - 19:00) with free access to either normal chow or a high fat diet (60% fat by caloric content; D12492 diet; Research Diets, New Jersey, USA) and water at all times. After three weeks consumption of chow/HFD, the HFD groups were stratified into three groups on the basis of body weight and mechanical withdrawal thresholds, and all rats then received either an i.p. injection of STZ (45mgkg^{-1}), or citric acid buffer. Blood samples were taken at day 18, 46 and 74. von Frey testing was carried out weekly.

4.2.2. *In vivo* electrophysiology

4.2.2.1. Induction of anaesthesia

To induce anaesthesia, the rat was placed in an induction chamber (a transparent plastic box), and isoflurane (Abbott, Kent, UK) was delivered at 3% in a mixture of 67% nitrous oxide and 33% oxygen (both BOC gases, UK) via a Vapotech series 3 vaporiser. Expelled gases were removed and absorbed by a Cardiff aldasorber (Datesand Ltd, Manchester, UK). Once an areflexic state was attained, the level of isoflurane was reduced to 2%. Areflexia was defined as the absence of a righting reflex when the induction chamber was gently tilted to the side, or the lack of a withdrawal reflex to a toe pinch.

4.2.2.2. Tracheal cannulation

The rat was transferred from the induction chamber to a mat, and placed in a nose-cone connected to a Y-connector and attached to the anaesthetic line through silicone Portex tubing. A small piece of skin was removed from the underside of the neck, exposing the muscle layers underneath, which were gently teased apart using blunt dissection to expose the trachea. Pointed forceps were placed under the trachea to support it, and two lengths of suture (Pearsall's Sutures Ltd., UK) were passed underneath the trachea and tied in loose knots. A small incision was made between two rings of cartilage approximately halfway along the exposed portion of the trachea, between the two threads. A bevelled-edged cannula, approximately 4cm in length and 2.08mm in diameter (Portex Ltd., UK) was inserted approximately 5mm and secured in place using the two sutures, and connected directly to the Y-connector. Response to a toe-pinch stimulus was checked to ensure the rat was sufficiently anaesthetised.

4.2.2.3. Laminectomy

The rat was transferred to a stereotaxic frame (University of Nottingham, Medical Faculty Workshops) and placed into ear bars in order to maintain a fixed head position throughout the experiment. Core body temperature was monitored by insertion of a rectal temperature probe and was maintained at $37\pm 0.5^{\circ}\text{C}$ by a heating blanket.

A midline incision was made through the skin and fur, from approximately 2cm above the base of the ribs. Two parallel incisions were made in the muscle on either side of the vertebral column, corresponding with L1-3, and the top clamp was tightly secured. A tear-drop shaped incision, approximately 1.5-2cm in length was then made along the dorsal surface of the spinal column, so that the centre of the incision lay over the base of the ribs, which approximately corresponds with the location of spinal segments L4-5. Connective tissue was

removed, creating a reservoir to hold future applications of saline, ensuring that the spinal cord was kept moist throughout the experiment.

Rongeurs were inserted gently into the gap between vertebrae, and used to expose segments L4-L5 of the spinal cord, which is innervated by primary afferent input from the hindpaws. The laminectomy was kept as small as possible to ensure stability of later electrophysiological recordings (Stanfa *et al.*, 2004). The *dura mater* was carefully removed using a pair of sharp forceps, leaving the *pia mater* intact. A second clamp was positioned around the vertebral column below the laminectomy to ensure that the area was held secure for later electrophysiological recordings. The skin of the rat was pulled tight around the clamps and secured with a crocodile clip to minimise loss of fluid and prevent dehydration of the rat. The level of isoflurane was reduced to 1.5% and maintained at this level for the remainder of the experiment. The rat was allowed a period of 30 minutes to adapt to the new level of anaesthesia. Hindpaw withdrawal and blink reflexes were regularly monitored throughout the rest of the experiment, and the spinal cord was kept moist by application of 50µl of 0.9% NaCl using a Hamilton syringe.

4.2.2.4. Electrophysiological recordings

Extracellular single-unit recordings of WDR dorsal horn neurones were made using glass coated tungsten electrodes (Merrill *et al.*, 1972), and a Neurolog system was used for spike discrimination and audio monitoring (Digitimer, Hertfordshire, UK). The system was grounded through the stereotaxic frame. The headstage (Neurolog NL100AK in A-B configuration) received input from the electrode inserted into the spinal cord and from a second indifferent electrode which was attached to the skin of the rat, allowing differential recording, and therefore reducing interference. The voltage signal was amplified (Neurolog NL104 x 2K, Neurolog 106 x 80) and filtered through low and high-pass filters (Neurolog NL125). The filtered signal was fed into a two channel

digital oscilloscope (Tektronix TDS210) providing a visual representation of the responses of the recorded neurones. Analogue spike signals were converted to a digital signal by the spike trigger (Neurolog NL201) with variable threshold, allowing only action potentials of a specified amplitude to be counted. This enabled the separation of action potentials recorded from a single neurone from recordings of other closely located neurones. Evoked firing of neurones was in the mV range with a typical signal to noise ratio of 4:1. The neuronal signals were digitised using a CED micro1401 interface and quantified using Spike 2 data acquisition software (Cambridge Electronic Design, Cambridge, UK).

An electrode was initially inserted level with the base of the ribs, close to the central vessel, and input from the hindpaw was confirmed by tapping the toes. The electrode was slowly withdrawn to the surface of the cord, and then lowered in 10 μ m steps using a SCAT-01 microdrive and an Epson HX210 Stepper (Digitimer) to a depth of around 500 μ m from the surface. It was then lowered further, whilst stimulating the toes, until a depth of around 1200 μ m. WDR neurones were selected if they displayed a sustained response to pinch stimuli, and a graded response to increasing stimulus intensity (Willis *et al.*, 2004). The receptive field was located and marked to allow accurate stimulation of the identified area throughout the experiment.

4.2.2.5. Characterising neurones

WDR neurones were characterised using transcutaneous electrical stimulation. Two metal pins (26 gauge syringe needles), connected to an electrical stimulator isolator (NL800), were inserted intradermally either side of the receptive field (or on adjacent toes), ensuring that the needles did not touch. The stimulus intensity was set to 1mA and the toes were stimulated using a single pulse, and the intensity was increased in 0.1mA steps up to 3mA, until a response with a C-fibre evoked latency was seen (90-300ms after stimulus). Once the threshold

for C-fibre-evoked response was determined, a train of 16 stimuli at 3 times the C-fibre threshold current were delivered using the period generator (NL304) at a frequency of 0.5Hz, with a 2ms pulse width, in order to stimulate neuronal wind-up. Using Spike 2, the neuronal responses were captured and displayed in a post-stimulus time histogram. The number of spikes evoked by each primary afferent fibre type were recorded and quantified ($A\beta$ -fibres, 0-20ms; $A\delta$ -fibres, 20-90 ms; C-fibres, 90-300 ms post stimulus), along with the number of post-discharge responses (300-800ms post-stimulus). Only neurones displaying ≥ 100 neuronal events for each fibre type were investigated further.

After a recovery period of at least ten minutes, the responses of the neurone to mechanical punctuate stimulation of the peripheral receptive field of the neurone on the hindpaw were characterised. The centre of the receptive field was mechanically stimulated with von Frey hairs of different bending forces (8, 10, 15, 26 and 60g) for 10 seconds in ascending order, with a 10s interval between each stimulation, and the mean firing frequency over the 10s stimulation period was recorded. The noxious withdrawal threshold to mechanical punctuate stimuli in conscious rats is 15g and so the range of von Frey hairs used included both innocuous and noxious stimuli (Chaplan *et al.*, 1994). Three sets of stimulations were recorded, with a 10 minute interval between each set. An average of 3 neurones were characterised from each rat.

4.2.2.6. Production of glass coated tungsten microelectrodes

A batch of 30 tungsten wires of equal length (Harvard Apparatus, Kent, UK) were loaded into a Perspex jig (75 x 50mm) and cleaned by gently brushing the length of the filament with 100% acetone. A piece of sellotape was attached to the end of the tungsten filaments, and then wrapped tightly around a cylindrical brass barrel, to ensure good contact between the barrel and the electrodes. The metal barrel was

attached to the arm of an electrode etcher (University of Nottingham, Medical Faculty Workshop) and lowered into a potassium nitrate (KNO_3 ; 90g/80 ml) electrolyte solution so that only 10 of the tungsten filaments were in contact with the solution at any one time. The circuit was completed by immersing a carbon electrode in the solution, and a current of 2.5mA was passed through the solution and the electrodes were allowed to etch until the current dropped to 2.0mA. The electrode barrel was then removed and the electrodes gently rinsed with distilled water.

Using a pair of forceps, a single electrode was removed from the barrel, and briefly passed through a burner to remove any sellotape residue. The filament was then placed in a glass capillary tube (Harvard Apparatus), and inserted into an electrode puller (University of Nottingham, Medical Faculty Workshops). A current was passed through a coil, causing the capillary tube to melt and pull apart, coating the filament with glass. The capillary tube with the tungsten filament was then placed into the holder of a light microscope and the tapered end was pushed gently towards a heated borax bead attached to the microscope. The current supply was then turned off, causing contraction of the borax bead, pulling off a small glass fragment to expose about 1-2 mm of the tungsten wire.

4.2.2.7. Choice of anaesthetic

The choice of anaesthetic was important as it was necessary that it would not have any overt effects on the responses of the dorsal horn neurones. Previously, decerebrate animals have often been used in electrophysiological studies (Clarke, 1985; Ogilvie *et al.*, 1999) as this method reduces the confounding analgesic effects of anaesthesia, but the generation of decerebrate animals involves additional surgical procedures and removes the descending pain pathways which modulate spinal dorsal horn neuronal responses.

Inhalation anaesthesia was chosen as it enables tight control of the amount of anaesthetic being delivered, and can be rapidly increased or decreased as required. Halothane was not chosen due to its potential for hepatotoxicity, and at the dose range used in these experiments halothane has a greater depressant effect on neuronal responses than isoflurane (Mitsuyo *et al.*, 2006). Isoflurane has been shown to have a minimal depressant effect on dorsal horn responses to noxious mechanical stimuli in rats *in vivo* (Antognini *et al.*, 1999; Kim *et al.*, 2007b). Isoflurane was used in combination with nitrous oxide so that a lower concentration of anaesthetic could be used.

4.2.3. Administration of drugs

All drug dosing was carried out blind to the treatment groups. Pioglitazone (10mgkg^{-1}), or 1% methylcellulose vehicle, was orally administered daily from day 21 to day 49 of the study, when the first cohort ($n=6$ for all groups) were used for electrophysiological experiments. A second cohort of rats ($n=6$ for lean/Veh, HFD/Veh and HFD/STZ and $n=5$ for HFD/STZ + pioglitazone) was assessed until day 78, (28 days after dosing with pioglitazone had ceased), when electrophysiological experiments were then conducted. Pioglitazone was purchased from Tocris Cookson (Bristol, UK) and was dissolved in 1% methylcellulose vehicle.

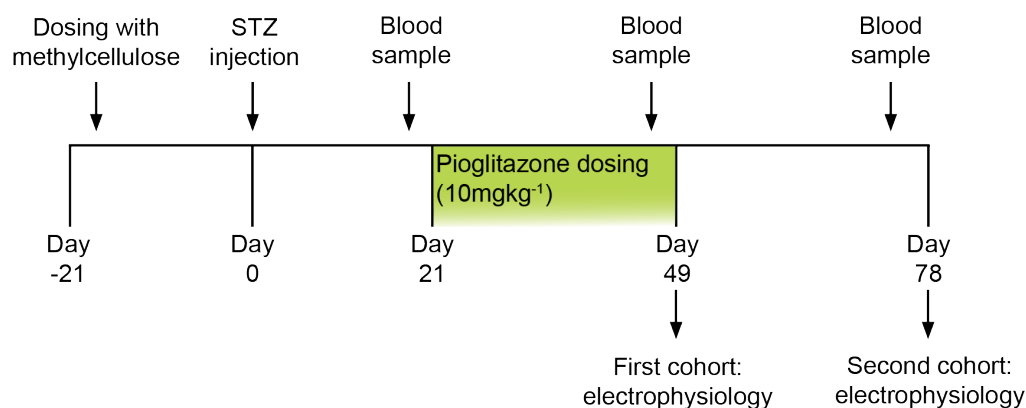


Figure 4.1 Timeline of the experiment

4.2.4. Statistics

Analysis of body weight, food intake and water intake was by an ANCOVA with Tukey's post-hoc test, with the average of day -7 to 0 as the covariate. Analysis of plasma glucose, plasma insulin, mechanical withdrawal thresholds, mechanically and electrically evoked neuronal responses and electrical thresholds and latencies was by a Kruskal-Wallis test with Dunn's post-hoc test. In all analyses, a p value of less than 0.05 was considered statistically significant.

Rats were excluded from analysis of pain behaviour if in the two weeks before injection with STZ the average hindpaw mechanical withdrawal threshold was <10g. In this study, this represented 5 rats – 1 lean/Veh, 1 HFD/Veh, 1 HFD/STZ + vehicle and 2 HFD/STZ + pioglitazone.

4.3. Results

4.3.1. Effects of HFD/STZ on hindpaw evoked responses of WDR neurones in the dorsal horn

This study examined the effects of the HFD/STZ model of diabetes on the activity of dorsal horn neurones *in vivo*, at day 49 and day 78. A total of 64 WDR dorsal horn neurones were characterized in 6 lean/Veh, 6 HFD/Veh, 6 HFD/STZ and 6 pioglitazone-treated HFD/STZ rats at day 49 (9, 18, 18 and 19 neurones per respective group), and a total of 79 WDR dorsal horn neurones were characterized in 6 lean/Veh, 6 HFD/Veh, 5 HFD/STZ and 6 pioglitazone-treated HFD/STZ rats at day 78 (20, 23, 17 and 19 neurones per respective group). The average depth of the dorsal horn neurones recorded from ranged between 756-887 μ m, which corresponds to laminae V-VI.

Prior to investigating the evoked responses of the WDR dorsal horn neurones, any spontaneous activity was recorded. The vast majority of neurones recorded exhibited negligible or no spontaneous firing activity. Two out of 18 neurones in both the vehicle and the pioglitazone treated HFD/STZ groups at day 49 had spontaneous firing above 1Hz (7.97 and 3.16Hz, and 6.85 and 1.12Hz, respectively), but no significant changes were seen between any of the groups (data not shown).

Both the electrically and mechanically evoked responses of the WDR dorsal horn neurones were quantified. The average latency and threshold values, as well as total number of action potentials produced by A β -, A δ - and C-fibres during a train of 16 electrical stimuli at three times the C-fibre threshold, as well as post-discharge, are presented in Table 4.3. Although there was a trend for the A β -fibre evoked response to be lower in the HFD/STZ rats, compared to the lean/Veh controls and HFD/Veh controls, this did not reach significance. An example trace of the response of a typical WDR neurone to the first 8 of a train of 16 electrical stimuli can be seen in Figure 4.2.

Stimulation of the hindpaw receptive field of dorsal horn neurones with a range of von Frey hairs evoked a stimulus intensity-dependant increase in the firing of these neurones in the lean/Veh controls, the HFD/Veh controls and the HFD/STZ group. An example histogram showing the graded response of a single dorsal horn neurone is provided in Figure 4.2. There was a trend towards a decrease in the mechanically-evoked responses of dorsal horn neurones in the HFD/STZ at each different weight at day 49, especially to the noxious stimuli (15-60g), although significance was not reached (Figure 4.3A), and an AUC analysis of the stimulus response functions for the three groups did not reveal a significant difference, perhaps due to the high variability in the data. This difference was not maintained at day 78.

Table 4.3 Comparison of the C- and A-fibre evoked responses of WDR dorsal horn neurones in the HFD/STZ model of diabetes, compared to HFD/Veh and lean/Veh controls at day 49. There were no significant differences in the C-fibre threshold and latency, total action potentials (APs) for A β -, A δ - and C-fibres, and also post-discharge firing, following a train of 16 electrical stimuli in the three groups. Pioglitazone (10mgkg⁻¹, p.o.) treatment from day 21-49 did not alter these properties of the dorsal horn neurones in the HFD/STZ model. All data represent mean \pm SEM, analysis was by a Kruskal-Wallis test.

	Lean/Veh n=6	HFD/Veh n=6	HFD/STZ + Vehicle n=6	HFD/STZ + Pioglitazone n= 6
C-fibre Threshold (mV)	1.5 \pm 0.2	1.3 \pm 0.1	1.2 \pm 0.1	1.4 \pm 0.1
Latency (ms)	228 \pm 13	189 \pm 11	192 \pm 19	214 \pm 14
A β (Total APs)	138 \pm 12	139 \pm 8	111 \pm 8	118 \pm 9
A δ (Total APs)	161 \pm 24	123 \pm 19	105 \pm 21	131 \pm 11
C (Total APs)	392 \pm 67	251 \pm 37	276 \pm 48	266 \pm 42
Post-discharge (Total APs)	440 \pm 98	309 \pm 48	402 \pm 82	378 \pm 60

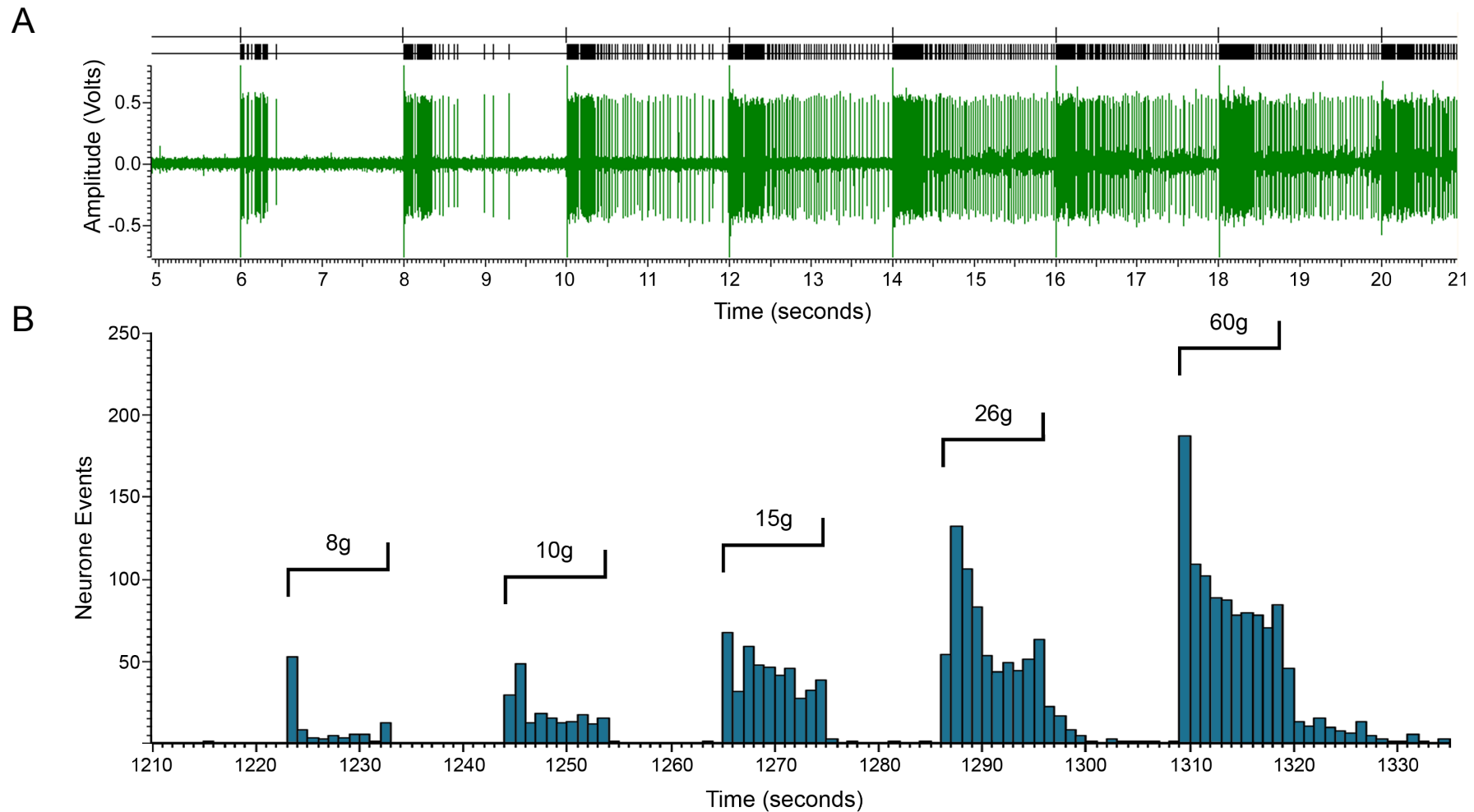


Figure 4.2 (A) Representative trace of electrically-evoked evoked responses of a single wide dynamic range dorsal horn neurone to the first 8 electrical stimuli of the train of 16 stimuli. **(B)** Representative trace of the evoked response of a single wide dynamic range dorsal horn neurone following mechanical (8, 10, 15, 26 and 60g) stimulation of the hindpaw receptive field in a HFD/Veh rat.

4.3.2. Effects of pioglitazone on mechanically evoked responses of dorsal horn neurones

The effects of pioglitazone (10 mgkg⁻¹, p.o., day 21-49) treatment on the magnitude of the mechanically-evoked responses of the WDR dorsal horn neurones in HFD/STZ rats were compared to the effects of vehicle treatment. Immediately following 28 days of pioglitazone treatment (day 49), mechanically evoked responses of dorsal horn neurones were significantly larger than evoked neuronal responses in HFD/STZ rats treated with vehicle. As shown in Figure 4.3B, there was a significant increase in the evoked firing of neurones in the spinal cord of HFD/STZ rats treated with pioglitazone. Twenty-eight days after cessation of pioglitazone treatment in the HFD/STZ rats, mechanically evoked responses of dorsal horn neurones had returned to a similar level to those in the vehicle treated HFD/STZ rats (Figure 4.3B).

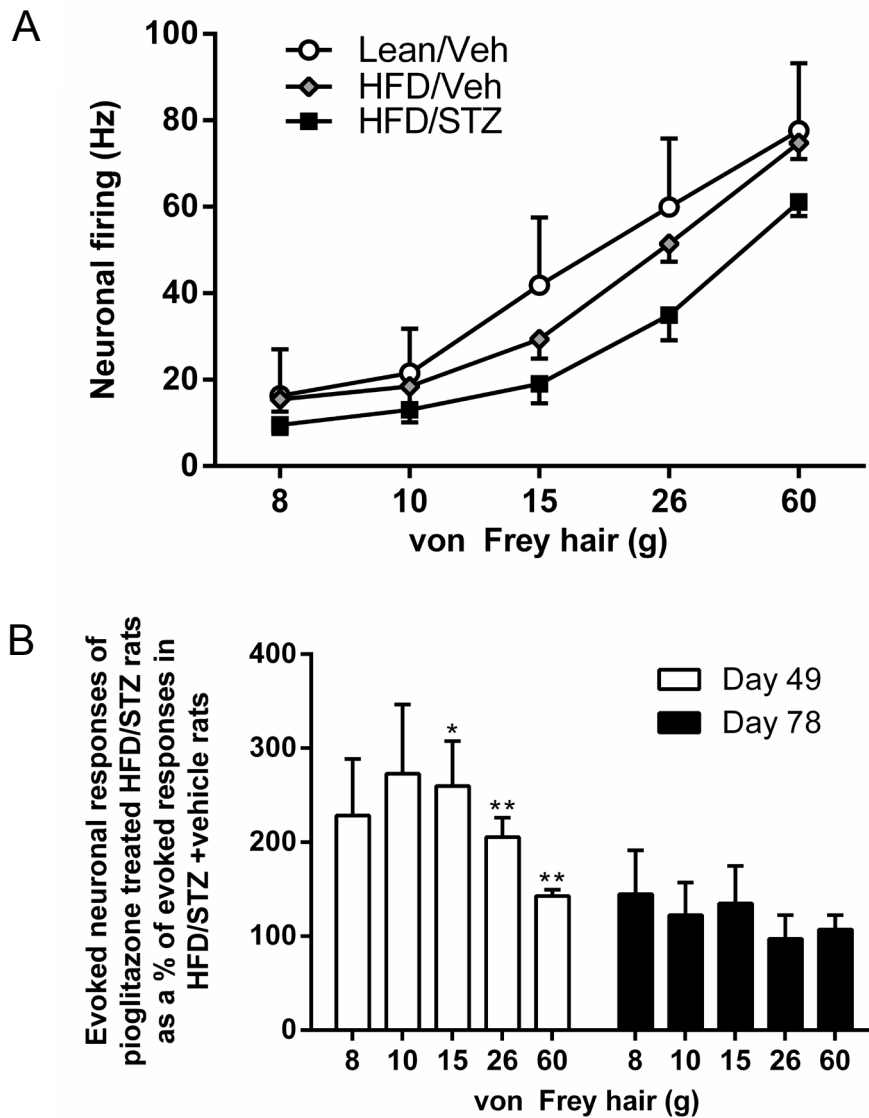


Figure 4.3 (A) Mechanically-evoked responses of WDR dorsal horn neurones in the HFD/STZ model of diabetes (n=6), compared to lean/Veh controls (n=6) and HFD/Veh controls (n=6). All data represent mean frequency of firing \pm SEM, analysis was by a Kruskal-Wallis test. **(B)** Effects of daily pioglitazone treatment (10 mg kg^{-1} , p.o., day 21-49) on mechanically-evoked responses of spinal neurones in HFD/STZ rats at day 49 (n=6 for both groups) and day 78 (n=5 for HFD/STZ, n=6 for HFD/STZ + pioglitazone). Data are mean neuronal firing in HFD/STZ + pioglitazone rats expressed as a % of evoked neuronal firing in HFD/STZ + vehicle rats. Analysis of original data, comparing HFD/STZ + vehicle and HFD/STZ + pioglitazone rats, was by a Mann-Whitney test: * $p < 0.05$, ** $p < 0.01$

4.3.3. Effects of pioglitazone on metabolic parameters

As described previously, induction of the HFD/STZ model leads to a threefold increase in plasma glucose levels ($p < 0.01$; Figure 4.4A), and a six-fold decrease in plasma insulin levels ($p < 0.001$; Figure 4.4B), compared to HFD/Veh controls. An increase in insulin levels can also be seen in the HFD/Veh group compared to the lean/Veh controls, as discussed in Chapter 3. Body weight gain was again stunted in the HFD/STZ rats ($p < 0.001$), water intake was increased four-fold ($p < 0.001$), and food intake was increased in all groups eating the HFD, although this was not significantly different between groups (data not shown). Systemic administration of pioglitazone from day 21 to 49 did not alter any of these parameters.

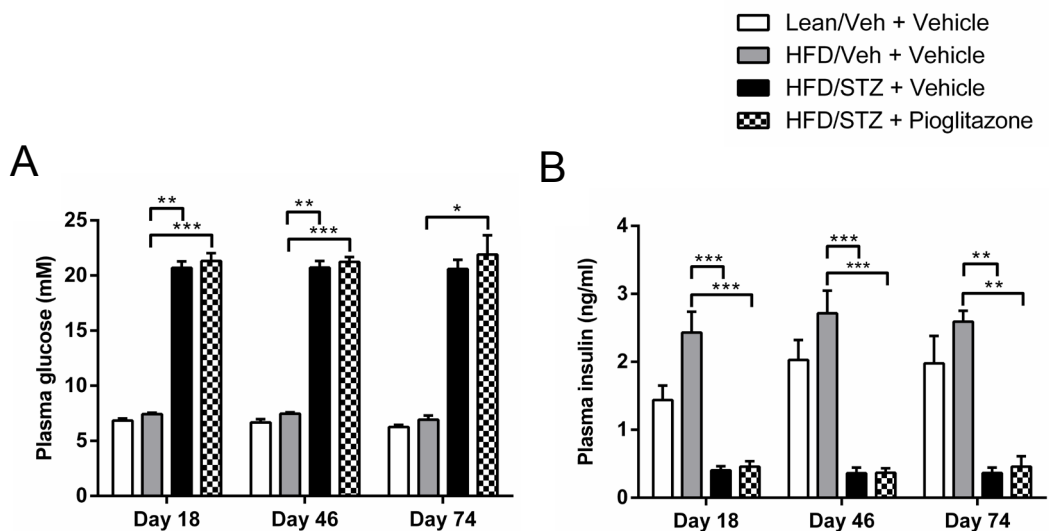


Figure 4.4 Effects of daily pioglitazone treatment (10 mg kg^{-1} , p.o., day 21-49) versus vehicle on **(A)** fasting plasma glucose and **(B)** fasting plasma insulin. Day 18 is pre-pioglitazone administration, day 46 is after 25 days of pioglitazone and day 74 is 25 days after pioglitazone administration had ceased. Day 18 and 46: $n=12$ for all, except $n=11$ for HFD/STZ + vehicle. Day 74: $n=6$ for all, except $n=5$ for HFD/STZ + vehicle. All data represent mean \pm SEM, analysis was by a Kruskal-Wallis test with Dunn's post-hoc test: (* vs. HFD/Veh)

* $p < 0.05$, ** $p < 0.01$, *** $p < 0.001$

4.3.4. Effects of pioglitazone on mechanical withdrawal thresholds

The mechanical withdrawal thresholds of the HFD/STZ group were significantly reduced compared to HFD/Veh controls from day 14 post-STZ injection, and the mean threshold decreased further up to day 70 (Figure 4.5). At day 49, when the first cohort was taken out for electrophysiological experiments, the mean mechanical withdrawal threshold of the HFD/STZ group was 8.7 ± 1.2 g, in comparison to 14.0 ± 0.6 g for the lean/Veh controls and 13.8 ± 0.6 g for the HFD/Veh controls. At day 70, just before the second set of electrophysiological experiments was performed, the mean mechanical withdrawal threshold of the HFD/STZ group was 7.0 ± 1.2 g, in comparison to 13.8 ± 0.8 g for the lean/Veh controls and 14.0 ± 1.0 g for the HFD/Veh controls.

Rats were dosed with 10mgkg^{-1} pioglitazone, or 1% methylcellulose vehicle, from day 21-49. Although there appears to be a separation between the decline in mechanical withdrawal thresholds in the HFD/STZ pioglitazone treated group compared to the HFD/STZ control group, there were no significant differences between the two groups over the period of treatment, and an area under the curve (AUC) analysis also revealed no significant difference (Figure 4.5). At the end of dosing with pioglitazone, day 49, the mean mechanical withdrawal threshold for this group was 10.8 ± 1.1 g compared to 8.7 ± 1.2 g in the HFD/STZ vehicle treated group.

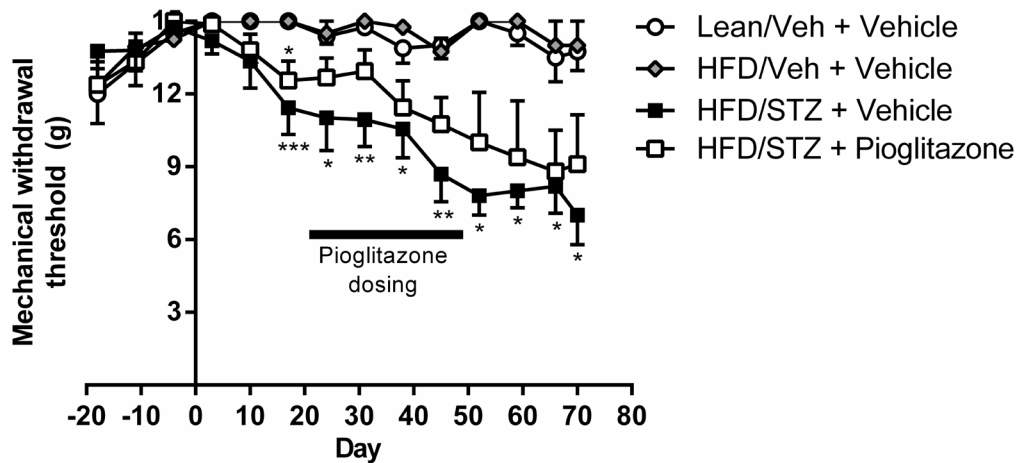


Figure 4.5 Effects of daily pioglitazone treatment (10 mgkg^{-1} , p.o., day 21-49) versus vehicle on hindpaw mechanical withdrawal thresholds. Up to day 49: $n=11$ for lean/Veh and HFD/Veh, and $n=10$ for HFD/STZ + vehicle and HFD/STZ + pioglitazone. Day 49 onwards: $n=6$ for lean/Veh and HFD/Veh, and $n=5$ for HFD/STZ + vehicle and HFD/STZ + pioglitazone. All data represent mean \pm SEM, analysis was by a Kruskal-Wallis test with Dunn's post-hoc test: (* vs. HFD/Veh)
 * $p<0.05$, ** $p<0.01$, *** $p<0.001$

4.4. Discussion

In the present study, I have demonstrated that the HFD/STZ model of diabetes, which is associated with mechanical hypersensitivity, is also associated with a trend towards a decrease in mechanically evoked responses of spinal neurones. This model was not associated with any changes in the threshold for electrical activation of C-fibres, nor any significant changes to electrically evoked responses. Although a trend towards a decrease in the electrical evoked A β -fibre activity of neurones was evident, significance wasn't reached. There was no change in spontaneous firing of neurones between any groups.

Pioglitazone treatment from day 21 to 49 did not significantly alter the progression of mechanical hypersensitivity in the HFD/STZ rats. However, electrophysiological studies revealed that the pioglitazone treatment was associated with a significant increase in the magnitude of the mechanically-evoked responses of WDR dorsal horn neurones in the HFD/STZ rats which received pioglitazone, compared to vehicle treatment. This effect was significant immediately following pioglitazone treatment but was not maintained and evoked responses returned to levels similar to that in the untreated HFD/STZ group 4 weeks after pioglitazone treatment had ceased.

4.4.1. Effects of the HFD/STZ model on electrophysiological parameters

Previous studies have investigated the involvement of A β -, A δ - and C-fibres, as well as higher order neurones in diabetic neuropathy, and how these might contribute to the painful symptoms experienced. Hyper-responsiveness, a decrease in mechanical thresholds and an increase in spontaneous activity and wind-up in both primary afferent fibres, as well as higher order neurones has been shown in the STZ model (Ahlgren *et al.*, 1994; Ahlgren *et al.*, 1992; Chen *et al.*, 2002a;

Chen *et al.*, 2003; Chen *et al.*, 2001; Fischer *et al.*, 2009; Khan *et al.*, 2002; Kimura *et al.*, 2005; Suzuki *et al.*, 2002).

This increase in activity has been postulated to be due to sensitisation of the central nervous system due to the aberrant activity in afferent nerves (Kamiya *et al.*, 2005a), and impairments to descending pain modulation (Morgado *et al.*, 2011b). The increased levels of GABA in the STZ model (Malmberg *et al.*, 2006; Morgado *et al.*, 2008) have been shown to have an excitatory rather than an inhibitory effect due to a decrease in the expression of KCC2 (Jolivald *et al.*, 2008; Morgado *et al.*, 2008), resulting in enhanced activity of spinal neurones, and therefore increased facilitation.

The affect of the STZ model on neurones in the dorsal horn of the spinal cord has previously been examined with contrasting findings. An increase in spontaneous activity, enlarged receptive fields and increased peripherally evoked responses to brush, press, pinch and von Frey stimuli have been observed (Chen *et al.*, 2002a; Ghorbani *et al.*, 2011; Tan *et al.*, 2012). Pertovaara *et al.* (2001) also found an increase in spontaneous activity, but no change in noxious heat-evoked responses, after discharges, or receptive field size, and a decrease in the responses evoked by mechanical stimulation in STZ treated rats. In the present study, a trend towards lower firing frequencies in response to mechanical stimulation was observed in the HFD/STZ group. A decrease in the evoked neuronal response to mechanical stimulation has also been seen in other models; SNL (Chapman *et al.*, 1998), spinal cord injury (Hao *et al.*, 2004) and cisplatin-induced chemoneuropathy (Cata *et al.*, 2008). However, this mismatch between the mechanical hypersensitivity observed in the HFD/STZ model, and the lowered mechanically evoked responses in this electrophysiology study, which would normally infer sensory deficits, is difficult to explain. Cata *et al.* (2008) hypothesised that the rats might be experiencing paresthesias such as tingling and numbness, which are routinely observed in humans with diabetic neuropathy (Ziegler, 2008). It was

proposed that these symptoms might result in enhanced vigilance of the rats to von Frey stimulation, rather than them actively becoming more sensitive to lower-threshold stimuli. The processing of pain in neuropathic conditions is very complex, and so there may be a variety of other mechanisms which that are responsible for the hypersensitivity that is observed in this model.

While the observed decrease in evoked responses to mechanical stimulation reported herein is consistent with previous studies, the majority of earlier reports have found an increase in spontaneous activity, both in the diabetic model (Pertovaara *et al.*, 2001; Tan *et al.*, 2012), and in a variety of other models of neuropathic pain (Cata *et al.*, 2008; Chapman *et al.*, 1998; Laird *et al.*, 1993; Palecek *et al.*, 1992). The basis for these differences is unclear, but may relate to the criteria used when searching for neurones. During this process, the neurone had to display three characteristics before it was taken further. It needed to; be responsive to both brush and pinch stimuli; have a graded response to stimulation with von Frey hairs; and display wind-up in response to a train of electrical stimuli. Neurones which displayed a large amount of spontaneous activity may have been disregarded due to the difficulty in making the assessment of these three characteristics. As the main purpose of this study was to determine whether HFD/STZ influenced mechanically-evoked responses, and to compare this to the changes seen in the behavioural experiments, this search criteria was necessary. Therefore it is possible that any increase in spontaneous firing that might have been seen in the HFD/STZ model was lost through the process of selecting neurones to follow, and so in a future study, it would be of great interest to conduct a similar experiment, but to be more inclusive of which neurones were followed, to allow any changes that might have been lost in the present study to be seen.

4.4.2. Metabolic effects of pioglitazone in the HFD/STZ model

The lack of effect of pioglitazone on glucose or insulin levels is in agreement with previous similar studies in STZ treated rats (Majithiya *et al.*, 2005; Wiggin *et al.*, 2008; Yamagishi *et al.*, 2008). In type 2 diabetes, pioglitazone acts as an insulin sensitiser in peripheral tissues, as well as improving β -cell function (Kawasaki *et al.*, 2005; Miyazaki *et al.*, 2001). However, in this model, a large proportion of the β -cells are destroyed by the STZ, and fasting plasma insulin levels are six-fold lower than in the HFD/Veh controls. This means that the rats are insulin-deficient, rather than insulin-resistant, and so improving the peripheral insulin sensitivity is ineffective due to the low levels of circulating insulin. As the insulin levels were also unchanged, this indicates that the β -cells are probably working at full capacity, and pioglitazone was therefore unable to stimulate more β -cell insulin secretion. Previously, Srinivasan *et al.* (2005) gave 10mgkg^{-1} of pioglitazone for 7 days to HFD/STZ rats, who had received either 35, 45 or 55mgkg^{-1} of STZ. In the rats which received the lowest dose of STZ, plasma insulin levels were only reduced to a level seen in rats fed a normal diet, and in these rats, pioglitazone was able to produce a significant reduction in plasma glucose levels. In the rats that had been given a higher dose of STZ (45 or 55mgkg^{-1}), there was a much greater reduction in insulin levels, and pioglitazone was then ineffective at reducing plasma glucose. This suggests that pioglitazone is most effective when it is able to improve whole body insulin sensitivity by decreasing lipolysis and enhancing insulin-mediated glucose disposal in skeletal muscle (Kahn *et al.*, 2000). However, when insulin levels are reduced beyond a certain level, such as in the current study, pioglitazone is unable to affect levels of glucose or insulin.

4.4.3. Effects of pioglitazone on pain behaviour and neuronal responses in the HFD/STZ model

In the current study, administration of 10mgkg⁻¹ pioglitazone three weeks after injection with STZ had no significant effect on the development of mechanical hypersensitivity, compared to the vehicle controls. The rationale behind administering the drug at this timepoint was that I wanted to model the clinical situation, where the drug would be administered once painful symptoms had first appeared. On the basis of the recent publication by Morgenweck *et al.* (2013), a higher dose of pioglitazone may be required to produce an analgesic effect once the model is established

Interestingly, despite the lack of effect on pain behaviour, in my electrophysiological experiments pioglitazone produced a significant increase in evoked neuronal responses in the HFD/STZ rats, with this effect not maintained 4 weeks after cessation of pioglitazone treatment. Pioglitazone treatment effectively restored mechanically evoked responses of spinal neurones in HFD/STZ rats to levels higher than lean/Veh controls. Given that this effect was not associated with a change in mechanical hypersensitivity, the biological relevance of this finding is unclear

Pioglitazone, and other thiazolidinediones, have been shown to be effective at alleviating mechanical hypersensitivity in a variety of models: carrageenan (Cuzzocrea *et al.*, 2004; Morgenweck *et al.*, 2010; Taylor *et al.*, 2002), post-incisional pain (Hasegawa-Moriyama *et al.*, 2012), spinal cord injury (Park *et al.*, 2007), spinal nerve transection (Jia *et al.*, 2013; Jia *et al.*, 2010), partial sciatic nerve ligation (Iwai *et al.*, 2008; Maeda *et al.*, 2008; Takahashi *et al.*, 2011), tibial and sural nerve transection (Jain *et al.*, 2009), and spared nerve injury (Churi *et al.*, 2008; Morgenweck *et al.*, 2013). Since the levels of glucose and insulin are not altered in these models, TZDs must have an analgesic effect that is not just due to insulin sensitisation.

Indeed, TZDs have marked effects on macrophage recruitment and activation state, and this has profound anti-inflammatory effects in models of inflammatory pain (Hasegawa-Moriyama *et al.*, 2012; Taylor *et al.*, 2002).

TZDs' analgesic effects in neuropathic pain models also seem to be predominantly mediated by an anti-inflammatory effect. TZDs are able to: decrease astrogliosis and microglial activation (Iwai *et al.*, 2008; Morgenweck *et al.*, 2013; Park *et al.*, 2007), inhibit the activation of NF κ B (Costa *et al.*, 2008; Jia *et al.*, 2013; Jia *et al.*, 2010), decrease the expression of various pro-inflammatory factors, such as TNF α and IL-1 β (Costa *et al.*, 2008; Jia *et al.*, 2013; Jia *et al.*, 2010; Park *et al.*, 2007; Qiang *et al.*, 1998), increase the expression of anti-oxidant enzymes (Park *et al.*, 2007), and attenuate the decrease in reduced glutathione, and the increase in myeloperoxidase activity (a specific marker of inflammation) (Jain *et al.*, 2009). The decrease in the production of pro-inflammatory cytokines may be partly responsible for the suppression of glial activation. TZDs have also been shown to reduce oxidative stress in the STZ model (Majithiya *et al.*, 2005), perhaps by activating genes with oxidoreductase activity (Wiggin *et al.*, 2008). This ability of pioglitazone to decrease pro-inflammatory cytokines could play an important role in diabetic neuropathy, as levels of NF κ B and pro-inflammatory cytokines are increased in both diabetic animals and patients (as reviewed in Wilson *et al.*, 2012a).

Therefore, from all the accumulating evidence as to the effects of pioglitazone in models of pain, it would seem logical that pioglitazone might have had an analgesic effect in the HFD/STZ model. However, many of these studies have shown that the TZDs are most effective when given at the time of injury. Indeed TZD treatment at day 26-28 after PNL is far less effective than when given at days 1-3 (Takahashi *et al.*, 2011). This group hypothesised that rosiglitazone may only be effective if given in the initial phase before macrophages are activated and recruited to the site of injury, where they exacerbate acute

inflammation. As pioglitazone was not seen to be effective in alleviating neuropathic pain in this study, experiments in the final chapter go on to investigate other antidiabetics, and other types of analgesics.

Chapter 5.

Comparison of analgesic versus antidiabetic interventions on aberrant pain responses in the HFD/STZ model

5.1. Introduction

Having established that the HFD/STZ model leads to development of mechanical hypersensitivity, and having investigated some of the mechanisms underlying these responses, the next series of experiments investigated the effects of different types of interventions, analgesic versus antidiabetic, on aberrant pain responses in this model.

5.1.1. Existing and novel analgesics for diabetic neuropathy

It is generally understood that one of the most important factors in the treatment of diabetic neuropathy is for diabetic patients to maintain tight control of their blood glucose concentration. Maintaining these levels with intensive insulin therapy has been shown to delay, or prevent the development of diabetic neuropathy, especially in type 1 diabetes (DCCT 1995; for review see Callaghan *et al.*, 2012; Gaede *et al.*, 1999), and this effect can still be seen over 10 years later (Albers *et al.*, 2010).

Alternatively, inhibiting the pain responses directly can ameliorate the painful symptoms (Ziegler, 2008). Neuropathic pain, however, has proved difficult to treat, with little efficacy seen from conventional analgesics such as non-steroidal anti-inflammatory drugs and opiates, the latter of which has a number of side effects including nausea, constipation and sedation, and can also be addictive, with tolerance developing with prolonged usage (Benyamin *et al.*, 2008).

There are a variety of drugs that can be prescribed to offer pain relief to diabetic patients. NICE guidelines recommend duloxetine as the first line treatment, followed by either amitriptyline or pregabalin (NICE, 2010), and the FDA has also approved tapentadol (FDA, 2004). A recent in-depth review of the literature recommended pregabalin as the first choice (Bril *et al.*, 2011).

5.1.1.1. Pregabalin

Both gabapentin and pregabalin are licensed for treatment of DPNP, with pregabalin being the gold-standard (Bril *et al.*, 2011). Both drugs alleviate painful symptoms, as well as improving quality of life and sleep problems. They are, however, associated with side effects such as dizziness and somnolence (Freeman *et al.*, 2008; Freynhagen *et al.*, 2005; Quilici *et al.*, 2009; Stacey *et al.*, 2008). Gabapentin and pregabalin are derivatives of the neurotransmitter GABA (but do not interact with the GABA receptor itself) (Lanneau *et al.*, 2001). They bind to the $\alpha 2\delta$ -1 auxiliary subunits of presynaptic voltage-gated calcium channels (Field *et al.*, 2006; Gee *et al.*, 1996), with pregabalin having a six-fold higher binding affinity than gabapentin at the $\alpha 2\delta$ -1 subunit (Vinik *et al.*, 2013).

The $\alpha 2\delta$ subunit enhances trafficking of $\text{Ca}_v\alpha 1$ to the plasma membrane, increasing the number of functional channels present, which results in an increase in Ca^{2+} currents (Davies *et al.*, 2007). The gabapentinoids bind to $\alpha 2\delta$ -1, and it has been postulated that their mechanism of action is to displace an endogenous protein ligand that normally acts as a positive modulator of $\alpha 2\delta$ -1, impairing its ability to traffic the calcium channel from DRG cell bodies to the plasma membrane of presynaptic terminals in the dorsal horn (Bauer *et al.*, 2009; Hendrich *et al.*, 2008). The consequence of this is less calcium entry into the nociceptive primary afferent fibres via this channel, which is located on these fibres, resulting in a reduction in transmitter release from the primary afferent terminals in the dorsal horn (Taylor, 2004; Taylor, 2009), and decreased activation of dorsal horn neurones in the spinal cord.

Importantly, $\alpha 2\delta$ -1 subunit expression has been shown to be up-regulated in the DRGs (Martinez *et al.*, 2012; Yusaf *et al.*, 2001) and dorsal horn of the spinal cord in STZ diabetic rats (Luo *et al.*, 2002). Electron microscopy and quantitative RT-PCR studies have provided

evidence that the elevation in $\alpha 2\delta$ -1 in the SNL model of neuropathic pain occurs exclusively on the presynaptic terminals of primary sensory afferents (Bauer *et al.*, 2009). Over-expression of the $\alpha 2\delta$ -1 subunit in mice results in the manifestation of mechanical hypersensitivity and thermal hyperalgesia (Li *et al.*, 2006), illustrating a fundamental role of this channel in influencing nociceptive thresholds.

Both gabapentin and pregabalin attenuate mechanical hypersensitivity in the STZ model of diabetes (Field *et al.*, 1999b; Martinez *et al.*, 2012; Wodarski *et al.*, 2009; Yamamoto *et al.*, 2009; Zhang *et al.*, 2013). In addition, gabapentin also suppressed the flinching response during the formalin test in diabetic rats (Ceseña *et al.*, 1999). Pregabalin led to a decrease in the calcium channels expressing $\alpha 2\delta$ -1 in the dorsal horn in diabetic rats (Martinez *et al.*, 2012), and gabapentin has been shown to significantly reduce enhanced excitability by decreasing the rise in expression of $\text{Na}_v1.7$ and p-ERK1/2 in STZ rats (Zhang *et al.*, 2013).

5.1.1.2. Cannabinoid ligands

Another target showing promise in its ability to alleviate pain associated with diabetic neuropathy is the endocannabinoid system. Endocannabinoids exert their effects through two GPCRs; CB_1 and CB_2 (cannabinoid receptors 1 and 2). CB_1 receptors are located in the periphery, but are found most abundantly in the CNS, including the spinal cord, PAG and thalamus (Tsou *et al.*, 1998). CB_2 receptors are primarily expressed by immune cells in the periphery with high concentrations in the spleen (Munro *et al.*, 1993), but are also expressed by microglia in the CNS (Romero-Sandoval *et al.*, 2008b) and neurones in the brain (Gong *et al.*, 2006; Van Sickle *et al.*, 2005). These receptors can be activated by cannabinoids such as $\Delta 9$ -tetrahydrocannabinol (THC) and cannabidiol, and also by endogenous cannabinoids (endocannabinoids) such as anandamide (AEA) and 2-arachidonoylglycerol (2-AG), which are synthesised and released on demand (Booker *et al.*, 2012), and rapidly broken down by the enzymes

fatty acid amide hydrolase (FAAH) and monoacylglycerol lipase (MAGL) respectively (for review see Muccioli, 2010). Figure 5.1 summaries the breakdown of these endocannabinoids, and the receptors that they are ligands for.

The effects of cannabinoids on pain responses in models of diabetes have been fairly widely studied. Systemic administration of WIN55212-2 (a mixed CB₁ and CB₂ receptor agonist) attenuated mechanical hypersensitivity in STZ mice (Dogrul *et al.*, 2004; Toth *et al.*, 2010), STZ rats (Ulugol *et al.*, 2004; Vera *et al.*, 2012) and ZDF rats (Vera *et al.*, 2012). Cannabidiol, which has a multitude of low potency targets including receptors CB₁ and CB₂, and inhibition of FAAH (Pertwee, 2004), was effective at preventing the development of mechanical hypersensitivity and thermal hyperalgesia in STZ mice when administered at the onset of diabetes, and for a further 2 months after discontinuation of the drug, although it was without effect when administered therapeutically once mechanical hypersensitivity was established (Toth *et al.*, 2010). In a more complicated behavioural assay, diabetic rats exhibited increased flinching behaviour compared to normoglycemic rats in the formalin test, and peripheral AM404 (an AEA reuptake inhibitor), AEA itself, and ACEA (a CB₁ receptor agonist) all attenuated flinching behaviour during the first and second phase of the formalin test in the diabetic rats (Schreiber *et al.*, 2012). Systemic administration of a cannabis extract decreased mechanical hypersensitivity, protected against oxidative stress (as evidenced by increased glutathione levels and decreased liver lipid peroxidation) and restored NGF levels in the sciatic nerve in the STZ model (Comelli *et al.*, 2009). Another study reported that the CB₁ receptor antagonist rimonabant was also able to attenuate mechanical hypersensitivity in diabetic mice (Comelli *et al.*, 2010).

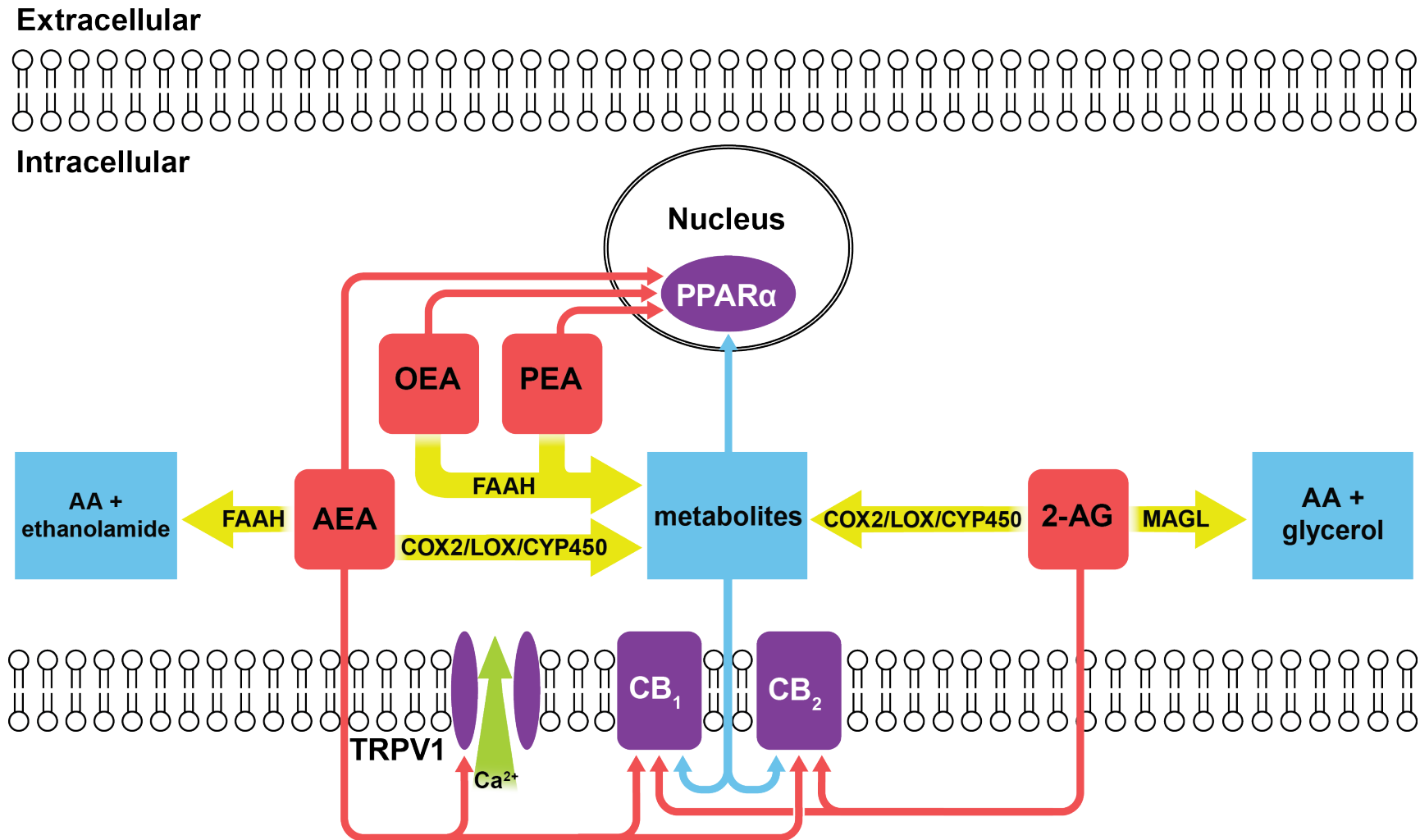


Figure 5.1. The key features of the endocannabinoid receptors and their breakdown. Both AEA and 2-AG can also be metabolised to form biologically activated metabolites. AA - arachidonic acid. Adapted from (Sagar *et al.*, 2009).

5.1.1.2.1. MAGL inhibitors

2-AG, is formed from DAG and phospholipase-C (Horváth *et al.*, 2012), and activates both CB₁ and CB₂ receptors, but binds with highest affinity to the CB₂ receptor (Mechoulam *et al.*, 1995). MAGL is one of the key enzymes responsible for its hydrolysis, and breaks 2-AG down to fatty acid and glycerol (Dinh *et al.*, 2002).

JZL184 is a selective, irreversible inhibitor of MAGL, effective at alleviating mechanical and cold allodynia in the neuropathic CCI mouse model (Schlosburg *et al.*, 2010). This effect was not seen in CB₁ receptor knock-out mice, but was present in CB₂ receptor knock-out mice (Kinsey *et al.*, 2010), suggesting a CB₁ receptor-selective mechanism of action is responsible for the inhibitory effects mediated by increased 2-AG. Interestingly, the ameliorative effect of FAAH inhibition on mechanical hypersensitivity was not present in either CB₁ or CB₂ receptor knockouts, suggesting that both receptors are required for the action of anandamide (see 5.1.2.2 for more on FAAH inhibition). This hypothesis was confirmed in a later study which demonstrated that the analgesic effects of JZL184 in the CCI mouse model were only blocked by a CB₁ receptor antagonist (Kinsey *et al.*, 2009).

An issue facing the use of JZL184 is that repeated administration of a high dose (40 mg/kg, i.p) caused tolerance, with mice showing similar responses to those of vehicle-treated mice in pain assays (Schlosburg *et al.*, 2010). However recent studies, using lower doses, have shown that repeated administration of JZL184 is effective at alleviating mechanical hypersensitivity in the carrageenan model, with only repeated high doses leading to tolerance (Ghosh *et al.*, 2013). This was substantiated with the demonstration that low doses of JZL184 increased levels of 2-AG in the brain, and decreased cold and mechanical hypersensitivity, with no tolerance developing with repeated dosing, an effect not seen with higher doses (Kinsey *et al.*, 2013).

Another problem with JZL184 is that it displays a 10-fold lower potency in the rat (Long *et al.*, 2009a). However a new compound, MJN110, has been developed that displays high selectivity for MAGL (IC₅₀ in rats <100nm, whereas the IC₅₀ for FAAH >10µM), and has a similar potency in both rat and mouse (Niphakis *et al.*, 2013), and so may be able to play a role in alleviating mechanical hypersensitivity in the HFD/STZ model.

5.1.1.2.2. FAAH inhibitors

FAAH is a membrane-bound serine hydrolase enzyme that breaks down fatty-acid ethanolamides (FAEs) such as AEA, N-palmitoylethanolamine (PEA) and oleoylethanolamide (OEA) (Cravatt *et al.*, 1996). AEA is broken down to arachidonic acid and ethanolamine (Devane *et al.*, 1992). It binds with a four-fold higher affinity to the CB₁ receptor than the CB₂ receptor (Pertwee *et al.*, 1995), and is also an agonist at TRPV1 (Tognetto *et al.*, 2001).

AEA was shown to have analgesic effects in models of inflammatory pain (Calignano *et al.*, 1998). PEA, which acts as a PPARα ligand, has also been shown to have both analgesic and anti-inflammatory effects (Calignano *et al.*, 1998; Conti *et al.*, 2002; Jaggar *et al.*, 1998; LoVerme *et al.*, 2006), as well as having an antinociceptive effect in the CCI model (Costa *et al.*, 2008).

The importance of FAAH has been demonstrated in knock-out mice (FAAH^{-/-}), which show a 15-fold increase in brain levels of AEA, and also exhibit reduced thermal and chemical pain sensation, which can be reversed by a CB₁ receptor antagonist (Cravatt *et al.*, 2001). Inhibitors of FAAH have been developed, such as URB597 (cyclohexyl carbamic acid 3'-carbamoyl-biphenyl-3-yl ester), which is a rapidly binding irreversible FAAH inhibitor, with no activity at cannabinoid receptors or MAGL (IC₅₀ in rats = 5nm for FAAH, >10µM for MAGL) (Piomelli *et al.*, 2006). Systemic administration of URB597 leads to profound inhibition of FAAH in the brain resulting in an increased accumulation of AEA in

the brain and spinal cord (Fegley *et al.*, 2005; Russo *et al.*, 2007). When administered to FAAH^{-/-} mice, the already increased levels of FAEs were not elevated further (Fegley *et al.*, 2005).

Repeated administration of URB597 causes a significant reduction in mechanical hypersensitivity and thermal hyperalgesia in the CCI model, and these effects were completely blocked by both CB₁ and CB₂ receptor antagonists (Kinsey *et al.*, 2009; Russo *et al.*, 2007). URB597 has antinociceptive efficacy in a variety of other models of pain, such as; the monosodium iodoacetate model of arthritis, and in Dunkin-Hartley guinea pigs where arthritis naturally occurs (Schuelert *et al.*, 2011); a model of cholestasis (Hasanein *et al.*, 2008); and the inflammatory carrageenan model (Okine *et al.*, 2012), where it blocked the expansion of the peripheral receptive field of WDR neurones in the spinal cord (Sagar *et al.*, 2008). URB597 has been shown to suppress the mechanically evoked responses of WDR neurones in sham-operated rats, but had no effect on these responses in the carrageenan (Sagar *et al.*, 2008) or the SNL model (Jhaveri *et al.*, 2006). Finally, it was also effective in alleviating mechanical hypersensitivity and thermal hyperalgesia in the complete Freund's adjuvant model (Jayamanne *et al.*, 2006), but conversely it had no effect in the PNL model.

Other FAAH inhibitors that have also been shown to have analgesic effects include OL135, a selective, reversible inhibitor, which caused substantial reversal of mechanical hypersensitivity in the mild thermal injury and SNL model (Chang *et al.*, 2006), as well as in the tail immersion, hot-plate and formalin tests, which were blocked by a CB₁ receptor antagonist (Lichtman *et al.*, 2004a). The effects of URB597 have also been investigated in the STZ model. URB597 produced an analgesic effect: lowering nociceptive scores in both phases of the formalin test, as well as increasing tail-flick latencies (Hasanein *et al.*, 2009a). ST4070, another FAAH inhibitor, alleviated established mechanical hypersensitivity in a dose-dependent manner in the STZ model (Caprioli *et al.*, 2012).

URB937, a peripherally restricted FAAH inhibitor, significantly reversed mechanical and thermal hyperalgesia in the carrageenan and SNL model, as well as the complete Freund's adjuvant model (Sasso *et al.*, 2012). Finally, a dual FAAH/MAGL inhibitor, JZL195, which causes a 10-fold elevation in both AEA and 2-AG in the brain, has a greater antinociceptive effect in the tail-flick test, than either JZL184 or PF-3845 (a FAAH inhibitor) alone (Long *et al.*, 2009b).

5.1.2. Antidiabetic drugs

5.1.2.1. Metformin

Metformin is an activator of AMPK, which can also be activated by low levels of cellular nutrients, or by other compounds such as AICAR or resveratrol. Its activation leads to the inhibition of mammalian target of rapamycin (mTOR) and ERK signalling (Tillu *et al.*, 2012), which results in a decrease in signalling to the translational machinery (Zoncu *et al.*, 2011), and decreased protein synthesis. The mTOR and ERK pathways (Ji *et al.*, 2009) have been linked to pathology in several animal models of pain. Norsted-Gregory *et al.* (2010) demonstrated an increase in downstream targets of mTOR in the ipsilateral dorsal horn in the carrageenan model of inflammatory pain, suggesting an increase in mTOR related signalling.

Metformin is effective in alleviating mechanical hypersensitivity, inhibiting translation regulation pathways and decreasing sensory neuronal excitability (Melemedjian *et al.*, 2011). In addition, resveratrol has been shown to reduce mechanical hypersensitivity in a model of post-surgery induced pain (Tillu *et al.*, 2012), as well as the formalin model (Torres-Lopez *et al.*, 2002), and the carrageenan model of inflammation (Gentilli *et al.*, 2001). Another method of inhibiting one of the mTOR complexes, mTORC1 (mammalian target of rapamycin complex 1), is through use of rapamycin itself, which alleviated mechanical hypersensitivity when applied locally in both an

inflammatory model (Geranton *et al.*, 2009) and a model of neuropathic pain (Jiménez-Díaz *et al.*, 2008), emphasising the important role the mTOR pathway plays in nociceptor sensitivity. Intrathecal administration of rapamycin was also effective at alleviating tactile and thermal hyperalgesia in the carrageenan model (Norsted Gregory *et al.*, 2010), and pain behaviour in the SNI (Geranton *et al.*, 2009) and formalin model (Asante *et al.*, 2010; Price *et al.*, 2007).

Obara *et al.* (2011), used temsirolimus (CCI-779), a rapamycin derivative, and Torin1, an inhibitor of both mTORC1 and mTORC2, and found that they were both effective in alleviating mechanical and cold hypersensitivity in the neuropathic SNI model, and mechanical hypersensitivity in the carrageenan model. As mTOR is mainly expressed in myelinated A-fibres in the peripheral nerve and dorsal roots, they postulated that this effect was mediated through A-fibres, leading to a decreased input to the dorsal horn. This hypothesis is supported by the observation that the carrageenan-induced thermal hypersensitivity, which is associated with peripheral sensitisation of C-fibres, was not altered by CCI-779.

Collectively there is strong evidence that metformin, through its activation of AMPK, may be able to play a role in alleviating the painful systems of diabetic neuropathy. One of the aims of the present study was to evaluate the potential analgesic effects of metformin in the HFD/STZ model.

5.1.2.2. Linagliptin

Preliminary evidence so far suggests that DPP-4 inhibitors, such as linagliptin, may also be able to play a role in alleviating painful symptoms. Two studies have investigated the effect of DPP-4 inhibitors on thermal/mechanical thresholds in the STZ model; PKF275-055 reversed thermal hypoalgesia and mechanical hypersensitivity (Bianchi

et al., 2012), and alogliptin improved thermal nociception (Davidson *et al.*, 2011a).

5.1.3. Aim of the Study

The aim of the first study was to investigate the ability of a new, more potent MAGL inhibitor, MJN110, to alter the already established mechanical hypersensitivity associated with the HFD/STZ model, as it has not yet been investigated in a neuropathic pain model. The inhibitory effects of this compound were compared to a well-studied FAAH inhibitor, URB597, as well as pregabalin, the gold standard treatment for DPNP, in the HFD/STZ model of diabetes.

The aim of the second study was to determine whether two currently prescribed oral antidiabetics (metformin and linagliptin) are able to alter the manifestation of mechanical hypersensitivity in the HFD/STZ model.

5.2. Methods

For detailed methods of induction of diabetes, blood sampling and von Frey testing see Chapter 2.

5.2.1. Animals

All experiments were carried out in accordance with the UK Home Office Animals (Scientific Procedures) Act 1986. 78 male Sprague-Dawley rats (200-250g), obtained from Charles River (Kent, UK), were individually housed on a normal light cycle (lights on: 07:00 - 19:00) with free access to a high fat diet (60% fat by caloric content; D12492 diet; Research Diets, New Jersey, USA) and water at all times. Food and water intake, and body weight were monitored twice weekly. After three weeks consumption of the HFD, rats received either an i.p. injection of STZ (45mgkg^{-1}), or citric acid buffer.

As specified in Chapter 2, any HFD/STZ rat with a plasma glucose concentration of $<15\text{mM}$ was to be excluded from the study, and two rats met this criteria in the present study and were excluded.

5.2.2. Administration of drugs

MJN110, URB597 and Pregabalin

The rats were divided into five stratified groups on the basis of body weight, blood glucose concentration and mechanical withdrawal thresholds. To assess the effect of systemic MJN110, URB597 and pregabalin on established pain behaviour, baseline von Frey testing was carried out 30 minutes before administration of the drug, and further testing was carried out at 1 hour and 3 hours after administration. MJN110 (5mgkg^{-1}) and URB597 (0.3mgkg^{-1}) were administered via i.p. injection, whereas pregabalin (10mgkg^{-1}) was administered orally, all at a volume of 1ml/kg . MJN110 and URB597 were dissolved in a vehicle of ethanol, Emulphor-620, and saline in a

ratio of 1:1:18, and pregabalin was dissolved in saline. Drug administration was carried out by two assistants to ensure that subsequent behaviour was assessed blind to treatment.

URB597 was given by i.p. injection in accordance with previous literature where it tends to be given via this route (or through local administration) (Hasanein *et al.*, 2009b; Jayamanne *et al.*, 2006; Kinsey *et al.*, 2009; Okine *et al.*, 2012), and MJN110 was therefore given via the same route, as has been shown to be effective in mice (Niphakis *et al.*, 2013). There are numerous literature reports on the delivery of pregabalin, and in the majority it is given orally, and so the oral route was used in this study (Field *et al.*, 1999b; Hahm *et al.*, 2012; Miyazaki *et al.*, 2012; Wodarski *et al.*, 2009; Yamamoto *et al.*, 2009).

Metformin and Linagliptin

HFD/STZ rats were divided into three stratified groups on the basis of body weight, blood glucose concentration and mechanical withdrawal thresholds. To assess the effect of systemic linagliptin (3mgkg^{-1}) and metformin (200mgkg^{-1}) on development of pain behaviour, animals were orally dosed daily with the drug, or saline vehicle, from day 4 until the conclusion of the study at day 40. All dosing was carried out blind to the treatment groups.

Both linagliptin and metformin were given orally in accordance with previous studies (Cheng *et al.*, 2006; Kern *et al.*, 2012; Kim *et al.*, 2012a; Klein *et al.*, 2012; Reed *et al.*, 2000; Vickers *et al.*, 2012). The dose of 3mgkg^{-1} of linagliptin was used as this dose is reported to improve glucose control when given once daily in animal models of diabetes (Hocher *et al.*, 2012), and it has been shown to significantly increase plasma GLP-1 in diet-induced obese rats and mice (Kern *et al.*, 2012; Vickers *et al.*, 2012), and to cause 67-80% DPP-4 inhibition (Kern *et al.*, 2012).

5.2.3. Quantification of endocannabinoids in spinal cord using liquid chromatography/tandem mass spectrometry (LC-MS/MS)

LC-MS/MS analysis was carried out to look at the changes induced in endocannabinoid levels in the spinal cord by URB597 and MJN110, compared to the 1:1:18 vehicle. Analysis was carried out by Dr Sarir Samad. Spinal cords were removed and stored at -80°C before analysis, and the extraction was performed on ice. Samples were weighed and transferred to homogenisation tubes. Internal standards (100µl of 2-AG-d8 (10µM) and 15 µl of AEA-d8 (28 µM); Cambridge Biosciences, Cambridge, UK) were added to each sample, blank sample, and endocannabinoid standard (Cambridge Biosciences). 5ml of ethyl acetate:hexane (9:1 vol./vol.) was added to each sample and homogenised thoroughly, then 3ml of deionised distilled water was added and the samples were homogenised further. Samples were then centrifuged (13000rpm, 10mins, 4 °C). The supernatants were transferred to glass tubes, and the procedure was repeated two more times and the supernatants pooled and then evaporated in a centrifugal evaporator. Prior to analysis, each sample extract was reconstituted in 200µl of acetonitrile. The injection volume was 5µl. Reproducibility was checked by repeated injections (n=6) of a mixed standard (1µM).

The HPLC system used was an Agilent 1100 series (Agilent Technologies, Germany). The HPLC Column used was a BDS Hypersil C8 column with BDS Hypersil C8 precolumn (100 x 2.1mm, 3µm) with guard column. Mobile phase A was water + 1g/L ammonium acetate +0.1% formic acid +10% ACN and mobile phase B was acetonitrile + 1g/L ammonium acetate +0.1% formic acid +10% H₂O. The starting flow rate was 300µL/min. The MS system used was a Micromass Quattro Ultima™ triple quadrupole mass spectrometer (Waters, Manchester, UK) equipped with an electro spray ionisation interface.

Quantification of the endocannabinoids was done using fully extracted calibration standards for each of the analytes. Quantification was performed using QuanLynx v4.1. Identification of each compound in plasma was confirmed by LC retention times of each standard and precursor and product ion *m/z* ratios. The peak area of each analyte was compared to a known amount of standard to determine the amount of target compound present. Measured concentrations of AEA, OEA, PEA and 2-AG in each sample were corrected for sample weight.

The standards used were:

Arachidonyl ethanolamide (*N*-(2-hydroxyethyl)-5Z,8Z,11Z,14Z-eicosatetraenamide, anandamide, AEA)

2-arachidonyl glycerol (2-AG, (5Z,8Z,11Z,14Z)-5,8,11,14-eicosatetraenoic acid, 2-hydroxy-1-(hydroxymethyl)ethyl ester)

Palmitoyl ethanolamide (PEA, *N*-(2-hydroxyethyl)-hexadecanamide)

Oleoyl ethanolamide (OEA, *N*-(2-hydroxyethyl)-9Z-octadecenamide)

Arachidonyl ethanolamide-d8 (*N*-(2-Hydroxyethyl)-5Z,8Z,11Z,14Z-eicosatetraenamide-d8, AEA-d8)

2-arachidonyl glycerol-d8 (2-AG-d8, (5Z,8Z,11Z,14Z)-5,8,11,14-Eicosatetraenoic acid-d8, 2-hydroxy-1-(hydroxymethyl)ethyl ester-d8)

5.2.4. Drugs

URB597 was purchased from Sigma Aldrich (Poole, UK), pregabalin was kindly provided by Pfizer (Cambridge, UK), and MJN110 was a kind gift from Micah Niphakis and Ben Cravatt (Scripps Research Institute, San Diego).

Metformin hydrochloride was purchased from Sigma Aldrich (Poole, UK), and linagliptin was a kind gift from Boehringer Ingelheim Pharmaceuticals (Ingelheim, Germany).

5.2.5. Statistics

MJN110, URB597 and Pregabalin

Analysis of plasma glucose was by a Repeated Measures ANOVA with Dunnett's post-hoc test. Analysis of changes in mechanical withdrawal thresholds, and plasma insulin was by Friedman test with Dunn's post-hoc test. Effects of drugs on mechanical withdrawal thresholds were analysed with a Kruskal-Wallis test with Dunn's post-hoc test.

Two rats were excluded from this study as the STZ injection did not cause an increase in plasma glucose concentration and so they could not be considered diabetic.

Metformin and Linagliptin

Analysis of plasma glucose and insulin, and mechanical withdrawal thresholds was by a Kruskal-Wallis test with Dunn's post-hoc test. Analysis of body weight, food intake and water intake was by an ANCOVA with Tukey's post-hoc test, with the average of day -7 to 0 as the covariate. In all analyses, a p value of less than 0.05 was considered statistically significant.

Two rats were excluded from this study as the STZ injection did not cause an increase in plasma glucose concentration and so they could not be considered diabetic. Additional rats were excluded from analysis of pain behaviour if in the week before injection with STZ the average hindpaw mechanical withdrawal threshold was < 10g. In this study, this represented 10 rats – 1 HFD/Veh, 3 HFD/STZ + vehicle, 3 HFD/STZ + metformin and 3 HFD/STZ + linagliptin.

5.3. Results

5.3.1. Acute effects of MJN110, URB597 and Pregabalin on established mechanical hypersensitivity

As described previously, induction of the HFD/STZ model leads to a significant increase ($p < 0.001$) in plasma glucose (Figure 5.2A), which is maintained throughout the study, and a significant decrease ($p < 0.001$) in plasma insulin at day 3, which decreased further by day 31 (Figure 5.2B). In addition, rats had a lower body weight following the induction of diabetes compared to basal body weight, and significantly increased water consumption ($p < 0.001$, data not shown).

By day 15 of the model, HFD/STZ rats exhibited lowered mechanical withdrawal thresholds to stimulation of the hindpaw (Figure 5.3A). At day 37 following model induction, the mechanical withdrawal threshold of the hindpaws was reduced to 6.7 ± 0.6 g, compared to basal values of 13.5 ± 0.4 g ($p < 0.001$). Systemic administration of MJN110 (5mgkg^{-1} , i.p.), URB597 (0.3mgkg^{-1} , i.p.) and pregabalin (10mgkg^{-1} , p.o.) reversed this decrease in mechanical withdrawal thresholds compared to the effects of vehicle treatment (Figure 5.3B). The effects of MJN110 and URB597 followed a similar pattern: an increase in the mechanical withdrawal thresholds was seen at 1 hour after administration of the drug, and this effect was further increased at 3 hours, although only the effects of MJN110 were significant. Pregabalin, however, had a maximal inhibitory effect at 1 hour post-administration, which was maintained, but not further increased at 3 hours post-administration.

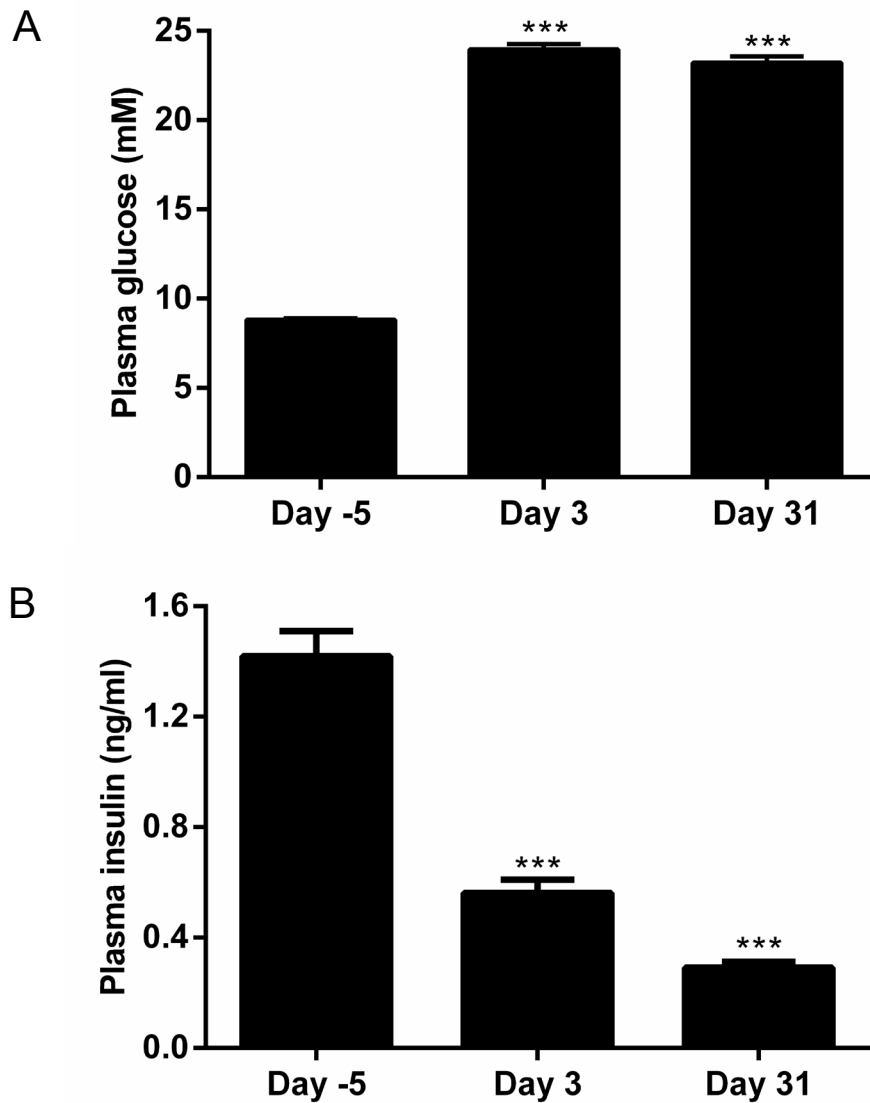


Figure 5.2 Fasting plasma **(A)** glucose and **(B)** insulin in HFD/STZ rats (n=36). All data represent mean \pm SEM, analysis of glucose was by a Repeated Measures ANOVA with Dunnett's Multiple Comparison post-hoc test, and analysis of plasma insulin was by a Friedman test with Dunn's post-hoc test:

*** $p < 0.001$, compared to baseline (day -5).

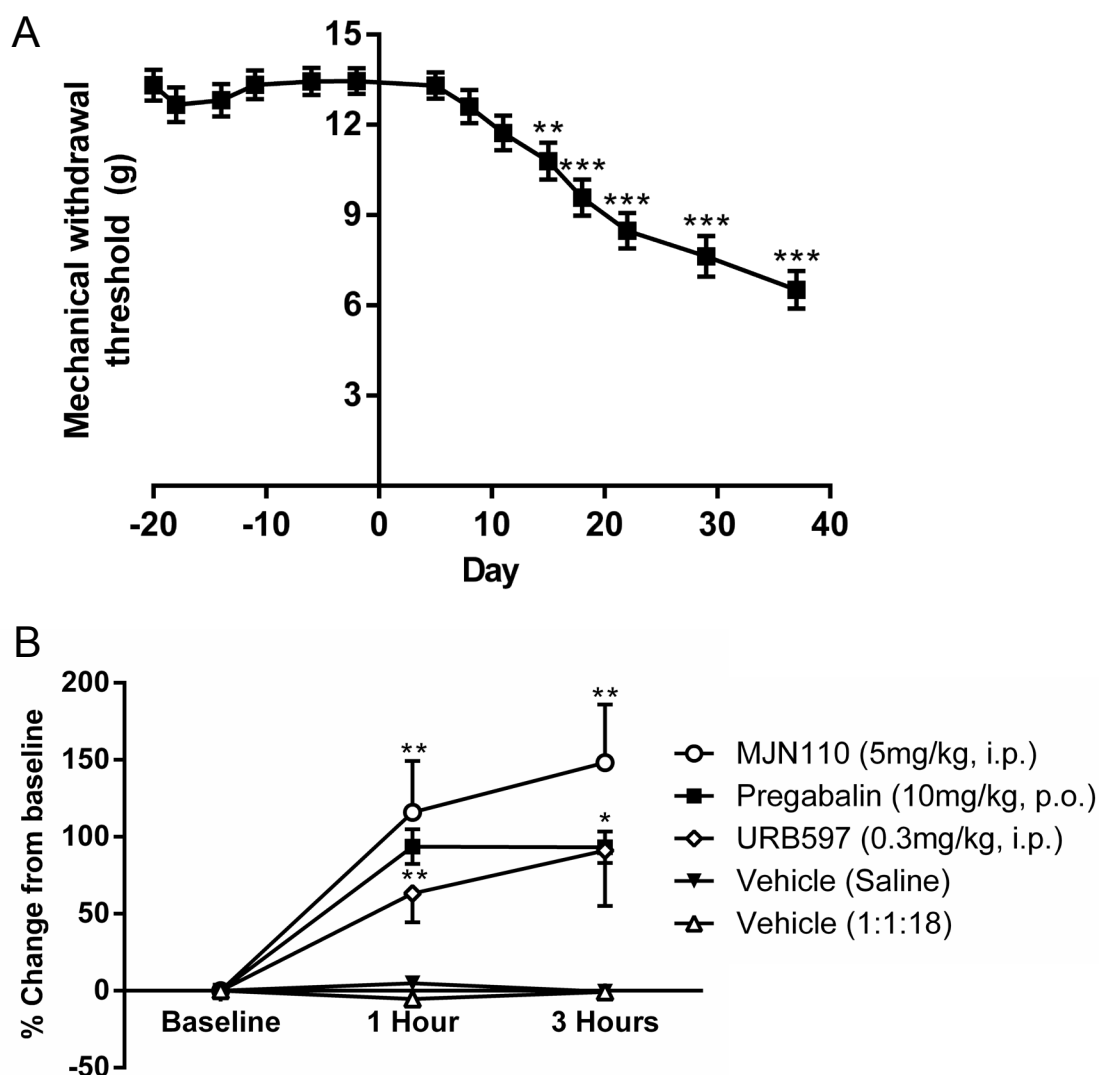


Figure 5.3 (A) Mechanical withdrawal thresholds of the hindpaw in HFD/STZ rats (n=36). All data represent mean \pm SEM, analysis was by a Friedman test with Dunn's post-hoc test: ** $p < 0.01$, *** $p < 0.001$, compared to baseline (day -2). **(B)** Effects of MJN110 (5mgkg^{-1} , i.p., n=8), URB597 (0.3mgkg^{-1} , i.p., n=8) and pregabalin (10mgkg^{-1} , p.o., n=9) on mechanical withdrawal thresholds in HFD/STZ rats (at day 37 post model induction) at 1 and 3 hours following drug administration. All data represent mechanical withdrawal thresholds expressed as a percentage of baseline values \pm SEM, analysis was by a Kruskal-Wallis test with Dunn's post-hoc test: * $p < 0.05$, ** $p < 0.01$

5.3.2. Acute effects of MJN110 and URB597 on endocannabinoid levels in spinal cord and brain

URB597 caused a significant increase in PEA and OEA levels in the spinal cord in comparison with the 1:1:18 vehicle ($p < 0.05$), and there was also a trend towards an increase in the level of AEA (Figure 5.4A-C). The same pattern is seen in the mid-brain where it caused a significant increase in all three FAEs (Figure 5.5A-C; $p < 0.01$). This indicates that URB597 was able to block FAAH, the enzyme responsible for degrading PEA, OEA and AEA, resulting in an increase in the levels of these endocannabinoids in both the brain and the spinal cord. MJN110, however, did not cause a significant increase in 2-AG in the spinal cord (Figure 5.4D), but a significant increase was seen in the mid-brain (Figure 5.5D; $p < 0.05$). This suggests that MJN110 was able to block MAGL, the enzyme responsible for breaking down 2-AG, resulting in an increase in the level of this endocannabinoid in the mid-brain.

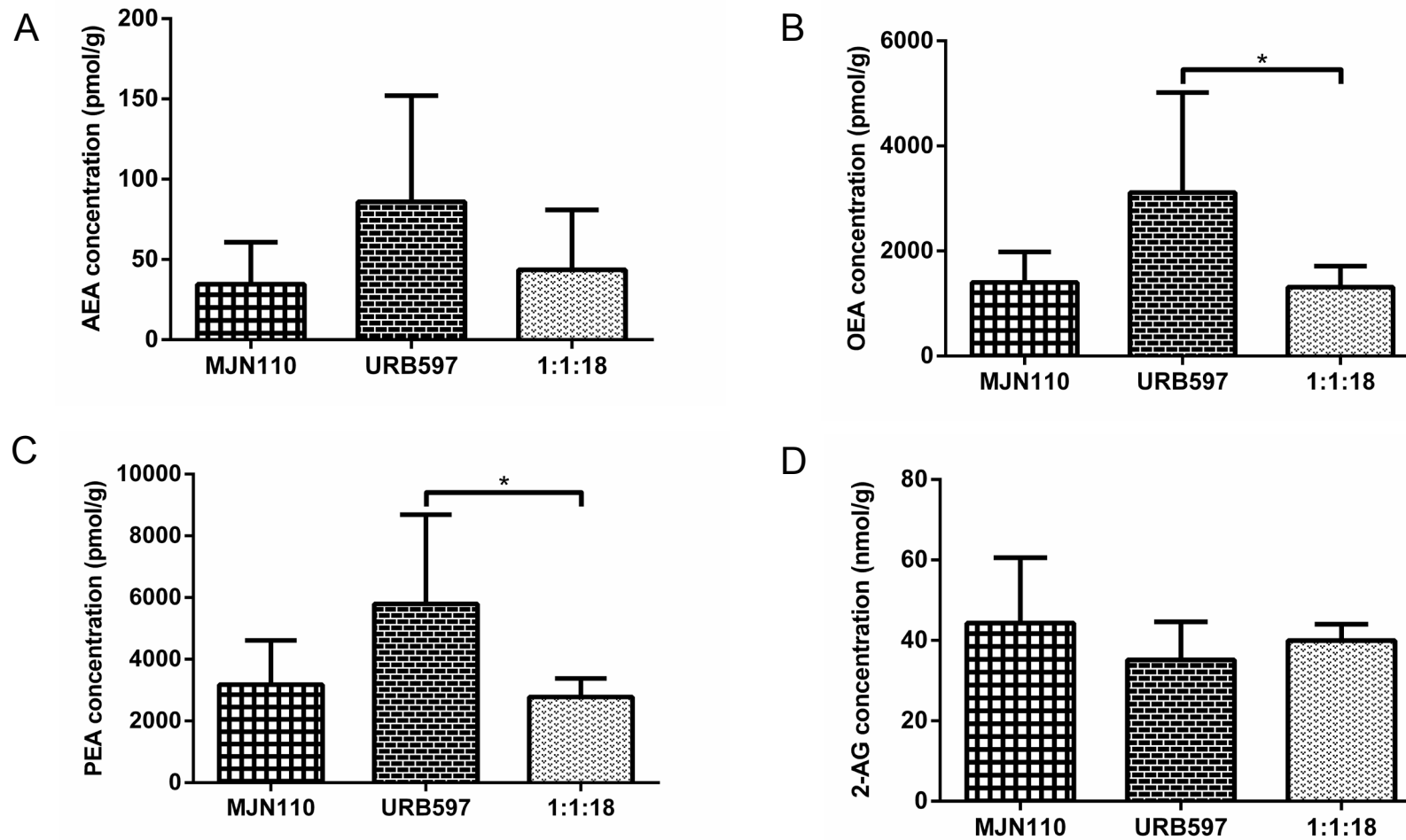


Figure 5.4 Effects of MJN110 (5mgkg^{-1} , i.p., $n=8$), URB597 (0.3mgkg^{-1} , i.p., $n=8$) and 1:1:18 vehicle ($n=5$) on levels of (A) AEA (B) PEA (C) OEA and (D) 2-AG in the spinal cord of HFD/STZ rats (at day 37 post model induction), approximately 4 hours after drug administration. All data represent mean \pm SEM, analysis was by a 1-way ANOVA with Tukey's post-hoc test: * $p<0.05$

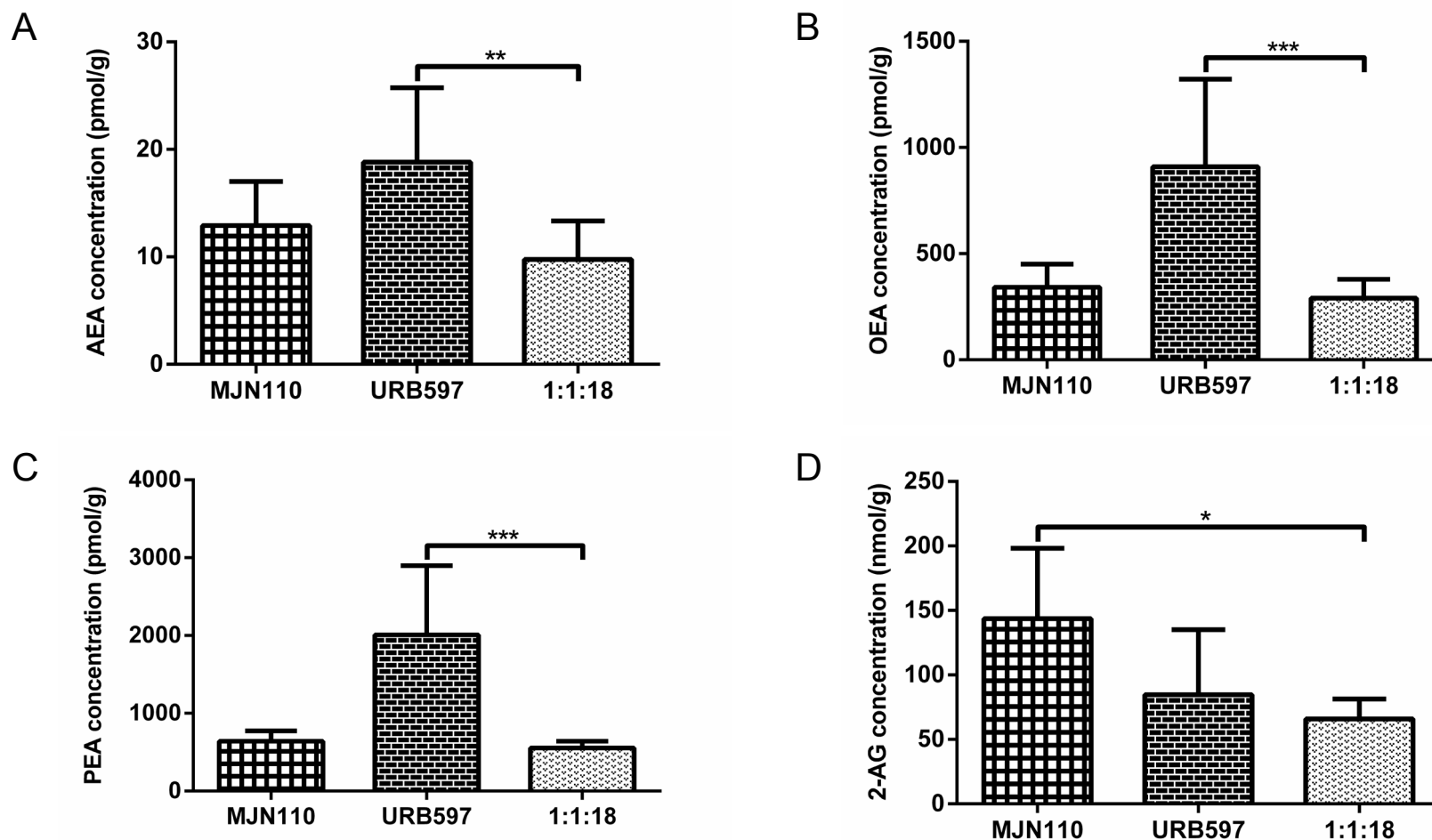


Figure 5.5 Effects of MJN110 (5mgkg^{-1} , i.p., $n=8$), URB597 (0.3mgkg^{-1} , i.p., $n=8$) and 1:1:18 vehicle ($n=5$) on levels of **(A)** AEA **(B)** PEA **(C)** OEA and **(D)** 2-AG in the mid-brain of HFD/STZ rats (at day 37 post model induction), approximately 4 hours after drug administration. All data represent mean \pm SEM, analysis was by a 1-way ANOVA with Tukey's post-hoc test:

* $p < 0.05$, ** $p < 0.01$, *** $p < 0.001$

5.3.3. Effects of Metformin and Linagliptin on metabolic parameters

As previously described there was a threefold increase in plasma glucose in all three HFD/STZ groups, in comparison to the HFD/Veh group (Figure 5.6A). Neither linagliptin (3mgkg^{-1}) nor metformin (200mgkg^{-1}) altered plasma glucose in HFD/STZ rats. The threefold decrease in plasma insulin in all the HFD/STZ rats, compared with the HFD/Veh group, was also not attenuated by linagliptin or metformin treatment (Figure 5.6B).

The growth rate of the HFD/STZ rats was severely stunted in comparison to the HFD/Veh animals (Figure 5.7A), with no effect of intervention with linagliptin or metformin. There was no significant change in food intake in the HFD/STZ rats compared to HFD/Veh controls, and this was also not altered by either antidiabetic drug (Figure 5.7B). Finally, the water intake in the HFD/STZ rats was significantly increased compared to the HFD/Veh rats (Figure 5.7C), with no effect of treatment except for around day 31 when the water intake was significantly higher in the linagliptin group, in comparison to the metformin group ($p < 0.05$).

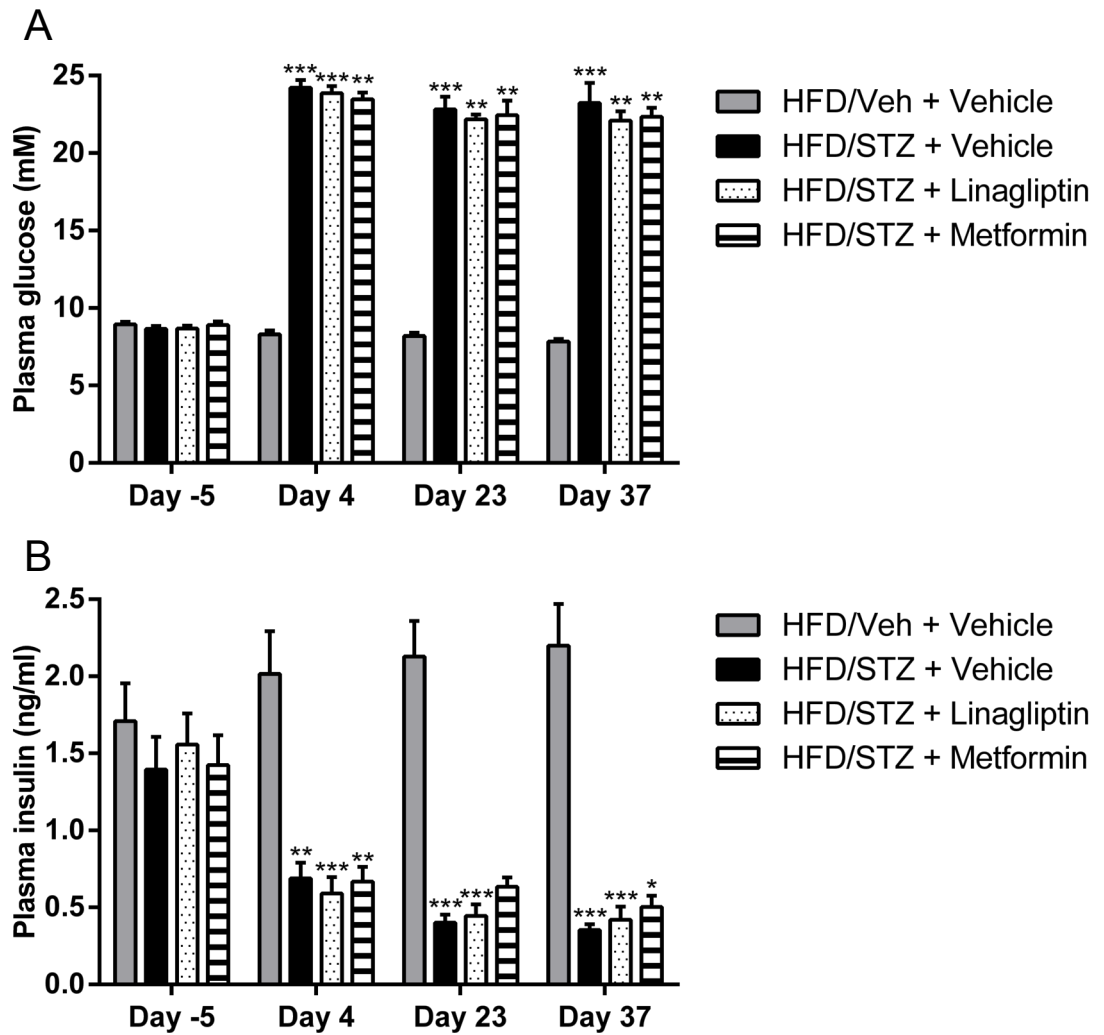


Figure 5.6 Effects of linagliptin (3mgkg^{-1} , p.o.; $n=10$) and metformin (200mgkg^{-1} , p.o.; $n=9$), given daily from day 4 onwards, on **(A)** fasting plasma glucose and **(B)** fasting plasma insulin, in comparison with vehicle treated HFD/Veh ($n=9$) and HFD/STZ ($n=11$) rats. All data represent mean \pm SEM, analysis was by a Kruskal-Wallis test with Dunn's post-hoc test: * $p<0.05$, ** $p<0.01$, *** $p<0.001$

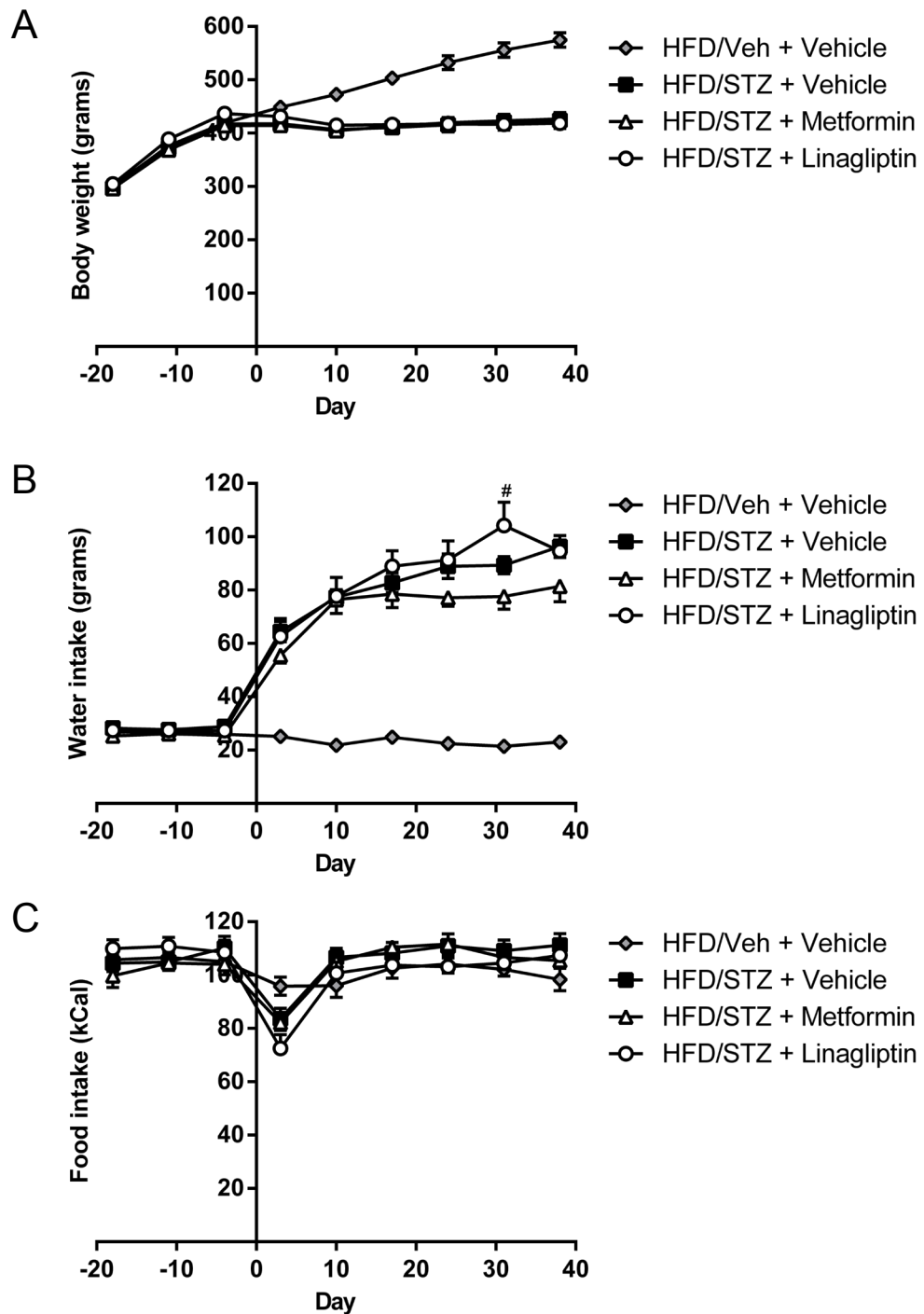


Figure 5.7 Effect of linagliptin (3mgkg^{-1} , p.o.; $n=10$) and metformin (200mgkg^{-1} , p.o.; $n=9$) on **(A)** body weight, **(B)** water intake, and **(C)** food intake, in comparison with vehicle treated HFD/Veh ($n=9$) and HFD/STZ ($n=11$) rats. All data represent mean \pm SEM, analysis was by an ANCOVA (with the average of day -7 to 0 as a covariate) with Tukey's post-hoc test: # $p<0.05$.

In comparison to HFD/Veh controls, body weight and water intake, $p<0.001$ from day 3 for all HFD/STZ rats.

5.3.4. Effects of Metformin and Linagliptin on the development of mechanical hypersensitivity

Consistent with my earlier studies, HFD/STZ caused a decrease in mechanical withdrawal thresholds compared to HFD/Veh rats, which became significant at day 21 (Figure 5.8). Both linagliptin and metformin (treatment from day 4) prevented the decrease in mechanical withdrawal thresholds in HFD/STZ rats. The withdrawal thresholds of these rats were not significantly different from the HFD/Veh rats at any timepoint, but were significantly different from the vehicle treated HFD/STZ rats from day 24, with this significance increasing as the study progressed.

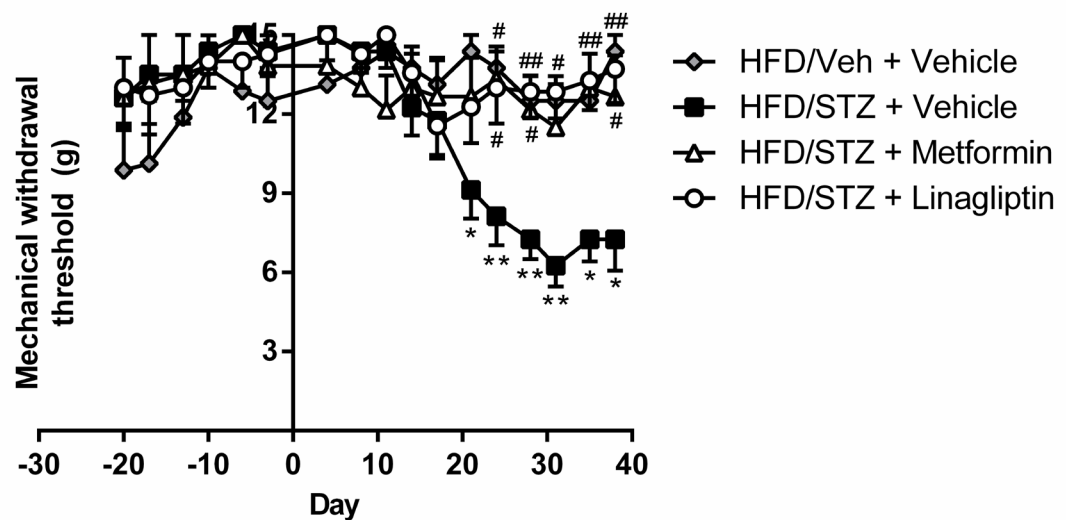


Figure 5.8 Effects of linagliptin (3mgkg^{-1} , p.o.; $n=7$) and metformin (200mgkg^{-1} , p.o.; $n=6$) on mechanical withdrawal thresholds of the hindpaws, in comparison with vehicle treated HFD/Veh ($n=8$) and HFD/STZ ($n=8$) rats. All data represent mean \pm SEM, analysis was by a Kruskal-Wallis test with Dunn's post-hoc test:

* $p < 0.05$, ** $p < 0.01$, in comparison with HFD/Veh + Vehicle

$p < 0.05$, ## $p < 0.01$, in comparison with HFD/STZ + Vehicle

5.4. Discussion

One of the problems facing patients with diabetic neuropathy today is the lack of medication that is effective at alleviating the neuropathic pain that can accompany this disease. One of the key objectives is therefore to develop new drugs, or to find alternative uses of current drugs, that are able to provide symptomatic relief of pain. In the present study it was demonstrated that MJN110, a novel MAGL inhibitor, was as effective as pregabalin at alleviating established mechanical hypersensitivity in the HFD/STZ model, highlighting a possible role of endocannabinoids in providing pain relief in diabetes. It was also demonstrated that two antidiabetic drugs, metformin and linagliptin, showed promise in preventing the development of mechanical hypersensitivity in this model when administered early on. It is worth investigating these findings further as both of these drugs are already licensed and have undergone all necessary safety testing, and so they could rapidly be put to use if effective.

5.4.1. Cannabinoids in the HFD/STZ model

The first study investigated the effects of two modulators of the endocannabinoids: MJN110 – a novel MAGL inhibitor, and URB597 – a FAAH inhibitor, in the HFD/STZ model of diabetes, and compared their effects to those of pregabalin, one of the first-line treatments for pain in diabetic neuropathy.

Mechanical hypersensitivity was well established by day 37, when a single acute administration of MJN110 produced a significant inhibition of mechanical hypersensitivity. Indeed, hindpaw withdrawal thresholds were returned close to control values in the presence of MJN110, demonstrating that it can block established hypersensitivity in this model of diabetic neuropathy. The inhibitory effects of MJN110 were comparable to those produced by the gold standard treatment, pregabalin, and even became more significant at the 3 hour timepoint.

URB597 was also effective, and showed the same response pattern as the other two drugs, but its effects did not reach significance at either timepoint, suggesting that significance could likely be reached with a slightly higher dose. LC-MS/MS analysis showed that URB597 significantly increased levels of the three FAEs in the spinal cord and mid-brain, and that MJN110 significantly increased levels of 2-AG in the mid-brain. These results indicate that endocannabinoid modulation may have a promising future in the treatment of diabetic neuropathy.

The analgesic effects of a variety of cannabinoids have previously been investigated in the STZ model (as discussed in the introduction), including WIN55212-2 (Dogrul *et al.*, 2004; Toth *et al.*, 2010; Ulugol *et al.*, 2004; Vera *et al.*, 2012), cannabidiol (Toth *et al.*, 2010) and cannabis extract (Comelli *et al.*, 2009). However the usefulness of these cannabinoid agonists is often limited clinically by the occurrence of unwanted psychotropic side effects.

My findings are consistent with previous reports that FAAH inhibitors possess analgesic activity in a wide variety of rodent models of nociception (Cravatt *et al.*, 2001). URB597 has shown analgesic properties in two models of hyperalgesia in STZ rats (Hasanein *et al.*, 2009a), and ST4070, another FAAH inhibitor, increased mechanical thresholds in STZ rats (Caprioli *et al.*, 2012). In the same study, they showed ST4070 to be more effective than URB597 or pregabalin in the CCI model.

One of the limitations of my study was that only a single acute dose of each drug was studied, which does not accurately reflect the situation in the clinic where the correct dose is titrated up, and long-term exposure may be required to see the full clinical efficacy (Berge, 2011). A single high dose may produce a different drug distribution and lead to unexpected effects, such as recruitment of antinociceptive mechanisms that would not be activated by a repeated dosing regime with a lower dose, and this could explain why drugs that seem efficacious in animal

models often fail in the clinic (Berge, 2011). It is therefore important to investigate the effect of repeated administration, to see whether the same effects would be seen, and if these could be maintained, or whether any tolerance would develop. Furthermore, if given from an earlier timepoint, it could be investigated whether either of these inhibitors would be able to prevent the development of neuropathic pain.

The effects of repeated administration of a FAAH inhibitor has been examined in several models with mixed results. In the CCI model, administration of URB597 (10mgkg⁻¹ p.o.) for four days was more effective at alleviating hypersensitivity than a single administration (Russo *et al.*, 2007), and the same group found that URB937 (1mgkg⁻¹ i.p.) given daily for 7 days was indistinguishable from single drug dosing (Clapper *et al.*, 2010). In agreement with this, PF3845, another FAAH inhibitor, maintained its anti-allodynic effect in the CCI model when given for 6 days (Schlosburg *et al.*, 2010), but, in the carrageenan model, 4 days of URB597 (0.3mgkg⁻¹ i.p.) was unable to reduce inflammatory hyperalgesia compared to a single acute dose (Okine *et al.*, 2012). Additionally, FAAH^{-/-} mice exhibit reduced pain behaviour in the tail immersion, hot-plate and formalin tests (Cravatt *et al.*, 2001), and the carrageenan model, but not in the CCI model, which Lichtman *et al.*, (2004b) postulated may be due to adaptive changes caused by nerve injury itself. From these results, it would appear that FAAH inhibitors are able to maintain their efficacy following repeated dosing in neuropathic models of pain, but studies with longer duration would be needed to see what the effects of long-time use might be.

Conversely, repeated dosing of the MAGL inhibitor JZL184 for six days, seems to lead to tolerance when given at high doses (40mgkg⁻¹). It loses its analgesic effects in both the CCI model (Kinsey *et al.*, 2013; Schlosburg *et al.*, 2010) and the carrageenan model (Ghosh *et al.*, 2013), but when given at a lower dose (4mgkg⁻¹) it is able to maintain its effectiveness in both models (Ghosh *et al.*, 2013; Kinsey *et al.*, 2013).

Furthermore, *Mgl1^{-/-}* mice, although displaying a 10-fold increase in 2-AG levels in the brain, display similar tail-withdrawal latencies to wild-type mice. These studies help to reinforce the importance of selecting an appropriate dose when planning any future studies with repeated dosing to avoid the possibility of tolerance developing.

Modulation of the endocannabinoid system is also showing promise in other areas of diabetes such as diabetic nephropathy, retinopathy and also cardiovascular complications (as reviewed by Horváth *et al.*, 2012). Additionally, with obesity becoming a growing problem, blockade of CB₁ receptors has shown promise, but its use so far has been limited due to its effect of increasing anxiety in patients. Several trials have found that in obese patients, rimonabant (a CB₁ receptor antagonist) is not only able to promote weight loss, but also decreases weight circumference and produces significant improvements in HDL-cholesterol, triglycerides and fasting insulin (Despres *et al.*, 2005; Pi-Sunyer *et al.*, 2006; Rosenstock *et al.*, 2008; Scheen *et al.*, 2006; Van Gaal *et al.*, 2005). However, a more recent trial had to be stopped prematurely as rimonabant was found to have serious neuropsychiatric side-effects, causing an increased risk of suicide (Topol *et al.*, 2010). This study highlights the importance of evaluating the risk of side-effects, and emphasises that perhaps modulation of levels of endocannabinoids may be a better way of tackling the problems associated with diabetes.

5.4.2. Antidiabetics in the HFD/STZ model

In the previous study in Chapter 4, the antidiabetic pioglitazone was administered 21 days after injection with STZ, and no significant alleviation of mechanical hypersensitivity was seen. As this drug was administered once pain behaviour was established, it was decided to administer the antidiabetic drugs in this study from day 4 after injection with STZ to see whether they could slow or prevent the development of mechanical hypersensitivity.

The two currently prescribed antidiabetic drugs investigated in this study were metformin and linagliptin, both of which significantly prevented the development of mechanical hypersensitivity. These findings are consistent with the report of analgesic effects of metformin in the SNI and SNL models (Melemedjian *et al.*, 2011; Melemedjian *et al.*, 2013). Resveratrol, another AMPK activator, has also been shown to be effective in acute, inflammatory, and chronic rodent pain models (Gentilli *et al.*, 2001; Tillu *et al.*, 2012; Torres-Lopez *et al.*, 2002).

Metformin is currently prescribed in diabetes for its ability to improve glycemic control and decrease blood sugar levels through multiple mechanisms, and in this study it was shown to also be effective at attenuating the development of mechanical allodynia. As metformin and other AMPK activators are effective in models of pain which do not have metabolic syndrome associated with them, I would hypothesise that it has a direct analgesic effect through activation of AMPK, and the inhibition of mTOR and ERK signalling pathways (Melemedjian *et al.*, 2011; Melemedjian *et al.*, 2013; Soares *et al.*, 2013). Inhibition of mTOR leads to inhibition of local protein synthesis (Jiménez-Díaz *et al.*, 2008), and blockade of ERK signalling has a multitude of effects, including decreased phosphorylation of Na_v1.7, (which prevents the changes in channel gating properties toward a hyperexcitable state (Stamboulian *et al.*, 2010)) resulting in a decrease in sensory neuronal excitability.

Further evidence of the effectiveness of inhibiting mTOR as a way to alleviate pain comes from the use of rapamycin, which inhibits mTORC1, and has been shown to alleviate mechanical hypersensitivity in preclinical models of inflammation (Geranton *et al.*, 2009) and neuropathic pain (Jiménez-Díaz *et al.*, 2008) when applied locally. CCI-779 and Torin1 (a rapamycin derivative, and an inhibitor of both mTORC1 and mTORC2 respectively) both reduced mechanical hypersensitivity in a mouse model of neuropathic pain when given systemically (Obara *et al.*, 2011). They hypothesised that the effects of mTORC1 inhibitors are mediated through A-fibres, where mTOR and its

active form (P-mTOR) are localised (Jiménez-Díaz *et al.*, 2008; Obara *et al.*, 2011).

Although metformin crosses the blood-brain-barrier, it appears that this drug and other AMPK activators, as well as direct mTORC1 inhibitors, have their effects on mechanical hypersensitivity through a peripheral mechanism of action. Both local (intraplantar) and systemic injections of CCI-779 produced comparable reductions in neuropathic sensitivity and systemic Torin1, which has limited access to the CNS, reduced mechanical and cold hypersensitivity (Obara *et al.*, 2011). Metformin caused a reversal of PNI-induced enhanced nascent protein synthesis, implying a direct action on the injured peripheral nervous system (Melemedjian *et al.*, 2011).

The findings of current studies suggest that AMPK activators may be a novel solution for the current problem of neuropathic pain, including that of painful diabetic neuropathy, and they warrant further investigation for the role they may be able to play clinically. Attention should also be paid to the development of more efficacious AMPK activators.

An unexpected outcome of this study was the inability of metformin to reduce blood glucose levels after prolonged administration. Other studies have found that dosing with metformin for four weeks causes a significant decrease in glucose levels in diabetic animals (Alhaider *et al.*, 2011; Erejuwa *et al.*, 2011). However only the higher dose of 500mgkg^{-1} is effective after 4 weeks of administration, and 100mgkg^{-1} does not have a significant effect until after 8 weeks (Alhaider *et al.*, 2011). Further studies have shown that long-term daily dosing with $300\text{--}350\text{mgkg}^{-1}$ metformin did not cause a change in blood glucose (Hauton, 2011; Kim *et al.*, 2012a), and finally, in other studies where metformin causes a decrease in glucose, blood samples were only taken shortly after an acute dose of metformin (Cheng *et al.*, 2006; Reed *et al.*, 2000; Wilson *et al.*, 2012b). It is possible that an acute effect of metformin on blood glucose levels was missed because dosing of metformin was

always carried out before blood samples were taken, or that a higher dose of metformin was needed in these rats to have a significant effect on blood glucose. Metformin's effect on AMPK, and the activation of the downstream signalling pathways, would still account for its analgesic properties.

To date, the effects of DPP4-inhibitors on pain behaviour have not been widely studied, with only two groups showing their ability to improve thermal nociception and reverse mechanical hypersensitivity (Bianchi *et al.*, 2012; Davidson *et al.*, 2011a). The findings in this chapter build on these previous studies, highlighting the ability of linagliptin to prevent the development of mechanical hypersensitivity in the HFD/STZ model.

The mechanism of action through which linagliptin is able to alleviate mechanical hypersensitivity has not yet been fully elucidated. Treatment with a DPP-4 inhibitor for 32 weeks was able to improve sensory thresholds to pressure, vibration, pain and temperature in the current perception threshold test in the STZ model, as well as decreasing the IENF loss (Jin *et al.*, 2009). This suggests that the GLP-1 pathway may play a role in attenuating nerve damage, as well as its metabolic effects on lowering glucose levels.

GLP-1 receptors are present in sciatic nerve and DRGs (Himeno *et al.*, 2011; Jolivald *et al.*, 2011; Kan *et al.*, 2012; Liu *et al.*, 2011), and these receptors have been shown to have a neuroprotective effect (During *et al.*, 2003). Exendin-4, which functions as a GLP-1R agonist is able to attenuate cutaneous nerve fibre damage, alleviate hypoesthesia as implied by the current perception threshold, protect Schwann cells and reduce the loss of IENFs in the STZ model without lowering glucose levels, suggesting that it a mechanism independent of glycemic control is responsible for these effects (Liu *et al.*, 2011). Other studies using exendin-4 showed it was able to ameliorate impaired neurite outgrowth of DRGs under high-glucose conditions *in vitro* (Himeno *et al.*, 2011; Perry *et al.*, 2002b), as well as improving: reduced sensory perception,

slowed NCV, and decreased IENF density in the plantar skin *in vivo* (Himeno *et al.*, 2011; Jolivald *et al.*, 2011). Exendin-4 also significantly improved slowing of sensory NCV in type 1 diabetic STZ mice and motor NCV in type 2 diabetic db/db mice, and was also able to improve thermal withdrawal latencies and restore mechanical sensitivity in the STZ mice (Kan *et al.*, 2012). However, in the db/db mice, exendin-4 caused a lowering of the thermal withdrawal latency, and had no effect on the loss of mechanical sensation (Kan *et al.*, 2012). Finally, GLP-1 and exendin-4 were also able to improve indices of pyridoxine-induced sensory peripheral neuropathy in rats (Perry *et al.*, 2007). It has been hypothesised that the neuroprotective effects of GLP-1 may be mediated by a cascade involving cAMP, and work through increasing trophic support (Kan *et al.*, 2012; Perry *et al.*, 2002a; Perry *et al.*, 2002b), or by coupling to anti-apoptotic signalling pathways (Li *et al.*, 2003).

In this study, linagliptin did not change either fasting glucose or insulin levels, which is consistent with other studies of DPP-4 inhibitors (Poucher *et al.*, 2012). Inhibition of DPP-4, and changes in GLP-1 were not measured in this study, but previous studies have reported decreased DPP-4 activity (Davidson *et al.*, 2011a), and an increase in GLP-1 (Jin *et al.*, 2009; Klein *et al.*, 2012; Pipatpiboon *et al.*, 2013).

My data suggest that the increase in GLP-1 by DPP-4 inhibition may contribute to the prevention of the development of mechanical hypersensitivity, but other substrates of DPP-4, such as stromal cell-derived factor-1a have also been shown to modulate neuropathic pain behaviour (Oh *et al.*, 2001). Further consolidation of evidence showing how DPP-4 inhibitors and GLP-1 agonists modulate altered fibre function and pain responses is needed to identify whether this treatment has any promise for diabetic neuropathic pain.

In conclusion, the results of the present study demonstrated that modulation of levels of endocannabinoids through use of a MAGL

inhibitor was as effective at alleviating the pain behaviour in the HFD/STZ model as the commonly prescribed first-line treatment pregabalin. These data provide an interesting first look at how these compounds might have a future in the treatment of painful diabetic neuropathy, but the long term effects of dosing with these compounds has yet to be investigated. Furthermore, metformin and linagliptin, two antidiabetic treatments, also showed promise in preventing the development of mechanical hypersensitivity in the HFD/STZ model, and this, combined with results from other recent studies, suggests they may be able to play a bigger role in diabetes than just their current role in glucose control.

Chapter 6.

General Discussion

The aim of this thesis was to assess the validity of the HFD/STZ model as one of type 2 diabetes, and also of diabetic neuropathy. The phenotype of the HFD/STZ model is summarised in Table 6.1. The model was found to produce some symptoms similar to the STZ-alone model: a rapid rise in plasma glucose and a rapid fall in plasma insulin, coupled with a huge increase in water intake and urine excretion. HFD/STZ was also found to produce a robust decrease in mechanical withdrawal thresholds, a behavioural correlate of mechanical hypersensitivity, compared to both lean/Veh and HFD/Veh controls. As the HFD/STZ combination resulted in a reproducible model of diabetic neuropathy, various aspects were examined further. There was no evidence for neuronal degeneration in DRGs or the spinal cord up to 50 days after model induction, but there was a decrease in GFAP expression, and in activated microglia in the spinal cord at this timepoint. Furthermore, there was a trend towards a decrease in the mechanically evoked responses of dorsal horn WDR neurones, but no changes in spontaneous firing or electrically evoked responses of these neurones. The pain behaviour associated with the HFD/STZ model of diabetic neuropathy was responsive to the gold standard analgesic gabapentin, antidiabetic treatments and two novel analgesic approaches.

Table 6.1 Summary of major findings

MWT – Mechanical withdrawal threshold

↔ no change

↑ or ↓ trend towards an increase/decrease

↑↑ or ↓↓ significant increase/decrease

	Lean	HFD	HFD/STZ
Body weight	↑	↑↑	↓↓
Water intake	↔	↔	↑↑
Food intake	↔	↑	↑↑
Glucose	↔	↑	↑↑
Insulin	↔	↑	↓↓
MWT	↔	↔	↓↓

Immunohistochemistry:

Microglia	↔	↔	↓↓
GFAP	↔	↔	↓↓
CGRP	↔	↔	↔
Fluoro-Jade B	↔	↔	↔

Electrophysiology:

Mechanically evoked	↔	↔	↓
Electrically evoked	↔	↔	↔
Spontaneous firing	↔	↔	↔
C-fibre threshold	↔	↔	↔
C-fibre latency	↔	↔	↔

6.1. HFD/STZ: a model of type 2 diabetes?

The HFD/STZ model has emerged as an interesting alternative to the STZ-alone model, which has been widely characterised and produces a robust model of type 1 diabetes (for review see King, 2012). As the vast majority of diabetic patients suffer from type 2 diabetes (Cheng, 2005), and as there have been some reports that diabetic neuropathy can vary between type 1 and type 2 diabetes (Arnold *et al.*, 2013; Loseth *et al.*,

2010; Sima *et al.*, 2006), it is important that we use animal models that are relevant to the clinical situation.

The HFD/STZ model is often referred to as a model of type 2 diabetes, but I think the model used in this thesis could be further refined to more closely reflect the clinical situation. The current model is based on feeding a high fat diet for a three week period before injection with STZ, but in reality this does not mimic the duration of the pre-diabetic stage in humans, which has been shown to last years before full-blown diabetes develops (Meigs *et al.*, 2003). β -cell dysfunction also develops slowly as the body becomes less able to compensate for insulin resistance (Rydén *et al.*, 2007), and during this period plasma insulin levels are fairly comparable to those seen in non-diabetic individuals (Reaven *et al.*, 1993). To further improve the model, a lower dose of STZ could also be used so that only a proportion of the β -cells are destroyed, allowing the rat to maintain a relatively normal level of insulin.

However, there has only been one previous report of pain assessment in the HFD/STZ model, and in this study, which used a lower dose of STZ (35mgkg^{-1}), there was no change in mechanical withdrawal thresholds (Ferhatovic *et al.*, 2013). This may not be surprising since the diabetic symptoms were much milder, with lower blood glucose concentrations, and greater gains in body mass (Ferhatovic *et al.*, 2013). Since the aim of this thesis was to investigate the signs of mechanical hypersensitivity that are associated with diabetic neuropathy and to explore the effects of a variety of therapeutic interventions on mechanical hypersensitivity, I selected the 45mgkg^{-1} dose of STZ. However, it is feasible that with a longer period of exposure to HFD prior to STZ treatment, a lower dose of STZ would then produce significant changes in pain behaviour.

Although the HFD/STZ model does not exactly reproduce diabetic neuropathy as it develops in humans, it aids in the understanding of some of the complex mechanisms underlying the development of

chronic pain associated with the disease, and it is important to remember that diabetic patients are themselves a heterogeneous population. It also highlights the importance of choosing an appropriate animal model for the endpoint you are interested in. If the goal of research is to specifically model the progression of type 2 diabetes, this would best be achieved with genetic models. However, if the aim is to investigate the mechanisms of chronic pain associated with type 2 diabetes, then the HFD/STZ (45mgkg⁻¹) model which mimics aspects of type 2 diabetes and exhibits robust pain behaviour is appropriate.

6.2. Assessment of mechanical hypersensitivity in the HFD/STZ model

Assessment of the development of mechanical hypersensitivity in this model used calibrated von Frey hairs. It has been suggested that these tests are not a direct measure of pain itself, but that they are a reflection of the hypersensitivity that develops alongside pain (Le Bars *et al.*, 2001; Mogil, 2009). Whilst allodynia and hyperalgesia are both associated with diabetic neuropathy, spontaneous pain is also an important symptom. There are a variety of proposed methods to assess spontaneous pain in animal models, but their use in the diabetic model is limited.

A video-tape can be used to monitor spontaneous, unprovoked pain behaviour, looking at factors such as immobility, locomotion, grooming, rearing and elevation of the paw, which can be scored by a blinded observer. While this method minimises handling, which may influence the behavioural response itself, it is very time consuming, and large numbers of rats are needed due to the high variability in behaviour (Olmaker *et al.*, 2002). It is also an indirect measure of pain, as while immobility, elevation of the paw and rearing can be interpreted as signs of spontaneous pain, they could also be altered by a variety of other factors. This method may prove useful in surgical models where

development of pain is rapid and very pronounced; but its application to the slower development of pain in the diabetic model is more questionable. Rats are prey animals and so any behaviour indicating pain which could be interpreted as weakness must be hidden, even though the underlying pain state may persist. The Rat Grimace Scale has recently been proposed as a method of quantifying pain through facial expressions such as orbital tightening, nose/cheek flattening, ear changes, and whisker changes (Sotocinal *et al.*, 2011). However it has only been shown to be effective up to 48 hours after the induction of inflammatory pain (Sotocinal *et al.*, 2011), and the SNI model in mice, which is of longer duration, is not associated with a 'pain face' (Langford *et al.*, 2010). Therefore the limited duration of facial grimacing is not applicable for models of neuropathic pain, such as diabetic neuropathy. These methods could therefore provide utility in other animal models, but in this thesis the effect of HFD/STZ was only assessed on evoked responses, as it was considered impractical to use any of the current methods that may be able to assess spontaneous pain in other shorter-term models.

In future studies, it would be interesting to quantify dynamic mechanical hypersensitivity in the HFD/STZ model, as this symptom is more often observed clinically, such as when clothing brushes against the skin. Static mechanical hypersensitivity is measured by the change in withdrawal threshold induced by von Frey hairs, whereas dynamic mechanical hypersensitivity is studied by light stroking with a cotton bud and measuring the withdrawal latency (Field *et al.*, 1999a). Field *et al.* (1999b) reported static mechanical hypersensitivity in the majority of diabetic rats within 10 days after injection with STZ, whereas the development of dynamic mechanical hypersensitivity had a slower onset, with fewer rats displaying sensitivity to stimulation with the cotton bud. They postulated that static mechanical hypersensitivity could be caused by the activation of A δ - and C-fibres, whereas dynamic mechanical hypersensitivity may be due to inappropriate activation of A β -fibres, and may be the result of more severe nerve damage. This

has been confirmed by studies in humans which have also shown that dynamic mechanical hypersensitivity is signalled by large myelinated A β -fibres, whereas the static component of mechanical hypersensitivity is signalled by unmyelinated fibres (Koltzenburg *et al.*, 1992). In the future, it would be valuable to determine whether the same pattern is observed in the HFD/STZ model, and whether any drug intervention is effective against both of these parameters, to ensure any results are more likely to show relevance in the clinical situation.

6.3. Mechanisms underlying the development of mechanical hypersensitivity

It is important to consider how the temporal development of the model is related to the progression of pain behaviour. Figure 6.1 shows a timeline of the progression of the HFD/STZ model, which brings about the question: what causes the switch to the development of mechanical hypersensitivity?

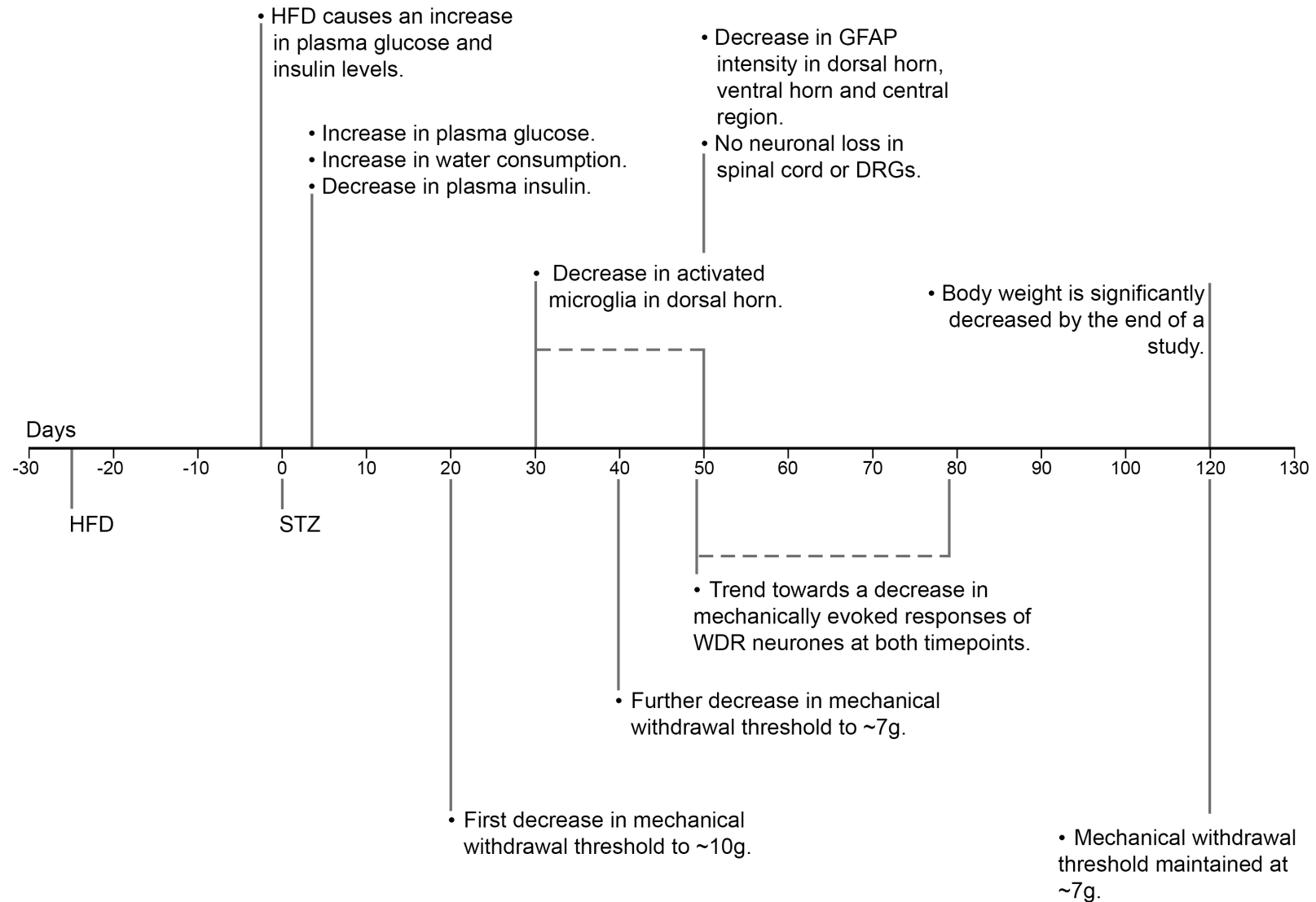


Figure 6.1 Temporal development of the HFD/STZ model of diabetes

As can be seen in Figure 6.1, it is not the rapid rise in plasma glucose, or the rapid decrease in plasma insulin that is directly responsible for the development of mechanical hypersensitivity, but it must be longer-term changes that underlie the later development of diabetic neuropathy. This would suggest that pain is not a direct consequence of hyperglycaemia, but it is the result of a variety of slower and longer-term molecular changes that are brought into play by elevated blood glucose and/or decreased insulin. Mechanisms, such as an increase in oxidative stress, may eventually lead to damage to neurones and altered function. On the basis of the findings of previous studies, it is likely that damage to these neurones induces a whole raft of changes, such as an increase in sodium channels and ectopic discharges, and neurochemical changes at the spinal cord level, which both lead to, and are influenced by, activation of glia. All of these slower changes are known to contribute to the manifestation of hypersensitivity in models of neuropathy, as well as other aberrant pain responses that are experienced in humans with diabetic neuropathy. Therefore it makes sense that the painful symptoms in this model take a few weeks to develop. A number of possible underlying mechanisms were investigated in this thesis.

The potential contribution of changes in spinal excitability to the manifestation of mechanical hypersensitivity was determined using electrophysiology. There was a trend towards a decrease in evoked responses of WDR dorsal horn neurones to mechanical stimulation, which has been observed previously in both the diabetic (Pertovaara *et al.*, 2001), SNL (Chapman *et al.*, 1998), spinal cord injury (Hao *et al.*, 2004) and cisplatin-induced chemoneuropathy (Cata *et al.*, 2008) models of neuropathic pain. Fluoro-Jade B staining was examined in both the DRGs and spinal cord to assess whether neuronal death might be responsible for this decrease in evoked responses, but very little positive staining was observed in any of the groups, with no increase in Fluoro-Jade B staining in the HFD/STZ group. However, it is possible that the neurones are already in an early damaged state, but have not

yet started to degenerate and produce the molecule that is detected by Fluoro-Jade B. It is feasible that in this state they are unable to function properly, resulting in the trend towards a decrease in evoked neuronal responses. If the model was taken out to a much later stage, I would expect an increase in the number of Fluoro-Jade B positive cells in the DRGs, consistent with previous studies of later stage apoptosis in the STZ animal model (Russell *et al.*, 1999; Schmeichel *et al.*, 2003; Zochodne *et al.*, 2001).

The importance of the role of astrocytes and microglia in the development and maintenance of neuropathic pain has been widely studied, and the results from the HFD/STZ model complement what has been reported so far. While an increase in astrocytes has been observed in many neuropathic pain models (Garrison *et al.*, 1991; Obata *et al.*, 2006; Raghavendra *et al.*, 2004; Sweitzer *et al.*, 1999; Wang *et al.*, 2009), in diabetic models a decrease in the amount of GFAP staining in the spinal cord is generally reported (Afsari *et al.*, 2008; Wodarski *et al.*, 2009). In my hands, a significant decrease in the mean grey intensity of GFAP staining was observed in both the dorsal and the ventral horn, as well as the central region, with greater changes seen in the dorsal and ventral horn at day 50 compared to the other timepoints. It has been hypothesised that this decrease is due to the reduction in the levels of circulating plasma insulin, as insulin has been shown to be important in the development of astrocytes (Aizenman *et al.*, 1987), and so a decrease may contribute to the reduction in the amount of GFAP staining in diabetic models. A decrease in glutamate transporters is observed in activated astrocytes in various pain models (Sung *et al.*, 2003; Wang *et al.*, 2006; Xin *et al.*, 2009). It would be interesting to investigate whether the decrease in the amount of GFAP staining is associated with a decrease in the expression of glutamate transporters, as increased levels of glutamate could lead to excitotoxicity (Nakagawa *et al.*, 2010), which could be one of the factors responsible for the pain experienced in diabetic neuropathy. As well as effects on the development of astrocytes, prolonged low levels of

insulin, as well as hyperglycaemia, have been proposed to contribute to the development of painful diabetic neuropathy. Insulin treatment has been shown to prevent or reverse mechanical hypersensitivity (Calcutt *et al.*, 1996; Hoybergs *et al.*, 2007; Otto *et al.*, 2011), and levels of insulin have been shown to be correlated with mechanical hypersensitivity (Romanovsky *et al.*, 2006). The impact of insulin deficiency on the function of sensory afferent fibres warrants further investigation.

Whilst the decrease in GFAP staining was as expected, the decrease in the number of activated microglia in the spinal cord was not. My data emphasise the importance of not just relying on phenotypic changes in microglia to assess whether they are activated, but to measure the change in markers, such as iNOS and CD16/32 for classically activated M1 microglia, and arginase-1 and CD206 for alternatively activated M2 microglia (Hirai *et al.*, 2013; Mantovani *et al.*, 2004). Another option would be to stain with p-erbB2, the receptor for the growth factor NRG1, which has been shown to be upregulated within activated microglia in the SNL model, correlating with the development of microgliosis (Calvo *et al.*, 2010), and also activates the ERK pathway (Calvo *et al.*, 2011). It would therefore be beneficial to double-label cells with markers for phospho-ERK (Morgado *et al.*, 2011a; Sweitzer *et al.*, 2004; Tsuda *et al.*, 2008) and phospho-p38 (Morgado *et al.*, 2011a; Sweitzer *et al.*, 2004), to see whether these pathways, which are switched on by microglia, are also activated in the HFD/STZ model. Further investigations would help to tease apart whether the numbers of classically activated, pro-inflammatory microglia are increased, regardless of whether they would be assessed as activated through morphology alone, helping to explain why an initial decrease was observed in this model.

If further studies were to be carried out in this model, it would be beneficial to examine the changes in sensory neurone morphology, in order to be able to make more conclusive statements about what is

happening at the level of the nerve, as in this thesis the main focus was the spinal cord.

6.4. Possible treatments for diabetic neuropathy

The current treatments for diabetic neuropathic pain are limited, and are often ineffective. It is therefore of major clinical importance to investigate the analgesic potential of current treatments as well as investigating the effects of novel compounds on diabetic neuropathic pain responses. This thesis was able to investigate both of these possibilities.

Pioglitazone, linagliptin and metformin, or drugs that bind to/activate the same target, have all recently shown promise at alleviating painful symptoms in animal models of neuropathic pain, through a variety of different mechanisms (Bianchi *et al.*, 2012; Churi *et al.*, 2008; Iwai *et al.*, 2008; Jain *et al.*, 2009; Jia *et al.*, 2013; Jia *et al.*, 2010; Maeda *et al.*, 2008; Melemedjian *et al.*, 2011; Morgenweck *et al.*, 2010; Morgenweck *et al.*, 2013; Takahashi *et al.*, 2011; Tillu *et al.*, 2012).

Both linagliptin and metformin, two currently prescribed antidiabetics, prevented the development of mechanical hypersensitivity in the HFD/STZ model when given 4 days after injection with STZ, without altering glucose or insulin levels. Whether these interventions can influence established pain behaviour requires future investigation. Given the large number of people currently being treated with these types of drugs, an epidemiological investigation of the prevalence of neuropathic pain in diabetic patients being treated with these different classes of compounds may help to provide much needed clinical evidence for whether these antidiabetic drugs alter the manifestation of chronic neuropathic pain. As both of these drugs were able to prevent the development of mechanical hypersensitivity without altering the changes in plasma glucose and insulin, this suggests that their effects must arise through their influence on mechanisms independent of

glycemic control. This lends further support to the hypothesis that it is not just the altered plasma glucose and insulin levels themselves which are directly responsible for the development of mechanical hypersensitivity, but other slower, molecular changes.

As discussed in Chapter 5, the analgesic properties of metformin have been demonstrated in other rodent models of neuropathic pain, suggesting that in the HFD/STZ model these effects may also be due to activation of AMPK. AMPK activation results in the inhibition of mTOR and ERK signalling pathways and insulin receptor substrate (IRS)-mediated feedback signalling, causing multiple effects such as inhibition of local protein synthesis and decreased phosphorylation of the Na_v1.7 channel, and it is thought that these effects are due to a peripheral mechanism of action. DPP-4 inhibitors such as linagliptin are also thought to have a peripheral action, as they improve sensory thresholds, and decrease nerve fibre loss (Jin *et al.*, 2009), suggesting an attenuation of nerve damage through the GLP-1 pathway. This is strengthened by the fact that GLP-1R agonists are able to attenuate nerve damage without lowering glucose levels, suggesting a mechanism independent of glycemic control (Himeno *et al.*, 2011; Jolivald *et al.*, 2011; Liu *et al.*, 2011).

Further studies should be carried out to confirm whether these are the mechanisms by which these drugs are effective. For example, the effects of GLP-1R agonists could be investigated in this model, as well as quantifying changes in IENF density in the HFD/STZ model, and the effects of DPP-4 inhibitors and GLP-1R agonists on this parameter. Experiments to determine the localisation of GLP-1 receptors in peripheral nerve would also be advisable. To further consolidate the evidence, it would be important to quantify changes in: the activity of mTOR and ERK; phosphorylation of their downstream targets; and the levels of proteins involved in RNA processing and transport in the sciatic nerve of HFD/STZ rats; as well as the level of eIF4F complex formation and nascent protein synthesis. From here it would be possible

to investigate whether administration of metformin, or other AMPK activators such as resveratrol or A769662, is able to change these levels, helping to identify whether it is the activation of AMPK, and the inhibition of mTOR and ERK, that is responsible for the changes in pain behaviour. If these changes in the activity of mTOR and nascent protein synthesis are partly responsible for the development of pain behaviour in this model, it would help to explain why the slower changes in the development of mechanical hypersensitivity do not happen in parallel with the rapid changes in glucose and insulin.

Previous studies have reported that early intervention with pioglitazone can also alter neuropathic pain symptoms in rodent models of peripheral nerve injury or spinal nerve transection (Iwai *et al.*, 2008; Jia *et al.*, 2013; Jia *et al.*, 2010; Maeda *et al.*, 2008; Morgenweck *et al.*, 2013). Treatment with the PPAR γ ligand pioglitazone once pain behaviour was established (3 weeks after STZ injection) was unable to reverse decreases in mechanical withdrawal thresholds. This raises the important issue that while identifying drugs that are able to prevent the development of mechanical hypersensitivity in an animal model may be a promising first step, whether they will show any efficacy when given to a diabetic patient who may have had the condition for many years before it was diagnosed, is unknown. This was the rationale behind giving pioglitazone at a relatively late timepoint, as it seemed that it would give a better indication of whether it would produce a clinically relevant result. It does highlight that whilst the results obtained from the antidiabetic drugs may show some promise, rigorous testing must be undertaken to see if they can be effective in patients when not administered under ideal conditions.

In the last study, an acute dose of pregabalin was shown to alleviate the well-established mechanical hypersensitivity at day 37 in the model. Pregabalin is one of the gold standard drugs prescribed for the treatment of neuropathic pain (Bril *et al.*, 2011). It has been shown to be effective at attenuating mechanical hypersensitivity in the STZ model of

diabetes (Field *et al.*, 1999b; Martinez *et al.*, 2012; Yamamoto *et al.*, 2009; Zhang *et al.*, 2013), as well as alleviating painful symptoms in diabetic patients, where it has been shown to be beneficial even in those patients who have had an unsatisfactory response to other treatments (Freeman *et al.*, 2008; Freynhagen *et al.*, 2005; Quilici *et al.*, 2009; Stacey *et al.*, 2008). My observation that gabapentin can alleviate established pain behaviour in the HFD/STZ model provides important new evidence of the translational value of this model for diabetic neuropathic pain. This is promising for the results that were obtained with the novel MAGL inhibitor, MJN110, and hopefully forward translation of this work might result in another effective treatment being made available to patients. MJN110 was found to be as effective as pregabalin at attenuating mechanical hypersensitivity in this study, and at 3 hours after administration it caused a greater attenuation of mechanical withdrawal thresholds than pregabalin itself. The FAAH inhibitor, URB597, also showed a trend towards increasing withdrawal thresholds, but this did not reach significance.

6.5. Conclusions

In conclusion, this thesis has highlighted the role that the HFD/STZ model can play in investigating underlying mechanisms of diabetic peripheral neuropathic pain, and its use in exploring potential new therapeutic options for alleviating this pain. There is a potential role of endocannabinoid modulators such as MJN110, and currently prescribed drugs such as linagliptin and metformin in the future treatment of the pain associated with this disease, as a diverse range and a combination of treatments will prove to be important in the future management of DPNP.

References

(1995). The effect of intensive diabetes therapy on the development and progression of neuropathy. The Diabetes Control and Complications Trial Research Group. *Ann Intern Med* **122**(8): 561-568.

Abbott CA, Malik RA, van Ross ER, Kulkarni J, Boulton AJ (2011). Prevalence and characteristics of painful diabetic neuropathy in a large community-based diabetic population in the U.K. *Diabetes Care* **34**(10): 2220-2224.

Adeghate E, Rashed H, Rajbandari S, Singh J (2006). Pattern of distribution of calcitonin gene-related Peptide in the dorsal root ganglion of animal models of diabetes mellitus. *Ann N Y Acad Sci* **1084**: 296-303.

Afsari ZH, Renno WM, Abd-El-Basset E (2008). Alteration of glial fibrillary acidic proteins immunoreactivity in astrocytes of the spinal cord diabetic rats. *Anatomical Record-Advances in Integrative Anatomy and Evolutionary Biology* **291**(4): 390-399.

Ahlgren SC, Levine JD (1993). Mechanical hyperalgesia in streptozotocin-diabetic rats. *Neuroscience* **52**(4): 1049-1055.

Ahlgren SC, Levine JD (1994). Protein kinase C inhibitors decrease hyperalgesia and C-fiber hyperexcitability in the streptozotocin-diabetic rat. *J Neurophysiol* **72**(2): 684-692.

Ahlgren SC, White DM, Levine JD (1992). Increased responsiveness of sensory neurons in the saphenous nerve of the streptozotocin-diabetic rat. *J Neurophysiol* **68**(6): 2077-2085.

Ahmed N (2005). Advanced glycation endproducts—role in pathology of diabetic complications. *Diabetes Research and Clinical Practice* **67**(1): 3-21.

Aizenman Y, de Vellis J (1987). Synergistic action of thyroid hormone, insulin and hydrocortisone on astrocyte differentiation. *Brain Res* **414**(2): 301-308.

Albers JW, Herman WH, Pop-Busui R, Feldman EL, Martin CL, Cleary PA, *et al.* (2010). Effect of prior intensive insulin treatment during the Diabetes Control and Complications Trial (DCCT) on peripheral neuropathy in type 1 diabetes during the Epidemiology of Diabetes Interventions and Complications (EDIC) Study. *Diabetes Care* **33**(5): 1090-1096.

Alhaider AA, Korashy HM, Sayed-Ahmed MM, Mobark M, Kfoury H, Mansour MA (2011). Metformin attenuates streptozotocin-induced diabetic nephropathy in rats through modulation of oxidative stress genes expression. *Chem Biol Interact* **192**(3): 233-242.

Ali Z, Ringkamp M, Hartke TV, Chien HF, Flavahan NA, Campbell JN, *et al.* (1999). Uninjured C-fiber nociceptors develop spontaneous activity and alpha-adrenergic sensitivity following L6 spinal nerve ligation in monkey. *J Neurophysiol* **81**(2): 455-466.

Anderson KJ, Fugaccia I, Scheff SW (2003). Fluoro-jade B stains quiescent and reactive astrocytes in the rodent spinal cord. *J Neurotrauma* **20**(11): 1223-1231.

Antognini JF, Carstens E (1999). Increasing Isoflurane from 0.9 to 1.1 Minimum Alveolar Concentration Minimally Affects Dorsal Horn Cell Responses to Noxious Stimulation. *Anesthesiology* **90**(1): 208-214.

Arner P (1995). Differences in lipolysis between human subcutaneous and omental adipose tissues. *Ann Med* **27**(4): 435-438.

Arnold R, Kwai N, Lin CS, Poynten AM, Kiernan MC, Krishnan AV (2013). Axonal dysfunction prior to neuropathy onset in type 1 diabetes. *Diabetes Metab Res Rev* **29**(1): 53-59.

Aronoff S, Rosenblatt S, Braithwaite S, Egan JW, Mathisen AL, Schneider RL (2000). Pioglitazone hydrochloride monotherapy improves glycemic control in the treatment of patients with type 2 diabetes: a 6-month randomized placebo-controlled dose-response study. The Pioglitazone 001 Study Group. *Diabetes Care* **23**(11): 1605-1611.

Asante CO, Wallace VC, Dickenson AH (2010). Mammalian target of rapamycin signaling in the spinal cord is required for neuronal plasticity and behavioral hypersensitivity associated with neuropathy in the rat. *J Pain* **11**(12): 1356-1367.

Association AD (2013). Standards of Medical Care in Diabetes—2013. *Diabetes Care* **36**(Supplement 1): S11-S66.

Atkinson MA, Eisenbarth GS (2001). Type 1 diabetes: new perspectives on disease pathogenesis and treatment. *The Lancet* **358**(9277): 221-229.

Aubel B, Kayser V, Mauborgne A, Farre A, Hamon M, Bourgoin S (2004). Antihyperalgesic effects of cizolirtine in diabetic rats: behavioral and biochemical studies. *Pain* **110**(1-2): 22-32.

Averill S, McMahon SB, Clary DO, Reichardt LF, Priestley JV (1995). Immunocytochemical localization of trkA receptors in chemically

identified subgroups of adult rat sensory neurons. *Eur J Neurosci* **7**(7): 1484-1494.

Barber AJ, Antonetti DA, Gardner TW (2000). Altered expression of retinal occludin and glial fibrillary acidic protein in experimental diabetes. The Penn State Retina Research Group. *Invest Ophthalmol Vis Sci* **41**(11): 3561-3568.

Basbaum AI, Bautista DM, Scherrer G, Julius D (2009). Cellular and molecular mechanisms of pain. *Cell* **139**(2): 267-284.

Bauer CS, Nieto-Rostro M, Rahman W, Tran-Van-Minh A, Ferron L, Douglas L, *et al.* (2009). The increased trafficking of the calcium channel subunit alpha2delta-1 to presynaptic terminals in neuropathic pain is inhibited by the alpha2delta ligand pregabalin. *J Neurosci* **29**(13): 4076-4088.

Baydas G, Nedzvetskii VS, Tuzcu M, Yasar A, Kirichenko SV (2003). Increase of glial fibrillary acidic protein and S-100B in hippocampus and cortex of diabetic rats: effects of vitamin E. *Eur J Pharmacol* **462**(1-3): 67-71.

Begon S, Pickering G, Eschalier A, Dubray C (2000). Magnesium and MK-801 have a similar effect in two experimental models of neuropathic pain. *Brain Res* **887**(2): 436-439.

Bennett DL, Averill S, Clary DO, Priestley JV, McMahon SB (1996). Postnatal changes in the expression of the trkA high-affinity NGF receptor in primary sensory neurons. *Eur J Neurosci* **8**(10): 2204-2208.

Bennett DL, Michael GJ, Ramachandran N, Munson JB, Averill S, Yan Q, *et al.* (1998). A distinct subgroup of small DRG cells express GDNF receptor components and GDNF is protective for these neurons after nerve injury. *J Neurosci* **18**(8): 3059-3072.

Bennett GJ, Kajander KC, Sahara Y, Iadarola MJ, Sugimoto T (1989). Neurochemical and anatomical changes in the dorsal horn of rats with an experimental painful peripheral neuropathy. In: (ed)^(eds). *Processing of sensory information in the superficial dorsal horn of the spinal cord*, edn: Springer. pp 463-471.

Benyamin R, Trescot AM, Datta S, Buenaventura R, Adlaka R, Sehgal N, *et al.* (2008). Opioid complications and side effects. *Pain Physician* **11**(2 Suppl): S105-120.

Berge OG (2011). Predictive validity of behavioural animal models for chronic pain. *British Journal of Pharmacology* **164**(4): 1195-1206.

Berger J, Moller DE (2002). The mechanisms of action of PPARs. *Annu Rev Med* **53**: 409-435.

Berger JP, Akiyama TE, Meinke PT (2005). PPARs: therapeutic targets for metabolic disease. *Trends Pharmacol Sci* **26**(5): 244-251.

Bernardo A, Minghetti L (2008). Regulation of Glial Cell Functions by PPAR-gamma Natural and Synthetic Agonists. *PPAR Res* **2008**: 864140.

Bianchi R, Cervellini I, Porretta-Serapiglia C, Oggioni N, Burkey B, Ghezzi P, *et al.* (2012). Beneficial effects of PKF275-055, a novel, selective, orally bioavailable, long-acting dipeptidyl peptidase IV inhibitor in streptozotocin-induced diabetic peripheral neuropathy. *J Pharmacol Exp Ther* **340**(1): 64-72.

Bierhaus A, Fleming T, Stoyanov S, Leffler A, Babes A, Neacsu C, *et al.* (2012). Methylglyoxal modification of Nav1.8 facilitates nociceptive neuron firing and causes hyperalgesia in diabetic neuropathy. *Nat Med* **18**(6): 926-933.

Bierhaus A, Haslbeck KM, Humpert PM, Liliensiek B, Dehmer T, Morcos M, *et al.* (2004). Loss of pain perception in diabetes is dependent on a receptor of the immunoglobulin superfamily. *J Clin Invest* **114**(12): 1741-1751.

Binns BC, Huang Y, Goettl VM, Hackshaw KV, Stephens Jr RL (2005). Glutamate uptake is attenuated in spinal deep dorsal and ventral horn in the rat spinal nerve ligation model. *Brain Research* **1041**(1): 38-47.

Bishnoi M, Bosgraaf CA, Abooj M, Zhong L, Premkumar LS (2011). Streptozotocin-Induced Early Thermal Hyperalgesia is independent of Glycemic State of Rats: Role of Transient Receptor Potential Vanilloid 1 (TRPV1) and Inflammatory mediators. *Molecular Pain* **7**.

Bluestone JA, Herold K, Eisenbarth G Genetics, pathogenesis and clinical interventions in type 1 diabetes. *Nature* **464**(7293): 1293-1300.

Bock G, Dalla Man C, Campioni M, Chittilapilly E, Basu R, Toffolo G, *et al.* (2006). Pathogenesis of Pre-Diabetes. *Diabetes* **55**(12): 3536-3549.

Booker L, Kinsey SG, Abdullah RA, Blankman JL, Long JZ, Ezzili C, *et al.* (2012). The fatty acid amide hydrolase (FAAH) inhibitor PF-3845 acts in the nervous system to reverse LPS-induced tactile allodynia in mice. *Br J Pharmacol* **165**(8): 2485-2496.

Bree AJ, Puente EC, Daphna-Iken D, Fisher SJ (2009). Diabetes increases brain damage caused by severe hypoglycemia. *Am J Physiol Endocrinol Metab* **297**(1): E194-201.

Brewster WJ, Diemel LT, Leach RM, Tomlinson DR (1994). Reduced sciatic nerve substance P and calcitonin gene-related peptide in rats

with short-term diabetes or central hypoxaemia co-exist with normal messenger RNA levels in the lumbar dorsal root ganglia. *Neuroscience* **58**(2): 323-330.

Bril V, England J, Franklin GM, Backonja M, Cohen J, Del Toro D, *et al.* (2011). Evidence-based guideline: Treatment of painful diabetic neuropathy. *Neurology* **76**(20): 1758-1765.

Brown MJ, Martin JR, Asbury AK (1976). Painful diabetic neuropathy. A morphometric study. *Arch Neurol* **33**(3): 164-171.

Brownlee M (2001). Biochemistry and molecular cell biology of diabetic complications. *Nature* **414**(6865): 813-820.

Brownlee M (2005). The pathobiology of diabetic complications - A unifying mechanism. *Diabetes* **54**(6): 1615-1625.

Brussee V, Guo G, Dong Y, Cheng C, Martinez JA, Smith D, *et al.* (2008). Distal Degenerative Sensory Neuropathy in a Long-Term Type 2 Diabetes Rat Model. *Diabetes* **57**(6): 1664-1673.

Burgess GM, Mullaney I, McNeill M, Dunn PM, Rang HP (1989). Second messengers involved in the mechanism of action of bradykinin in sensory neurons in culture. *J Neurosci* **9**(9): 3314-3325.

Burgess PR, Perl ER (1967). Myelinated afferent fibres responding specifically to noxious stimulation of the skin. *The Journal of Physiology* **190**(3): 541-562.

Calcutt NA (2002). Potential mechanisms of neuropathic pain in diabetes. In: David T (ed)^(eds). *International Review of Neurobiology*, edn, Vol. Volume 50: Academic Press. p^pp 205-228.

Calcutt NA, Chaplan SR (1997). Spinal pharmacology of tactile allodynia in diabetic rats. *Br J Pharmacol* **122**(7): 1478-1482.

Calcutt NA, Chen P, Hua XY (1998). Effects of diabetes on tissue content and evoked release of calcitonin gene-related peptide-like immunoreactivity from rat sensory nerves. *Neurosci Lett* **254**(3): 129-132.

Calcutt NA, Jorge MC, Yaksh TL, Chaplan SR (1996). Tactile allodynia and formalin hyperalgesia in streptozotocin-diabetic rats: effects of insulin, aldose reductase inhibition and lidocaine. *Pain* **68**(2-3): 293-299.

Calignano A, La Rana G, Giuffrida A, Piomelli D (1998). Control of pain initiation by endogenous cannabinoids. *Nature* **394**(6690): 277-281.

Callaghan BC, Little AA, Feldman EL, Hughes RA (2012). Enhanced glucose control for preventing and treating diabetic neuropathy. *Cochrane Database Syst Rev* **6**: CD007543.

Calvo M, Zhu N, Grist J, Ma Z, Loeb JA, Bennett DL (2011). Following nerve injury neuregulin-1 drives microglial proliferation and neuropathic pain via the MEK/ERK pathway. *Glia* **59**(4): 554-568.

Calvo M, Zhu N, Tsantoulas C, Ma Z, Grist J, Loeb JA, *et al.* (2010). Neuregulin-ErbB signaling promotes microglial proliferation and chemotaxis contributing to microgliosis and pain after peripheral nerve injury. *J Neurosci* **30**(15): 5437-5450.

Cameron NE, Cotter MA, Maxfield EK (1993). Anti-oxidant treatment prevents the development of peripheral nerve dysfunction in streptozotocin-diabetic rats. *Diabetologia* **36**(4): 299-304.

Campbell IW, Mariz S (2007). Beta-cell preservation with thiazolidinediones. *Diabetes Res Clin Pract* **76**(2): 163-176.

Campbell JN, LaMotte RH (1983). Latency to detection of first pain. *Brain Research* **266**(2): 203-208.

Campbell JN, Meyer RA (2006). Mechanisms of neuropathic pain. *Neuron* **52**(1): 77-92.

Campbell RK (2009). Type 2 diabetes: Where we are today: An overview of disease burden, current treatments, and treatment strategies. *Journal of the American Pharmacists Association* **49**: S3-S9.

Candelario-Jalil E, de Oliveira A, Graf S, Bhatia H, Hull M, Munoz E, *et al.* (2007). Resveratrol potently reduces prostaglandin E2 production and free radical formation in lipopolysaccharide-activated primary rat microglia. *Journal of Neuroinflammation* **4**(1): 25.

Caprioli A, Coccurello R, Rapino C, Di Serio S, Di Tommaso M, Vertechy M, *et al.* (2012). The Novel Reversible Fatty Acid Amide Hydrolase Inhibitor ST4070 Increases Endocannabinoid Brain Levels and Counteracts Neuropathic Pain in Different Animal Models. *Journal of Pharmacology and Experimental Therapeutics* **342**(1): 188-195.

Cata JP, Weng HR, Dougherty PM (2008). Behavioral and electrophysiological studies in rats with cisplatin-induced chemoneuropathy. *Brain Res* **1230**: 91-98.

Caterina MJ, Julius D (2001). The vanilloid receptor: a molecular gateway to the pain pathway. *Annu Rev Neurosci* **24**: 487-517.

Caterina MJ, Schumacher MA, Tominaga M, Rosen TA, Levine JD, Julius D (1997). The capsaicin receptor: a heat-activated ion channel in the pain pathway. *Nature* **389**(6653): 816-824.

Cesare P, McNaughton P (1996). A novel heat-activated current in nociceptive neurons and its sensitization by bradykinin. *Proceedings of the National Academy of Sciences* **93**(26): 15435-15439.

Ceseña RM, Calcutt NA (1999). Gabapentin prevents hyperalgesia during the formalin test in diabetic rats. *Neuroscience Letters* **262**(2): 101-104.

Chang L, Luo L, Palmer JA, Sutton S, Wilson SJ, Barbier AJ, et al. (2006). Inhibition of fatty acid amide hydrolase produces analgesia by multiple mechanisms. *Br J Pharmacol* **148**(1): 102-113.

Chaplan SR, Bach FW, Pogrel JW, Chung JM, Yaksh TL (1994). Quantitative assessment of tactile allodynia in the rat paw. *Journal of Neuroscience Methods* **53**(1): 55-63.

Chapman V, Suzuki R, Dickenson AH (1998). Electrophysiological characterization of spinal neuronal response properties in anaesthetized rats after ligation of spinal nerves L5-L6. *The Journal of Physiology* **507**(3): 881-894.

Chattopadhyay M, Zhou Z, Hao S, Mata M, Fink D (2012). Reduction of voltage gated sodium channel protein in DRG by vector mediated miRNA reduces pain in rats with painful diabetic neuropathy. *Molecular Pain* **8**(1): 17.

Chatzigeorgiou A, Halapas A, Kalafataki K, Kamper E (2009). The Use of Animal Models in the Study of Diabetes Mellitus. *In Vivo* **23**(2): 245-258.

Chen L, Huang LY (1992). Protein kinase C reduces Mg²⁺ block of NMDA-receptor channels as a mechanism of modulation. *Nature* **356**(6369): 521-523.

Chen SR, Pan HL (2002a). Hypersensitivity of spinothalamic tract neurons associated with diabetic neuropathic pain in rats. *Journal of Neurophysiology* **87**(6): 2726-2733.

Chen SR, Sweigart KL, Lakoski JM, Pan HL (2002b). Functional mu opioid receptors are reduced in the spinal cord dorsal horn of diabetic rats. *Anesthesiology* **97**(6): 1602-1608.

Chen X, Levine JD (2003). Altered temporal pattern of mechanically evoked C-fiber activity in a model of diabetic neuropathy in the rat. *Neuroscience* **121**(4): 1007-1015.

Chen X, Levine JD (2001). Hyper-responsivity in a subset of C-fiber nociceptors in a model of painful diabetic neuropathy in the rat. *Neuroscience* **102**(1): 185-192.

Cheng D (2005). Prevalence, predisposition and prevention of type II diabetes. *Nutr Metab (Lond)* **2**: 29.

Cheng JT, Huang CC, Liu IM, Tzeng TF, Chang CJ (2006). Novel mechanism for plasma glucose-lowering action of metformin in streptozotocin-induced diabetic rats. *Diabetes* **55**(3): 819-825.

Cherian PV, Kamijo M, Angelides KJ, Sima AAF Nodal Na⁺-channel displacement is associated with nerve-conduction slowing in the chronically diabetic BB/W rat: Prevention by aldose reductase inhibition. *Journal of Diabetes and its Complications* **10**(4): 192-200.

Chung SSM, Ho ECM, Lam KSL, Chung SK (2003). Contribution of Polyol Pathway to Diabetes-Induced Oxidative Stress. *Journal of the American Society of Nephrology* **14**(suppl 3): S233-S236.

Churi SB, Abdel-Aleem OS, Tumber KK, Scuderi-Porter H, Taylor BK (2008). Intrathecal rosiglitazone acts at peroxisome proliferator-activated receptor-gamma to rapidly inhibit neuropathic pain in rats. *Journal of Pain* **9**(7): 639-649.

Clapper JR, Moreno-Sanz G, Russo R, Guijarro A, Vacondio F, Duranti A, *et al.* (2010). Anandamide suppresses pain initiation through a peripheral endocannabinoid mechanism. *Nat Neurosci* **13**(10): 1265-1270.

Clarke RW (1985). The effects of decerebration and destruction of nucleus raphe magnus, periaqueductal grey matter and brainstem lateral reticular formation on the depression due to surgical trauma of the jaw-opening reflex evoked by tooth-pulp stimulation in the cat. *Brain Research* **332**(2): 231-236.

Coderre TJ, Katz J (1997). Peripheral and central hyperexcitability: differential signs and symptoms in persistent pain. *Behav Brain Sci* **20**(3): 404-419; discussion 435-513.

Coggeshall RE, Carlton SM (1997). Receptor localization in the mammalian dorsal horn and primary afferent neurons. *Brain Res Brain Res Rev* **24**(1): 28-66.

Colburn RW, Rickman AJ, DeLeo JA (1999). The effect of site and type of nerve injury on spinal glial activation and neuropathic pain behavior. *Exp Neurol* **157**(2): 289-304.

Coleman E, Judd R, Hoe L, Dennis J, Posner P (2004). Effects of diabetes mellitus on astrocyte GFAP and glutamate transporters in the CNS. *Glia* **48**(2): 166-178.

Coleman ES, Dennis JC, Braden TD, Judd RL, Posner P (2010). Insulin treatment prevents diabetes-induced alterations in astrocyte glutamate uptake and GFAP content in rats at 4 and 8 weeks of diabetes duration. *Brain Research* **1306**: 131-141.

Comelli F, Bettoni I, Colleoni M, Giagnoni G, Costa B (2009). Beneficial effects of a *Cannabis sativa* extract treatment on diabetes-induced neuropathy and oxidative stress. *Phytotherapy Research* **9999**(9999): n/a.

Comelli F, Bettoni I, Colombo A, Fumagalli P, Giagnoni G, Costa B (2010). Rimonabant, a cannabinoid CB1 receptor antagonist, attenuates mechanical allodynia and counteracts oxidative stress and nerve growth factor deficit in diabetic mice. *European Journal of Pharmacology* **637**(1-3): 62-69.

Conti S, Costa B, Colleoni M, Parolaro D, Giagnoni G (2002). Antiinflammatory action of endocannabinoid palmitoylethanolamide and the synthetic cannabinoid nabilone in a model of acute inflammation in the rat. *Br J Pharmacol* **135**(1): 181-187.

Costa B, Comelli F, Bettoni I, Colleoni M, Giagnoni G (2008). The endogenous fatty acid amide, palmitoylethanolamide, has anti-allodynic and anti-hyperalgesic effects in a murine model of neuropathic pain: involvement of CB1, TRPV1 and PPAR[γ] receptors and neurotrophic factors. *Pain* **139**(3): 541-550.

Costigan M, Mannion RJ, Kendall G, Lewis SE, Campagna JA, Coggeshall RE, *et al.* (1998). Heat Shock Protein 27: Developmental Regulation and Expression after Peripheral Nerve Injury. *The Journal of Neuroscience* **18**(15): 5891-5900.

Coull JA, Beggs S, Boudreau D, Boivin D, Tsuda M, Inoue K, *et al.* (2005). BDNF from microglia causes the shift in neuronal anion gradient underlying neuropathic pain. *Nature* **438**(7070): 1017-1021.

Coull JA, Boudreau D, Bachand K, Prescott SA, Nault F, Sik A, *et al.* (2003). Trans-synaptic shift in anion gradient in spinal lamina I neurons as a mechanism of neuropathic pain. *Nature* **424**(6951): 938-942.

Courteix C, Bardin M, Massol J, Fialip J, Lavarenne J, Eschalier A (1996). Daily insulin treatment relieves long-term hyperalgesia in streptozocin diabetic rats. *Neuroreport* **7**(12): 1922-1924.

Courteix C, Eschalier A, Lavarenne J (1993). Streptozocin-induced diabetic rats: behavioural evidence for a model of chronic pain. *Pain* **53**(1): 81-88.

Coyle DE (1998). Partial peripheral nerve injury leads to activation of astroglia and microglia which parallels the development of allodynic behavior. *Glia* **23**(1): 75-83.

Crandall M, Kwash J, Yu W, White G (2002). Activation of protein kinase C sensitizes human VR1 to capsaicin and to moderate decreases in pH at physiological temperatures in *Xenopus* oocytes. *Pain* **98**(1-2): 109-117.

Craner MJ, Klein JP, Renganathan M, Black JA, Waxman SG (2002). Changes of sodium channel expression in experimental painful diabetic neuropathy. *Ann Neurol* **52**(6): 786-792.

Cravatt BF, Demarest K, Patricelli MP, Bracey MH, Giang DK, Martin BR, *et al.* (2001). Supersensitivity to anandamide and enhanced endogenous cannabinoid signaling in mice lacking fatty acid amide hydrolase. *Proc Natl Acad Sci U S A* **98**(16): 9371-9376.

Cravatt BF, Giang DK, Mayfield SP, Boger DL, Lerner RA, Gilula NB (1996). Molecular characterization of an enzyme that degrades neuromodulatory fatty-acid amides. *Nature* **384**(6604): 83-87.

Cuzzocrea S, Pisano B, Dugo L, Ianaro A, Maffia P, Patel NS, *et al.* (2004). Rosiglitazone, a ligand of the peroxisome proliferator-activated receptor-gamma, reduces acute inflammation. *Eur J Pharmacol* **483**(1): 79-93.

Damjanac M, Bilan AR, Barrier L, Pontcharraud R, Anne C, Hugon J, *et al.* (2007). Fluoro-Jade® B staining as useful tool to identify activated microglia and astrocytes in a mouse transgenic model of Alzheimer's disease. *Brain Research* **1128**(0): 40-49.

Dandona P, Aljada A (2004). Endothelial dysfunction in patients with type 2 diabetes and the effects of thiazolidinedione antidiabetic agents. *J Diabetes Complications* **18**(2): 91-102.

Daousi C, MacFarlane IA, Woodward A, Nurmikko TJ, Bundred PE, Benbow SJ (2004). Chronic painful peripheral neuropathy in an urban community: a controlled comparison of people with and without diabetes. *Diabetic Medicine* **21**(9): 976-982.

Dauch JR, Yanik BM, Hsieh W, Oh SS, Cheng HT (2012). Neuron-astrocyte signaling network in spinal cord dorsal horn mediates painful neuropathy of type 2 diabetes. *Glia* **60**(9): 1301-1315.

Daulhac L, Mallet C, Courteix C, Etienne M, Duroux E, Privat A-M, *et al.* (2006). Diabetes-induced mechanical hyperalgesia involves spinal mitogen-activated protein kinase activation in neurons and microglia via N-methyl-D-aspartate-dependent mechanisms. *Molecular Pharmacology* **70**(4): 1246-1254.

Davidson E, Coppey L, Lu B, Arballo V, Calcutt NA, Gerard C, *et al.* (2009). The roles of streptozotocin neurotoxicity and neutral endopeptidase in murine experimental diabetic neuropathy. *Exp Diabetes Res* **2009**: 431980.

Davidson EP, Coppey LJ, Dake B, Yorek MA (2011a). Treatment of streptozotocin-induced diabetic rats with alogliptin: effect on vascular and neural complications. *Exp Diabetes Res* **2011**: 810469.

Davidson EP, Coppey LJ, Holmes A, Dake B, Yorek MA (2011b). Effect of treatment of high fat fed/low dose streptozotocin-diabetic rats with lilepatril on vascular and neural complications. *European Journal of Pharmacology* **668**(3): 497-506.

Davidson EP, Coppey LJ, Holmes A, Yorek MA (2012). Effect of inhibition of angiotensin converting enzyme and/or neutral endopeptidase on vascular and neural complications in high fat fed/low dose streptozotocin-diabetic rats. *European Journal of Pharmacology* **677**(1-3): 180-187.

Davies A, Hendrich J, Van Minh AT, Wratten J, Douglas L, Dolphin AC (2007). Functional biology of the alpha(2)delta subunits of voltage-gated calcium channels. *Trends Pharmacol Sci* **28**(5): 220-228.

de Senna PN, Ilha J, Baptista PP, do Nascimento PS, Leite MC, Paim MF, *et al.* (2011). Effects of physical exercise on spatial memory and astroglial alterations in the hippocampus of diabetic rats. *Metab Brain Dis* **26**(4): 269-279.

Despres JP, Golay A, Sjostrom L (2005). Effects of rimonabant on metabolic risk factors in overweight patients with dyslipidemia. *N Engl J Med* **353**(20): 2121-2134.

Desvergne B, Wahli W (1999). Peroxisome Proliferator-Activated Receptors: Nuclear Control of Metabolism. *Endocrine Reviews* **20**(5): 649-688.

Devane WA, Hanus L, Breuer A, Pertwee RG, Stevenson LA, Griffin G, *et al.* (1992). Isolation and structure of a brain constituent that binds to the cannabinoid receptor. *Science* **258**(5090): 1946-1949.

Devor M (2006). Response of nerves to injury in relation to neuropathic pain. In: Wall PD, Melzack R (ed) (eds). *Textbook of Pain*, edn. New York: Churchill Livingstone. p^pp.

Devor M (2005). Response of nerves to injury in relation to neuropathic pain. In: Wall PD, Melzack R (ed)^(eds). *Textbook of Pain*, edn. New York: Churchill Livingstone. p^pp.

Di Piero V, Jones AK, Iannotti F, Powell M, Perani D, Lenzi GL, *et al.* (1991). Chronic pain: a PET study of the central effects of percutaneous high cervical cordotomy. *Pain* **46**(1): 9-12.

Diamant M, Heine RJ (2003). Thiazolidinediones in type 2 diabetes mellitus - Current clinical evidence. *Drugs* **63**(13): 1373-1405.

Dickenson AH, Matthews EA, Suzuki R (2002). Neurobiology of neuropathic pain: mode of action of anticonvulsants. *European Journal of Pain* **6**(Supplement 1): 51-60.

Dickenson AH, Sullivan AF (1987). Evidence for a role of the NMDA receptor in the frequency dependent potentiation of deep rat dorsal horn nociceptive neurones following C fibre stimulation. *Neuropharmacology* **26**(8): 1235-1238.

Diemel LT, Brewster WJ, Fernyhough P, Tomlinson DR (1994). Expression of neuropeptides in experimental diabetes; effects of treatment with nerve growth factor or brain-derived neurotrophic factor. *Brain Res Mol Brain Res* **21**(1-2): 171-175.

Diemel LT, Stevens EJ, Willars GB, Tomlinson DR (1992). Depletion of substance P and calcitonin gene-related peptide in sciatic nerve of rats with experimental diabetes; effects of insulin and aldose reductase inhibition. *Neurosci Lett* **137**(2): 253-256.

Dinh TP, Freund TF, Piomelli D (2002). A role for monoglyceride lipase in 2-arachidonoylglycerol inactivation. *Chem Phys Lipids* **121**(1-2): 149-158.

Dixon WJ (1980). Efficient analysis of experimental observations. *Annu Rev Pharmacol Toxicol* **20**: 441-462.

Djouhri L, Lawson SN (2004). Abeta-fiber nociceptive primary afferent neurons: a review of incidence and properties in relation to other afferent A-fiber neurons in mammals. *Brain Res Brain Res Rev* **46**(2): 131-145.

Dobretsov M, Hastings SL, Romanovsky D, Stimers JR, Zhang J-M (2003). Mechanical hyperalgesia in rat models of systemic and local hyperglycemia. *Brain Research* **960**(1-2): 174-183.

Dobretsov M, Romanovsky D, Stimers JR (2007). Early diabetic neuropathy: Triggers and mechanisms. *World Journal of Gastroenterology* **13**(2): 175-191.

Dogrul A, Gül H, Yildiz O, Bilgin F, Güzeldemir ME (2004). Cannabinoids blocks tactile allodynia in diabetic mice without attenuation of its antinociceptive effect. *Neuroscience Letters* **368**(1): 82-86.

Dostrovsky JO, Craig AD (2006). Ascending projection systems. In: Wall PD, Melzack R (ed)^(eds). *Textbook of pain*, edn: Churchill Livingstone. p^pp.

Dostrovsky JO, Craig AD (2005). Ascending projection systems. In: Wall PD, Melzack R (ed)^(eds). *Textbook of pain*, edn: Churchill Livingstone. p^pp.

Dray A, Bettaney J, Forster P, Perkins MN (1988). Bradykinin-induced stimulation of afferent fibres is mediated through protein kinase C. *Neurosci Lett* **91**(3): 301-307.

Dreyer C, Krey G, Keller H, Givel F, Helftenbein G, Wahli W (1992). Control of the peroxisomal beta-oxidation pathway by a novel family of nuclear hormone receptors. *Cell* **68**(5): 879-887.

Driver JP, Serreze DV, Chen YG (2011). Mouse models for the study of autoimmune type 1 diabetes: a NOD to similarities and differences to human disease. *Semin Immunopathol* **33**(1): 67-87.

Drucker DJ (2006). The biology of incretin hormones. *Cell Metab* **3**(3): 153-165.

Drucker DJ, Nauck MA (2006). The incretin system: glucagon-like peptide-1 receptor agonists and dipeptidyl peptidase-4 inhibitors in type 2 diabetes. *Lancet* **368**(9548): 1696-1705.

Duby JJ, Campbell RK, Setter SM, White JR, Rasmussen KA (2004). Diabetic neuropathy: An intensive review. *American Journal of Health-System Pharmacy* **61**(2): 160-173.

During MJ, Cao L, Zuzga DS, Francis JS, Fitzsimons HL, Jiao X, *et al.* (2003). Glucagon-like peptide-1 receptor is involved in learning and neuroprotection. *Nat Med* **9**(9): 1173-1179.

Eckhardt M, Langkopf E, Mark M, Tadayyon M, Thomas L, Nar H, *et al.* (2007). 8-(3-(R)-aminopiperidin-1-yl)-7-but-2-ynyl-3-methyl-1-(4-methylquinazolin-2-ylmethyl)-3,7-dihydropurine-2,6-dione (BI 1356), a highly potent, selective, long-acting, and orally bioavailable DPP-4 inhibitor for the treatment of type 2 diabetes. *J Med Chem* **50**(26): 6450-6453.

Edwards JL, Vincent AM, Cheng HT, Feldman EL (2008). Diabetic neuropathy: Mechanisms to management. *Pharmacology & Therapeutics* **120**(1): 1-34.

Ellington HC, Cotter MA, Cameron NE, Ross RA (2002). The effect of cannabinoids on capsaicin-evoked calcitonin gene-related peptide (CGRP) release from the isolated paw skin of diabetic and non-diabetic rats. *Neuropharmacology* **42**(7): 966-975.

Erejuwa OO, Sulaiman SA, Wahab MS, Sirajudeen KN, Salleh MS, Gurtu S (2011). Glibenclamide or metformin combined with honey improves glycemic control in streptozotocin-induced diabetic rats. *Int J Biol Sci* **7**(2): 244-252.

Eriksson NP, Persson JK, Svensson M, Arvidsson J, Molander C, Aldskogius H (1993). A quantitative analysis of the microglial cell reaction in central primary sensory projection territories following peripheral nerve injury in the adult rat. *Exp Brain Res* **96**(1): 19-27.

FDA (2004). FDA Approves Drug for Neuropathic Pain Associated With Diabetes. Maryland: U.S. Food and Drug Administration.

Fegley D, Gaetani S, Duranti A, Tontini A, Mor M, Tarzia G, *et al.* (2005). Characterization of the fatty acid amide hydrolase inhibitor cyclohexyl carbamic acid 3'-carbamoylester (URB597): effects on anandamide and oleoylethanolamide deactivation. *J Pharmacol Exp Ther* **313**(1): 352-358.

Ferhatovic L, Banozic A, Kostic S, Kurir TT, Novak A, Vrdoljak L, *et al.* (2013). Expression of Calcium/Calmodulin-Dependent Protein Kinase II and Pain-Related Behavior in Rat Models of Type 1 and Type 2 Diabetes. *Anesthesia & Analgesia* **116**(3): 712-721.

Field MJ, Bramwell S, Hughes J, Singh L (1999a). Detection of static and dynamic components of mechanical allodynia in rat models of neuropathic pain: are they signalled by distinct primary sensory neurones? *Pain* **83**(2): 303-311.

Field MJ, Cox PJ, Stott E, Melrose H, Offord J, Su TZ, *et al.* (2006). Identification of the alpha2-delta-1 subunit of voltage-dependent calcium channels as a molecular target for pain mediating the analgesic actions of pregabalin. *Proc Natl Acad Sci U S A* **103**(46): 17537-17542.

Field MJ, McCleary S, Hughes J, Singh L (1999b). Gabapentin and pregabalin, but not morphine and amitriptyline, block both static and dynamic components of mechanical allodynia induced by streptozocin in the rat. *Pain* **80**(1-2): 391-398.

Fields HL, Basbaum AI, Heinricher MM (1999). Central nervous system mechanisms of pain modulation. In: Wall PD, Melzack R (eds). *Textbook of Pain*, edn: Churchill Livingstone. p^{pp}.

Fields HL, Basbaum AI, Heinricher MM (2005). Central nervous system mechanisms of pain modulation. In: Wall PD, Melzack R (eds). *Textbook of Pain*, edn. New York: Churchill Livingstone. p[^]pp.

Fields HL, Bry J, Hentall I, Zorman G (1983). The activity of neurons in the rostral medulla of the rat during withdrawal from noxious heat. *J Neurosci* **3**(12): 2545-2552.

Fields HL, Heinricher MM, Mason P (1991). Neurotransmitters in nociceptive modulatory circuits. *Annu Rev Neurosci* **14**: 219-245.

Fischer TZ, Tan AM, Waxman SG (2009). Thalamic neuron hyperexcitability and enlarged receptive fields in the STZ model of diabetic pain. *Brain Research* **1268**: 154-161.

Forbes JM, Cooper ME (2013). Mechanisms of Diabetic Complications. *Physiological Reviews* **93**(1): 137-188.

Fox A, Eastwood C, Gentry C, Manning D, Urban L (1999). Critical evaluation of the streptozotocin model of painful diabetic neuropathy in the rat. *Pain* **81**(3): 307-316.

Francis G, Martinez J, Liu W, Nguyen T, Ayer A, Fine J, *et al.* (2009). Intranasal insulin ameliorates experimental diabetic neuropathy. *Diabetes* **58**(4): 934-945.

Freeman R, Durso-Decruz E, Emir B (2008). Efficacy, safety, and tolerability of pregabalin treatment for painful diabetic peripheral neuropathy: findings from seven randomized, controlled trials across a range of doses. *Diabetes Care* **31**(7): 1448-1454.

Freyenhagen R, Strojek K, Griesing T, Whalen E, Balkenohl M (2005). Efficacy of pregabalin in neuropathic pain evaluated in a 12-week, randomised, double-blind, multicentre, placebo-controlled trial of flexible- and fixed-dose regimens. *Pain* **115**(3): 254-263.

Fu KY, Light AR, Maixner W (2000). Relationship between nociceptor activity, peripheral edema, spinal microglial activation and long-term hyperalgesia induced by formalin. *Neuroscience* **101**(4): 1127-1135.

Fu KY, Light AR, Matsushima GK, Maixner W (1999). Microglial reactions after subcutaneous formalin injection into the rat hind paw. *Brain Res* **825**(1-2): 59-67.

Fuchs D, Birklein F, Reeh PW, Sauer SK (2010). Sensitized peripheral nociception in experimental diabetes of the rat. *Pain* **151**(2): 496-505.

Gaede P, Vedel P, Parving HH, Pedersen O (1999). Intensified multifactorial intervention in patients with type 2 diabetes mellitus and

microalbuminuria: the Steno type 2 randomised study. *Lancet* **353**(9153): 617-622.

Gallwitz B (2013). Emerging DPP-4 inhibitors: focus on linagliptin for type 2 diabetes. *Diabetes Metab Syndr Obes* **6**: 1-9.

Gao X, Kim HK, Chung JM, Chung K (2005). Enhancement of NMDA receptor phosphorylation of the spinal dorsal horn and nucleus gracilis neurons in neuropathic rats. *Pain* **116**(1-2): 62-72.

Gao YJ, Ji RR (2010). Targeting astrocyte signaling for chronic pain. *Neurotherapeutics* **7**(4): 482-493.

Garcia-Larrea L, Maarrawi J, Peyron R, Costes N, Mertens P, Magnin M, *et al.* (2006). On the relation between sensory deafferentation, pain and thalamic activity in Wallenberg's syndrome: a PET-scan study before and after motor cortex stimulation. *Eur J Pain* **10**(8): 677-688.

Garrido-Mesa N, Zarzuelo A, Galvez J (2013). What is behind the non-antibiotic properties of minocycline? *Pharmacol Res* **67**(1): 18-30.

Garrison CJ, Dougherty PM, Kajander KC, Carlton SM (1991). Staining of glial fibrillary acidic protein (GFAP) in lumbar spinal cord increases following a sciatic nerve constriction injury. *Brain Research* **565**(1): 1-7.

Garry MG, Hargreaves KM (1992). Enhanced release of immunoreactive CGRP and substance P from spinal dorsal horn slices occurs during carrageenan inflammation. *Brain Res* **582**(1): 139-142.

Gee NS, Brown JP, Dissanayake VUK, Offord J, Thurlow R, Woodruff GN (1996). The novel anticonvulsant drug, gabapentin (Neurontin), binds to the alpha(2)delta subunit of a calcium channel. *Journal of Biological Chemistry* **271**(10): 5768-5776.

Gehrmann J, Banati RB (1995). Microglial turnover in the injured CNS: activated microglia undergo delayed DNA fragmentation following peripheral nerve injury. *J Neuropathol Exp Neurol* **54**(5): 680-688.

Gentilli M, Mazoit JX, Bouaziz H, Fletcher D, Casper RF, Benhamou D, *et al.* (2001). Resveratrol decreases hyperalgesia induced by carrageenan in the rat hind paw. *Life Sci* **68**(11): 1317-1321.

Geranton SM, Jimenez-Diaz L, Torsney C, Tochiki KK, Stuart SA, Leith JL, *et al.* (2009). A rapamycin-sensitive signaling pathway is essential for the full expression of persistent pain states. *J Neurosci* **29**(47): 15017-15027.

Ghorbani MLM, Qin C, Wu MY, Farber JP, Sheykhzade M, Fjalland B, *et al.* (2011). Characterization of upper thoracic spinal neurons

receiving noxious cardiac and/or somatic inputs in diabetic rats. *Auton. Neurosci-Basic Clin.* **165**(2): 168-177.

Ghosh S, Wise LE, Chen Y, Gujjar R, Mahadevan A, Cravatt BF, *et al.* (2013). The monoacylglycerol lipase inhibitor JZL184 suppresses inflammatory pain in the mouse carrageenan model. *Life Sci* **92**(8-9): 498-505.

Giacco F, Brownlee M (2010). Oxidative Stress and Diabetic Complications. *Circulation Research* **107**(9): 1058-1070.

Ginhoux F, Lim S, Hoeffel G, Low D, Huber T (2013). Origin and differentiation of microglia. *Front Cell Neurosci* **7**: 45.

Gong JP, Onaivi ES, Ishiguro H, Liu QR, Tagliaferro PA, Brusco A, *et al.* (2006). Cannabinoid CB2 receptors: immunohistochemical localization in rat brain. *Brain Res* **1071**(1): 10-23.

Guastella V, Mick G (2009). Strategies for the diagnosis and treatment of neuropathic pain secondary to diabetic peripheral sensory polyneuropathy. *Diabetes & Metabolism* **35**(1): 12-19.

Guasti L, Richardson D, Jhaveri M, Eldeeb K, Barrett D, Elphick M, *et al.* (2009). Minocycline treatment inhibits microglial activation and alters spinal levels of endocannabinoids in a rat model of neuropathic pain. *Molecular Pain* **5**(1): 35.

Gutniak M, Ørkov C, Holst JJ, Ahrén B, Efendić S (1992). Antidiabetogenic Effect of Glucagon-like Peptide-1 (7–36)amide in Normal Subjects and Patients with Diabetes Mellitus. *New England Journal of Medicine* **326**(20): 1316-1322.

Hahm TS, Ahn HJ, Ryu S, Gwak MS, Choi SJ, Kim JK, *et al.* (2012). Combined carbamazepine and pregabalin therapy in a rat model of neuropathic pain. *Br J Anaesth* **109**(6): 968-974.

Hanisch UK (2002). Microglia as a source and target of cytokines. *Glia* **40**(2): 140-155.

Hao JX, Kupers RC, Xu XJ (2004). Response characteristics of spinal cord dorsal horn neurons in chronic allodynic rats after spinal cord injury. *J Neurophysiol* **92**(3): 1391-1399.

Hardie DG (2007). AMP-activated/SNF1 protein kinases: conserved guardians of cellular energy. *Nat Rev Mol Cell Biol* **8**(10): 774-785.

Hargreaves K, Dubner R, Brown F, Flores C, Joris J (1988). A new and sensitive method for measuring thermal nociception in cutaneous hyperalgesia. *Pain* **32**(1): 77-88.

- Harris JA, Corsi M, Quartaroli M, Arban R, Bentivoglio M (1996). Upregulation of spinal glutamate receptors in chronic pain. *Neuroscience* **74**(1): 7-12.
- Hasanein P, Keshavarz M, Parviz M, Roohbakhsh A (2009a). URB597, an inhibitor of fatty acid amide hydrolase, reduces hyperalgesia in diabetic rats. *Canadian Journal of Physiology and Pharmacology* **87**(6): 432+.
- Hasanein P, Parviz M, Keshavarz M, Roohbakhsh A (2009b). URB597, an inhibitor of fatty acid amide hydrolase, reduces hyperalgesia in diabetic rats. *Can J Physiol Pharmacol* **87**(6): 432-439.
- Hasanein P, Shahidi S, Komaki A, Mirazi N (2008). Effects of URB597 as an inhibitor of fatty acid amide hydrolase on modulation of nociception in a rat model of cholestasis. *Eur J Pharmacol* **591**(1-3): 132-135.
- Hasegawa-Moriyama M, Ohnou T, Godai K, Kurimoto T, Nakama M, Kanmura Y (2012). Peroxisome proliferator-activated receptor-gamma agonist rosiglitazone attenuates postincisional pain by regulating macrophage polarization. *Biochemical and Biophysical Research Communications* **426**(1): 76-82.
- Hauton D (2011). Does long-term metformin treatment increase cardiac lipoprotein lipase? *Metabolism* **60**(1): 32-42.
- Heinricher MM, Tavares I, Leith JL, Lumb BM (2009). Descending control of nociception: Specificity, recruitment and plasticity. *Brain Res Rev* **60**(1): 214-225.
- Hendrich J, Van Minh AT, Hebllich F, Nieto-Rostro M, Watschingert K, Striessnig J, *et al.* (2008). Pharmacological disruption of calcium channel trafficking by the alpha(2)delta ligand gabapentin. *Proceedings of the National Academy of Sciences of the United States of America* **105**(9): 3628-3633.
- Hide I, Tanaka M, Inoue A, Nakajima K, Kohsaka S, Inoue K, *et al.* (2000). Extracellular ATP triggers tumor necrosis factor-alpha release from rat microglia. *J Neurochem* **75**(3): 965-972.
- Himeno T, Kamiya H, Naruse K, Harada N, Ozaki N, Seino Y, *et al.* (2011). Beneficial effects of exendin-4 on experimental polyneuropathy in diabetic mice. *Diabetes* **60**(9): 2397-2406.
- Hirade M, Yasuda H, Omatsu-Kanbe M, Kikkawa R, Kitasato H (1999). Tetrodotoxin-resistant sodium channels of dorsal root ganglion neurons are readily activated in diabetic rats. *Neuroscience* **90**(3): 933-939.

Hirai T, Uchida K, Nakajima H, Guerrero AR, Takeura N, Watanabe S, *et al.* (2013). The Prevalence and Phenotype of Activated Microglia/Macrophages within the Spinal Cord of the Hyperostotic Mouse (*twy/twy*) Changes in Response to Chronic Progressive Spinal Cord Compression: Implications for Human Cervical Compressive Myelopathy. *PLoS ONE* **8**(5): e64528.

Hocher B, Reichetzedler C, Alter ML (2012). Renal and Cardiac Effects of DPP4 Inhibitors – from Preclinical Development to Clinical Research. *Kidney and Blood Pressure Research* **36**(1): 65-84.

Hong S, Morrow TJ, Paulson PE, Isom LL, Wiley JW (2004). Early Painful Diabetic Neuropathy Is Associated with Differential Changes in Tetrodotoxin-sensitive and -resistant Sodium Channels in Dorsal Root Ganglion Neurons in the Rat. *Journal of Biological Chemistry* **279**(28): 29341-29350.

Hong S, Wiley JW (2006). Altered expression and function of sodium channels in large DRG neurons and myelinated A-fibers in early diabetic neuropathy in the rat. *Biochem Biophys Res Commun* **339**(2): 652-660.

Horváth B, Mukhopadhyay P, Haskó G, Pacher P (2012). The Endocannabinoid System and Plant-Derived Cannabinoids in Diabetes and Diabetic Complications. *The American Journal of Pathology* **180**(2): 432-442.

Hotamisligil GS, Peraldi P, Budavari A, Ellis R, White MF, Spiegelman BM (1996). IRS-1-mediated inhibition of insulin receptor tyrosine kinase activity in TNF- α - and obesity-induced insulin resistance. *Science* **271**(5249): 665-668.

Hotamisligil GS, Shargill NS, Spiegelman BM (1993). Adipose expression of tumor necrosis factor- α : direct role in obesity-linked insulin resistance. *Science* **259**(5091): 87-91.

Howe JF, Loeser JD, Calvin WH (1977). Mechanosensitivity of dorsal root ganglia and chronically injured axons: a physiological basis for the radicular pain of nerve root compression. *Pain* **3**(1): 25-41.

Hoybergs YM, Biermans RL, Meert TF (2008). The impact of bodyweight and body condition on behavioral testing for painful diabetic neuropathy in the streptozotocin rat model. *Neurosci Lett* **436**(1): 13-18.

Hoybergs YMJJ, Meert TF (2007). The effect of low-dose insulin on mechanical sensitivity and allodynia in type I diabetes neuropathy. *Neuroscience Letters* **417**(2): 149-154.

IDF (2012). The Global Burden. Brussels: International Diabetes Federation.

Inoue K, Tsuda M, Tozaki-Saitoh H (2007). Modification of neuropathic pain sensation through microglial ATP receptors. *Purinergic Signal* **3**(4): 311-316.

Ishii H, Jirousek MR, Koya D, Takagi C, Xia P, Clermont A, *et al.* (1996). Amelioration of vascular dysfunctions in diabetic rats by an oral PKC beta inhibitor. *Science* **272**(5262): 728-731.

Issemann I, Green S (1990). Activation of a member of the steroid hormone receptor superfamily by peroxisome proliferators. *Nature* **347**(6294): 645-650.

Iwai S, Maeda T, Kiguchi N, Kobayashi Y, Fukazawa Y, Ozaki M, *et al.* (2008). Pioglitazone attenuates tactile allodynia and microglial activation in mice with peripheral nerve injury. *Drug discoveries & therapeutics* **2**(6): 353-356.

Jaggari SI, Hasnie FS, Sellaturay S, Rice AS (1998). The anti-hyperalgesic actions of the cannabinoid anandamide and the putative CB2 receptor agonist palmitoylethanolamide in visceral and somatic inflammatory pain. *Pain* **76**(1-2): 189-199.

Jain V, Jaggi AS, Singh N (2009). Ameliorative potential of rosiglitazone in tibial and sural nerve transection-induced painful neuropathy in rats. *Pharmacological Research* **59**(6): 385-392.

Jancso G (1992). Pathobiological reactions of C-fibre primary sensory neurones to peripheral nerve injury. *Exp Physiol* **77**(3): 405-431.

Jang JH, Nam TS, Paik KS, Leem JW (2004). Involvement of peripherally released substance P and calcitonin gene-related peptide in mediating mechanical hyperalgesia in a traumatic neuropathy model of the rat. *Neurosci Lett* **360**(3): 129-132.

Jayamanne A, Greenwood R, Mitchell VA, Aslan S, Piomelli D, Vaughan CW (2006). Actions of the FAAH inhibitor URB597 in neuropathic and inflammatory chronic pain models. *Br J Pharmacol* **147**(3): 281-288.

Jhaveri MD, Richardson D, Kendall DA, Barrett DA, Chapman V (2006). Analgesic effects of fatty acid amide hydrolase inhibition in a rat model of neuropathic pain. *J Neurosci* **26**(51): 13318-13327.

Ji RR, Gereau RWt, Malcangio M, Strichartz GR (2009). MAP kinase and pain. *Brain Res Rev* **60**(1): 135-148.

Jia HB, Wang XM, Qiu LL, Liu XY, Shen JC, Ji Q, *et al.* (2013). Spinal neuroimmune activation inhibited by repeated administration of pioglitazone in rats after L5 spinal nerve transection. *Neurosci Lett*.

Jia HB, Zhu SH, Ji Q, Hui KL, Duan ML, Xu JG, *et al.* (2010). Repeated Administration of Pioglitazone Attenuates Development of Hyperalgesia in a Rat Model of Neuropathic Pain. *Experimental and Clinical Psychopharmacology* **18**(4): 359-365.

Jiang Y, Nyengaard JR, Zhang JS, Jakobsen J (2004). Selective loss of calcitonin gene-related Peptide-expressing primary sensory neurons of the a-cell phenotype in early experimental diabetes. *Diabetes* **53**(10): 2669-2675.

Jiménez-Díaz L, Géranton SM, Passmore GM, Leith JL, Fisher AS, Berliocchi L, *et al.* (2008). Local Translation in Primary Afferent Fibers Regulates Nociception. *PLoS ONE* **3**(4): e1961.

Jin HY, Liu WJ, Park JH, Baek HS, Park TS (2009). Effect of dipeptidyl peptidase-IV (DPP-IV) inhibitor (Vildagliptin) on peripheral nerves in streptozotocin-induced diabetic rats. *Arch Med Res* **40**(7): 536-544.

Johansson BL, Borg K, Fernqvist-Forbes E, Kernell A, Odergren T, Wahren J (2000). Beneficial effects of C-peptide on incipient nephropathy and neuropathy in patients with Type 1 diabetes mellitus. *Diabet Med* **17**(3): 181-189.

Jolivalt CG, Fineman M, Deacon CF, Carr RD, Calcutt NA (2011). GLP-1 signals via ERK in peripheral nerve and prevents nerve dysfunction in diabetic mice. *Diabetes Obes Metab* **13**(11): 990-1000.

Jolivalt CG, Lee CA, Ramos KM, Calcutt NA (2008). Allodynia and hyperalgesia in diabetic rats are mediated by GABA and depletion of spinal potassium-chloride co-transporters. *Pain* **140**(1): 48-57.

Julius D, Basbaum AI (2001). Molecular mechanisms of nociception. *Nature* **413**(6852): 203-210.

Kahn BB, Alquier T, Carling D, Hardie DG (2005). AMP-activated protein kinase: ancient energy gauge provides clues to modern understanding of metabolism. *Cell Metab* **1**(1): 15-25.

Kahn CR, Chen L, Cohen SE (2000). Unraveling the mechanism of action of thiazolidinediones. *The Journal of Clinical Investigation* **106**(11): 1305-1307.

Kajander KC, Wakisaka S, Bennett GJ (1992). Spontaneous discharge originates in the dorsal root ganglion at the onset of a painful peripheral neuropathy in the rat. *Neurosci Lett* **138**(2): 225-228.

Kamiya H, Murakawa Y, Zhang W, Sima AA (2005a). Unmyelinated fiber sensory neuropathy differs in type 1 and type 2 diabetes. *Diabetes Metab Res Rev* **21**(5): 448-458.

Kamiya H, Zhang W, Sima AA (2004). C-peptide prevents nociceptive sensory neuropathy in type 1 diabetes. *Ann Neurol* **56**(6): 827-835.

Kamiya H, Zhang W, Sima AA (2006). Degeneration of the Golgi and neuronal loss in dorsal root ganglia in diabetic BioBreeding/Worcester rats. *Diabetologia* **49**(11): 2763-2774.

Kamiya H, Zhangm W, Sima AA (2005b). Apoptotic stress is counterbalanced by survival elements preventing programmed cell death of dorsal root ganglions in subacute type 1 diabetic BB/Wor rats. *Diabetes* **54**(11): 3288-3295.

Kan M, Guo G, Singh B, Singh V, Zochodne DW (2012). Glucagon-like peptide 1, insulin, sensory neurons, and diabetic neuropathy. *J Neuropathol Exp Neurol* **71**(6): 494-510.

Karanth SS, Springall DR, Francavilla S, Mirrlees DJ, Polak JM (1990). Early increase in CGRP- and VIP-immunoreactive nerves in the skin of streptozotocin-induced diabetic rats. *Histochemistry* **94**(6): 659-666.

Katsuki A, Sumida Y, Murashima S, Murata K, Takarada Y, Ito K, *et al.* (1998). Serum levels of tumor necrosis factor-alpha are increased in obese patients with noninsulin-dependent diabetes mellitus. *J Clin Endocrinol Metab* **83**(3): 859-862.

Kawamura M, Kuraishi Y, Minami M, Satoh M (1989). Antinociceptive effect of intrathecally administered antiserum against calcitonin gene-related peptide on thermal and mechanical noxious stimuli in experimental hyperalgesic rats. *Brain Res* **497**(1): 199-203.

Kawasaki F, Matsuda M, Kanda Y, Inoue H, Kaku K (2005). Structural and functional analysis of pancreatic islets preserved by pioglitazone in db/db mice. *Am J Physiol Endocrinol Metab* **288**(3): E510-518.

Kawasaki Y, Xu ZZ, Wang X, Park JY, Zhuang ZY, Tan PH, *et al.* (2008). Distinct roles of matrix metalloproteases in the early- and late-phase development of neuropathic pain. *Nat Med* **14**(3): 331-336.

Kawashima S, Matsuoka TA, Kaneto H, Tochino Y, Kato K, Yamamoto K, *et al.* (2011). Effect of alogliptin, pioglitazone and glargine on pancreatic beta-cells in diabetic db/db mice. *Biochem Biophys Res Commun* **404**(1): 534-540.

Kern M, Klötting N, Niessen HG, Thomas L, Stiller D, Mark M, *et al.* (2012). Linagliptin Improves Insulin Sensitivity and Hepatic Steatosis in Diet-Induced Obesity. *PLoS ONE* **7**(6): e38744.

Khan GM, Chen SR, Pan HL (2002). Role of primary afferent nerves in allodynia caused by diabetic neuropathy in rats. *Neuroscience* **114**(2): 291-299.

Kim D, Kim MA, Cho IH, Kim MS, Lee S, Jo EK, *et al.* (2007a). A critical role of toll-like receptor 2 in nerve injury-induced spinal cord glial cell activation and pain hypersensitivity. *J Biol Chem* **282**(20): 14975-14983.

Kim D, You B, Jo E-K, Han S-K, Simon MI, Lee SJ (2010). NADPH oxidase 2-derived reactive oxygen species in spinal cord microglia contribute to peripheral nerve injury-induced neuropathic pain. *Proceedings of the National Academy of Sciences* **107**(33): 14851-14856.

Kim J, Shon E, Kim CS, Kim JS (2012a). Renal podocyte injury in a rat model of type 2 diabetes is prevented by metformin. *Exp Diabetes Res* **2012**: 210821.

Kim J, Yao A, Atherley R, Carstens E, Jinks SL, Antognini JF (2007b). Neurons in the Ventral Spinal Cord Are More Depressed by Isoflurane, Halothane, and Propofol Than Are Neurons in the Dorsal Spinal Cord. *Anesthesia & Analgesia* **105**(4): 1020-1026.

Kim SH, Kwon JK, Kwon YB (2012b). Pain modality and spinal glia expression by streptozotocin induced diabetic peripheral neuropathy in rats. *Lab Anim Res* **28**(2): 131-136.

Kimura S, Tanabe M, Honda M, Ono H (2005). Enhanced wind-up of the C-fiber-mediated nociceptive flexor reflex movement following painful diabetic neuropathy in mice. *Journal of Pharmacological Sciences* **97**(2): 195-202.

King AJF (2012). The use of animal models in diabetes research. *British Journal of Pharmacology* **166**(3): 877-894.

Kinsey SG, Long JZ, Cravatt BF, Lichtman AH (2010). Fatty acid amide hydrolase and monoacylglycerol lipase inhibitors produce anti-allodynic effects in mice through distinct cannabinoid receptor mechanisms. *J Pain* **11**(12): 1420-1428.

Kinsey SG, Long JZ, O'Neal ST, Abdullah RA, Poklis JL, Boger DL, *et al.* (2009). Blockade of endocannabinoid-degrading enzymes attenuates neuropathic pain. *J Pharmacol Exp Ther* **330**(3): 902-910.

Kinsey SG, Wise LE, Ramesh D, Abdullah R, Selley DE, Cravatt BF, *et al.* (2013). Repeated Low Dose Administration of the Monoacylglycerol Lipase Inhibitor JZL184 Retains CB1 Receptor Mediated Antinociceptive and Gastroprotective Effects. *J Pharmacol Exp Ther*.

Kishi M, Tanabe J, Schmelzer JD, Low PA (2002). Morphometry of Dorsal Root Ganglion in Chronic Experimental Diabetic Neuropathy. *Diabetes* **51**(3): 819-824.

Klein T, Niessen HG, Ittrich C, Mayoux E, Mueller HP, Cheetham S, *et al.* (2012). Evaluation of body fat composition after linagliptin treatment in a rat model of diet-induced obesity: a magnetic resonance spectroscopy study in comparison with sibutramine. *Diabetes Obes Metab* **14**(11): 1050-1053.

Koenig RJ, Peterson CM, Jones RL, Saudek C, Lehrman M, Cerami A (1976). Correlation of glucose regulation and hemoglobin Alc in diabetes mellitus. *N Engl J Med* **295**(8): 417-420.

Koltzenburg M, Lundberg LER, Torebjörk HE (1992). Dynamic and static components of mechanical hyperalgesia in human hairy skin. *Pain* **51**(2): 207-219.

Kota BP, Huang TH, Roufogalis BD (2005). An overview on biological mechanisms of PPARs. *Pharmacol Res* **51**(2): 85-94.

Kramer D, Shapiro R, Adler A, Bush E, Rondinone CM (2001). Insulin-sensitizing effect of rosiglitazone (BRL-49653) by regulation of glucose transporters in muscle and fat of Zucker rats. *Metabolism* **50**(11): 1294-1300.

Kreutzberg GW (1996). Microglia: a sensor for pathological events in the CNS. *Trends Neurosci* **19**(8): 312-318.

Kudo Y, Ohtaki H, Dohi K, Yin L, Nakamachi T, Endo S, *et al.* (2006). Neuronal damage in rat brain and spinal cord after cardiac arrest and massive hemorrhagic shock. *Crit Care Med* **34**(11): 2820-2826.

Kumar NP, Annamalai AR, Thakur RS (2009). Antinociceptive property of *Embllica officinalis* Gaertn (Amla) in high fat diet-fed/low dose streptozotocin induced diabetic neuropathy in rats. *Indian J. Exp. Biol.* **47**(9): 737-742.

Kuraishi Y, Nanayama T, Ohno H, Minami M, Satoh M (1988). Antinociception induced in rats by intrathecal administration of antiserum against calcitonin gene-related peptide. *Neurosci Lett* **92**(3): 325-329.

Laird JM, Bennett GJ (1993). An electrophysiological study of dorsal horn neurons in the spinal cord of rats with an experimental peripheral neuropathy. *J Neurophysiol* **69**(6): 2072-2085.

Lamigeon C, Bellier JP, Sacchettoni S, Rujano M, Jacquemont B (2001). Enhanced neuronal protection from oxidative stress by

coculture with glutamic acid decarboxylase-expressing astrocytes. *J Neurochem* **77**(2): 598-606.

LaMotte RH, Shain CN, Simone DA, Tsai EF (1991). Neurogenic hyperalgesia: psychophysical studies of underlying mechanisms. *J Neurophysiol* **66**(1): 190-211.

Langford DJ, Bailey AL, Chanda ML, Clarke SE, Drummond TE, Echols S, *et al.* (2010). Coding of facial expressions of pain in the laboratory mouse. *Nat Methods* **7**(6): 447-449.

Lanneau C, Green A, Hirst WD, Wise A, Brown JT, Donnier E, *et al.* (2001). Gabapentin is not a GABAB receptor agonist. *Neuropharmacology* **41**(8): 965-975.

Latreoliere A, Woolf CJ (2009). Central sensitization: a generator of pain hypersensitivity by central neural plasticity. *J Pain* **10**(9): 895-926.

Lazaridis I, Charalampopoulos I, Alexaki V-I, Avlonitis N, Padiaditakis I, Efstathopoulos P, *et al.* (2011). Neurosteroid Dehydroepiandrosterone Interacts with Nerve Growth Factor (NGF) Receptors, Preventing Neuronal Apoptosis. *PLoS Biol* **9**(4): e1001051.

Le Bars D, Gozariu M, Cadden SW (2001). Animal models of nociception. *Pharmacol Rev* **53**(4): 597-652.

Lechuga-Sancho AM, Arroba AI, Frago LM, Garcia-Caceres C, de Celix AD, Argente J, *et al.* (2006). Reduction in the number of astrocytes and their projections is associated with increased synaptic protein density in the hypothalamus of poorly controlled diabetic rats. *Endocrinology* **147**(11): 5314-5324.

Ledeboer A, Sloane EM, Milligan ED, Frank MG, Mahony JH, Maier SF, *et al.* (2005). Minocycline attenuates mechanical allodynia and proinflammatory cytokine expression in rat models of pain facilitation. *Pain* **115**(1-2): 71-83.

Lenzen S (2008). The mechanisms of alloxan- and streptozotocin-induced diabetes. *Diabetologia* **51**(2): 216-226.

Li CY, Zhang XL, Matthews EA, Li KW, Kurwa A, Boroujerdi A, *et al.* (2006). Calcium channel $\alpha_2\delta_1$ subunit mediates spinal hyperexcitability in pain modulation. *Pain* **125**(1-2): 20-34.

Li F, Szabo C, Pacher P, Southan GJ, Abatan OI, Charniauskaya T, *et al.* (2004). Evaluation of orally active poly(ADP-ribose) polymerase inhibitor in streptozotocin-diabetic rat model of early peripheral neuropathy. *Diabetologia* **47**(4): 710-717.

- Li N, Lundeberg T, Yu LC (2001). Involvement of CGRP and CGRP1 receptor in nociception in the nucleus accumbens of rats. *Brain Res* **901**(1-2): 161-166.
- Li Y, Hansotia T, Yusta B, Ris F, Halban PA, Drucker DJ (2003). Glucagon-like peptide-1 receptor signaling modulates beta cell apoptosis. *J Biol Chem* **278**(1): 471-478.
- Liao YH, Zhang GH, Jia D, Wang P, Qian NS, He F, *et al.* (2011). Spinal astrocytic activation contributes to mechanical allodynia in a mouse model of type 2 diabetes. *Brain Res* **1368**: 324-335.
- Liaw WJ, Stephens RL, Jr., Binns BC, Chu Y, Sepkuty JP, Johns RA, *et al.* (2005). Spinal glutamate uptake is critical for maintaining normal sensory transmission in rat spinal cord. *Pain* **115**(1-2): 60-70.
- Lichtman AH, Leung D, Shelton CC, Saghatelian A, Hardouin C, Boger DL, *et al.* (2004a). Reversible inhibitors of fatty acid amide hydrolase that promote analgesia: evidence for an unprecedented combination of potency and selectivity. *J Pharmacol Exp Ther* **311**(2): 441-448.
- Lichtman AH, Shelton CC, Advani T, Cravatt BF (2004b). Mice lacking fatty acid amide hydrolase exhibit a cannabinoid receptor-mediated phenotypic hypoalgesia. *Pain* **109**(3): 319-327.
- Lindner MD, Bourin C, Chen P, McElroy JF, Leet JE, Hogan JB, *et al.* (2006). Adverse effects of gabapentin and lack of anti-allodynic efficacy of amitriptyline in the streptozotocin model of painful diabetic neuropathy. *Exp Clin Psychopharmacol* **14**(1): 42-51.
- Liu CN, Wall PD, Ben-Dor E, Michaelis M, Amir R, Devor M (2000). Tactile allodynia in the absence of C-fiber activation: altered firing properties of DRG neurons following spinal nerve injury. *Pain* **85**(3): 503-521.
- Liu WJ, Jin HY, Lee KA, Xie SH, Baek HS, Park TS (2011). Neuroprotective effect of the glucagon-like peptide-1 receptor agonist, synthetic exendin-4, in streptozotocin-induced diabetic rats. *Br J Pharmacol* **164**(5): 1410-1420.
- Long JZ, Nomura DK, Cravatt BF (2009a). Characterization of monoacylglycerol lipase inhibition reveals differences in central and peripheral endocannabinoid metabolism. *Chem Biol* **16**(7): 744-753.
- Long JZ, Nomura DK, Vann RE, Walentiny DM, Booker L, Jin X, *et al.* (2009b). Dual blockade of FAAH and MAGL identifies behavioral processes regulated by endocannabinoid crosstalk in vivo. *Proc Natl Acad Sci U S A* **106**(48): 20270-20275.

- Loseth S, Mellgren SI, Jorde R, Lindal S, Stalberg E (2010). Polyneuropathy in type 1 and type 2 diabetes: comparison of nerve conduction studies, thermal perception thresholds and intraepidermal nerve fibre densities. *Diabetes Metab Res Rev* **26**(2): 100-106.
- LoVerme J, Russo R, La Rana G, Fu J, Farthing J, Mattace-Raso G, *et al.* (2006). Rapid broad-spectrum analgesia through activation of peroxisome proliferator-activated receptor- α . *J Pharmacol Exp Ther* **319**(3): 1051-1061.
- Luo J, Quan J, Tsai J, Hobensak C, Sullivan C, Hector R, *et al.* (1998). Streptozotocin-induced diabetes in fat-fed mice: A new rodent model of non-insulin-dependent diabetes mellitus. *Journal of Investigative Medicine* **46**(1): 145A-145A.
- Luo ZD, Calcutt NA, Higuera ES, Valder CR, Song YH, Svensson CI, *et al.* (2002). Injury type-specific calcium channel $\alpha 2$ delta-1 subunit up-regulation in rat neuropathic pain models correlates with antiallodynic effects of gabapentin. *J Pharmacol Exp Ther* **303**(3): 1199-1205.
- Maeda T, Kiguchi N, Kobayashi Y, Ozaki M, Kishioka S (2008). Pioglitazone Attenuates Tactile Allodynia and Thermal Hyperalgesia in Mice Subjected to Peripheral Nerve Injury. *Journal of Pharmacological Sciences* **108**(3): 341-347.
- Magistretti PJ, Pellerin L (1999). Astrocytes Couple Synaptic Activity to Glucose Utilization in the Brain. *News Physiol Sci* **14**: 177-182.
- Majithiya JB, Paramar AN, Balaraman R (2005). Pioglitazone, a PPAR γ agonist, restores endothelial function in aorta of streptozotocin-induced diabetic rats. *Cardiovasc Res* **66**(1): 150-161.
- Malan TP, Mata HP, Porreca F (2002). Spinal GABA(A) and GABA(B) receptor pharmacology in a rat model of neuropathic pain. *Anesthesiology* **96**(5): 1161-1167.
- Malcangio M, Tomlinson DR (1998). A pharmacologic analysis of mechanical hyperalgesia in streptozotocin/diabetic rats. *Pain* **76**(1-2): 151-157.
- Malmberg AB, O'Connor WT, Glennon JC, Cesena R, Calcutt NA (2006). Impaired formalin-evoked changes of spinal amino acid levels in diabetic rats. *Brain Res* **1115**(1): 48-53.
- Mantovani A, Sica A, Sozzani S, Allavena P, Vecchi A, Locati M (2004). The chemokine system in diverse forms of macrophage activation and polarization. *Trends Immunol* **25**(12): 677-686.

Marchand F, Perretti M, McMahon SB (2005). Role of the immune system in chronic pain. *Nat Rev Neurosci* **6**(7): 521-532.

Marmioli P, Rodriguez-Menendez V, Rigamonti L, Tonoli E, Rigolio R, Cavaletti G, *et al.* (2009). Neuropathological changes in the peripheral nervous system and spinal cord in a transgenic mouse model of Niemann-Pick disease type A. *Clin Neuropathol* **28**(4): 263-274.

Martinez JA, Kasamatsu M, Rosales-Hernandez A, Hanson LR, Frey WH, Toth CC (2012). Comparison of central versus peripheral delivery of pregabalin in neuropathic pain states. *Mol Pain* **8**: 3.

Masiello P, Broca C, Gross R, Roye M, Manteghetti M, Hillaire-Buys D, *et al.* (1998). Experimental NIDDM: development of a new model in adult rats administered streptozotocin and nicotinamide. *Diabetes* **47**(2): 224-229.

Mayer DJ (1984). Analgesia produced by electrical stimulation of the brain. *Prog Neuropsychopharmacol Biol Psychiatry* **8**(4-6): 557-564.

Mayer DJ, Price DD (1976). Central nervous system mechanisms of analgesia. *Pain* **2**(4): 379-404.

Mayer DJ, Wolfle TL, Akil H, Carder B, Liebeskind JC (1971). Analgesia from electrical stimulation in the brainstem of the rat. *Science* **174**(4016): 1351-1354.

Mayer ML, Armstrong N (2004). Structure and function of glutamate receptor ion channels. *Annu Rev Physiol* **66**: 161-181.

McGill JB (2012). Linagliptin for type 2 diabetes mellitus: a review of the pivotal clinical trials. *Ther Adv Endocrinol Metab* **3**(4): 113-124.

McGuirk SM, Dolphin AC (1992). G-protein mediation in nociceptive signal transduction: an investigation into the excitatory action of bradykinin in a subpopulation of cultured rat sensory neurons. *Neuroscience* **49**(1): 117-128.

McMahon SB, Koltzenburg M (2005).

Mechoulam R, Ben-Shabat S, Hanus L, Ligumsky M, Kaminski NE, Schatz AR, *et al.* (1995). Identification of an endogenous 2-monoglyceride, present in canine gut, that binds to cannabinoid receptors. *Biochem Pharmacol* **50**(1): 83-90.

Meigs JB, Muller DC, Nathan DM, Blake DR, Andres R (2003). The Natural History of Progression From Normal Glucose Tolerance to Type 2 Diabetes in the Baltimore Longitudinal Study of Aging. *Diabetes* **52**(6): 1475-1484.

- Melemedjian OK, Asiedu MN, Tillu DV, Sanoja R, Yan J, Lark A, *et al.* (2011). Targeting adenosine monophosphate-activated protein kinase (AMPK) in preclinical models reveals a potential mechanism for the treatment of neuropathic pain. *Mol Pain* **7**: 70.
- Melemedjian OK, Khoutorsky A, Sorge RE, Yan J, Asiedu MN, Valdez A, *et al.* (2013). mTORC1 inhibition induces pain via IRS-1-dependent feedback activation of ERK. *Pain* **154**(7): 1080-1091.
- Meller ST, Dykstra C, Grzybycki D, Murphy S, Gebhart GF (1994). The possible role of glia in nociceptive processing and hyperalgesia in the spinal cord of the rat. *Neuropharmacology* **33**(11): 1471-1478.
- Mendell LM (1966). Physiological properties of unmyelinated fiber projection to the spinal cord. *Exp Neurol* **16**(3): 316-332.
- Merrill EG, Ainsworth A (1972). Glass-coated platinum-plated tungsten microelectrodes. *Med Biol Eng* **10**(5): 662-672.
- Messinger RB, Naik AK, Jagodic MM, Nelson MT, Lee WY, Choe WJ, *et al.* (2009). In vivo silencing of the CaV3.2 T-type calcium channels in sensory neurons alleviates hyperalgesia in rats with streptozocin-induced diabetic neuropathy. *Pain* **145**(1–2): 184-195.
- Meyer RA, Ringkamp M, Campbell JN, Raja SN (2005). Peripheral mechanisms of cutaneous nociception. In: Wall PD, Melzack R (ed)^(eds). *Textbook of Pain*, edn. New York: Churchill Livingstone. p^pp.
- Miki K, Fukuoka T, Tokunaga A, Noguchi K (1998). Calcitonin gene-related peptide increase in the rat spinal dorsal horn and dorsal column nucleus following peripheral nerve injury: up-regulation in a subpopulation of primary afferent sensory neurons. *Neuroscience* **82**(4): 1243-1252.
- Millan MJ (2002). Descending control of pain. *Prog Neurobiol* **66**(6): 355-474.
- Millan MJ (1999). The induction of pain: an integrative review. *Prog Neurobiol* **57**(1): 1-164.
- Milligan ED, Watkins LR (2009). Pathological and protective roles of glia in chronic pain. *Nat Rev Neurosci* **10**(1): 23-36.
- Misawa S, Sakurai K, Shibuya K, Iose S, Kanai K, Ogino J, *et al.* (2009). Neuropathic pain is associated with increased nodal persistent Na(+) currents in human diabetic neuropathy. *J Peripher Nerv Syst* **14**(4): 279-284.

Mitsuyo T, Dutton RC, Antognini JF, Carstens E (2006). The Differential Effects of Halothane and Isoflurane on Windup of Dorsal Horn Neurons Selected in Unanesthetized Decerebrated Rats. *Anesthesia & Analgesia* **103**(3): 753-760.

Miyazaki R, Yamamoto T (2012). The efficacy of morphine, pregabalin, gabapentin, and duloxetine on mechanical allodynia is different from that on neuroma pain in the rat neuropathic pain model. *Anesth Analg* **115**(1): 182-188.

Miyazaki Y, Mahankali A, Matsuda M, Glass L, Mahankali S, Ferrannini E, *et al.* (2001). Improved Glycemic Control and Enhanced Insulin Sensitivity in Type 2 Diabetic Subjects Treated With Pioglitazone. *Diabetes Care* **24**(4): 710-719.

Miyazaki Y, Mahankali A, Matsuda M, Mahankali S, Hardies J, Cusi K, *et al.* (2002). Effect of pioglitazone on abdominal fat distribution and insulin sensitivity in type 2 diabetic patients. *J Clin Endocrinol Metab* **87**(6): 2784-2791.

Mizisin A, Jolivalt C, Calcutt N (2007). Spinal Cord. In: Veves A, Malik R (ed)[^](eds). *Diabetic Neuropathy*, edn: Humana Press. p[^]pp 165-185.

Mogil JS (2009). Animal models of pain: progress and challenges. *Nat. Rev. Neurosci.* **10**(4): 283-294.

Molliver DC, Wright DE, Leitner ML, Parsadarian AS, Doster K, Wen D, *et al.* (1997). IB4-binding DRG neurons switch from NGF to GDNF dependence in early postnatal life. *Neuron* **19**(4): 849-861.

Montgomery DL (1994). Astrocytes: form, functions, and roles in disease. *Vet Pathol* **31**(2): 145-167.

Moreno S, Farioli-Vecchioli S, Ceru MP (2004). Immunolocalization of peroxisome proliferator-activated receptors and retinoid X receptors in the adult rat CNS. *Neuroscience* **123**(1): 131-145.

Morgado C, Pereira-Terra P, Cruz CD, Tavares I (2011a). Minocycline completely reverses mechanical hyperalgesia in diabetic rats through microglia-induced changes in the expression of the potassium chloride co-transporter 2 (KCC2) at the spinal cord. *Diabetes Obes. Metab.* **13**(2): 150-159.

Morgado C, Pinto-Ribeiro F, Tavares I (2008). Diabetes affects the expression of GABA and potassium chloride cotransporter in the spinal cord: a study in streptozotocin diabetic rats. *Neurosci Lett* **438**(1): 102-106.

Morgado C, Silva L, Pereira-Terra P, Tavares I (2011b). Changes in serotonergic and noradrenergic descending pain pathways during

painful diabetic neuropathy: The preventive action of IGF1. *Neurobiology of Disease* **43**(1): 275-284.

Morgado C, Tavares I (2007). C-fos expression at the spinal dorsal horn of streptozotocin-induced diabetic rats. *Diabetes Metab Res Rev* **23**(8): 644-652.

Morgenweck J, Abdel-aleem OS, McNamara KC, Donahue RR, Badr MZ, Taylor BK (2010). Activation of peroxisome proliferator-activated receptor [gamma] in brain inhibits inflammatory pain, dorsal horn expression of Fos, and local edema. *Neuropharmacology* **58**(2): 337-345.

Morgenweck J, Griggs RB, Donahue RR, Zadina JE, Taylor BK (2013). PPAR γ activation blocks development and reduces established neuropathic pain in rats. *Neuropharmacology*(0).

Morton CR, Hutchison WD (1989). Release of sensory neuropeptides in the spinal cord: studies with calcitonin gene-related peptide and galanin. *Neuroscience* **31**(3): 807-815.

Muccioli GG (2010). Endocannabinoid biosynthesis and inactivation, from simple to complex. *Drug Discov Today* **15**(11-12): 474-483.

Munro S, Thomas KL, Abu-Shaar M (1993). Molecular characterization of a peripheral receptor for cannabinoids. *Nature* **365**(6441): 61-65.

Nadig PD, Revankar RR, Dethe SM, Narayanswamy SB, Aliyar MA (2012). Effect of *Tinospora cordifolia* on experimental diabetic neuropathy. *Indian J Pharmacol* **44**(5): 580-583.

Nakagawa T, Kaneko S (2010). Spinal astrocytes as therapeutic targets for pathological pain. *J Pharmacol Sci* **114**(4): 347-353.

Nakagawa T, Wakamatsu K, Zhang N, Maeda S, Minami M, Satoh M, *et al.* (2007). Intrathecal administration of ATP produces long-lasting allodynia in rats: differential mechanisms in the phase of the induction and maintenance. *Neuroscience* **147**(2): 445-455.

Nakamura J, Kato K, Hamada Y, Nakayama M, Chaya S, Nakashima E, *et al.* (1999). A protein kinase C-beta-selective inhibitor ameliorates neural dysfunction in streptozotocin-induced diabetic rats. *Diabetes* **48**(10): 2090-2095.

Nauck MA, Heimesaat MM, Orskov C, Holst JJ, Ebert R, Creutzfeldt W (1993). Preserved incretin activity of glucagon-like peptide 1 [7-36 amide] but not of synthetic human gastric inhibitory polypeptide in patients with type-2 diabetes mellitus. *J Clin Invest* **91**(1): 301-307.

Negi G, Kumar A, Kaundal RK, Gulati A, Sharma SS Functional and biochemical evidence indicating beneficial effect of Melatonin and Nicotinamide alone and in combination in experimental diabetic neuropathy. *Neuropharmacology* **58**(3): 585-592.

Neugebauer V (2009). CGRP in Spinal Cord Pain Mechanisms. In: Malcangio M (ed)^(eds). *Synaptic Plasticity in Pain*, edn: Springer New York. p^pp 175-197.

Neugebauer V, Rumenapp P, Schaible HG (1996). Calcitonin gene-related peptide is involved in the spinal processing of mechanosensory input from the rat's knee joint and in the generation and maintenance of hyperexcitability of dorsal horn-neurons during development of acute inflammation. *Neuroscience* **71**(4): 1095-1109.

Nguyen MD, D'Aigle T, Gowing G, Julien JP, Rivest S (2004). Exacerbation of motor neuron disease by chronic stimulation of innate immunity in a mouse model of amyotrophic lateral sclerosis. *J Neurosci* **24**(6): 1340-1349.

NICE (2010). Neuropathic pain: the pharmacological management of neuropathic pain in adults in non-specialist settings. London: National Institute for Health and Clinical Excellence.

Nielsen CK, Ross FB, Lotfipour S, Saini KS, Edwards SR, Smith MT (2007). Oxycodone and morphine have distinctly different pharmacological profiles: radioligand binding and behavioural studies in two rat models of neuropathic pain. *Pain* **132**(3): 289-300.

Niphakis MJ, Cognetta AB, Chang JW, Buczynski MW, Parsons LH, Byrne F, *et al.* (2013). Evaluation of NHS carbamates as a potent and selective class of endocannabinoid hydrolase inhibitors. *ACS Chem Neurosci*.

Noguchi K, Kawai Y, Fukuoka T, Senba E, Miki K (1995). Substance P induced by peripheral nerve injury in primary afferent sensory neurons and its effect on dorsal column nucleus neurons. *J Neurosci* **15**(11): 7633-7643.

Norsted Gregory E, Codeluppi S, Gregory JA, Steinauer J, Svensson CI (2010). Mammalian target of rapamycin in spinal cord neurons mediates hypersensitivity induced by peripheral inflammation. *Neuroscience* **169**(3): 1392-1402.

Nukada H, McMorran PD, Baba M, Ogasawara S, Yagihashi S (2011). Increased susceptibility to ischemia and macrophage activation in STZ-diabetic rat nerve. *Brain Research* **1373**: 172-182.

Obara I, Tochiki KK, Geranton SM, Carr FB, Lumb BM, Liu Q, *et al.* (2011). Systemic inhibition of the mammalian target of rapamycin

(mTOR) pathway reduces neuropathic pain in mice. *Pain* **152**(11): 2582-2595.

Obata H, Eisenach JC, Hussain H, Bynum T, Vincler M (2006). Spinal Glial Activation Contributes to Postoperative Mechanical Hypersensitivity in the Rat. *The Journal of Pain* **7**(11): 816-822.

Obrosova I (2009a). Diabetic painful and insensate neuropathy: Pathogenesis and potential treatments. *Neurotherapeutics* **6**(4): 638-647.

Obrosova IG (2009b). Diabetic Painful and Insensate Neuropathy: Pathogenesis and Potential Treatments. *Neurotherapeutics* **6**(4): 638-647.

Ogilvie J, Simpson DAA, Clarke RW (1999). Tonic adrenergic and serotonergic inhibition of a withdrawal reflex in rabbits subjected to different levels of surgical preparation. *Neuroscience* **89**(4): 1247-1258.

Oh SB, Tran PB, Gillard SE, Hurley RW, Hammond DL, Miller RJ (2001). Chemokines and Glycoprotein120 Produce Pain Hypersensitivity by Directly Exciting Primary Nociceptive Neurons. *The Journal of Neuroscience* **21**(14): 5027-5035.

Okine BN, Norris LM, Woodhams S, Burston J, Patel A, Alexander SP, *et al.* (2012). Lack of effect of chronic pre-treatment with the FAAH inhibitor URB597 on inflammatory pain behaviour: evidence for plastic changes in the endocannabinoid system. *Br J Pharmacol* **167**(3): 627-640.

Oku R, Satoh M, Fujii N, Otaka A, Yajima H, Takagi H (1987). Calcitonin gene-related peptide promotes mechanical nociception by potentiating release of substance P from the spinal dorsal horn in rats. *Brain Res* **403**(2): 350-354.

Okuno A, Tamemoto H, Tobe K, Ueki K, Mori Y, Iwamoto K, *et al.* (1998). Troglitazone increases the number of small adipocytes without the change of white adipose tissue mass in obese Zucker rats. *J Clin Invest* **101**(6): 1354-1361.

Oliveira ACP, Bertollo CM, Rocha LTS, Nascimento JEB, Costa KA, Coelho MM (2007). Antinociceptive and antiedematogenic activities of fenofibrate, an agonist of PPAR alpha, and pioglitazone, an agonist of PPAR gamma. *European Journal of Pharmacology* **561**(1-3): 194-201.

Olmarker K, Storkson R, Berge OG (2002). Pathogenesis of sciatic pain: a study of spontaneous behavior in rats exposed to experimental disc herniation. *Spine (Phila Pa 1976)* **27**(12): 1312-1317.

Orendacova J, Ondrejcek T, Kucharova K, Cizkova D, Jergova S, Mitruskova B, *et al.* (2005). Fluoro-Jade B evidence of induced ischemic tolerance in the rat spinal cord ischemia: physiological, neurological and histopathological consequences. *Gen Physiol Biophys* **24**(1): 75-87.

Otto KJ, Wyse BD, Cabot PJ, Smith MT (2011). Insulin Implants Prevent the Temporal Development of Mechanical Allodynia and Opioid Hyposensitivity for 24-Wks in Streptozotocin (STZ)-Diabetic Wistar Rats. *Pain Medicine* **12**(5): 782-793.

Pabbidi R, Yu S-Q, Peng S, Khardori R, Pauza M, Premkumar L (2008a). Influence of TRPV1 on diabetes-induced alterations in thermal pain sensitivity. *Molecular Pain* **4**(1): 9.

Pabbidi RM, Cao DS, Parihar A, Pauza ME, Premkumar LS (2008b). Direct role of streptozotocin in inducing thermal hyperalgesia by enhanced expression of transient receptor potential vanilloid 1 in sensory neurons. *Mol Pharmacol* **73**(3): 995-1004.

Pabreja K, Dua K, Sharma S, Padi SSV, Kulkarni SK (2011). Minocycline attenuates the development of diabetic neuropathic pain: Possible anti-inflammatory and anti-oxidant mechanisms. *European Journal of Pharmacology* **661**(1-3): 15-21.

Padi SS, Kulkarni SK (2008). Minocycline prevents the development of neuropathic pain, but not acute pain: possible anti-inflammatory and antioxidant mechanisms. *Eur J Pharmacol* **601**(1-3): 79-87.

Palecek J, Paleckova V, Dougherty PM, Carlton SM, Willis WD (1992). Responses of spinothalamic tract cells to mechanical and thermal stimulation of skin in rats with experimental peripheral neuropathy. *J Neurophysiol* **67**(6): 1562-1573.

Park SW, Yi JH, Miranpuri G, Satriotomo I, Bowen K, Resnick DK, *et al.* (2007). Thiazolidinedione class of peroxisome proliferator-activated receptor gamma agonists prevents neuronal damage, motor dysfunction, myelin loss, neuropathic pain, and inflammation after spinal cord injury in adult rats. *Journal of Pharmacology and Experimental Therapeutics* **320**(3): 1002-1012.

Perry T, Haughey NJ, Mattson MP, Egan JM, Greig NH (2002a). Protection and reversal of excitotoxic neuronal damage by glucagon-like peptide-1 and exendin-4. *J Pharmacol Exp Ther* **302**(3): 881-888.

Perry T, Holloway HW, Weerasuriya A, Mouton PR, Duffy K, Mattison JA, *et al.* (2007). Evidence of GLP-1-mediated neuroprotection in an animal model of pyridoxine-induced peripheral sensory neuropathy. *Exp Neurol* **203**(2): 293-301.

Perry T, Lahiri DK, Chen D, Zhou J, Shaw KT, Egan JM, *et al.* (2002b). A novel neurotrophic property of glucagon-like peptide 1: a promoter of nerve growth factor-mediated differentiation in PC12 cells. *J Pharmacol Exp Ther* **300**(3): 958-966.

Pertovaara A, Wei H, Kalmari J, Ruotsalainen M (2001). Pain behavior and response properties of spinal dorsal horn neurons following experimental diabetic neuropathy in the rat: Modulation by nitecapone, a COMT inhibitor with antioxidant properties. *Experimental Neurology* **167**(2): 425-434.

Pertwee R (2004). Pharmacological and therapeutic targets for $\Delta 9$ tetrahydrocannabinol and cannabidiol. *Euphytica* **140**(1-2): 73-82.

Pertwee R, Griffin G, Fernando S, Li X, Hill A, Makriyannis A (1995). AM630, a competitive cannabinoid receptor antagonist. *Life Sci* **56**(23-24): 1949-1955.

Pi-Sunyer FX, Aronne LJ, Heshmati HM, Devin J, Rosenstock J (2006). Effect of rimonabant, a cannabinoid-1 receptor blocker, on weight and cardiometabolic risk factors in overweight or obese patients: RIO-North America: a randomized controlled trial. *JAMA* **295**(7): 761-775.

Piomelli D, Tarzia G, Duranti A, Tontini A, Mor M, Compton TR, *et al.* (2006). Pharmacological profile of the selective FAAH inhibitor KDS-4103 (URB597). *CNS Drug Rev* **12**(1): 21-38.

Pipatpiboon N, Pintana H, Pratchayasakul W, Chattipakorn N, Chattipakorn SC (2013). DPP4-inhibitor improves neuronal insulin receptor function, brain mitochondrial function and cognitive function in rats with insulin resistance induced by high-fat diet consumption. *European Journal of Neuroscience* **37**(5): 839-849.

Pirart J (1978). Diabetes Mellitus and Its Degenerative Complications: A Prospective Study of 4,400 Patients Observed Between 1947 and 1973. *Diabetes Care* **1**(3): 168-188.

Piriz J, Torres-Aleman I, Nuñez A (2009). Independent alterations in the central and peripheral somatosensory pathways in rat diabetic neuropathy. *Neuroscience* **160**(2): 402-411.

Pop-Busui R, Sullivan KA, Van Huysen C, Bayer L, Cao XH, Towns R, *et al.* (2001). Depletion of taurine in experimental diabetic neuropathy: Implications for nerve metabolic, vascular, and functional deficits. *Experimental Neurology* **168**(2): 259-272.

Porreca F, Ossipov MH, Gebhart GF (2002). Chronic pain and medullary descending facilitation. *Trends Neurosci* **25**(6): 319-325.

Poucher SM, Cheetham S, Francis J, Zinker B, Kirby M, Vickers SP (2012). Effects of saxagliptin and sitagliptin on glycaemic control and pancreatic beta-cell mass in a streptozotocin-induced mouse model of type 2 diabetes. *Diabetes Obes Metab* **14**(10): 918-926.

Price DD, Hayes RL, Ruda M, Dubner R (1978). Spatial and temporal transformations of input to spinothalamic tract neurons and their relation to somatic sensations. *J Neurophysiol* **41**(4): 933-947.

Price TJ, Rashid MH, Millecamps M, Sanoja R, Entrena JM, Cervero F (2007). Decreased nociceptive sensitization in mice lacking the fragile X mental retardation protein: role of mGluR1/5 and mTOR. *J Neurosci* **27**(51): 13958-13967.

Qiang X, Satoh J, Sagara M, Fukuzawa M, Masuda T, Sakata Y, *et al.* (1998). Inhibitory effect of troglitazone on diabetic neuropathy in streptozotocin-induced diabetic rats. *Diabetologia* **41**(11): 1321-1326.

Quilici S, Chancellor J, Lothgren M, Simon D, Said G, Le T, *et al.* (2009). Meta-analysis of duloxetine vs. pregabalin and gabapentin in the treatment of diabetic peripheral neuropathic pain. *BMC Neurology* **9**(1): 6.

Raghavendra V, Tanga F, DeLeo JA (2003). Inhibition of Microglial Activation Attenuates the Development but Not Existing Hypersensitivity in a Rat Model of Neuropathy. *Journal of Pharmacology and Experimental Therapeutics* **306**(2): 624-630.

Raghavendra V, Tanga FY, DeLeo JA (2004). Complete Freund's adjuvant-induced peripheral inflammation evokes glial activation and proinflammatory cytokine expression in the CNS. *European Journal of Neuroscience* **20**(2): 467-473.

Rang HP, Ritchie JM (1988). Depolarization of nonmyelinated fibers of the rat vagus nerve produced by activation of protein kinase C. *The Journal of neuroscience : the official journal of the Society for Neuroscience* **8**(7): 2606-2617.

Rauch T, Graefe-Mody U, Deacon CF, Ring A, Holst JJ, Woerle HJ, *et al.* (2012). Linagliptin increases incretin levels, lowers glucagon, and improves glycemic control in type 2 diabetes mellitus. *Diabetes Ther* **3**(1): 10.

Reaven GM, Chen YD, Hollenbeck CB, Sheu WH, Ostrega D, Polonsky KS (1993). Plasma insulin, C-peptide, and proinsulin concentrations in obese and nonobese individuals with varying degrees of glucose tolerance. *J Clin Endocrinol Metab* **76**(1): 44-48.

Reed MJ, Meszaros K, Entes LJ, Claypool MD, Pinkett JG, Gadbois TM, *et al.* (2000). A new rat model of type 2 diabetes: The fat-fed, streptozotocin-treated rat. *Metab.-Clin. Exp.* **49**(11): 1390-1394.

Reed MJ, Scribner KA (1999). In-vivo and in-vitro models of type 2 diabetes in pharmaceutical drug discovery. *Diabetes Obes Metab* **1**(2): 75-86.

Rees DA, Alcolado JC (2005). Animal models of diabetes mellitus. *Diabetic Medicine* **22**(4): 359-370.

Regalia J, Cai F, Helke C (2002). Streptozotocin-induced diabetes and the neurochemistry of vagal afferent neurons. *Brain Res* **938**(1-2): 7-14.

Regan MR, Huang YH, Kim YS, Dykes-Hoberg MI, Jin L, Watkins AM, *et al.* (2007). Variations in promoter activity reveal a differential expression and physiology of glutamate transporters by glia in the developing and mature CNS. *J Neurosci* **27**(25): 6607-6619.

Renno WM, Al-Banaw AG, George P, Abu-Ghefreh AA, Akhtar S, Benter IF (2012). Angiotensin-(1-7) Via the Mas Receptor Alleviates the Diabetes-Induced Decrease in GFAP and GAP-43 Immunoreactivity with Concomitant Reduction in the COX-2 in Hippocampal Formation: An Immunohistochemical Study. *Cellular and Molecular Neurobiology* **32**(8): 1323-1336.

Rexed B (1952). The cytoarchitectonic organization of the spinal cord in the cat. *The Journal of Comparative Neurology* **96**(3): 415-495.

Romanovsky D, Cruz NF, Diemel GA, Dobretsov M (2006). Mechanical hyperalgesia correlates with insulin deficiency in normoglycemic streptozotocin-treated rats. *Neurobiology of Disease* **24**(2): 384-394.

Romanovsky D, Hastings SL, Stimers JR, Dobretsov M (2004). Relevance of hyperglycemia to early mechanical hyperalgesia in streptozotocin-induced diabetes. *J Peripher Nerv Syst* **9**(2): 62-69.

Romanovsky D, Wang J, Al-Chaer ED, Stimers JR, Dobretsov M (2010). Comparison of metabolic and neuropathy profiles of rats with streptozotocin-induced overt and moderate insulinopenia. *Neuroscience* **170**(1): 337-347.

Romero-Sandoval A, Chai N, Natile-McMenemy N, Deleo JA (2008a). A comparison of spinal Iba1 and GFAP expression in rodent models of acute and chronic pain. *Brain Res* **1219**: 116-126.

Romero-Sandoval A, Natile-McMenemy N, DeLeo JA (2008b). Spinal microglial and perivascular cell cannabinoid receptor type 2 activation reduces behavioral hypersensitivity without tolerance after peripheral nerve injury. *Anesthesiology* **108**(4): 722-734.

Rosenblatt S, Miskin B, Glazer NB, Prince MJ, Robertson KE (2001). The impact of pioglitazone on glycemic control and atherogenic dyslipidemia in patients with type 2 diabetes mellitus. *Coron Artery Dis* **12**(5): 413-423.

Rosenstock J, Hollander P, Chevalier S, Iranmanesh A (2008). SERENADE: the Study Evaluating Rimonabant Efficacy in Drug-naive Diabetic Patients: effects of monotherapy with rimonabant, the first selective CB1 receptor antagonist, on glycemic control, body weight, and lipid profile in drug-naive type 2 diabetes. *Diabetes Care* **31**(11): 2169-2176.

Rothstein JD, Martin L, Levey AI, Dykes-Hoberg M, Jin L, Wu D, *et al.* (1994). Localization of neuronal and glial glutamate transporters. *Neuron* **13**(3): 713-725.

Rungger-Brandle E, Dosso AA, Leuenberger PM (2000). Glial reactivity, an early feature of diabetic retinopathy. *Invest Ophthalmol Vis Sci* **41**(7): 1971-1980.

Russell JW, Golovoy D, Vincent AM, Mahendru P, Olzmann JA, Mentzer A, *et al.* (2002). High glucose-induced oxidative stress and mitochondrial dysfunction in neurons. *FASEB J* **16**(13): 1738-1748.

Russell JW, Sullivan KA, Windebank AJ, Herrmann DN, Feldman EL (1999). Neurons Undergo Apoptosis in Animal and Cell Culture Models of Diabetes. *Neurobiology of Disease* **6**(5): 347-363.

Russo R, Loverme J, La Rana G, Compton TR, Parrott J, Duranti A, *et al.* (2007). The fatty acid amide hydrolase inhibitor URB597 (cyclohexylcarbamic acid 3'-carbamoylbiphenyl-3-yl ester) reduces neuropathic pain after oral administration in mice. *J Pharmacol Exp Ther* **322**(1): 236-242.

Rydén L, Standl E, Bartnik M, Van den Berghe G, Betteridge J, de Boer M-J, *et al.* (2007). Guidelines on diabetes, pre-diabetes, and cardiovascular diseases: executive summary. *European Heart Journal* **28**(1): 88-136.

Saganová K, Burda J, Orendáčová J, Čížková D, Vanický I (2006). Fluoro-Jade B Staining Following Zymosan Microinjection into the Spinal Cord White Matter. *Cellular and Molecular Neurobiology* **26**(7): 1461-1471.

Sagar DR, Burston JJ, Hathway GJ, Woodhams SG, Pearson RG, Bennett AJ, *et al.* (2011). The contribution of spinal glial cells to chronic pain behaviour in the monosodium iodoacetate model of osteoarthritic pain. *Mol Pain* **7**: 88.

Sagar DR, Gaw AG, Okine BN, Woodhams SG, Wong A, Kendall DA, *et al.* (2009). Dynamic regulation of the endocannabinoid system: implications for analgesia. *Mol Pain* **5**: 59.

Sagar DR, Kendall DA, Chapman V (2008). Inhibition of fatty acid amide hydrolase produces PPAR- α -mediated analgesia in a rat model of inflammatory pain. *British Journal of Pharmacology* **155**(8): 1297-1306.

Said G (2007). Diabetic neuropathy - a review. *Nature Clinical Practice Neurology* **3**(6): 331-340.

Sarashina A, Sesoko S, Nakashima M, Hayashi N, Taniguchi A, Horie Y, *et al.* (2010). Linagliptin, a dipeptidyl peptidase-4 inhibitor in development for the treatment of type 2 diabetes mellitus: a Phase I, randomized, double-blind, placebo-controlled trial of single and multiple escalating doses in healthy adult male Japanese subjects. *Clin Ther* **32**(6): 1188-1204.

Saravia FE, Revsin Y, Gonzalez Deniselle MC, Gonzalez SL, Roig P, Lima A, *et al.* (2002). Increased astrocyte reactivity in the hippocampus of murine models of type 1 diabetes: the nonobese diabetic (NOD) and streptozotocin-treated mice. *Brain Res* **957**(2): 345-353.

Sasaki H, Schmelzer JD, Zollman PJ, Low PA (1997). Neuropathology and blood flow of nerve, spinal roots and dorsal root ganglia in longstanding diabetic rats. *Acta Neuropathol* **93**(2): 118-128.

Sasso O, Bertorelli R, Bandiera T, Scarpelli R, Colombano G, Armirotti A, *et al.* (2012). Peripheral FAAH inhibition causes profound antinociception and protects against indomethacin-induced gastric lesions. *Pharmacol Res* **65**(5): 553-563.

Schaible HG, Freudenberger U, Neugebauer V, Stiller RU (1994). Intraspinous release of immunoreactive calcitonin gene-related peptide during development of inflammation in the joint in vivo--a study with antibody microprobes in cat and rat. *Neuroscience* **62**(4): 1293-1305.

Scheen AJ, Finer N, Hollander P, Jensen MD, Van Gaal LF (2006). Efficacy and tolerability of rimonabant in overweight or obese patients with type 2 diabetes: a randomised controlled study. *Lancet* **368**(9548): 1660-1672.

Schlosburg JE, Blankman JL, Long JZ, Nomura DK, Pan B, Kinsey SG, *et al.* (2010). Chronic monoacylglycerol lipase blockade causes functional antagonism of the endocannabinoid system. *Nat Neurosci* **13**(9): 1113-1119.

Schmeichel AM, Schmelzer JD, Low PA (2003). Oxidative Injury and Apoptosis of Dorsal Root Ganglion Neurons in Chronic Experimental Diabetic Neuropathy. *Diabetes* **52**(1): 165-171.

Schmidt R, Schmelz M, Forster C, Ringkamp M, Torebjork E, Handwerker H (1995). Novel classes of responsive and unresponsive C nociceptors in human skin. *J Neurosci* **15**(1 Pt 1): 333-341.

Schmued LC, Hopkins KJ (2000). Fluoro-Jade B: a high affinity fluorescent marker for the localization of neuronal degeneration. *Brain Research* **874**(2): 123-130.

Schouenborg J, Dickenson A (1985). Effects of a distant noxious stimulation on A and C fibre-evoked flexion reflexes and neuronal activity in the dorsal horn of the rat. *Brain Res* **328**(1): 23-32.

Schreiber AK, Neufeld M, Jesus CHA, Cunha JM (2012). Peripheral antinociceptive effect of anandamide and drugs that affect the endocannabinoid system on the formalin test in normal and streptozotocin-diabetic rats. *Neuropharmacology* **63**(8): 1286-1297.

Schuelert N, Johnson MP, Oskins JL, Jassal K, Chambers MG, McDougall JJ (2011). Local application of the endocannabinoid hydrolysis inhibitor URB597 reduces nociception in spontaneous and chemically induced models of osteoarthritis. *Pain* **152**(5): 975-981.

Sears DD, Hsiao A, Ofrecio JM, Chapman J, He W, Olefsky JM (2007). Selective modulation of promoter recruitment and transcriptional activity of PPARgamma. *Biochem Biophys Res Commun* **364**(3): 515-521.

Selvarajah D, Wilkinson ID, Emery CJ, Shaw PJ, Griffiths PD, Gandhi R, *et al.* (2008). Thalamic neuronal dysfunction and chronic sensorimotor distal symmetrical polyneuropathy in patients with type 1 diabetes mellitus. *Diabetologia* **51**(11): 2088-2092.

Severinsen K, Jakobsen J (2007). Diabetes does not accelerate neuronal loss following nerve injury. *J Peripher Nerv Syst* **12**(4): 262-268.

Sharma AK, Thomas PK (1974). Peripheral nerve structure and function in experimental diabetes. *Journal of the Neurological Sciences* **23**(1): 1-15.

Sherrington CS (1906). *The Integrative Action of the Nervous System*.

Sidenius P, Jakobsen J (1980). Reduced perikaryal volume of lower motor and primary sensory neurons in early experimental diabetes. *Diabetes* **29**(3): 182-186.

Silva M, Amorim D, Almeida A, Tavares I, Pinto-Ribeiro F, Morgado C (2013). Pronociceptive changes in the activity of rostroventromedial medulla (RVM) pain modulatory cells in the streptozotocin-diabetic rat. *Brain Res Bull* **96**: 39-44.

Sima AAF (2003). New insights into the metabolic and molecular basis for diabetic neuropathy. *Cellular and Molecular Life Sciences* **60**(11): 2445-2464.

Sima AAF, Kamiya H (2006). Diabetic neuropathy differs in type 1 and type 2 diabetes. *Diabetes Mellitus and Its Complications* **1084**: 235-249.

Singhal A, Cheng C, Sun H, Zochodne DW (1997). Near nerve local insulin prevents conduction slowing in experimental diabetes. *Brain Research* **763**(2): 209-214.

Skalska S, Kucera P, Goldenberg Z, Stefek M, Kyselova Z, Jariabka P, *et al.* (2010). Neuropathy in a rat model of mild diabetes induced by multiple low doses of streptozotocin: effects of the antioxidant stobadine in comparison with a high-dose alpha-lipoic acid treatment. *Gen Physiol Biophys* **29**(1): 50-58.

Smith HS (2010). Activated Microglia in Nociception. *Pain Physician* **13**(3): 295-304.

Soares HP, Ni Y, Kisfalvi K, Sinnott-Smith J, Rozengurt E (2013). Different Patterns of Akt and ERK Feedback Activation in Response to Rapamycin, Active-Site mTOR Inhibitors and Metformin in Pancreatic Cancer Cells. *PLoS ONE* **8**(2): e57289.

Sorensen L, Siddall PJ, Trenell MI, Yue DK (2008). Differences in metabolites in pain-processing brain regions in patients with diabetes and painful neuropathy. *Diabetes Care* **31**(5): 980-981.

Sotocinal S, Sorge R, Zaloum A, Tuttle A, Martin L, Wieskopf J, *et al.* (2011). The Rat Grimace Scale: A partially automated method for quantifying pain in the laboratory rat via facial expressions. *Molecular Pain* **7**(1): 55.

Srinivasan K, Ramarao P (2007). Animal models in type 2 diabetes research: An overview. *Indian J. Med. Res.* **125**(3): 451-472.

Srinivasan K, Viswanad B, Asrat L, Kaul CL, Ramarao P (2005). Combination of high-fat diet-fed and low-dose streptozotocin-treated rat: A model for type 2 diabetes and pharmacological screening. *Pharmacological Research* **52**(4): 313-320.

Stacey BR, Dworkin RH, Murphy K, Sharma U, Emir B, Griesing T (2008). Pregabalin in the Treatment of Refractory Neuropathic Pain:

Results of a 15-Month Open-Label Trial. *Pain Medicine* **9**(8): 1202-1208.

Stamboulian S, Choi JS, Ahn HS, Chang YW, Tyrrell L, Black JA, *et al.* (2010). ERK1/2 mitogen-activated protein kinase phosphorylates sodium channel Na(v)1.7 and alters its gating properties. *J Neurosci* **30**(5): 1637-1647.

Stanfa LC, Dickenson AH (2004). In vivo electrophysiology of dorsal-horn neurons. *Methods Mol Med* **99**: 139-153.

Study RE, Kral MG (1996). Spontaneous action potential activity in isolated dorsal root ganglion neurons from rats with a painful neuropathy. *Pain* **65**(2-3): 235-242.

Stumvoll M, Goldstein BJ, van Haeften TW (2005). Type 2 diabetes: principles of pathogenesis and therapy. *Lancet* **365**(9467): 1333-1346.

Stumvoll M, Nurjhan N, Perriello G, Dailey G, Gerich JE (1995). Metabolic Effects of Metformin in Non-Insulin-Dependent Diabetes Mellitus. *New England Journal of Medicine* **333**(9): 550-554.

Sugimoto K, Murakawa Y, Sima AAF (2000). Diabetic neuropathy - a continuing enigma. *Diabetes/Metabolism Research and Reviews* **16**(6): 408-433.

Sun RQ, Lawand NB, Lin Q, Willis WD (2004a). Role of calcitonin gene-related peptide in the sensitization of dorsal horn neurons to mechanical stimulation after intradermal injection of capsaicin. *J Neurophysiol* **92**(1): 320-326.

Sun RQ, Lawand NB, Willis WD (2003). The role of calcitonin gene-related peptide (CGRP) in the generation and maintenance of mechanical allodynia and hyperalgesia in rats after intradermal injection of capsaicin. *Pain* **104**(1-2): 201-208.

Sun RQ, Tu YJ, Lawand NB, Yan JY, Lin Q, Willis WD (2004b). Calcitonin gene-related peptide receptor activation produces PKA- and PKC-dependent mechanical hyperalgesia and central sensitization. *J Neurophysiol* **92**(5): 2859-2866.

Sung B, Lim G, Mao J (2003). Altered expression and uptake activity of spinal glutamate transporters after nerve injury contribute to the pathogenesis of neuropathic pain in rats. *J Neurosci* **23**(7): 2899-2910.

Suzuki N, Hasegawa-Moriyama M, Takahashi Y, Kamikubo Y, Sakurai T, Inada E (2011). Lidocaine attenuates the development of diabetic-induced tactile allodynia by inhibiting microglial activation. *Anesth Analg* **113**(4): 941-946.

Suzuki Y, Sato J, Kawanishi M, Mizumura K (2002). Lowered response threshold and increased responsiveness to mechanical stimulation of cutaneous nociceptive fibers in streptozotocin-diabetic rat skin in vitro--correlates of mechanical allodynia and hyperalgesia observed in the early stage of diabetes. *Neuroscience Research* **43**(2): 171-178.

Sweitzer SM, Colburn RW, Rutkowski M, DeLeo JA (1999). Acute peripheral inflammation induces moderate glial activation and spinal IL-1 β expression that correlates with pain behavior in the rat. *Brain Research* **829**(1-2): 209-221.

Sweitzer SM, Medicherla S, Almirez R, Dugar S, Chakravarty S, Shumilla JA, *et al.* (2004). Antinociceptive action of a p38alpha MAPK inhibitor, SD-282, in a diabetic neuropathy model. *Pain* **109**(3): 409-419.

Szkudelski T (2001). The mechanism of alloxan and streptozotocin action in B cells of the rat pancreas. *Physiological Research* **50**(6): 537-546.

Szkudelski T (2012). Streptozotocin-nicotinamide-induced diabetes in the rat. Characteristics of the experimental model. *Experimental Biology and Medicine* **237**(5): 481-490.

Takada J, Machado MA, Peres SB, Brito LC, Borges-Silva CN, Costa CE, *et al.* (2007). Neonatal streptozotocin-induced diabetes mellitus: a model of insulin resistance associated with loss of adipose mass. *Metabolism* **56**(7): 977-984.

Takahashi Y, Hasegawa-Moriyama M, Sakurai T, Inada E (2011). The Macrophage-Mediated Effects of the Peroxisome Proliferator-Activated Receptor-Gamma Agonist Rosiglitazone Attenuate Tactile Allodynia in the Early Phase of Neuropathic Pain Development. *Anesth. Analg.* **113**(2): 398-404.

Tal M, Eliav E (1996). Abnormal discharge originates at the site of nerve injury in experimental constriction neuropathy (CCI) in the rat. *Pain* **64**(3): 511-518.

Talbot S, Chahmi E, Dias J, Couture R (2010). Key role for spinal dorsal horn microglial kinin B1 receptor in early diabetic pain neuropathy. *Journal of Neuroinflammation* **7**(1): 36.

Taliyan R, Sharma PL (2012). Possible mechanism of protective effect of thalidomide in STZ-induced-neuropathic pain behavior in rats. *Inflammopharmacology* **20**(2): 89-97.

Tan AM, Samad OA, Fischer TZ, Zhao P, Persson AK, Waxman SG (2012). Maladaptive Dendritic Spine Remodeling Contributes to Diabetic Neuropathic Pain. *Journal of Neuroscience* **32**(20): 6795-6807.

Tan NS, Michalik L, Desvergne B, Wahli W (2005). Multiple expression control mechanisms of peroxisome proliferator-activated receptors and their target genes. *J Steroid Biochem Mol Biol* **93**(2-5): 99-105.

Tanga FY, Raghavendra V, DeLeo JA (2004). Quantitative real-time RT-PCR assessment of spinal microglial and astrocytic activation markers in a rat model of neuropathic pain. *Neurochem Int* **45**(2-3): 397-407.

Taylor BK, Dadia N, Yang CB, Krishnan S, Badr M (2002). Peroxisome proliferator-activated receptor agonists inhibit inflammatory edema and hyperalgesia. *Inflammation* **26**(3): 121-127.

Taylor CP (2004). The biology and pharmacology of calcium channel alpha2-delta proteins Pfizer Satellite Symposium to the 2003 Society for Neuroscience Meeting. Sheraton New Orleans Hotel, New Orleans, LA November 10, 2003. *CNS Drug Rev* **10**(2): 183-188.

Taylor CP (2009). Mechanisms of analgesia by gabapentin and pregabalin – Calcium channel $\alpha 2\text{-}\delta$ [Cava2- δ] ligands. *Pain* **142**(1–2): 13-16.

Terenghi G, Chen S, Carrington AL, Polak JM, Tomlinson DR (1994). Changes in sensory neuropeptides in dorsal root ganglion and spinal cord of spontaneously diabetic BB rats. A quantitative immunohistochemical study. *Acta Diabetol* **31**(4): 198-204.

Tesfaye S, Stevens LK, Stephenson JM, Fuller JH, Plater M, Ionescu-Tirgoviste C, *et al.* (1996). Prevalence of diabetic peripheral neuropathy and its relation to glycaemic control and potential risk factors: the EURODIAB IDDM Complications Study. *Diabetologia* **39**(11): 1377-1384.

Tikka TM, Koistinaho JE (2001). Minocycline Provides Neuroprotection Against N-Methyl-d-aspartate Neurotoxicity by Inhibiting Microglia. *The Journal of Immunology* **166**(12): 7527-7533.

Tillu DV, Melemedjian OK, Asiedu MN, Qu N, De Felice M, Dussor G, *et al.* (2012). Resveratrol engages AMPK to attenuate ERK and mTOR signaling in sensory neurons and inhibits incision-induced acute and chronic pain. *Mol Pain* **8**: 5.

Tkacs NC, Pan Y, Raghupathi R, Dunn-Meynell AA, Levin BE (2005). Cortical Fluoro-Jade staining and blunted adrenomedullary response to hypoglycemia after noncoma hypoglycemia in rats. *J Cereb Blood Flow Metab* **25**(12): 1645-1655.

Tognetto M, Amadesi S, Harrison S, Creminon C, Trevisani M, Carreras M, *et al.* (2001). Anandamide excites central terminals of dorsal root

ganglion neurons via vanilloid receptor-1 activation. *J Neurosci* **21**(4): 1104-1109.

Tomiyama M, Furusawa K, Kamijo M, Kimura T, Matsunaga M, Baba M (2005). Upregulation of mRNAs coding for AMPA and NMDA receptor subunits and metabotropic glutamate receptors in the dorsal horn of the spinal cord in a rat model of diabetes mellitus. *Brain Res Mol Brain Res* **136**(1-2): 275-281.

Topol EJ, Bousser MG, Fox KA, Creager MA, Despres JP, Easton JD, *et al.* (2010). Rimonabant for prevention of cardiovascular events (CRESCENDO): a randomised, multicentre, placebo-controlled trial. *Lancet* **376**(9740): 517-523.

Toran-Allerand CD, Bentham W, Miranda RC, Anderson JP (1991). Insulin influences astroglial morphology and glial fibrillary acidic protein (GFAP) expression in organotypic cultures. *Brain Res* **558**(2): 296-304.

Torres-Lopez JE, Ortiz MI, Castaneda-Hernandez G, Alonso-Lopez R, Asomoza-Espinosa R, Granados-Soto V (2002). Comparison of the antinociceptive effect of celecoxib, diclofenac and resveratrol in the formalin test. *Life Sci* **70**(14): 1669-1676.

Toth C, Rong LL, Yang C, Martinez J, Song F, Ramji N, *et al.* (2008). Receptor for advanced glycation end products (RAGEs) and experimental diabetic neuropathy. *Diabetes* **57**(4): 1002-1017.

Toth CC, Jedrzejewski NM, Ellis CL, Frey WH, 2nd (2010). Cannabinoid-mediated modulation of neuropathic pain and microglial accumulation in a model of murine type I diabetic peripheral neuropathic pain. *Mol Pain* **6**: 16.

Tracey I, Mantyh PW (2007). The cerebral signature for pain perception and its modulation. *Neuron* **55**(3): 377-391.

Treede RD, Meyer RA, Campbell JN (1998). Myelinated mechanically insensitive afferents from monkey hairy skin: heat-response properties. *J Neurophysiol* **80**(3): 1082-1093.

Treede RD, Meyer RA, Raja SN, Campbell JN (1995). Evidence for two different heat transduction mechanisms in nociceptive primary afferents innervating monkey skin. *J Physiol* **483** (Pt 3): 747-758.

Tsou K, Brown S, Sanudo-Pena MC, Mackie K, Walker JM (1998). Immunohistochemical distribution of cannabinoid CB1 receptors in the rat central nervous system. *Neuroscience* **83**(2): 393-411.

Tsuda M, Inoue K, Salter MW (2005). Neuropathic pain and spinal microglia: a big problem from molecules in 'small' glia. *Trends in Neurosciences* **28**(2): 101-107.

Tsuda M, Masuda T, Tozaki-Saitoh H, Inoue K (2013). Microglial regulation of neuropathic pain. *J Pharmacol Sci* **121**(2): 89-94.

Tsuda M, Ueno H, Kataoka A, Tozaki-Saitoh H, Inoue K (2008). Activation of dorsal horn microglia contributes to diabetes-induced tactile allodynia via extracellular signal-regulated protein kinase signaling. *Glia* **56**(4): 378-386.

Ulrich P, Cerami A (2001). Protein Glycation, Diabetes, and Aging. *Recent Prog Horm Res* **56**(1): 1-22.

Ulugol A, Karadag HC, Ipci Y, Tamer M, Dokmeci I (2004). The effect of WIN 55,212-2, a cannabinoid agonist, on tactile allodynia in diabetic rats. *Neuroscience Letters* **371**(2-3): 167-170.

Van Gaal LF, Rissanen AM, Scheen AJ, Ziegler O, Rossner S (2005). Effects of the cannabinoid-1 receptor blocker rimonabant on weight reduction and cardiovascular risk factors in overweight patients: 1-year experience from the RIO-Europe study. *Lancet* **365**(9468): 1389-1397.

van Rossum D, Hanisch UK, Quirion R (1997). Neuroanatomical localization, pharmacological characterization and functions of CGRP, related peptides and their receptors. *Neurosci Biobehav Rev* **21**(5): 649-678.

Van Sickle MD, Duncan M, Kingsley PJ, Mouihate A, Urbani P, Mackie K, *et al.* (2005). Identification and functional characterization of brainstem cannabinoid CB2 receptors. *Science* **310**(5746): 329-332.

Vanegas H, Schaible HG (2004). Descending control of persistent pain: inhibitory or facilitatory? *Brain Res Brain Res Rev* **46**(3): 295-309.

Velazquez KT, Mohammad H, Sweitzer SM (2007). Protein kinase C in pain: involvement of multiple isoforms. *Pharmacol Res* **55**(6): 578-589.

Vera G, Lopez-Miranda V, Herradon E, Martin MI, Abalo R (2012). Characterization of cannabinoid-induced relief of neuropathic pain in rat models of type 1 and type 2 diabetes. *Pharmacol Biochem Behav* **102**(2): 335-343.

Verge GM, Milligan ED, Maier SF, Watkins LR, Naeve GS, Foster AC (2004). Fractalkine (CX3CL1) and fractalkine receptor (CX3CR1) distribution in spinal cord and dorsal root ganglia under basal and neuropathic pain conditions. *Eur J Neurosci* **20**(5): 1150-1160.

Veves A, Backonja M, Malik RA (2008). Painful diabetic neuropathy: Epidemiology, natural history, early diagnosis, and treatment options. *Pain Medicine* **9**(6): 660-674.

Vickers SP, Cheetham SC, Birmingham GD, Rowley HL, Headland KR, Dickinson K, *et al.* (2012). Effects of the DPP-4 inhibitor, linagliptin, in diet-induced obese rats: a comparison in naive and exenatide-treated animals. *Clin Lab* **58**(7-8): 787-799.

Vincent A, Feldman E (2004a). New Insights into the Mechanisms of Diabetic Neuropathy. *Reviews in Endocrine & Metabolic Disorders* **5**(3): 227-236.

Vincent AM, Russell JW, Low P, Feldman EL (2004b). Oxidative Stress in the Pathogenesis of Diabetic Neuropathy. *Endocrine Reviews* **25**(4): 612-628.

Vinik AI, Casellini CM (2013). Guidelines in the management of diabetic nerve pain: clinical utility of pregabalin. *Diabetes Metab Syndr Obes* **6**: 57-78.

Vinik AI, Park TS, Stansberry KB, Pittenger GL (2000). Diabetic neuropathies. *Diabetologia* **43**(8): 957-973.

Wall PD, Devor M (1983). Sensory afferent impulses originate from dorsal root ganglia as well as from the periphery in normal and nerve injured rats. *Pain* **17**(4): 321-339.

Wang S, Lim G, Yang L, Sung B, Mao J (2006). Downregulation of spinal glutamate transporter EAAC1 following nerve injury is regulated by central glucocorticoid receptors in rats. *Pain* **120**(1-2): 78-85.

Wang W, Wang W, Mei X, Huang J, Wei Y, Wang Y, *et al.* (2009). Crosstalk between Spinal Astrocytes and Neurons in Nerve Injury-Induced Neuropathic Pain. *PLoS ONE* **4**(9): e6973.

Wattiez A, DA DB, Dupuis A, Courteix C (2012). Rodent Models of Painful Diabetic Neuropathy: What Can We Learn from Them? *Journal of Diabetes and Metabolism* **S5**:(008).

Wautier MP, Chappey O, Corda S, Stern DM, Schmidt AM, Wautier JL (2001). Activation of NADPH oxidase by AGE links oxidant stress to altered gene expression via RAGE. *Am J Physiol Endocrinol Metab* **280**(5): E685-694.

Weng HR, Chen JH, Cata JP (2006). Inhibition of glutamate uptake in the spinal cord induces hyperalgesia and increased responses of spinal dorsal horn neurons to peripheral afferent stimulation. *Neuroscience* **138**(4): 1351-1360.

Wiggin TD, Kretzler M, Pennathur S, Sullivan KA, Brosius FC, Feldman EL (2008). Rosiglitazone treatment reduces diabetic neuropathy in streptozotocin-treated DBA/2J mice. *Endocrinology* **149**(10): 4928-4937.

Willis WD, Coggeshall RE (2004). *Sensory mechanisms of the spinal cord*. 3rd Edition. edn. Kluwer Academic/Plenum Publishers, New York.

Willson TM, Brown PJ, Sternbach DD, Henke BR (2000). The PPARs: from orphan receptors to drug discovery. *J Med Chem* **43**(4): 527-550.

Wilson NM, Wright DE (2012a). Inflammatory Mediators in Diabetic Neuropathy. *Journal of Diabetes & Metabolism* **01**(S5).

Wilson RD, Islam MS (2012b). Fructose-fed streptozotocin-injected rat: an alternative model for type 2 diabetes. *Pharmacol Rep* **64**(1): 129-139.

Wodarski R, Clark AK, Grist J, Marchand F, Malcangio M (2009). Gabapentin reverses microglial activation in the spinal cord of streptozotocin-induced diabetic rats. *European Journal of Pain* **13**(8): 807-811.

Won SJ, Yoo BH, Kauppinen TM, Choi BY, Kim JH, Jang BG, *et al.* (2012). Recurrent/moderate hypoglycemia induces hippocampal dendritic injury, microglial activation, and cognitive impairment in diabetic rats. *J Neuroinflammation* **9**: 182.

Woolf CJ (1983). Evidence for a central component of post-injury pain hypersensitivity. *Nature* **306**(5944): 686-688.

Woolf CJ, Thompson SW (1991). The induction and maintenance of central sensitization is dependent on N-methyl-D-aspartic acid receptor activation; implications for the treatment of post-injury pain hypersensitivity states. *Pain* **44**(3): 293-299.

Xie Y, Zhang J, Petersen M, LaMotte RH (1995). Functional changes in dorsal root ganglion cells after chronic nerve constriction in the rat. *J Neurophysiol* **73**(5): 1811-1820.

Xin W-J, Weng H-R, Dougherty P (2009). Plasticity in expression of the glutamate transporters GLT-1 and GLAST in spinal dorsal horn glial cells following partial sciatic nerve ligation. *Molecular Pain* **5**(1): 15.

Xu GY, Li G, Liu N, Huang LY (2011). Mechanisms underlying purinergic P2X3 receptor-mediated mechanical allodynia induced in diabetic rats. *Mol Pain* **7**: 60.

Xu H, Barnes GT, Yang Q, Tan G, Yang D, Chou CJ, *et al.* (2003). Chronic inflammation in fat plays a crucial role in the development of obesity-related insulin resistance. *J Clin Invest* **112**(12): 1821-1830.

Yagihashi S, Yamagishi SI, Wada R, Baba M, Hohman TC, Yabe-Nishimura C, *et al.* (2001). Neuropathy in diabetic mice overexpressing

human aldose reductase and effects of aldose reductase inhibitor. *Brain* **124**: 2448-2458.

Yamagishi S-I, Ogasawara S, Mizukami H, Yajima N, Wada R-i, Sugawara A, *et al.* (2008). Correction of protein kinase C activity and macrophage migration in peripheral nerve by pioglitazone, peroxisome proliferator activated- γ -ligand, in insulin-deficient diabetic rats. *Journal of Neurochemistry* **104**(2): 491-499.

Yamamoto H, Shimoshige Y, Yamaji T, Murai N, Aoki T, Matsuoka N (2009). Pharmacological characterization of standard analgesics on mechanical allodynia in streptozotocin-induced diabetic rats. *Neuropharmacology* **57**(4): 403-408.

Yan SD, Schmidt AM, Anderson GM, Zhang J, Brett J, Zou YS, *et al.* (1994). Enhanced cellular oxidant stress by the interaction of advanced glycation end products with their receptors/binding proteins. *J Biol Chem* **269**(13): 9889-9897.

Yang XY, Sun L, Xu P, Gong LL, Qiang GF, Zhang L, *et al.* (2011). Effects of salvianolic acid A on plantar microcirculation and peripheral nerve function in diabetic rats. *European Journal of Pharmacology* **665**(1-3): 40-46.

Yang Y, Santamaria P (2006). Lessons on autoimmune diabetes from animal models. *Clin Sci (Lond)* **110**(6): 627-639.

Ye Z, Wimalawansa SJ, Westlund KN (1999). Receptor for calcitonin gene-related peptide: localization in the dorsal and ventral spinal cord. *Neuroscience* **92**(4): 1389-1397.

Yoon YW, Na HS, Chung JM (1996). Contributions of injured and intact afferents to neuropathic pain in an experimental rat model. *Pain* **64**(1): 27-36.

Youssef J, Badr M (2004). Role of peroxisome proliferator-activated receptors in inflammation control. *BioMed Research International* **2004**(3): 156-166.

Yu LC, Hansson P, Lundeberg T (1996). The calcitonin gene-related peptide antagonist CGRP8-37 increases the latency to withdrawal responses bilaterally in rats with unilateral experimental mononeuropathy, an effect reversed by naloxone. *Neuroscience* **71**(2): 523-531.

Yu Y, Lundeberg T, Yu LC (2002). Role of calcitonin gene-related peptide and its antagonist on the evoked discharge frequency of wide dynamic range neurons in the dorsal horn of the spinal cord in rats. *Regul Pept* **103**(1): 23-27.

Yusaf SP, Goodman J, Gonzalez IM, Bramwell S, Pinnock RD, Dixon AK, *et al.* (2001). Streptozocin-induced neuropathy is associated with altered expression of voltage-gated calcium channel subunit mRNAs in rat dorsal root ganglion neurones. *Biochem Biophys Res Commun* **289**(2): 402-406.

Zhang J, De Koninck Y (2006a). Spatial and temporal relationship between monocyte chemoattractant protein-1 expression and spinal glial activation following peripheral nerve injury. *Journal of Neurochemistry* **97**(3): 772-783.

Zhang JL, Yang JP, Zhang JR, Li RQ, Wang J, Jan JJ, *et al.* (2013). Gabapentin reduces allodynia and hyperalgesia in painful diabetic neuropathy rats by decreasing expression level of Nav1.7 and p-ERK1/2 in DRG neurons. *Brain Res* **1493**: 13-18.

Zhang L, Hoff AO, Wimalawansa SJ, Cote GJ, Gagel RF, Westlund KN (2001a). Arthritic calcitonin/alpha calcitonin gene-related peptide knockout mice have reduced nociceptive hypersensitivity. *Pain* **89**(2-3): 265-273.

Zhang M, Lv XY, Li J, Xu ZG, Chen L (2008). The Characterization of High-Fat Diet and Multiple Low-Dose Streptozotocin Induced Type 2 Diabetes Rat Model. *Experimental Diabetes Research*.

Zhang W, Murakawa Y, Wozniak KM, Slusher B, Sima AA (2006b). The preventive and therapeutic effects of GCPII (NAALADase) inhibition on painful and sensory diabetic neuropathy. *J Neurol Sci* **247**(2): 217-223.

Zhang W, Yorek M, Pierson CR, Murakawa Y, Breidenbach A, Sima AA (2001b). Human C-peptide dose dependently prevents early neuropathy in the BB/Wor-rat. *Int J Exp Diabetes Res* **2**(3): 187-193.

Zhou G, Myers R, Li Y, Chen Y, Shen X, Fenyk-Melody J, *et al.* (2001a). Role of AMP-activated protein kinase in mechanism of metformin action. *J Clin Invest* **108**(8): 1167-1174.

Zhou Y, Zhou ZS, Zhao ZQ (2001b). PKC regulates capsaicin-induced currents of dorsal root ganglion neurons in rats. *Neuropharmacology* **41**(5): 601-608.

Zhou Z, Peng X, Hagshenas J, Insolera R, Fink DJ, Mata M (2010). A novel cell-cell signaling by microglial transmembrane TNFalpha with implications for neuropathic pain. *Pain* **151**(2): 296-306.

Zhuang HX, Wuarin L, Fei ZJ, Ishii DN (1997). Insulin-like growth factor (IGF) gene expression is reduced in neural tissues and liver from rats with non-insulin-dependent diabetes mellitus, and IGF treatment ameliorates diabetic neuropathy. *J Pharmacol Exp Ther* **283**(1): 366-374.

Zhuo M, Gebhart GF (1992). Characterization of descending facilitation and inhibition of spinal nociceptive transmission from the nuclei reticularis gigantocellularis and gigantocellularis pars alpha in the rat. *J Neurophysiol* **67**(6): 1599-1614.

Zhuo M, Gebhart GF (1990). Characterization of descending inhibition and facilitation from the nuclei reticularis gigantocellularis and gigantocellularis pars alpha in the rat. *Pain* **42**(3): 337-350.

Zhuo M, Wu G, Wu LJ (2011). Neuronal and microglial mechanisms of neuropathic pain. *Mol Brain* **4**: 31.

Ziegler D (2008). Painful diabetic neuropathy: treatment and future aspects. *Diabetes-Metabolism Research and Reviews* **24**: S52-S57.

Zimmermann M (2001). Pathobiology of neuropathic pain. *European Journal of Pharmacology* **429**(1-3): 23-37.

Zinman B, Hanley AJ, Harris SB, Kwan J, Fantus IG (1999). Circulating tumor necrosis factor-alpha concentrations in a native Canadian population with high rates of type 2 diabetes mellitus. *J Clin Endocrinol Metab* **84**(1): 272-278.

Zochodne DW (2007). Diabetes mellitus and the peripheral nervous system: Manifestations and mechanisms. *Muscle & Nerve* **36**(2): 144-166.

Zochodne DW, Verge VM, Cheng C, Sun H, Johnston J (2001). Does diabetes target ganglion neurones? Progressive sensory neurone involvement in long-term experimental diabetes. *Brain* **124**(Pt 11): 2319-2334.

Zoncu R, Efeyan A, Sabatini DM (2011). mTOR: from growth signal integration to cancer, diabetes and ageing. *Nat Rev Mol Cell Biol* **12**(1): 21-35.

Zuo ZF, Wang W, Niu L, Kou ZZ, Zhu C, Zhao XH, *et al.* (2011). RU486 (mifepristone) ameliorates cognitive dysfunction and reverses the down-regulation of astrocytic N-myc downstream-regulated gene 2 in streptozotocin-induced type-1 diabetic rats. *Neuroscience* **190**: 156-165.